

31 1146450 8

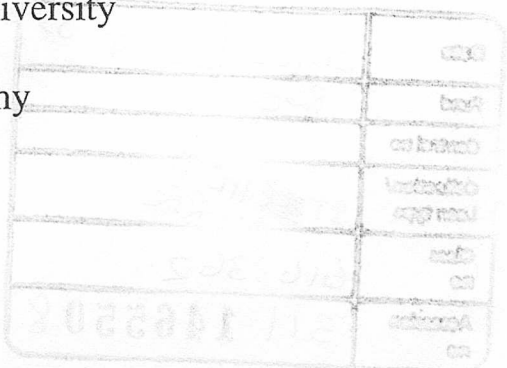


Molecular responses of iron regulatory proteins
to iron overload in human liver

Maria Neonaki

A thesis submitted in partial fulfilment of the requirements of
London Metropolitan University
for the degree of
Doctor of Philosophy

October 2006



Date	20/02/2007
Paid	803
Control no	
Collection/ Loan type	ST HL PREM RFC
Class no	616.362
Accession no	311 146550 8

Abstract

Iron is one of the most abundant metals in nature and a necessary element for life. It is not iron *per se* but rather its implication in the generation of reactive oxygen species that makes the metal harmful when present in excess as seen in iron overload disorders, such as in hereditary haemochromatosis (HH). And although the intricate mechanisms that maintain iron homeostasis are beginning to transpire, the aetiology of this disorder remains elusive despite knowledge of the causative mutations in HFE. In an attempt to gain an insight into the complexity of HH, transcript and protein levels of key iron-related molecules were investigated in liver specimens from patients with *HFE*-related HH. Protein levels of iron regulatory protein 1 (IRP1), a known regulator of iron uptake and storage in cells, were found to be consistently down-regulated in the liver of patients with *HFE*-related HH and also in a human hepatoma cell line exposed to ferric ammonium citrate. The intracellular localisation of the protein was also studied and in addition to the cytoplasmic and perinuclear presence of IRP1, a nuclear existence was also evident in transiently transfected cells. Protein levels of transferrin receptor 2 (TfR2) were found to be up-regulated in the liver of both untreated as well as treated HH patients, and correlated directly, irrespective of mutations in HFE, with the degree of transferrin saturation, reaching saturable levels at high hepatic iron concentrations. The underlying mechanism of the observed decrease in IRP1 and increase in TfR2 protein levels in these patients was further investigated at the mRNA level and pointed to a post-transcriptional level of control for both molecules. Hepcidin has recently been dubbed as the main regulator of dietary iron absorption and levels of the transcript in the liver of HH patients failed to respond to the extent of the iron burden, pointing to a central role of this molecule in the aetiology of this disorder.

Acknowledgements

My utmost gratitude goes to my supervisor Dr. Kenneth White and our collaborator Dr. Adrian Bomford (Institute of Liver Studies, King's College Hospital), without whose help, excellent guidance and continuous support this work would have been impossible. Special thanks go to both Dr. White and Prof. Christopher Branford-White, director of the Institute for Health Research and Policy at London Metropolitan University, for providing me with the opportunity to work for the Institute and the Department of Health and Human Sciences, hence ensuring my financial support as well as my professional development. I am indebted to Dr. Christopher Gove (Randal Centre for Molecular Mechanisms of Cell Function, King's College London) for his invaluable help with the real-time PCR experiments and Mrs Rongrong Cheng (Molecular Biology Unit, King's College London) for the numerous sequencing reactions. I am thankful to Mr Allan Bashal (Department of Health and Human Sciences, London Metropolitan University) for his help with the atomic absorption spectrometry experiments. Thanks also to Jordi Gracia Sancho and Gerard Folch Codera, Socrates-Erasmus students (at the time) from the University of Tarragona in Spain, for providing stepping stones to certain aspects of this work, and whose pneuma of enthusiasm and perseverance in the lab was inspiring. I would also like to thank all the members of the Institute and fellow students for their encouragement, and finally my warmest thanks go to my friends and family and especially my mother for her unlimited support throughout the years.

In memory of my father

Table of Contents

ABBREVIATIONS	14-17
CHAPTER I. INTRODUCTION	18-58
1.1 THE IRONIC PROTAGONIST	18-20
1.1.1 Brief background on iron	18-19
1.1.2 The “dark” side of iron	19-20
1.2 THE IRON TREK – UPTAKE, DISTRIBUTION, AND STORAGE OF IRON IN HUMANS	20-34
1.2.1 Dietary iron uptake	21-22
1.2.1.1 Non-haem iron uptake	22-23
1.2.1.2 Haem iron uptake	23-25
1.2.1.3 Iron uptake by target cells via the Tf cycle	26-28
1.2.1.4 Additional and/or alternative mechanisms of iron uptake by target cells	29-32
1.2.2 Distribution and storage of iron	33-34
1.3 REGULATION OF IRON HOMEOSTASIS	34-42
1.3.1 The iron responsive element/iron regulatory protein system	34-40
1.3.2 Regulation of iron homeostasis at the level of intestinal absorption	40-42
1.4 HEREDITARY IRON OVERLOAD	42-57
1.4.1 Types of hereditary haemochromatosis	42-54
1.4.1.1 Type 1 or <i>HFE</i> -related hereditary haemochromatosis	43-51
1.4.1.2 Non <i>HFE</i> -related HH (Types 2, 3 and 4)	51-54
1.4.2 Pathogenesis of hereditary haemochromatoses	55-57
1.5 AIMS AND OBJECTIVES OF THE THESIS	58
CHAPTER II. MATERIALS AND METHODS	59-97
2.1 MATERIALS	59-60
2.1.1 Liver Tissue	59
2.1.2 Cell lines	59
2.1.3 Bacterial strains	60
2.2. REAGENTS AND GENERAL EQUIPMENT	60-61
2.2.1 Chemicals and reagents	60
2.2.2 Molecular weight markers	60
2.2.3 Cell culture reagents	60
2.2.4 Commonly used equipment	61
2.3 CELL CULTURE	61-62
2.3.1 Culturing of cell lines	61

2.3.2 Counting cells with a haemocytometer	62
2.3.3 Cryopreservation of cells and revival of frozen stock	62
2.4 RNA AND DNA PREPARATIONS	63-66
2.4.1 Extraction of RNA from cultured cells or liver tissue	63-64
2.4.2 Purification of plasmid DNA from bacterial cells	64-65
2.4.2.1 Mini preparation of plasmid DNA from bacterial cells	64
2.4.2.2 Maxi preparation of plasmid DNA from bacterial cells	64-65
2.4.3 Spectrophotometric determination of the amount of RNA/DNA	65-66
2.5 STANDARD METHODS INVOLVING DNA	66-71
2.5.1 Restriction enzyme digestions	66
2.5.2 'Fill in' reactions using Klenow Polymerase	66-67
2.5.3 Alkaline phosphatase treatment (dephosphorylation of cut vectors)	67
2.5.4 DNA ligation	67
2.5.5 Concentration of DNA by phenol extraction and ethanol precipitation	67-68
2.5.6 Agarose gel electrophoresis	68
2.5.7 Purification of DNA fragments from a low-melting point agarose gel	68-69
2.5.7.1 Purification of DNA fragments for subcloning	68-69
2.5.7.2 Purification of DNA fragments for use as standards and for sequencing	69
2.5.8 Transformation of bacteria	69-70
2.5.8.1 Transformation of competent cells	69-70
2.5.8.2 Perfectly blunt cloning kit transformation	70
2.5.9 Antibiotic selection	70-71
2.6 PLASMIDS	71-72
2.7 CELL MANIPULATION	73-75
2.7.1 Transient transfection of eukaryotes	73-74
2.7.1.1 Transfection of mammalian cells using DEAE-Dextran	73
2.7.1.2 Transfection of mammalian cells by electroporation	74
2.7.2 Treatment of mammalian cells with ferric ammonium citrate	74
2.7.3 Atomic absorption spectrometry of iron	74-75
2.8 PROTEIN EXTRACTION AND WESTERN BLOTTING	75-82
2.8.1 Protein extraction from cultured cells	76-77
2.8.1.1 Extraction of endogenous IRP1 and IRP1-GFP	76
2.8.1.2 Cytoplasmic, membrane and nuclear fractionation of IRP1-GFP	76-77
2.8.1.3 Extraction of TfR2	77
2.8.2 Protein extraction from liver tissue	77-78
2.8.2.1 Extraction of IRP1 from liver tissue	77
2.8.2.2 Extraction of TfR2 from liver tissue	78

2.8.3 Determination of protein concentration	78
2.8.3.1 Determination of protein concentration by the Lowry method	78
2.8.3.2 Determination of protein concentration by the Bradford method	78
2.8.4 Separation of proteins using SDS-PAGE	79-80
2.8.4.1 Preparation of the samples for Western Blotting	79
2.8.4.2 Preparation of the SDS polyacrylamide gel	79
2.8.4.3 Preparation and running of the SDS polyacrylamide gel	79-80
2.8.4.4 Coomassie Brilliant Blue staining	80
2.8.5 Western blotting	80-82
2.8.5.1 Immunodetection of IRP1	81
2.8.5.2 Immunodetection of TfR2	81
2.8.5.3 Immunodetection of GFP and actin	82
2.8.5.4 Colorimetric detection	82
2.9 FIRST STRAND SYNTHESIS AND REAL TIME POLYMERASE CHAIN REACTION	83-92
2.9.1 Synthesis of cDNA Strand for nested PCR analysis	83
2.9.2 Synthesis of cDNA Strand for real time PCR analysis	83
2.9.3 Nested PCR	84
2.9.4 Real-time quantitative PCR	84-86
2.9.4.1 Optimisation of real-time PCR runs	87-88
2.9.4.2 Preparation of standards	89
2.9.4.3 Reaction components and cycling parameters	89-91
2.9.4.4 Confirmation of PCR product identity	92
2.10 DATA ACQUISITION AND EVALUATION	92-97
2.10.1 LightCycler Data acquisition	92-94
2.10.2 Calculation of copy numbers	93
2.10.3 Image acquisition and processing	95-96
2.10.4 Statistical analysis	97
CHAPTER III. EXPRESSION OF LIVER IRP1 PROTEIN IN HH	98-138
3.1 INTRODUCTION	98-100
3.1.1 IRP1 protein expression	98-99
3.1.2 Subcellular distribution and alternatively spliced forms of IRP1	99-100
3.2 RESULTS	101-129
3.2.1 Down-regulation of liver IRP1 protein in iron overload	101-112
3.2.1.1 Evaluation of IRP1 protein levels in the liver of HH patients	101-105
3.2.1.2 Evaluation of IRP1 protein levels in COS and HepG2 cells	106-112
3.2.2 Alternative splicing of IRP1	113-116
3.2.3 Subcellular distribution of IRP1-GFP in cultured cells	117-121

3.2.4 Transient expression of IRP1-GFP in COS, HeLa and HepG2 cells	122-129
3.3 DISCUSSION	130-138
3.3.1 Hepatic IRP1 is down-regulated in response to iron loading	130-133
3.3.2 Smaller forms of IRP1	134
3.3.3 Intracellular localisation of IRP1	135-137
3.3.4 Future directions	137-138
CHAPTER IV.	
HEPATIC mRNA LEVELS OF HAMP, HJV, TfR1, TfR2 AND IRP1 IN HH	139-168
4.1 INTRODUCTION	139
4.2 RESULTS	140-158
4.2.1 Clinical characteristics of study groups	140
4.2.2 Real time PCR efficiency	141-143
4.2.3 Levels of hepatic HAMP, HJV, TfR1, TfR2 and IRP1 mRNA in iron loaded HH patients homozygous for the major mutation in <i>HFE</i> , patients with iron overload irrespective of their genotype and control subjects	144-147
4.2.4 Abundance of HAMP and IRP1 mRNA in human liver	148-149
4.2.5 Hepatic HAMP mRNA levels correlate with IRP1 and TfR2	150-153
4.2.6 Hepatic TfR2 and IRP1 mRNA levels correlate with levels of serum ferritin in the control group but not in HH patients	154-155
4.2.7 Hepatic HAMP and TfR2 mRNA levels and the hepatic iron concentration	156-157
4.2.8 Hepatic HJV and IRP1 mRNA levels and the total iron binding capacity	156-158
4.3 DISCUSSION	159-168
4.3.1 Hepatic hepcidin fails to respond to the iron burden	159-162
4.3.2 Abundance and correlation of HAMP and IRP1 mRNA in the human liver	163
4.3.3 Hepatic HAMP and TfR2 transcripts correlate with the HIC	163-164
4.3.4 Duodenal expression of molecules implicated in iron import and export	164-167
4.3.5 Future directions	168
CHAPTER V. EXPRESSION OF LIVER TfR2 PROTEIN IN HH	
5.1 INTRODUCTION	169-170
5.2 RESULTS	170-179
5.2.1 TfR2 protein expression in human liver	170-173
5.2.2 Correlation of hepatic TfR2 protein levels with clinical iron indices	174-177

5.2.3 Non-linear regression analysis of the associations between hepatic TfR2 protein levels and clinical iron indices	178-179
5.3 DISCUSSION	180-183
5.3.1 Hepatic TfR2 protein is up-regulated in HH	180-182
5.3.2 Saturable expression of liver TfR2 protein in HH	183
5.3.3 Future directions	183
CHAPTER VI. CONCLUSIONS	184-191
6.1 DOWN-REGULATION OF IRP1 PROTEIN IN HH IS A POST-TRANSCRIPTIONAL EVENT	184-185
6.2 TRANSCRIPT LEVELS OF IRON-RELATED MOLECULES EXPRESSED IN THE LIVER ARE NOT AFFECTED BY IRON OVERLOAD	185
6.3 SATURABILITY OF HEPATIC TfR2 PROTEIN EXPRESSION IN HH	185-186
6.4 SUMMARY OF OBSERVATIONS	186-190
6.5 REMAINING ISSUES	191
REFERENCES	192-225
APPENDIX I	226-227
APPENDIX II	228-230
APPENDIX III	231-245

List of figures

CHAPTER I. INTRODUCTION

Figure 1.1 Proposed model for the uptake of dietary iron across the apical membrane of the absorptive enterocyte.	25
Figure 1.2 Uptake of iron into cells via the Tf cycle.	28
Figure 1.3 Mechanisms of iron uptake by hepatocytes and macrophages.	32
Figure 1.4 Structure of human IRP1.	37
Figure 1.5 The co-ordinated post-transcriptional regulation of TfR1 and ferritin mRNAs via the IRE/IRP system.	39
Figure 1.6 Diagrammatic representation of the HFE molecule.	46
Figure 1.7 Unifying pathogenic model for the development of HH.	57

CHAPTER II. MATERIALS AND METHODS

Figure 2.1 Diagrammatic representation of the pEGFP-N3 vector.	72
Figure 2.2 Real-time PCR optimisation via magnesium chloride titration and use of appropriate acquisition temperature (T_m).	88
Figure 2.3 Real-time PCR of TfR2 mRNA levels in human liver tissue.	94
Figure 2.4 Analysis of immunoblotted membranes using ImageJ.	96

CHAPTER III. EXPRESSION OF LIVER IRP1 PROTEIN IN HH

Figure 3.1 Expression of IRP1 protein in liver sections from an HH patient before and after phlebotomy treatment.	102
Figure 3.2 Western blotting analysis of IRP1 in human liver using anti peptide A of IRP1 anti-serum.	104
Figure 3.3 Western blotting analysis of IRP1 in human liver using anti peptide B of IRP1 anti-serum.	105
Figure 3.4 Effect of iron loading treatment on COS and HepG2 cells.	108
Figure 3.5 Effect of iron loading on IRP1 protein levels in COS cells as assessed by Western blotting using a polyclonal anti-peptide A of human IRP1 antiserum.	109
Figure 3.6 Effect of iron loading on IRP1 protein levels in COS cells as assessed by Western blotting using anti-peptide B and anti-whole of human IRP1 antiserum.	110
Figure 3.7 Effect of iron loading on IRP1 protein levels in HepG2 cells as assessed by Western blotting using a polyclonal	

anti-peptide A of human IRP1 antiserum.	111
Figure 3.8 Effect of iron loading on IRP1 protein levels in HepG2 cells as assessed by Western blotting using anti-peptide B and anti-whole of human IRP1 antiserum.	112
Figure 3.9 Location of peptides on IRP1 sequence recognised by anti-peptide A and anti-peptide B anti-sera.	113
Figure 3.10 Electrophoretic analysis of Nested PCR products derived from HepG2 cells.	116
Figure 3.11 Transient expression of IRP1-GFP and REX-GFP constructs in COS cells.	120
Figure 3.12 Subcellular distribution of IRP1 in COS cells.	121
Figure 3.13 Fluorescence microscopy of GFP protein in HeLa transfected cells.	123
Figure 3.14 Fluorescence microscopy of IRP1-GFP protein in transfected HeLa cells.	124
Figure 3.15 Fluorescence microscopy of GFP protein in transfected HepG2 cells.	125
Figure 3.16 Fluorescence microscopy of Rex-GFP protein in HepG2 cells.	126
Figure 3.17 Fluorescence microscopy of IRP1-GFP protein in HepG2 cells.	127
Figure 3.18 Confocal microscopy of IRP1-GFP protein in transfected COS cells.	128
Figure 3.19 Evidence of IRP1-GFP protein expression in the nucleus.	129

CHAPTER IV.

HEPATIC mRNA LEVELS OF HAMP, HJV, TfR1, TfR2 AND IRP1 IN HH

Figure 4.1 Melting curve and gel analysis of the HAMP, HJV and TfR1 transcripts.	142
Figure 4.2 Melting curve and gel analysis of the IRP1, TfR2, and β -actin transcripts.	143
Figure 4.3 Hepatic mRNA expression of HAMP, HJV, TfR1, TfR2 and IRP1 in HH patients homozygous for the C282Y mutation and control individuals.	146
Figure 4.4 Hepatic mRNA expression of HAMP, HJV, TfR1, TfR2 and IRP1 in patients with iron overload irrespective of genotype and control individuals.	147
Figure 4.5 Abundance of HAMP and IRP1 expression in the liver.	149
Figure 4.6 Linear regression analysis of the correlation between hepatic HAMP and IRP1 mRNA expression.	151
Figure 4.7 Linear regression analysis of the correlation between hepatic HAMP and TfR2 mRNA expression.	152
Figure 4.8 Linear regression analysis of the correlation between hepatic TfR2 and IRP1 mRNA expression.	153

Figure 4.9 Linear regression analysis of the correlation between serum ferritin and hepatic mRNA expression of the IRP1 and TfR2 transcripts.	155
Figure 4.10 Linear regression analysis of the correlation between hepatic iron concentration and hepatic mRNA expression of the TfR2 and HAMP transcripts.	157
Figure 4.11 Linear regression analysis of the correlation between TIBC and hepatic mRNA expression of the HJV and IRP1 transcripts.	158
CHAPTER V. EXPRESSION OF LIVER TfR2 PROTEIN IN HH	
Figure 5.1 Western blotting analysis of TfR2 in human liver.	172
Figure 5.2 Western blotting analysis of hepatic TfR2 in untreated and treated HH patients.	173
Figure 5.3 Linear regression analysis of the correlation between hepatic TfR2 protein expression and clinical iron status indices in the whole study group.	175
Figure 5.4 Linear regression analysis of the correlation between hepatic TfR2 protein expression and the TS, SF and the HIC in control subjects or untreated HH patients.	176
Figure 5.5 Linear regression analysis of the correlation between hepatic TfR2 protein expression and the SI and TIBC in control subjects and untreated HH patients.	177
Figure 5.6 Non-linear regression analysis of the correlation between the hepatic TfR2 protein expression and clinical iron status indices in the whole study group.	179

CHAPTER VI. CONCLUSIONS

Figure 6.1 Mechanisms regulating iron absorption are abrogated in HFE-related HH.	190
---	-----

List of tables

CHAPTER I. INTRODUCTION

Table 1.1 Laboratory measurements of iron status in HH patients	49
Table 1.2 Genetic Haemochromatoses	54

CHAPTER II. MATERIALS AND METHODS

Table 2.1.1 Sequences of primers, orientation, size of amplicon and regions amplified for quantification of genes in qRT-PCR	86
Table 2.1.2 Optimal cycling conditions for quantification of HAMP, HJV, IRP1, TfR1, TfR2 and β-actin in qRT-PCR	86
Table 2.2 Specific cycling conditions for quantification of HAMP, HJV, IRP1, TfR1, TfR2 and β-actin in qRT-PCR	91

CHAPTER III. EXPRESSION OF LIVER IRP1 PROTEIN IN HH

Table 3.1 Clinical characteristics and iron indices of study groups in Chapter III	101
Table 3.2 Alternative splicing patterns of IRP1	114
Table 3.3 Expression of IRP1 in response to iron	133

CHAPTER IV. HEPATIC mRNA LEVELS OF HAMP, HJV, TfR1, TfR2 AND IRP1 IN HH

Table 4.1 Clinical characteristics and iron indices of study groups in Chapter IV	140
Table 4.2 Summary of mRNA expression levels of studied genes	145
Table 4.3 Comparative levels of HAMP, HJV, IRP1, TfR1 and TfR2 in human liver	148
Table 4.4 Hepatic mRNA expression of iron-related genes in studies using material from human subjects and cell lines	160
Table 4.5 Hepatic mRNA expression of iron-related genes in the animal model of HH	161
Table 4.6 Duodenal mRNA expression of iron-related genes in patients with HFE associated HH	166
Table 4.7 Duodenal mRNA expression of iron-related genes in animal models of HH and mice on iron rich diet	167

CHAPTER V. EXPRESSION OF LIVER TfR2 PROTEIN IN HH

Table 5.1 Clinical characteristics and iron indices of study groups in Chapter V	170
Table 5.2 Hepatic TfR2 protein expression in cell lines and animal models	182

Abbreviations

A ₂₆₀	Absorbance at 260 nm
A ₂₈₀	Absorbance at 280 nm
aa	Amino acids
AMVRT	Avian myeloblastosis virus reverse transcriptase
AP	Alkaline phosphatase
APS	Ammonium perodoxisulphate
ATP	Adenosine triphosphate
BCIP	5-bromo 4-chloro 3-indoylphosphate
bp	Base pairs
BPB	Bromophenol blue
BSA	Bovine serum albumin
C/EBPa	CCAAT/enhancer binding protein
cDNA	Complementary DNA
CIP	Calf intestinal alkaline phosphatase
C _p	Crossing points
Cp	Ceruloplasmin
Dcytb	Duodenal cytochrome b
DEAE	Diethylaminoethyl
DMF	Dimethylformamide
DMSO	Dimethylsulphoxide
DMT1	Divalent metal transporter 1
DNA	Deoxyribonucleic acid
dNTPs	Deoxyribonucleotide triphosphates
DOC	Deoxycholate
ds	double stranded
DTT	Dithiothreitol
EDTA	Ethylene-diamine-tetra-acetic acid
eIF4F	Eukaryotic initiation factor-4F
FAC	Ferric ammonium citrate
FBS	Fetal bovine serum
Fe	Iron

Fe ²⁺	Ferrous iron
Fe ³⁺	Ferric iron
Fe ³⁺ -Tf	Diferric transferrin
FP1	Ferroportin 1
FR	Ferritin receptor
GFP	Green fluorescent protein
GI	Gastrointestinal
HAMP	Hepcidin gene/transcript
Hb	Haemoglobin
HCP1	Haem carrier protein 1
HH	Hereditary haemochromatosis
HIC	Hepatic iron concentration
HII	Hepatic iron index
HIV-1	Human immunodeficiency virus type 1
HJV	Hemojuvelin
HLA	Human leukocyte antigen
HO1	Haem oxygenase 1
Hp	Hephaestin
Htb	Haptoglobin
HTLV-1	Human T-cell leukemia virus type 1
Hx	Haemopexin
IL-6	Interleukin-6
IRE(s)	Iron response element(s)
IRE/IRP	Iron responsive element/iron regulatory protein
IRP(s)	Iron regulatory protein(s)
IRP1	Iron regulatory protein 1
IRP2	Iron regulatory protein 2
4Fe-4S	Iron-sulphur cluster
JH	Juvenile haemochromatosis
Kbp	Kilo base pairs
kDa	Kilo Dalton
KO	Knockout
-/-	Deficient
LB	Luria-Bertani broth

LIP	Labile iron pool
MCS	Multiple cloning site
MHC	Major histocompatibility
MOPS	3-(N-Morpholino)-propanesulfonic acid
M _r	Molecular weight
mRNA	Messenger RNA
NBT	Nitro blue tetrazolium
NEAA	Non-essential amino acids
NH	Neonatal haemochromatosis
NLS	Nuclear localization signal
NTBI	Non transferrin bound iron
OMIM	Online Mendelian Inheritance in Man
PAGE	Polyacrylamide gel electrophoresis
PBS	Phosphate buffer saline
PCR	Polymerase chain reaction
PKD	Pyruvate kinase deficiency
ppm	Parts per million
qRT-PCR	Quantitative real-time PCR
RBC(s)	Red blood cell(s)
RE	Restriction enzyme
RGM	Repulsive guidance molecules
RNA	Ribonucleic acid
ROS	Reactive oxygen species
rpm	Rounds per minute
RRE	Rev responsive element
RT	Reverse transcriptase
RXRE	Rex responsive element
SD	Standard deviation
SDS	Sodium dodecyl sulphate
SF	Serum ferritin
SFT	Stimulator of Fe transport
SI	Serum iron
SOD1	Superoxide dismutase 1
STAT	Signal transducer and activator of transcription

Strep-AP	Streptavidin alkaline phosphatase
$t_{1/2}$	Half-life
TBS	Tris buffered saline
TE	Tris EDTA
TEMED	N,N,N',N'-Tetramethylethylenediamine
Tf	Transferrin
TfR(s)	Transferrin receptor(s)
TfR1	Transferrin receptor 1
TfR2	Transferrin receptor 2
TGF	Transforming growth factor
TIBC	Total iron binding capacity
T_m	Melting temperature
tRNA	Transfer RNA
TS	Transferrin saturation
TTB	Towbin transfer buffer
U	Unit
UTR	Untranslated regions
Usf2	Upstream stimulatory factor 2
v/v	Volume/volume
w/v	Weight/volume
β 2m	β 2-microglobulin
β -Me	β -mercaptoethanol

Chapter I

Introduction

1.1 The ironic protagonist

1.1.1 Brief background on iron

Life is thought to have evolved in a milieu composed of inorganic molecules. Current theories on the origin of life and cells suggest that iron, in the form of iron pyrite or structured iron sulphide, may have been the procreator in the formation of complex organic compounds in the primordial Hadean ocean floor billions of years ago and in the generation of some of the atmospheric oxygen (Huber and Wachtershauser 1998, Martin and Russell 2003). Nowadays, the significance of the existence of this metal is exemplified by the fact that all living organisms from the simplest bacteria, with the *Lactobacillus* and some strains of the *Bacillus* family being the only exceptions, to the most complex organisms, depend on iron for survival (reviewed in Crichton *et al* 2002). Iron was one of the first elements to have been identified as an essential component of the human diet from as early as 1664 (O'Dell and Sunde 1997) and there are records indicating that the ancient Egyptian, Greek and Roman civilisations, though ignorant of its nutritional significance, had recognised its potential therapeutic properties (Beard and Dawson 1997).

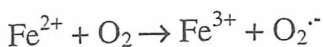
Iron (Fe), which got its symbol from the Latin word for iron, *ferrum*, is the most abundant transition metal, in terms of its cosmic abundance as well as its concentration in the Earth's crust (Harris 2002). Iron (atomic weight 55.85, atomic number 26) is located in the middle of the elements of the first transition series (group 8, period 4) in the periodic table, and its oxidation states vary from -II to +VI. The reduced divalent ferrous form (Fe II or Fe²⁺) and the oxidised trivalent ferric form (Fe III or Fe³⁺) are the principal ones - and the only states that are stable in the aqueous environment of the human body and in food - allowing iron to coordinate electron donors and participate in oxidation-reduction processes. In the human body, iron is a teeming element, making 0.004% of the human body's mass, at approximately 4.5g and is an essential component of, and cofactor for, numerous proteins and enzymes, including the oxygen carrying proteins, catalases,

cytochromes, ribonucleotide reductases, and aconitases to name but a few (Wrigglesworth and Baum 1980).

Iron plays key roles in processes that rely on its one-electron donations and its ability to bind certain proteins to form the iron-containing proteins known as metalloproteins. Iron, in the ferrous form, combines with haem, a pigment that is synthesised from the universal precursor 5-aminolevulinic acid to form haem iron (iron-protoporphyrin IX). The result of the joining of haem iron to various protein moieties, is the formation of the haemoproteins, the most abundant of which are haemoglobin (Hb) and myoglobin, and various cytochromes (cytochrome oxidase, peroxidase and the cytochromes of the mitochondrial respiratory chain), which are involved in oxygen and electron transport, respectively (Crichton and Boelaert 2001). Non-haem iron is also known to combine in equimolar amounts with acid labile sulphur forming iron-sulphur clusters, which are also involved in electron transport. Moreover, both haem and non-haem iron (either in the ferrous or ferric form) are essential cofactors for an extensive list of enzymes (over 40) that are involved in numerous reactions (Beard and Dawson 1997). Iron therefore in its different “costumes” has major roles in oxygen transport, electron transfer, respiration, synthesis of deoxy- and ribo-nucleic acids (DNA, RNA) and proteins, transcriptional regulation, formation of neurotransmitters and hormones, and xenobiotic metabolism (reviewed in Lieu *et al* 2001 and Zecca *et al* 2004).

1.1.2 The “dark” side of iron

Transition metals have an incomplete outer shell of d electrons and can undergo changes in oxidation states involving one electron. The ability of iron to participate in one-electron transfer reactions makes this element an important biological catalyst but at the same time a potential threat to the cell. Free iron can participate in reactions involving oxygen, which can lead to the formation of unstable intermediates with unpaired electrons, known as free radicals or reactive oxygen species (ROS) (reviewed in Aisen *et al* 2001 and Cadenas 1989). Iron can reduce dioxygen (O_2), resulting in superoxide (O_2^-) formation, which forms part of the Haber-Weiss-Fenton sequence of reactions, named after their discoverers (reviewed in Toyokuni 1996):



The resulting reactive hydroxyl ($\text{OH}^{\cdot-}$) radical is highly toxic due to its ability to react with almost every organic molecule found in living cells (reviewed in McCord 1998). Uncontrolled ROS production leads to oxidative damage of cellular components, often referred to as oxidative stress. ROS can cause oxidative damage to macromolecules leading to lipid peroxidation, DNA damage, and protein fragmentation due to the oxidation of the polypeptide backbone (reviewed in Aisen *et al* 2001). Most iron is tightly bound to proteins so that it would be unavailable to participate in ROS generating reactions, however a small pool of non-protein bound “free” iron could potentially provide iron for these reactions. Normally, this “free” iron pool, also referred to as the labile iron pool (LIP), is kept extremely small and the total amount of iron in the body is well controlled. Iron released from haem can also add to this pool but even haem iron may catalyse the formation of radicals, via the formation of oxoferryl intermediates (reviewed in Papanikolaou and Pantopoulos 2005). This “dark” side of iron has the potential to aggravate oxidative stress, which is implicated in over 60 human diseases (reviewed in Halliwell 1987). Oxidative stress can lead to accelerated tissue degeneration, which is evident in disorders of hereditary iron overload (haemochromatosis) and consequently iron has been implicated in the pathogenesis of atherosclerosis, neurodegenerative disorders, such as Parkinson’s and Alzheimer’s diseases, certain cancers, ageing, and dysfunction of main organs such as the heart, pancreas and the liver (reviewed in Weinberg 1996 and Youdim *et al* 1993 and Eisenstein 2000 and Zecca *et al* 2004).

1.2 The iron trek – uptake, distribution, and storage of iron in humans

About 3.5 billion years ago, in the earliest stages of life on Earth, large amounts of iron in the ferrous form were thought to be present in the low-oxygen environment. Later, the presence of oxygen in the Earth’s atmosphere reduced iron bioavailability and nowadays iron exists almost exclusively in the less soluble ferric form. Because of this insolubility and potential toxicity of iron, specialised molecules for the acquisition, transport and storage of this metal in a soluble non-toxic form have

evolved to meet cellular iron requirements. Humans, and most mammals, are equipped with a panoply of molecules that, through closely orchestrated mechanisms, aid iron uptake, sequestration, storage, and utilisation and carry the element through its trek inside the human body.

1.2.1 Dietary iron uptake

Dietary iron is present either as inorganic or non-haem iron when plant sources are ingested and organic or haem iron contained in Hb and to a less extent in myoglobin when meat sources are ingested (reviewed in Hallberg 1983). Haem iron accounts for a small portion (15%-35%) of iron uptake and its absorption is not thought to be influenced by other dietary factors or the individual's iron status. In contrast, non-haem iron, the main source of dietary iron seems to be influenced by both the iron status of the individual as well as dietary factors (reviewed in Hallberg 1983). Non-haem iron, bound to food components, needs to be hydrolysed or solubilised before it can be reduced to its more readily absorbed Fe^{2+} form (Groff and Gropper 2000). Certain food components, such as ascorbic acid, act as reductants and hence promote iron absorption, while others, such as carbonates, phytates, phosphates and tannates, form insoluble complexes or polymerise iron and thus decrease its absorption (reviewed in Conrad *et al* 1999). Absorption of iron can be further influenced by the presence of, or interaction with, other micronutrients, such as zinc and copper (Arredondo *et al* 2006).

Nutritional absorption of iron in the human gastrointestinal (GI) tract occurs mainly in the duodenum and is dependent on acid and mucin from the stomach that aid penetration of the mucosal layer (Muir and Hopfer 1985). The immature duodenal crypt cells have the unique ability of initiating iron absorption by maturing into intestinal villi (enterocytes). Mature enterocytes have a brush border surface oriented to the lumen of the GI tract and a basolateral surface oriented to the portal blood vein, and express all the necessary components for the translocation of iron from the intestinal lumen to the portal circulation. Depending on whether haem or non haem iron is absorbed, entrance to the enterocyte will occur via distinct pathways (Turnbull *et al* 1962). Regardless of the source of iron however, the overall mechanism of iron absorption is a two-step process: the first step involves iron absorption across the apical membrane of the enterocyte and intracellular translocation of iron across the

cytosol, and the second step the egress of iron across the basolateral membrane and into the portal circulation (Figure 1.1).

1.2.1.1 Non-haem iron uptake

Absorption of non-haem (free or inorganic) iron occurs predominantly in the proximal small intestine and specifically in the mature enterocytes of the duodenum and jejunum, with the lowest rate of absorption in the ileum (Wheby *et al* 1964). Free iron is present in the diet as oxidised ferric iron, which cannot easily be absorbed by the enterocyte, and is therefore reduced to the soluble ferrous form via means of duodenal cytochrome b (Dcytb), an ascorbate dependent ferric reductase located in the luminal surface of the duodenal enterocyte (McKie *et al* 2001). Following reduction, the ferrous form is transported across the brush border membrane via the divalent metal transporter 1 (DMT1) [formerly divalent cation transporter 1 (DCT1) or natural resistance associated macrophage protein 2 (Nramp2)], which was identified by cDNA expression cloning in *Xenopus laevis* oocytes (Gunshin *et al* 1997, Fleming *et al* 1997). DMT1 is a plasma membrane glycoprotein with 12 membrane spanning domains that can also transport a number of other divalent metals, such as copper (Arredondo *et al* 2003), cobalt (Forbes and Gros 2003), manganese, cadmium and lead (Gunshin *et al* 1997). Mutations in *DMT1* result in defects in iron uptake from the intestinal lumen both in the mouse model of microcytic anaemia (Fleming *et al* 1997, Cannone-Hergaus *et al* 2000) and in Belgrade rats (Fleming *et al* 1998), and there has recently been a single report of a human mutation in *DMT1* in a patient with severe microcytic anaemia and iron overload (Mims *et al* 2005).

Once inside the absorptive enterocyte, iron is stored within the cell, bound to the iron storage protein ferritin or moves towards the basolateral membrane. Mammalian ferritin is a spherical protein shell composed of 24 subunits of heavy and light chains, forming a cavity that can accommodate up to 4500 atoms of iron in its ferric hydroxide core (reviewed in Harrison and Arosio 1996, and Theil 2003). Iron that is not incorporated into one of the storage proteins is transported into the portal circulation. Iron leaves the enterocyte via means of the iron exporter ferroportin 1 (FP1), [also known as SLC40A1 (for solute carrier family 40, member 1), MTP1 (for metal transporter 1) and IREG1 (for iron-regulated messenger RNA)], a single-chain

glycoprotein with at least 10 transmembrane domains that is located at the basolateral membrane of the enterocyte (Donovan *et al* 2000, McKie *et al* 2000, Abboud and Haile 2000). The efflux of iron across the basolateral membrane is enhanced by the presence of hephaestin (Hp), a transmembrane-bound copper-dependent ferroxidase, that facilitates cellular iron release by promoting the oxidation of Fe^{2+} to Fe^{3+} (Vulpe *et al* 1999). Hp is also thought to have a supranuclear localisation inside the enterocyte aiding the effective loading of iron onto ferritin (Kuo *et al* 2004). A defective Hp has been associated with the sex-linked anaemia (sla) of the mouse (Vulpe *et al* 1999), however no human disease has been linked with Hp to date. Once across the basolateral membrane and into the plasma circulation, ferric iron will reversibly bind the serum, single chain glycoprotein transferrin (Tf) (reviewed in Ponka 1999). Tf has homologous N-terminal and C-terminal iron-binding domains that are well separated forming a large water-filled cleft that can accommodate a maximum of two ferric iron atoms when the protein is in the iron-free conformation (apo-Tf) (Holmberg and Laurell 1947). Diferric-Tf ($\text{Fe}^{3+}_2\text{-Tf}$ or holo-Tf) and mono-Tf ($\text{Fe}^{3+}\text{-Tf}$) will then transport iron via the portal system to the target cells and tissues.

1.2.1.2 Haem iron uptake

Haem uptake is of critical importance due to the greater bioavailability of haem iron (Turnbull *et al* 1962, Hallberg and Sölvell 1967), and the fact that it can contribute up to 35% of the iron entering the body (Bezwoda *et al* 1983, reviewed in Carpenter and Mahoney 1992). Absorption of haem iron also starts at the proximal end of the gut, being highest at the duodenum and lowest at the ileum, however it occurs via a different pathway than for inorganic iron. At first, haem, once it is enzymatically split from globin within the intestinal lumen by the action of several digestive enzymes, readily enters the absorptive cell as an intact metalloporphyrin (Turnbull *et al* 1962, Hallberg and Sölvell 1967, Conrad *et al* 1967), via the recently identified haem carrier protein 1 (HCP1) (Shayeghi *et al* 2005). Identification of a haem transporter supports the findings of earlier studies of an energy dependent transmembrane transport of haem (Noyer *et al* 1998, Worthington *et al* 2001), though the possibility of an additional pathway of haem uptake by diffusion through the cell membrane still stands (Light and Olson 1990). Within the enterocyte, haem is degraded by haem oxygenase 1 (HO1) and releases biliverdin, carbon monoxide

and ferrous iron (Raffin *et al* 1974), the latter of which joins the LIP of the enterocyte and is either stored or transported across the basolateral membrane via FP1. Whether all haem entering the absorptive enterocyte is broken down within it or whether some haem moieties enter the portal circulation intact remains unclear. Two recently characterised haem exporters, the feline leukaemic virus receptor (FLVCR) (Krishnamurthy *et al* 2004) and the ABCG2, formerly known as the breast cancer resistance gene (Bcrp) and ATP-binding cassette placenta (ABCP) (Quigley *et al* 2004) are likely candidates for the export of excess haem and/or of haem breakdown products, however further studies are necessary in order to establish their precise roles in the absorptive enterocyte (reviewed in Latunde-Dada *et al* 2006). Once in the portal circulation, regardless of the mechanism of absorption, iron will follow the common fate of binding onto Tf.

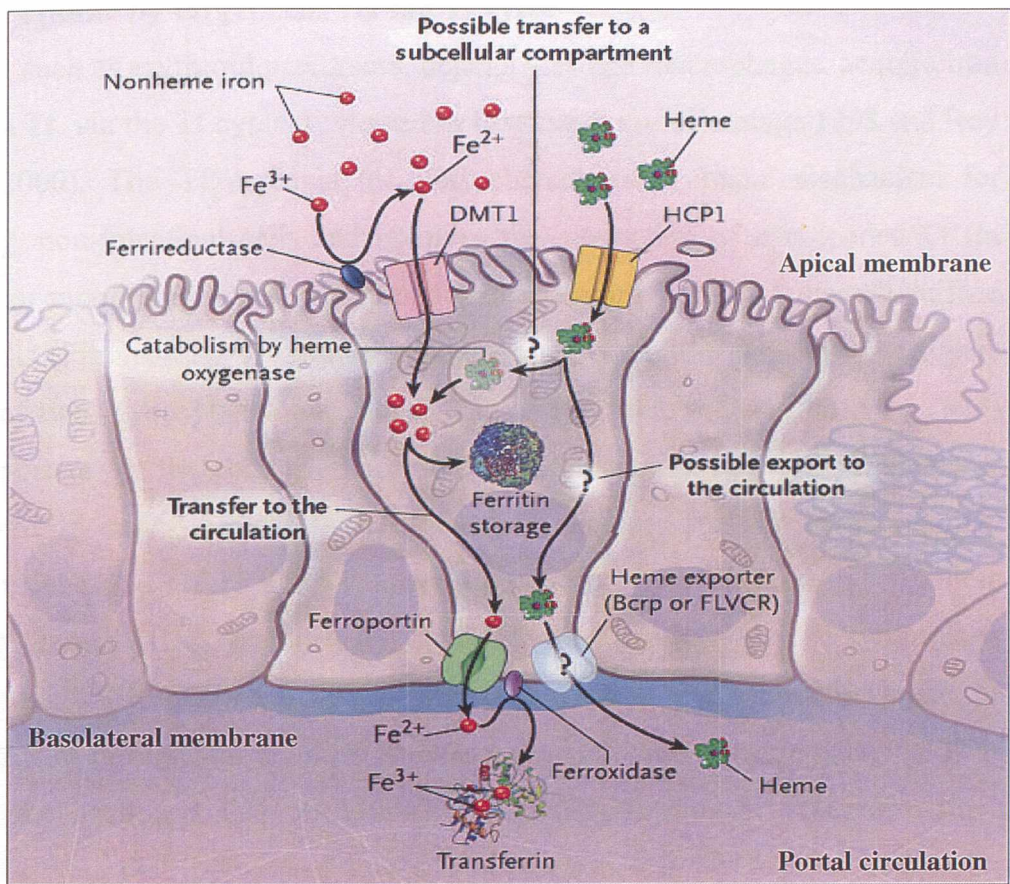


Figure 1.1 Proposed model for the uptake of dietary iron across the apical membrane of the absorptive enterocyte.

(Image adapted from Andrews 2005a)

Dietary iron in the lumen of the gut is present either as inorganic (Fe^{3+}) or haem-iron. Inorganic iron needs to be reduced to the Fe^{2+} form before it can be taken up by the enterocyte. The brush border ferric reductase Dcytb facilitates that conversion and the soluble ferrous iron is then transported across the apical membrane via DMT1. Uptake of haem iron within a haem moiety involves HCP1 on the apical membrane and catabolism of the haem moiety by HO1 once in the cytoplasm. The released iron from haem joins the inorganic iron that has been taken up via DMT1, forming a labile iron pool and is either stored as ferritin or exported across the basolateral membrane, into the plasma circulation via FP1. Iron is then reoxidised to the Fe^{3+} form via the action of Hp and enters the circulation loaded onto Tf, which will then find its way and deliver iron where it is required.

1.2.1.3 Iron uptake by target cells via the Tf cycle

Target cells, such as erythroid precursors, hepatocytes and macrophages, acquire iron from plasma Tf, via the Tf cycle (reviewed in Eisenstein and Blemings 1998 and Roy and Enns 2000). The Tf cycle is the best characterised uptake mechanism for proliferating, non-intestinal cells and involves the interaction of iron-loaded Tf (in the diferric or monoferric form) with transferrin receptors (TfRs) on the cell surface of target cells (Figure 1.2). TfRs are transmembrane, disulphide linked homodimers consisting of two glycosylated subunits of 760 amino acids (aa) (Kuhn *et al* 1984) and are important for the controlled access of Tf to the cells. All cell types, except mature erythroid cells, express a well described receptor for human Tf, namely transferrin receptor 1 (TfR1). TfR1 is a homodimeric type II membrane glycoprotein of 190 kilo Dalton (kDa), encoded by the *TfRC* gene on 3q29 whose synthesis is post-transcriptionally controlled in response to cellular iron levels such that when the demand for iron is high, the pool of receptors available to bind iron carrying Tf is increased (see section 1.3.1). A 190 kDa homologous dimeric receptor with a distinctly different distribution and levels of expression, namely transferrin receptor 2 (TfR2), has also been identified. The *TfR2* gene maps to 7q22 and gives rise to at least two alternatively spliced transcripts, α (TfR2- α) and β (TfR2- β). The TfR2- α extracellular domain is 45% identical and 66% similar to the TfR1 ectodomain. However, the N-terminal cytoplasmic regions of TfR1 and TfR2- α show no similarity. The TfR2- β transcript lacks exons 1–3 of TfR2, thus it does not contain a transmembrane or cytoplasmic domain. TfR1 and TfR2 are able to form heterodimers, but preferentially form homodimers. TfR2- α can also mediate cellular uptake of Tf-bound iron and is predominantly expressed in the liver (and in the hepatoma cell line HepG2), normal erythroid precursor cells, and to a less extent in spleen, lung, muscle, prostate, and peripheral blood mononuclear cells (Kawabata *et al* 1999, 2000).

Depending on the target cell and its iron requirements, the number of TfRs expressed on their cell surface will vary to accommodate those needs. TfR1 is known to be expressed with greater abundance in cells with high iron demands, such as developing erythroid precursors (for Hb production), placental syncytiotrophoblasts (for iron transfer) and tumour cells (for cell proliferation) (reviewed in Andrews

will have a higher affinity for diferric-Tf than mono-Tf and a much lower affinity for apo-Tf (Young *et al* 1984, reviewed in Aisen 2004). The Tf cycle initiates with the internalisation of the Fe³⁺-Tf/TfR complex into a clathrin-coated pit, with the aid of an adaptor protein complex (AP2), and its subsequent maturation into an endosome. The endosome undergoes acidification, resulting in a lowered pH (5.6) of the endosomal compartment, followed by the release of iron and its reduction to the ferrous form, possibly via the action of a putative endosomal ferric reductase, Steap3, (Ohgami *et al* 2005) and the transport of iron across the endosomal membrane via DMT1 (Fleming *et al* 1998, Gruenheid *et al* 1999). Iron then enters the LIP of the target cell and becomes available for intracellular usage or storage in ferritin, which is found in all cell types, and haemosiderin, found mostly in macrophages in the bone marrow, liver and spleen. The vesicle with the iron depleted Tf/TfR complex returns to the cell surface where the neutral pH of the blood will cause the receptor to release the empty Tf back to the circulation in search of more iron. The half-life ($t_{1/2}$) of apo-Tf is 7.6 days, while that of iron carrying Tf is 1.7 hours and it is estimated that Tf undergoes more than a hundred cycles before it is removed from the circulation (Crichton and Boelaert 2001).

The importance for the existence of two TfRs in the uptake of Tf-bound iron is unclear and a tissue specific function for TfR2 has been suggested. TfR2 senses diferric-Tf rather than mono-Tf (Johnson and Enns 2004) and has a 30-fold lower affinity for Tf compared with TfR1 (Kawabata *et al* 2000). Tf taken via TfR2 is not recycled as apo-Tf back to the cell surface after release of iron, but is instead intracellularly deposited and does not appear to be degraded (Robb *et al* 2004). Studies suggest that murine TfR2 is not able to compensate for the functional absence of TfR1, since *Tfr1* knockout (KO) mice are embryonic lethal (Levy *et al* 1999). However, mutagenesis of the murine *Tfr2* gene (Fleming *et al* 2002) and disabling mutations in *Tfr2* result in haemochromatosis (see section 1.4.1.2), observations that signify the importance of TfR2 in iron homeostasis. Finally, more recent observations of hepatic TfR2 protein levels correlating with changes in Tf saturation (Robb and Wessling-Resnick 2004), have brought TfR2 into the limelight as a sensor for iron status.

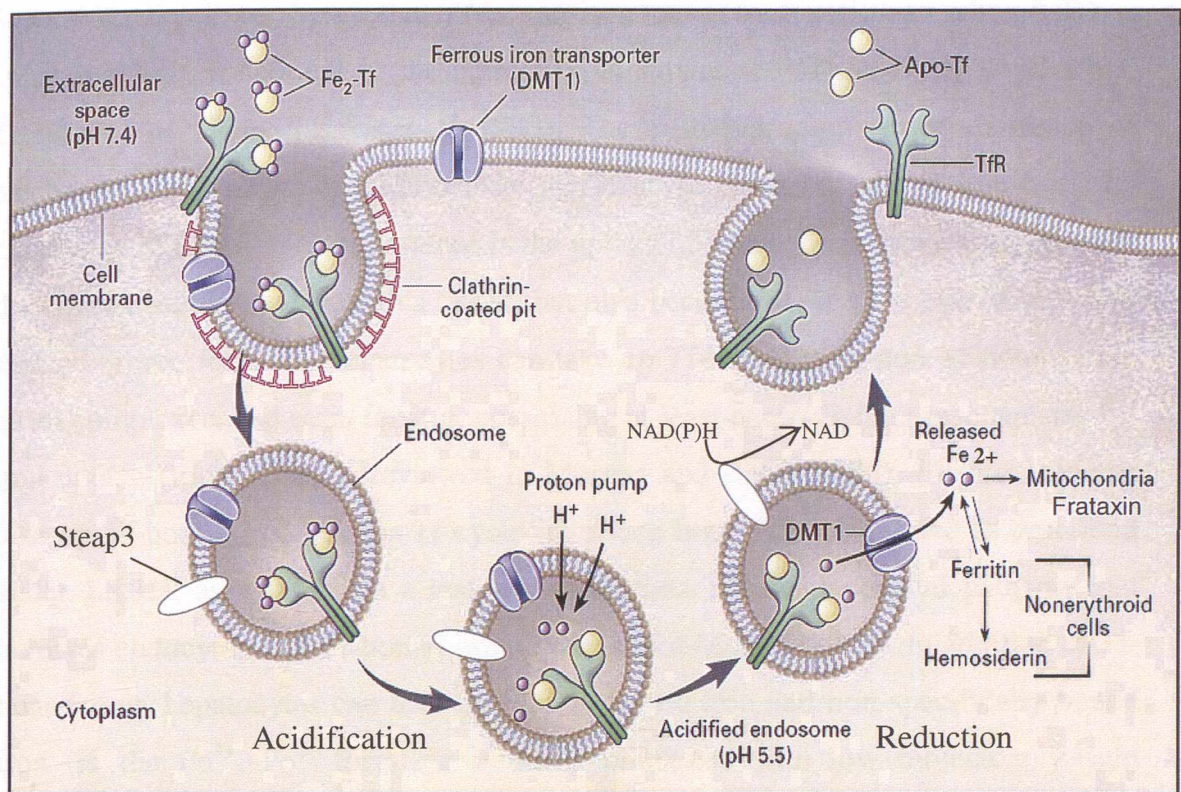


Figure 1.2 Uptake of iron into cells via the Tf cycle.

(Image adapted from Andrews 1999)

Diferric-Tf binds TfR1 on the cell surface and the complex is internalised in the form of an endosome. A proton pump acidifies the environment within the endosome and aids in the release of the iron atoms from the Tf/TfR1 complex. The released iron exits the endosome via means of DMT1 and is then stored in ferritin and haemosiderin or in mitochondrial frataxin. The iron free Tf/TfR1 complex is regurgitated to the cell surface where at neutral pH it dissociates and both Tf and TfR1 become available for more Tf cycles.

1.2.1.4 Additional and/or alternative mechanisms of iron uptake by target cells

Several studies have shown that Tf-bound iron can enter a cell even when TfR1 is either not fully functional or its expression is suppressed (Thorstensen *et al* 1995, Trinder *et al* 1996, Sasaki *et al* 1993). These studies support the existence of mechanisms alternative or additional to the Tf cycle for the uptake of iron from the circulation. Of particular importance is the uptake of iron by hepatocytes not only for the typical cellular needs of this tissue, but also because the liver is one of the main storage organs for iron. Hepatocytes can take up Tf-bound iron, non-Tf-bound iron, haem complexes, and even ferritin, possessing at least seven distinct mechanisms for iron uptake (Figure 1.3A) (reviewed in Morgan and Baker 1986). Hepatocytes can take up Tf-bound iron via the Tf cycle involving both TfR1 and TfR2 as described under 1.2.1.3, as well as via a less well described TfR1-independent pathway that involves endocytosis of Tf-bound iron (Trinder and Morgan 2002). In addition to Tf-bound iron, hepatocytes can take up non-Tf bound iron and non-specifically bound iron (in the Fe^{3+} , Fe^{2+} form, or as Fe^{2+} complexed with low molecular weight chelators). Non-Tf-bound iron is taken up via specific low-density lipoprotein receptor-related proteins (LPR1, also called CD91) in the form of Hb bound to haptoglobin (Htb) and haem bound to haemopexin (Hx) (Muller-Eberhard *et al* 1975, reviewed in Latunde-Dada *et al* 2006), while non-specifically bound iron is taken up via DMT1 (in the same way that intestinal cells take up ferrous iron), but also via the stimulator of Fe transport (SFT), another iron transport protein that is highly expressed in hepatocytes (Crichton and Boelaert 2001). In addition, hepatocytes are also in charge of clearing any ferritin molecules introduced into the plasmatic circulation, which may often be found in the plasma in very low amounts, via means of a ferritin receptor (FR) (Mack *et al* 1983). The process is thought to involve endocytosis of the ferritin/ferritin receptor complex, followed by possible lysosomal degradation of the protein (Unger and Hershko 1974). Finally, current studies on the recently identified haem carrier protein, HCP1, established expression of this molecule in the adult liver, thus opening a further pathway for haem uptake by hepatocytes (McKie 2005).

Reticuloendothelial macrophages are also important target cells as they carry out iron recycling and redistribution. They acquire iron via a pathway unique to these cells that involves the ingestion of senescent red blood cells (RBCs) and their lysis in a

phagolysosomal compartment, where Hb is degraded and iron is liberated from haem by HO1 (Figure 1.3B). Macrophages can also take up Hb-Htb complexes via surface CD163 receptors. The importance of HO1 activity not only in the liberation of iron from haem but also in the release of iron from these cells was exemplified in a study where HO1 deficient (-/-) mice developed anaemia with abnormally low iron plasma. Interestingly, these mice accumulated non haem iron in macrophages, hepatocytes as well as other tissues (reviewed in Ponka 1999).

The existence of additional receptors and uptake mechanisms in various target cells also supports the possibility of extra iron assimilation, in the non Tf-bound form. The exact mechanisms of non Tf-bound iron (NTBI) uptake remain to be explored however are expected to be similar to that of inorganic iron. NTBI in the circulation is present in the Fe^{3+} form and therefore needs to be reduced to the soluble Fe^{2+} form before it can be taken up by a cell. Recent studies by Vargas *et al* (2003) have established the ferric reductase activities of other molecules, including that of mouse cytochrome b561 and mouse and fly stromal cell-derived receptor 2 (SDR2), belonging to the same class of molecules as Dcytb, paving the future for identifying more pathways of iron uptake. Levels of *sdr2* messenger RNA (mRNA) were found to be highly expressed in the liver, but low in the hypotransferranaemic (*hpx*) mouse, therefore it is likely that such ferric reductases might have a role in iron metabolism and possibly in the uptake of NTBI (Vargas *et al* 2003).

Although cellular uptake might occur via several distinct routes, only one pathway of iron exit from macrophages and hepatocytes has been described to date, via FP1. The form of iron exported from target cells via FP1 into the plasma circulation is thought to be in the Fe^{2+} form and a copper containing ferroxidase homologous to Hp that is present abundantly in the plasma, ceruloplasmin (Cp), aids the loading of iron onto Tf, by oxidising it to the Fe^{3+} form. Mutations in Cp cause aceruloplasminaemia, a disorder characterised by iron loading in the central nervous system (Harris *et al* 1995). Data from animal studies on copper-deficient mice that develop microcytic hypochromic anaemia provide a basis for the hypothesis that copper regulates expression of FP1 mRNA and protein such that copper sufficiency is required for normal maintenance of iron export function. The identification of mutations in human FP1, leading to iron overload in reticuloendothelial macrophages, as well as

its recent interaction with hepcidin has revealed the essential role of FP1 in iron homeostasis (see section 1.3.2).

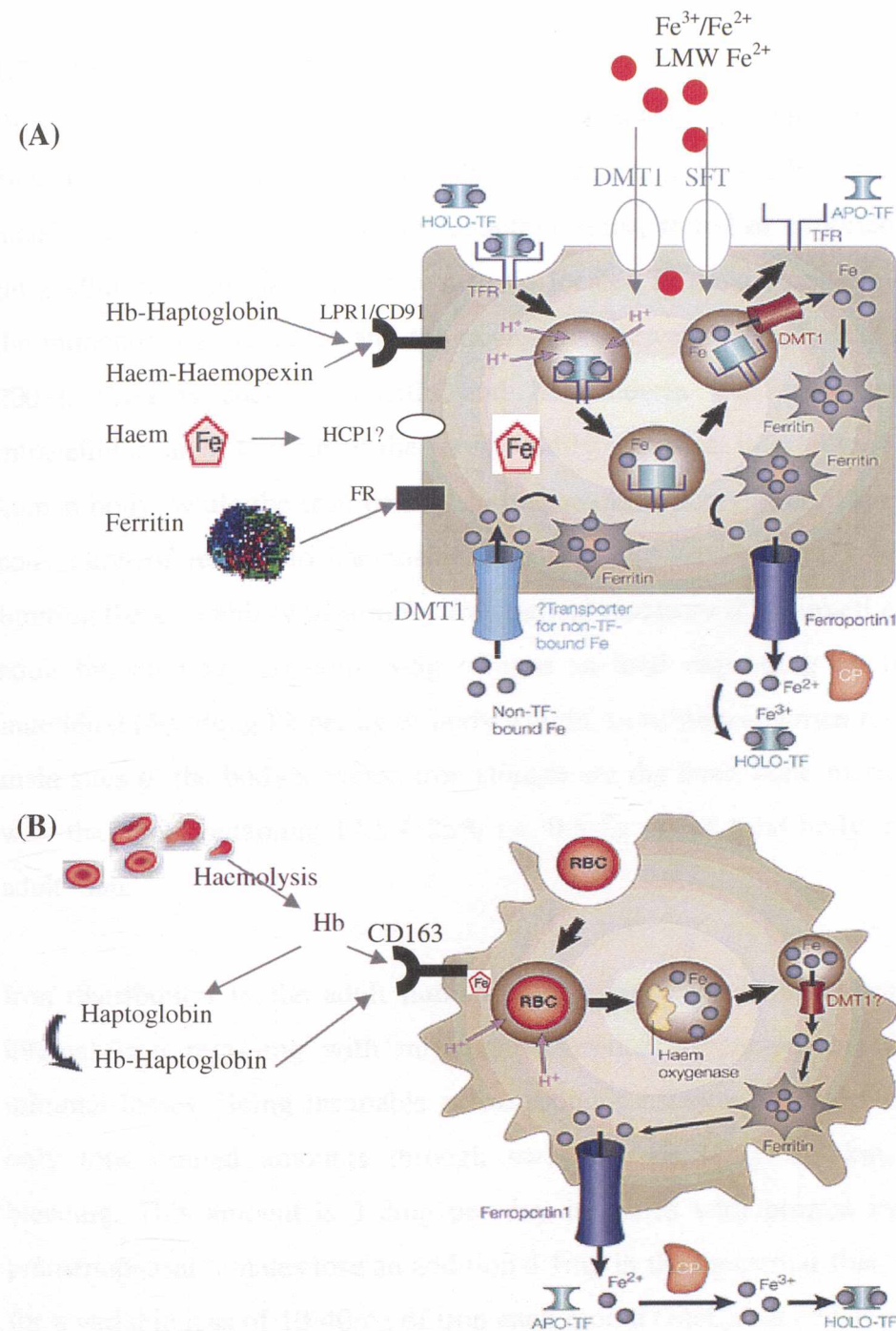


Figure 1.3 Mechanisms of iron uptake by hepatocytes and macrophages.

(Image adapted from Andrews 2000)

(A) Iron uptake by hepatocytes occurs via at least seven distinct pathways: TfR1/TfR2-mediated and TfR-independent endocytosis of Tf-bound iron; haem and haem-complexed receptor uptake via LPR1/CD91; DMT1 and SFT uptake of non-specifically bound iron; endocytosis of ferritin via a FR. (B) Iron uptake by macrophages involves the phagocytosis of RBCs and the subsequent degradation of Hb and liberation of iron from haem via HO1. An additional pathway of haem efflux exists through the uptake of Hb-Htb complexes via CD163 receptors. In both cell types iron efflux occurs via FP1 with the aid of Cp which reduces Fe^{2+} to the Fe^{3+} form that binds plasma Tf.

1.2.2 Distribution and storage of iron

Once in the cytoplasm of a target cell, iron enters the LIP and has several possible fates depending on the cell's iron status and metabolic needs. Iron will either be used metabolically for the synthesis of metalloproteins, stored or exported from the cell. Intracellularly iron has been shown to be located in most compartments, including the mitochondria, vacuoles and the nucleus (reviewed in De Freitas and Meneghini 2001). Proteins such as ferritin and hemosiderin will store iron to specific intracellular sites. Ferritin is the most readily available iron storage protein in the human body, while the iron present in hemosiderin is not easily accessible and thus conversion of ferritin to haemosiderin during iron overload may be protective by limiting the availability of iron for free radical reactions (O'Connell *et al* 1986). The adult human body contains 3-5g of iron in total depending on the size of the individual (40-50mg Fe per kg of body weight, in women and men respectively). The main sites of the body's excess iron storage are the liver, bone marrow, and spleen, with the liver containing 12.5%-25% i.e. 0.5-1g of the total body iron in a normal adult man.

Iron distribution in the adult human body relies on a well orchestrated cycle of internal iron recycling with minimal absorption to compensate for the equally minimal losses. Being incapable of excreting substantial amounts of iron, humans only lose limited amounts through sweating, shedding of skin, urination and bleeding. This amount is 1-2mg per day in males with normal iron stores while premenopausal females lose an additional 1mg in the menstrual flux, which accounts for a variable loss of 10-40mg of iron each month (McCance and Widdowson 1937). In an average Western diet, iron is estimated at no more than 5-7mg Fe per 1000kcal (Groff and Gropper 2000), and depending on the individual a healthy adult will absorb 1-2mg of iron daily, that once in the circulation, will join a pool of Tf-bound iron (3mg) which can be recycled over ten times daily (reviewed in Papanikolaou and Pantopoulos 2005). Up to 97% of iron needs are supplied internally, mainly through the recycling of Hb iron from senescent RBCs. Most iron in the human body is in the erythroid bone marrow (300mg), in macrophages (600mg) with the highest amount in mature erythrocytes (1800mg) (in the haem part of Hb). Iron for new RBCs is supplied by the reticuloendothelial macrophages, especially those of the spleen, but also those of the liver and bone marrow that will recycle iron from old

RBCs at the end of their 120 day life, back to the pool of Tf-bound iron, then to the bone marrow for erythropoiesis, and other tissues, thus completing a cycle of iron recycling. Stored iron is found in the hepatocytes of the liver, in ferritin (1000mg) and in muscle, in the form of myoglobin (300mg) (reviewed in Papanikolaou and Pantopoulos 2005).

1.3 Regulation of iron homeostasis

In pregnancy, iron overload or iron deficiency the distribution of iron is altered to accommodate body needs. Therefore and quoting the classic work of Drs McCance and Widdowson in 1937, “the amount of iron in the body must be regulated by controlled absorption”. Nearly two thirds of a century later, studies suggest that iron homeostasis indeed depends on the coordinated function of numerous genes that ultimately control iron absorption from the intestine. Humans maintain a constant body iron concentration of 60 parts per million (ppm) throughout life by balancing the uptake of iron during growing years with an equilibrium between absorption and loss in adult life (reviewed in Conrad *et al* 1999). In the absence of a mechanism for iron excretion, humans are equipped with specific mechanisms to maintain iron homeostasis which can be achieved at two levels of control, regulation at the cellular level and at the level of intestinal absorption.

1.3.1 The iron responsive element/iron regulatory protein system

The best characterised regulatory mechanism for the maintenance of iron homeostasis within a single cell is the iron responsive element/iron regulatory protein (IRE/IRP) system. The IRE/IRP system responds to changes in cellular iron status and through the interaction of iron regulatory proteins (IRPs) [formerly referred to as IRE-binding proteins (IRE-BPs), iron regulatory factors (IRFs), or ferritin repressor proteins (FRPs)] with iron responsive elements (IREs) present on mRNAs encoding iron-related molecules, regulates the amount of iron taken up and/or stored by an individual cell, according to its needs. IRPs are *trans*-acting RNA-binding proteins that interact with key mRNAs containing the 30-nucleotide long IREs. IREs are phylogenetically conserved, *cis*-acting, stem-loop structures, characterised by a six nucleotide, single stranded loop (5'CAGUGN) on a 9-10 base paired stem with an unpaired cytosine residue in a bulge (Casey *et al* 1988, Addess *et al* 1997). All IREs share the same structural features sufficient for IRP recognition and are present in the

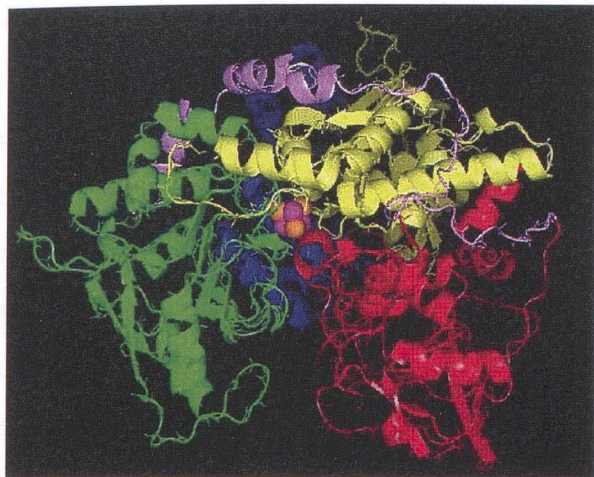
untranslated regions (UTRs) of mRNAs that code for proteins involved in iron uptake (3'UTR of TfR1 mRNA, 3'UTR of DMT1), storage (5'UTR of ferritin mRNA, both heavy and light chains), export (5'UTR of FP1 mRNA), utilisation (5'UTR of erythroid 5-aminolevulinic-synthase mRNA) as well as iron transduction signalling pathways (5'UTR of hexokinase III, 5'UTR of acid phosphatase) (Aziz and Munro 1987, Fleming *et al* 1999, reviewed in Melefors and Hentze 1993, and Harford 1994, and Hentze and Kuhn 1996, and Lieu *et al* 2001). IRE motifs have also been identified in transcripts not related to iron homeostasis as in the two mRNAs coding for enzymes of the Krebs cycle, namely the mitochondrial aconitase and the succinate dehydrogenase subunit β of *Drosophila melanogaster* (Kohler *et al* 1995). Lieu *et al* (2001) reports that bioinformatic searches using several public and private sequence databases revealed 70 novel genes in the human genome that contained at least one IRE in their 5' or 3'UTR.

Two IRPs have been characterised to date, namely IRP1 and IRP2, both capable of IRE binding, though at distinct binding sites, that are also conserved across species at 90% sequence identity (Henderson *et al* 1993, Samaniego *et al* 1994, Guo *et al* 1994, Guo *et al* 1995, Butt *et al* 1996). Encoded by the *IRP1* gene on 9q13-22, IRP1 (98kDa) is identical in sequence to cytosolic aconitase that catalyses the conversion of citrate to isocitrate via the intermediate *cis*-aconitate in the Krebs cycle (Rouault *et al* 1991, Hentze and Argos 1991). Earlier models of IRP1 based on the crystal structure of the homologous mitochondrial aconitase indicate that it is a 4 domain protein, with domain 4 linked by a hinge region to the other 3 domains, and a cleft forming between domains 1-3 and domain 4 (Figures 1.4A and 1.4B). These earlier predicted models have now been confirmed with the recent crystallisation of human IRP1 in its aconitase form (Dupuy *et al* 2005, 2006) and of IRP1 in complex with the ferritin IRE (Selezneva *et al* 2006) further supporting the importance of the cleft region in IRP1's mutually exclusive functions (Figure 1.4C). High cellular iron levels promote the formation of the iron sulphur cluster (4Fe-4S), which can occupy the cleft and determine the function of the protein, which acts either as an active cytosolic aconitase (holoprotein) or as an RNA binding protein (apoprotein) when the protein lacks this cluster (Constable *et al* 1992, Haile *et al* 1992) (Figure 1.5A). In the former scenario, binding of 4Fe-4S limits IRE access but allows the binding of

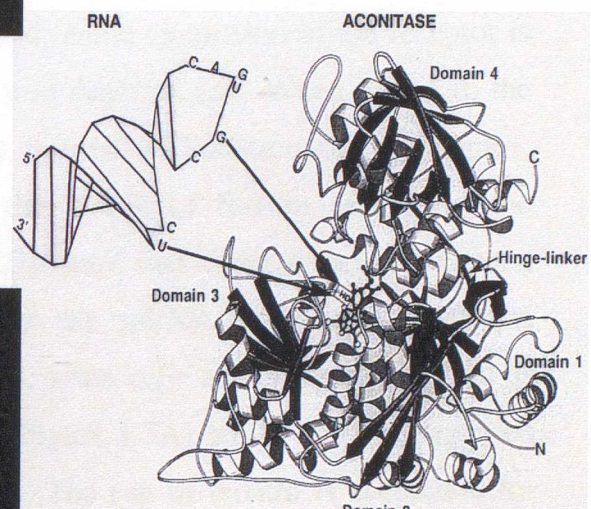
citrate, while in the latter case low levels of iron promote the disassembly of 4Fe-4S and the cleft widens enough to accommodate an RNA molecule, which is critical for the IRE/IRP interaction. In addition to iron levels, nitric oxide proved to be the first factor able to regulate the RNA binding activity of IRP1 to IREs (Drapier *et al* 1993) and soon thereafter further effectors of that interaction such as phosphorylation (Eisenstein *et al* 1993) and oxidative stress (Pantopoulos and Hentze 1995) emerged.

Human IRP2 (105kDa) shares 61% sequence identity and 79% aa sequence similarity to human IRP1 (Samaniego *et al* 1994). IRP2 is always active to bind IREs and unlike IRP1 appears neither to be enzymatically active nor post-translationally reversibly convertible between active and inactive RNA binding forms. IRP2 is regulated via *de novo* synthesis and proteasome-mediated degradation (Guo *et al* 1995, Iwai *et al* 1995) and although both IRPs have been found to be regulated by protein degradation in the presence of iron or haem (Guo *et al* 1995, Goessling *et al* 1998, Clarke *et al* 2006), this mechanism is more pronounced for IRP2. IRP2 (gene location 15) (962 aa) contains a 73 aa region encoded by a single exon not present in IRP1 (889 aa) that targets IRP2 for iron dependent degradation. The unique “iron dependent degradation domain” in IRP2 can bind free iron resulting in a localised oxidation site that forms or acts as the recognition signal for ubiquitination and the subsequent degradation of the protein (Iwai *et al* 1998). The oxidation of IRP2 has been proposed to be induced by haem, in iron-rich cells, as well as oxygen (Yamanaka *et al* 2003, Bourdon *et al* 2003), however other studies have suggested that the unique degradation domain is dispensable for both iron and oxygen mediated degradation (Hanson *et al* 2003), while additional stimuli may be involved in creating recognition signals within and outside the boundaries of this degradation domain (Wang *et al* 2004).

(A)



(B)



(C)

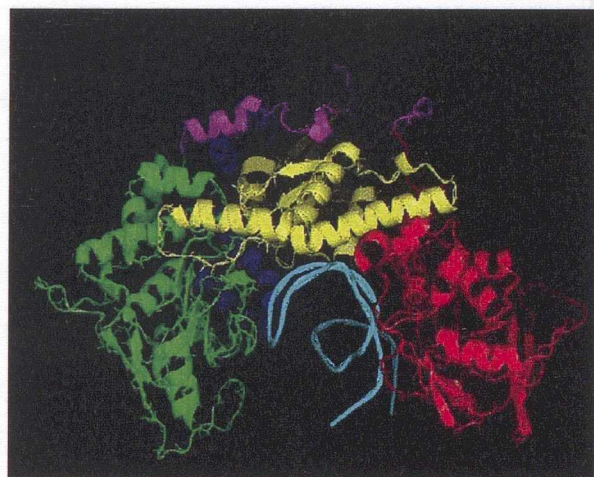


Figure 1.4 Structure of human IRP1.

(Image taken from http://www-dsv.cea.fr/art/images/Pascal/BMC_050.jpg and Basilion *et al* 1994)

(A) Ribbon diagram of the crystal structure of human cytosolic aconitase. Each of the four domains is represented in a different colour; the hinge linker domain is shown in mauve and the 4Fe-4S in the centre of the molecule in purple/orange balls. (B) Sketch of earlier postulated model of IRP1 based on the structure of mitochondrial aconitase showing the predicted region for IRE-binding between domains 1-3 and 4. (C) Ribbon diagram of the structure of human IRP1 based on the crystal structure of the cytosolic aconitase and using the same colour code as in A. The mauve hinge linker region joins domains 3 and 4. The cleft between the protein domains is thought to widen enough to accommodate an RNA molecule, represented in cyan.

Expression of many eukaryotic genes is regulated at the level of translation and can be mediated by altering the rate of transcription or by controlling the half-life of the transcript. Most eukaryotic mRNAs are stable ($t_{1/2}$ of 12hrs) unless a destabilising element is present that renders it unstable ($t_{1/2}$ of 15-60min). One well described paradigm of post-transcriptional control via the IRE/IRP system is the interaction between IRPs and the IREs on the mRNAs of ferritin and TfR1 (Figure 1.5). When levels of intracellular iron are low, disassembly of 4Fe-4S is promoted and both IRPs bind the IREs on the 5'UTR of ferritin and the 3'UTR of TfR1 (Haile *et al* 1992). Translation of the storage molecule is repressed, while expression of the receptor is maintained, so that more iron can enter the iron depleted cell. When bound to the ferritin IREs, IRPs block the binding of the translation initiation factor complex, eukaryotic initiation factor-4F (eIF4F), to the 5' cap of ferritin and hence the subsequent recruitment of the 40s ribosomal subunit and other associated factors, that make up the 43s initiation complex, to the mRNA to initiate translation (Muckenthaler *et al* 1998). On the other hand, when cells are iron replete, IRP1 is converted to the 4Fe-4S cluster holoprotein (Figure 1.5A) while IRP2 is degraded and hence both IRPs are unable to bind IREs. The cap of ferritin is accessible for binding by eIF4F and initiation of translation can proceed allowing storage of the excess iron in the iron replete cell (Figure 1.5B).

TfR1 mRNA, in addition to the five IREs in its 3'UTR, contains a 400 nucleotide long, destabilising element with a site for the endonucleolytic cleavage of the mRNA (Casey *et al* 1989, Erlitzki *et al* 2002). Binding of IRPs to the IREs on the 3'UTR of TfR1 mRNA, under low iron conditions, protects the mRNA from degradation by covering exposure of the destabilising element rendering it inaccessible for cleavage by endonucleases, thus increasing mRNA stability and hence promoting translation of the transcript whose 5' cap is available for binding by the eIF4F (Figure 1.5B) (reviewed in Hentze and Kuhn 1996 and Klausner *et al* 1993). Under high iron conditions on the other hand, IRPs are unable to bind IREs on the TfR1 mRNA and the destabilising element on TfR1 remains exposed, and hence accessible for endonucleolytic cleavage. TfR1 mRNA is then degraded which serves to protect further entry of iron into the already replete cell via this receptor (Figure 1.5B) (Binder *et al* 1994).

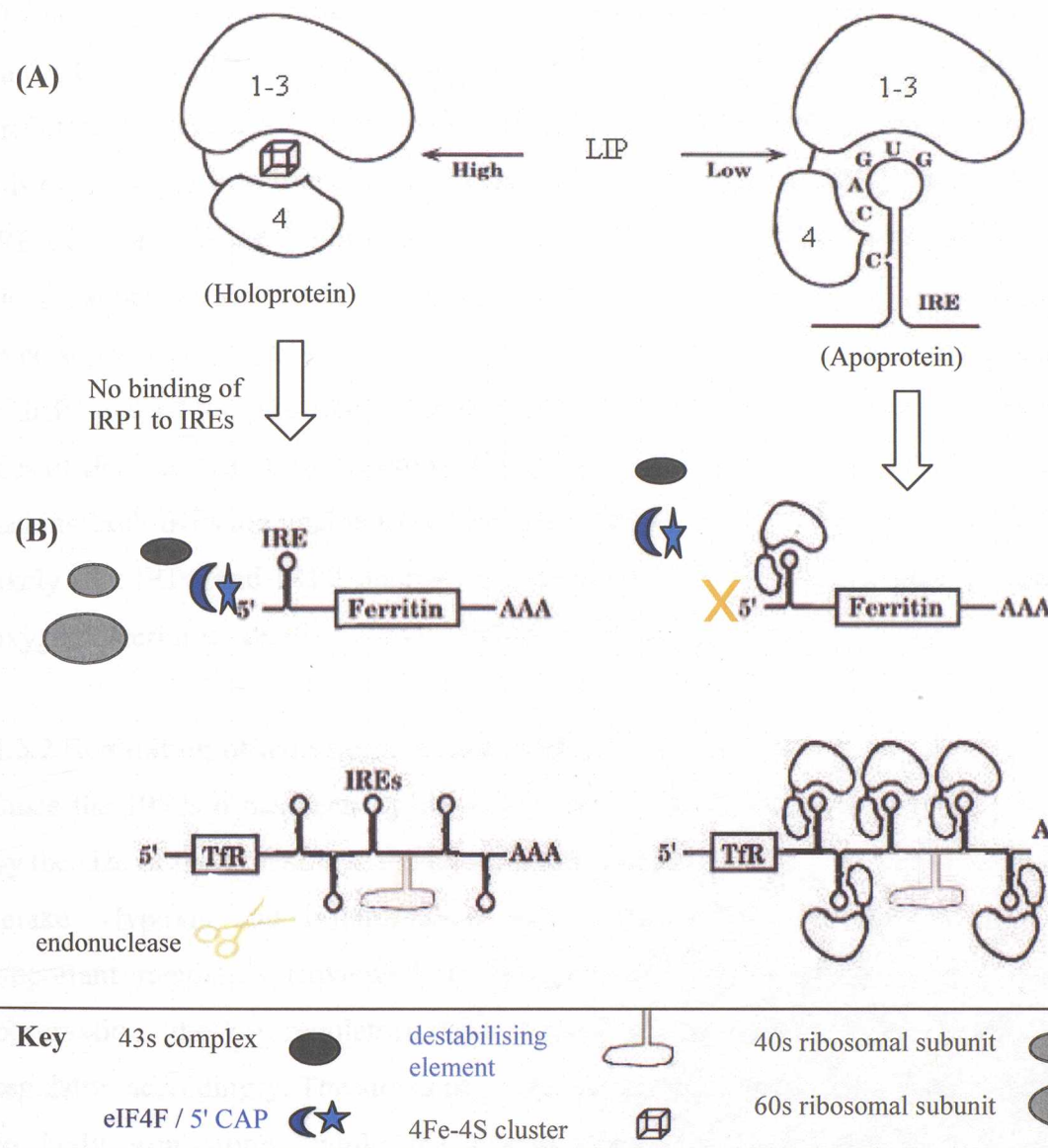


Figure 1.5 The co-ordinated post-transcriptional regulation of TfR1 and ferritin mRNAs via the IRE/IRP system.

(Diagram adapted from Lobmayr *et al* 2005)

(A) When the LIP of the cell is replete, formation of 4Fe-4S clusters is promoted, which then occupy the cleft on IRP1 (holoprotein) rendering it incapable of IRE binding. Depletion of the LIP allows the cleft on IRP1 (apoprotein) to remain accessible for IRE binding.

(B) When levels of iron are high, IRP1 cannot bind the IREs on the ferritin and TfR1 mRNAs, allowing therefore the expression of ferritin and the rapid degradation of TfR1. In contrast, when levels of iron are low, IRP1 binds the IREs on the 5'UTR of ferritin and blocks translation of the molecule, while binding of the apoprotein to the 3'UTR of TfR1 mRNA protects the transcript from nuclease digestion. The reciprocal regulation of these two transcripts enhances iron efflux into the cell while hindering its storage when the metal is scarce, whereas storage is enhanced and efflux is hindered when iron is in excess.

The necessity for the presence of two IRPs is not clearly understood, though based on the fact that IRP1 is more abundant than IRP2, IRP1 would be expected to be the predominant regulator (reviewed in Hentze and Kuhn 1996). The finding of a misregulation of iron homeostasis in *Ireb2*^{-/-} mice, lacking the mouse gene encoding IRP2, exemplifies the importance of IRP2 in iron homeostasis and suggests that IRP1 alone cannot regulate iron metabolism appropriately (LaVaute *et al* 2001). *Irpl*^{-/-} mice show only compromised normal iron metabolism in tissues in which the levels of IRP1 exceed those of IRP2, suggesting that unlike IRP1, IRP2 can compensate for loss of IRP1 activity by increasing IRP2 levels (Meyron-Holtz *et al* 2004a). Animals lacking both IRPs are unable to survive through gestation (Smith *et al* 2006) and it is likely that IRP1 and IRP2 operate in a continuum in which the partial pressure of oxygen determines relative activity (Meyron-Holtz *et al* 2004b).

1.3.2 Regulation of iron homeostasis at the level of intestinal absorption

Since the 1950s it has been hypothesised that intestinal iron absorption is regulated by the size of the iron stores, the rate of erythropoiesis and the amount of dietary iron intake. Hypoxia and inflammation have subsequently also been identified as important regulators (reviewed in Hentze *et al* 2004). Based on physiological observations the key regulators were termed the stores, erythropoietic and dietary regulator, accordingly. The stores regulator adjusts non-haem iron uptake in response to body iron stores, while the erythropoietic regulator balances the rate of erythropoiesis in the bone marrow with intestinal iron absorption, independent of iron stores. Both the stores and erythropoietic regulators were hypothesised to be soluble components of the plasma, as they must signal between the haematopoietic bone marrow and the intestine (reviewed in Roy and Enns 2000). Finally, the dietary regulator influences iron absorption based on recent dietary iron intake, with ingestion of a dietary iron bolus rendering enterocytes resistant to absorbing additional iron for several days, a phenomenon referred to as mucosal block (Stewart *et al* 1950). Changes in iron absorption do not occur until 2-3 days following an iron absorption stimulus and this time lag is identical to the time needed by duodenal crypt cells to migrate to the tip of the villus and mature into iron-absorbing enterocytes (Lombard *et al* 1997), an observation that led to the crypt-programming model and received wide support for decades.

Observations of a rapid response of hours rather than days in the rate of absorption following a change in the iron status, however cast doubt on the plausibility of the crypt hypothesis and the recent discovery of hepcidin as a major, evolutionarily conserved denominator of iron distribution unveiled a complex regulatory network that governs iron traffic rather than deposition (reviewed in Deicher and Hörl 2006). Hepcidin, a circulating antimicrobial peptide, is now proposed as the/or an important factor of the stores and/or erythropoietic regulator(s). This hypothesis brought a shift to the focus from the intestinal enterocytes to the liver, the site of hepcidin synthesis. Hepcidin was first isolated from urine by Krausse *et al* (2000) as a cDNA encoding hepcidin antimicrobial peptide which the authors called liver-expressed antimicrobial peptide 1 (LEAP1). Park *et al* (2001) also cloned hepcidin, and named it hepcidin from its liver origin (hep-) and antibacterial properties *in vitro* (-cidin). The hepcidin gene (*HAMP*) on 19q13.1 contains 3 exons encoding a propeptide of 84 aa that undergoes enzymatic cleavage into mature peptides of 20, 22, and 25 aa (Krause *et al* 2000, Park *et al* 2001, Pigeon *et al* 2001).

Several studies have suggested that hepcidin communicates the body signals of iron requirements to intestinal enterocytes. The first clue of this crucial involvement of hepcidin in iron homeostasis came from a study by Pigeon *et al* (2001), who observed hepcidin mRNA levels to increase in mice with secondary iron overload, while levels decreased in iron depletion. Further studies in mice lacking the upstream stimulatory factor 2 (*Usf2*^{-/-}) of hepcidin showed that these mice, which lacked hepcidin expression, developed hepatic iron overload associated with decreased iron in tissue macrophages (Nicolas *et al* 2001), while mice over-expressing hepcidin died shortly after birth from severe iron-deficiency anaemia (Nicolas *et al* 2002a). Consistent with these findings, injection of hepcidin peptide into mice induces a rapid drop in serum iron levels (Rivera *et al* 2005). Hepcidin expression is induced when iron stores are replete and during inflammation (Nemeth *et al* 2003), but is suppressed when iron stores are depleted and during erythropoiesis (Nicolas *et al* 2002b), thus fulfilling the role of both the erythropoietic and stores regulators.

It is now thought that hepcidin controls iron absorption by decreasing membrane levels of FP1. Nemeth *et al* (2004) found that the direct binding of human hepcidin to mouse ferroportin-green fluorescent protein (GFP) promoted internalisation and

lysosomal degradation of the iron exporter, while others have shown that synthetic human hepcidin inhibited iron export and decreased levels of transfected murine FP1 in J744 macrophages (Knutson *et al* 2005). The role of hepcidin therefore appears to be to block iron absorption by decreasing FP1 expression. Taken together these findings suggest that hepcidin is a negative regulator of intestinal iron absorption and an inhibitor of iron release from macrophages. The molecular mechanisms regulating *HAMP* gene expression in response to iron however is unknown. Sequence analysis of the 5' flanking region of the human and mouse *HAMP* gene has revealed the presence of several binding sites for liver enriched transcription factors such as the CCAAT/enhancer binding protein (C/EBPa) and the hepatocyte nuclear factor 4 (HNF4) (Ilyin *et al* 2003). Hepatic C/EBPa KO mice exhibit a pronounced decrease in *HAMP* gene expression, which is accompanied by iron accumulation in periportal hepatocytes. Iron overload results in an increase in both C/EBP protein and hepcidin transcripts. Interleukin-6 (IL-6) and the tumour necrosis factor alpha (TNFa) have also been shown to stimulate hepcidin expression in hepatocytes (Nemeth *et al* 2003), which establishes a link between cytokine production and hepcidin expression.

1.4 Hereditary iron overload

Iron related disorders in humans include defects in iron absorption, iron transport and secondary disorders induced by altered iron content in cells and tissues. Discussion of all is beyond the scope of this thesis, but to exemplify the importance of this metal, there are over 30 iron-related disorders that fall under one of the above mentioned categories. In the primary iron overload disorder, hereditary haemochromatosis (HH), a term that is derived from the Greek words αἷμα (haema) for blood and χρώματος (chromatos) for colour, iron absorption from the mucosa is inappropriately stimulated despite massive iron overload (Powell *et al* 1970). According to the Online Mendelian Inheritance in Man (OMIM) (<http://www.ncbi.nlm.nih.gov/omim>), there are currently four types of HH, classified according to the causative gene, with type 1 or *HFE*-related HH being the most common and the other forms of HH defined by numbers with an order that reflects their chronological recognition (Table 1.2).

1.4.1 Types of hereditary haemochromatosis

1.4.1.1 Type 1 or *HFE*-related hereditary haemochromatosis

Hereditary (primary or idiopathic) haemochromatosis (type 1 HH) (OMIM 235200) is an autosomal recessive disorder of excessive dietary iron absorption leading to the progressive deposition of iron and resultant dysfunction in several organ systems during the fourth or fifth decade of life. Type 1 HH affects 1 in 200-400 Caucasians of Western and Northern European descent, presenting a gene frequency as high as 1:9 or 11% of people with this ancestry (Edwards *et al* 1988, Merryweather-Clarke *et al* 1997). The genetic defect for HH is thought to have arisen in a Celtic population in the early middle ages, providing an advantage to people living under conditions in which iron deficiency was common (back when life expectancy was 40 years old). The disease has been recognised from as early as 1865, when Troussseau described the first haemochromatosis patient, and later in 1889, Von Recklinghausen introduced the term “haemochromatosis” to denote iron storage disease associated with widespread tissue injury. In 1935 Sheldon was the first to conclude that haemochromatosis is an inherited metabolic disorder that leads to increased iron accumulation (reviewed in Cuthbert 1997), however the inheritability of HH remained controversial for four decades until Simon *et al* (1977) found an association between haemochromatosis and the human leukocyte antigens (HLA) *HLA-A3* and *HLA-B14* on chromosome 6.

It took a further twenty years for the candidate gene to be discovered by Feder *et al* (1996) who identified a novel major histocompatibility (MHC) class I-like gene that was involved in iron homeostasis and was initially called *HLA-H*, H for haemochromatosis. This gene was subsequently designated *HFE* (Bodmer *et al* 1997) and mapped to 6p21.3, spanning approximately 10 kilobases (kb) and being 4.6 megabases telomeric from *HLA-A* (Rhodes and Trowsdale 1999). The genomic structure of the *HFE* gene is homologous to MHC class I molecules and each of the first six exons encodes a distinct domain of the 343-aa glycoprotein (reviewed in Britton *et al* 2002). Northern blot analysis showed the major transcript of the *HFE* gene to be about 4.2kb in size, though minor transcripts have been detected, probably due to alternative splicing of exon 7 (Thénié *et al* 2000). *HFE* is expressed on the cell surface as a heterodimer with β_2 -microglobulin (β_2m) (Feder *et al* 1996) and is

predicted to have three extracellular domains (α_1 , α_2 and α_3), with the latter having the binding site for β_2m , a transmembrane helix and a short intracellular domain (Figure 1.6). HFE has been localised to various cell types, including placental syncytiotrophoblasts (Parkkila *et al* 1997), Kupffer cells and endothelium of the liver (Bastin *et al* 1998), crypt enterocytes of the human duodenum (Waheed *et al* 1999), epithelial cells of the gastromucosa and on the cell surface of macrophages and monocytes (Parkkila *et al* 2000).

The *HFE* gene has been shown to be mutated in the majority of patients with type I HH, with the most common mutation (referred to as the major mutation) identified as a G-to-A transition at nucleotide 845 (G845A), resulting in a cysteine to tyrosine substitution at aa 282 (Cys282→Tyr, C282Y), disrupting a critical disulphide bridge in the α_3 loop of the HFE protein (Figure 1.6) (Feder *et al* 1996). A minor mutation, causing a C-to-G transversion at nucleotide position 187 (C187G) resulting in a change of histidine to aspartate (His63→Asp, H63D) (Figure 1.6), has also been described (Feder *et al* 1996), as well as further mutations in the *HFE* gene (another 9 missense mutations) that however, present isolated cases (Pointon *et al* 2000). Inheritance of the minor mutation does not contribute to HH unless inherited with the C282Y mutation, producing a compound heterozygous genotype (C282Y/H63D or CY). C282Y/H63D compound heterozygotes develop a milder form of iron overload, while homozygotes for the C282Y mutation develop severe iron overload. C282Y heterozygotes on the other hand, even though present with increased levels of circulating saturated Tf rarely have organ damage (Gottschalk *et al* 2000).

The association between HH and homozygosity for the major mutation is dependent on the population (reviewed in Lyon and Frank 2001). Up to 96.3% of English HH patients are homozygous for the major mutation (genotype C282Y/C282Y). The overall frequency of the major mutation in Europe is 84.5%, with the highest frequencies in Ireland, Scotland, and Wales and the lowest in southern Italy and Greece (reviewed in Camaschella *et al* 2002). In Australian HH patients of European descent, the percentage of homozygosity is 100% (Jazwinska *et al* 1996), whereas in Italian HH patients of European descent, the percentage of homozygosity is only 64.5% (Carella *et al* 1997). The major HH mutation appears not to be present or have

low frequencies in non-Caucasian populations, although emigration from Europe has introduced the mutation to America, Australia, New Zealand and South Africa (Merryweather-Clarke *et al* 2000).

It is important here to note that the presence of the HFE genotype does not always equate to clinical disease, but rather susceptibility to the development of the phenotype. In a study of white adults of northern European ancestry by Olynyk *et al* (1999), only half of the identified homozygotes for the C282Y mutation (0.5% of the population) presented with clinical features of HH. While another study conducted in the U.S.A., estimates that less than 1% of homozygotes develop the full clinical phenotype (Beutler *et al* 2002). Expression of the genotype may be influenced by gene penetrance and several environmental factors. Possible positive modifiers of the disease phenotype include pregnancy and menstruation in females, and regular blood donation in both males and females. Detrimental factors include alcohol abuse, excessive iron intake or other factors that increase iron stores (such as vitamin C).

Therapeutic options for HH

The mainstay of therapy for hemochromatosis is phlebotomy, which is aimed at removing excess iron from the body. It is important to remove all excess iron, as it can cause damage to organs such as the liver, heart, and pancreas, and result in cirrhosis. The protein of HFE and HFE-like genes is involved in the regulation of iron homeostasis.

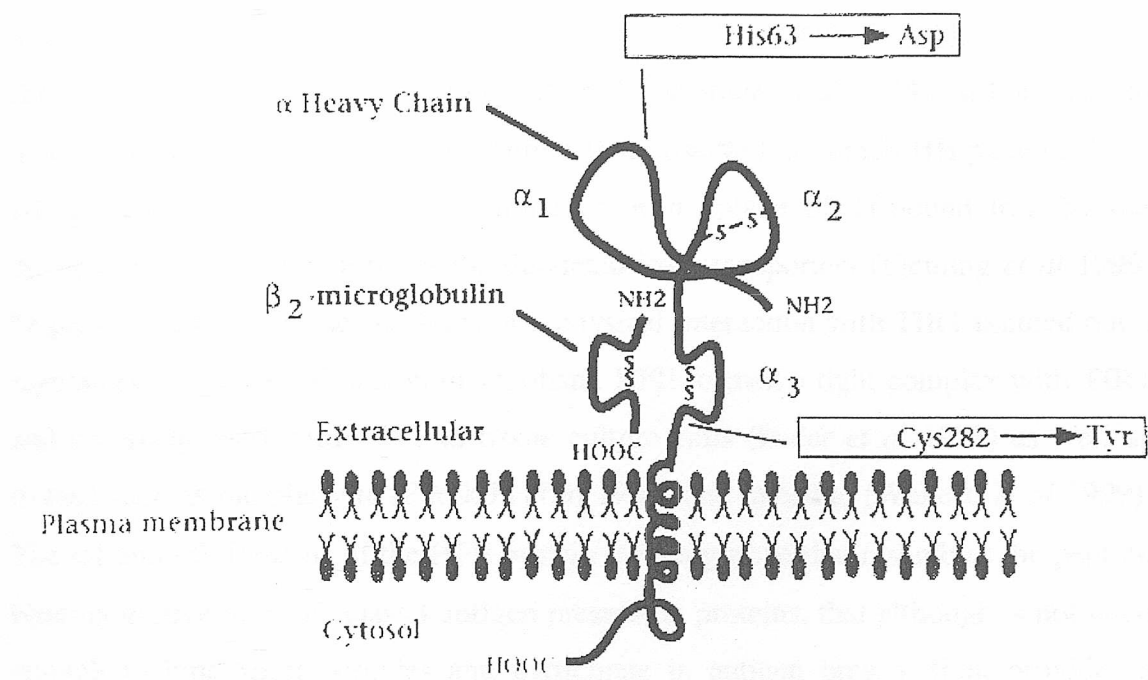


Figure 1.6 Diagrammatic representation of the HFE molecule.

(Image taken from Bacon 2001)

The HFE molecule is a type I transmembrane glycoprotein with 343 residues. The extracellular portion is composed of α_1 and α_2 domains and an immunoglobulin like α_3 domain that binds to or is physically associated with β_2 -microglobulin. The positions of C282Y and H63D are indicated.

The definitive proof of the involvement of HFE, which neither binds nor transports iron, in iron overload was given by the description of mice lacking HFE ($Hfe^{-/-}$) (Zhou *et al* 1998) and $\beta 2m$ KO mice ($\beta 2m^{-/-}$) (de Sousa *et al* 1994). In both animal models, the massive iron overload mimics that observed in human HH patients. Like HH patients, these animals, have impaired iron uptake of Tf-bound iron by the duodenum and up-regulation of the duodenal iron transporters (Fleming *et al* 1999, Dupic *et al* 2002). Further findings of a physical interaction with TfR1 pointed out a regulatory role for HFE in iron metabolism. HFE formed a tight complex with TfR1 and co-precipitated with TfR1 in tissue culture cells (Feder *et al* 1998) as well as tissues such as the placenta (Parkkila *et al* 1997) and intestine (Waheed *et al* 1999). The $\alpha 1$ and $\alpha 2$ domains of the HFE protein form a groove that resembles the peptide binding groove of MHC class I antigen presenting proteins, that although is not wide enough to bind short peptides and participate in antigen presentation, provides a binding site for the interaction between HFE and TfR1. In humans, the major mutation of the *HFE* gene alters both the structure of the protein as well as its association with $\beta 2m$, resulting in a lack of HFE expression on the cell surface (Lebron *et al* 1998), while the minor mutation has no effect on the association of HFE with $\beta 2m$ or on its expression at the cell surface (Waheed *et al* 1999). HFE and Fe₂-Tf are thought to bind TfR1 simultaneously (Lebron *et al* 1998) and HFE is thought to inhibit the Tf/TfR1 interaction (Feder *et al* 1998, Gross *et al* 1998) by binding near the Tf binding site on TfR1 (Lebron *et al* 1999). Normally, HFE on the cell surface binds TfR1 and results in a 10-fold reduction in the affinity of the receptor for iron loaded Tf, thereby reducing the overall uptake of iron into cells, maintaining low but sufficient intracellular levels of iron (Feder *et al* 1998, Lebron *et al* 1998, Riedel *et al* 1999). Therefore, in HH and in the absence of a functional HFE, iron transport into the cytoplasm of the HFE-deficient cell can proceed without negative regulation (Gottschalk *et al* 2000). Studies by Salter-Cid *et al* (1999) have presented further evidence that HFE not only blocks binding of Tf to TfR1 but also inhibits internalisation of the complex into the cytoplasm. However, others have reported that the binding of HFE to TfR1 does not affect the cycling or distribution of TfRs (Roy *et al* 1999). A more recent study by Cheng *et al* (2004) confirmed previous findings of an HFE-Tf competition by showing that the TfR1 dimer can accommodate one HFE and one Tf molecule on either side but not on the same side

of TfR1. And although previous studies have failed to demonstrate an *in vitro* interaction between the ectodomains of HFE and TfR2 (West *et al* 2000), a recent study by Goswami and Andrews (2006) concluded that HFE interacts specifically with both TfR1 and TfR2. Prior to the discovery of hepcidin, clues on the molecular mechanisms causing HH were sought in these often controversial observations and the crypt modelling hypothesis, based on the observations of increased expression of duodenal iron transporters in HH patients. It has since then been revealed that iron overload due to HH (at least for types 1, 2 and 3) is the result of a failed hepcidin response to the iron burden.

Diagnosis of *HFE*-related HH depends upon both indirect and direct markers of iron overload (Table 1.1). Indirect markers include biochemical measures of iron status, such as serum iron (SI), serum ferritin (SF), transferrin saturation (TS), and the total iron binding capacity (TIBC). A persistently elevated TS (<45%) and SF levels in the absence of other causes of iron overload strongly suggests HH (reviewed in Powell *et al* 1998). Measurement of the unsaturated iron binding capacity has also been proposed as a surrogate marker of TS that can be automated for large scale population screening programmes (Hickman *et al* 2000). Direct markers include *HFE* gene mutation analysis and liver biopsy for histopathology (using histochemical iron stains such as Perls' Prussian blue stain) and measurement of the hepatic iron concentration (HIC), with calculation of the hepatic iron index (HII) (quotient of HIC and the age of the patient). DNA analysis can identify up to 90% of the patients homozygous for the most common mutation, C282Y, in the *HFE* gene (The U.K. Haemochromatosis Consortium), while liver biopsy is used to establish the degree of iron loading. Iron grade or grade of siderosis denotes the degree of iron deposition, as classified by Scheuer *et al* (1962) with grade 0 being negative (no visible iron) and grades I (iron visible in very few hepatocytes), II (iron visible in 5-10% of hepatocytes), III (iron visible in ≥40% of hepatocytes) and IV (abundant iron visible in most hepatocytes), representing increasing amounts of stainable iron. Non invasive methods to measure hepatic iron overload include computed axial tomography, superconducting quantum interference device (SQUID) that measures magnetic susceptibility, and magnetic resonance imaging (the latter being the most promising) but liver biopsy remains an essential diagnostic tool in C282Y

homozygotes with hepatomegaly or SF levels higher than 1000ng·mL⁻¹ (reviewed in Pietrangelo 2004).

Table 1.1 Laboratory measurements of iron status in HH patients
(Table adapted from Bacon 2001 to utilise S.I. units)

	Normal Individuals	Patients with HH	
		Asymptomatic	Symptomatic
Indirect measures			
Serum Iron (μmoles·L ⁻¹)	10-30	<30	30-50
Serum Ferritin (ng·mL ⁻¹)			
Males	20-300	150-1000	500-6000
Females	20-200	120-1000	500-6000
Transferrin Saturation (%)	<30%	30%-60%	>45% to >100%
Total Iron Binding Capacity (μmoles·L ⁻¹)	53-85	53-85	40-60
Direct measures			
Hepatic Iron Concentration (μg Fe/g dry wt)	300-1500	2000-10000	8000-30000
Hepatic Iron Index	<1.0	1.0 to >1.9	>1.9
Grade of Siderosis	0 to I	II to III	III to IV
<i>HFE</i> mutation analysis	Normal/Normal	C282Y/C282Y C282Y/H63D	C282Y/C282Y C282Y/H63D

Total body iron stores normally range from 2-6g, however in HH patients iron stores can range from 5-40g, since the amount of iron transferred from the mucosa to the plasma circulation is higher (or a higher rate constant) than in normal subjects (McLaren *et al* 1991). HH patients absorb dietary iron at 2-3 times the normal rate and can thus accumulate iron at a rate of 0.5-1.0g per year (Bomford and Williams 1976). Symptoms of HH usually appear after 20g of iron have accumulated in the body and thus men tend to be symptomatic in middle age (40s), while women after menopause (60s) (Holman 1997). HH is ten times more common in men than women, who are less severely affected, being protected by the physiological loss of

iron during menstruation and in pregnancy (Yip 1998), but could also develop HH and have a full phenotypic expression of the disease (Moirand *et al* 1997). The *HFE*-related HH phenotype is characterised by both non-specific and specific clinical symptoms. Early non-specific clinical symptoms include severe fatigue, apathy, and weight loss, while specific symptoms reflecting target organ damage include chronic abdominal pain, arthralgia, diabetes, impotence in men or amenorrhea in women and arrhythmias. Specific signs include hepatomegaly, splenomegaly, arthritis, cardiomyopathy, skin bronzing or pigmentation (due to increased melanin deposition in the skin), and hypogonadism and hypopituitarism (reviewed in Harrison and Bacon 2003). The latter clinical signs that are evident in symptomatic HH patients reflect the iron burden in the respective organs (liver, joints, heart, skin, and endocrine). In healthy individuals only 30% of the circulating Tf binds iron however in pathological iron overload, iron gradually saturates the iron-binding capacity of Tf and in addition to the uptake of Tf-bound iron, excess iron in the plasma (in the form of NTBI or low molecular weight chelates) is also taken up into tissues resulting in cell damage and tissue injury. Type I HH is characterised by iron accumulation in periportal hepatocytes and to a less extent in Kupffer cells, while the bone marrow macrophages are spared of this iron burden (reviewed in Powell 2002). Hepatocellular carcinoma is a major complication and cause of mortality with prevalence more than 200 times than of the general population, while 10% of patients present with cirrhosis (reviewed in Stremmel *et al* 1995).

Treatment for HH is universally achieved by venesection or phlebotomy in which significant quantities of iron can be removed from the body. The long-term administration of iron-chelating agents, such as desferrioxamine, is only very occasionally required in patients who cannot tolerate venesection. Therapeutic phlebotomy, which is the method of choice being safest, most effective and economical, involves the weekly removal of approximately 1 unit (500mL) of blood over the course of one or two years to return the iron level to normal. Thereafter, three to four sessions a year, are sufficient to maintain normality (reviewed in Barton *et al* 1998 and Franchini 2006). Other preventative measures are often incorporated into the diet (such as avoidance of medicinal iron, mineral supplements, excess vitamin C) to reduce the amount of iron absorbed. Total long-term remission is possible in patients treated before the pathological process of iron overload has

produced irreversible lesions, emphasising the importance of early diagnosis (Niederau *et al* 1996). Deaths attributed to HH in Britain are rare, despite the fact that 1 in 250 of the 700,000 who die in Britain annually will be homozygous for the C282Y gene (Willis *et al* 2000). This is a clear indication that the C282Y mutation is of very low penetrance.

1.4.1.2 Non *HFE*-related HH (Types 2, 3 and 4)

Iron loading before the second and third decade of life is considered a distinct entity (OMIM 602390), known as juvenile haemochromatosis (JH). JH is a rare, autosomal recessive disorder that affects both sexes and presents with a clinical phenotype similar to that of type 1 HH, although with increased severity (Kelly *et al* 1998). There are two JH subtypes, type 2A (OMIM 608374) and type 2B (OMIM 606464), of which type 2A is the most common. Type 2A HH, is due to mutations in the hemojuvelin (*HJV*) gene, which was mapped by linkage analysis to the long arm of chromosome 1 at 1q21 by Roetto *et al* (1999), and type 2B is caused by mutations in the *HAMP* gene that maps to 19q13.1 (Roetto *et al* 2003). Numerous (mainly private) mutations have been described in the *HJV* gene (Papanikolaou *et al* 2004, Roetto *et al* 2004, Lee *et al* 2004, Huang *et al* 2004, Biasiotto *et al* 2004, Jánosi *et al* 2005), with one report identifying up to 16 novel mutations (Lanzara *et al* 2004), while comparatively only a few rare mutations have been identified in the *HAMP* gene (Roetto *et al* 2003, 2004). Nevertheless, the early onset of this disorder exemplifies the importance of the proper functioning of the *HJV* and hepcidin molecules in iron homeostasis.

HJV belongs to the family of repulsive guidance molecules (RGM), however unlike other RGMs which are expressed in neural tissue, *HJV* transcript expression has a distribution similar to that of hepcidin and is abundant in the liver, heart and skeletal muscle (Papanikolaou *et al* 2004). *HJV* is transcribed from a gene (also known as *HFE2*) of 4265 base pairs (bp) and four exons into a full-length transcript with five spliced isoforms (Papanikolaou *et al* 2004). The putative full-length protein from the longest transcript is 426 aa (Papanikolaou *et al* 2004). *HJV* contains multiple protein motifs consistent with a function as a membrane-bound receptor or secreted polypeptide hormone, which have been shown to reciprocally regulate hepcidin expression *in vitro* in response to changes in extracellular iron

concentrations (Lin *et al* 2005). The exact mechanism of action is not known but is expected to involve interaction with other proteins or an HJV receptor, since HJV lacks a cytoplasmic tail for direct signalling to the cell interior and since other members of the RGM family function as receptor ligands. Candidates for HJV transmembrane receptors include the receptors of the transforming growth factor/bone morphogenic protein (TGF β /BMP) superfamily whose signalling is transduced into the nucleus by SMADs, of which SMAD4, a tumor suppressor gene, has been found to activate hepcidin expression in hepatocytes (Wang *et al* 2005). HJV has been reported to act as a BMP co-receptor and the resulting signal transduction pathway was shown to induce hepcidin mRNA in hepatocyte cell lines. In addition, mice with liver specific knockout of SMAD4, a signalling adaptor used by several receptors of the TGF β R family, developed haemochromatosis, supporting the important role of the TGF β R family in iron homeostasis and in the regulation of hepcidin (Babitt *et al* 2006).

Classified as type 3 or *TfR2*-related HH (OMIM 604250) is an autosomal recessive disorder caused by homozygous nonsense or missense mutations in the *TfR2* gene. The precise role of TfR2 in iron metabolism has not yet been elucidated and there are findings to suggest that it is not merely a Tf receptor. The first mutation in the *TfR2* gene, a Y250X nonsense mutation, was detected in two families from Sicily (Camaschella *et al* 2000) and since then several other mutations have been identified in the Italian population (Roetto *et al* 2001). The clinical symptoms of this type of HH are similar to those of the *HFE*-related HH, although heterozygotes for any of the identified TfR2 mutations do not have clinical symptoms and show normal iron indices (reviewed in Roetto and Camaschella 2005).

Type 4 HH (also known as ferroportin disease, OMIM 606069) is an autosomal dominant disorder caused by heterozygous mutations in the *SCL40A1* gene on chromosome 2q32 that codes for FP1 (Montosi *et al* 2001, Njajou *et al* 2001). The most common mutation is a GTT triplet deletion that occurs in a GTT repeat at position 478-494 that leads to a valine deletion at position 160-162 (160-162delVal). Several other mutations in the *SCL40A1* gene have also been identified (Wallace *et al* 2002), however there is no clear correlation between genotype and phenotype in

this type of HH. FP1 mutations cause impairment of iron export from cells, especially from reticuloendothelial macrophages, which results in tissue iron accumulation, and a decrease in the iron that would be available for circulating Tf, indicated by a low or normal TS, possibly resulting in a mild anaemia. Iron deposition, especially in young patients, is found in the reticuloendothelial cells, which is an unusual feature in HH. During the third and fourth decade of life progressive tissue iron loading in this disorder occurs due to the impaired release of iron from the macrophages, but also an increase in iron absorption in response to the anaemia, resulting in parenchymal iron overload. In contrast to all other types of HH, patients with type 4 HH show reduced tolerance to phlebotomy and develop mild iron-deficient anaemia when an aggressive phlebotomy treatment is followed. A less aggressive phlebotomy regimen with the concomitant use of erythropoietin is recommended in this case (reviewed in Pietrangelo 2004).

Finally, two rare cases of iron overload, H-ferritin related iron overload and neonatal haemochromatosis (NH) also require mentioning. H-ferritin related iron overload (OMIM 134770) is an autosomal dominant iron overload that has up to date only been observed in a single Japanese family and is caused by a mutation in the 5' IRE in the gene on 11q13 that encodes the H-subunit of ferritin. This type of iron overload is characterised by heavy deposition of iron in hepatocytes and Kupffer cells (Kato *et al* 2001). NH (OMIM 231100) is a rare and as yet unexplained severe accumulation of iron occurring in newborn and unborn children in utero that has not been linked to any other types of HH (Kelly *et al* 2001). NH is characterised by widespread iron deposition in several organs, irreversible liver failure and raised ferritin levels (reviewed in Cox and Kelly 1998). In this type of iron overload the offspring rarely reaches full term (Hardy *et al* 1990) and survival is rare, though a few cases of survival have been documented (Muller-Berghaus *et al* 1997).

Table 1.2 Genetic Haemochromatoses

(Table adapted from Bomford 2002 and Pietrangelo 2004)

Disease	OMIM	Gene mutated	Locus	Mode of Inheritance	Clinical manifestations and main organs accumulating iron	References
Type 1 or <i>HFE</i> -related HH	235200	<i>HFE</i>	6p21.3	Autosomal recessive	Chronic increase in iron absorption leading to iron deposition in the liver, joints, heart, skin and endocrine glands.	Feder <i>et al</i> 1996
Type 2A or <i>HJV</i> -related HH	608374	<i>HJV/HFE2</i>	1q21	Autosomal recessive	Similar to Type 1 HH but with accelerated iron loading and death by third decade from heart failure.	Lee <i>et al</i> 2004, Papanikolaou <i>et al</i> 2004
Type 2B or <i>HAMP</i> -related HH	606464	<i>HAMP</i>	19q13.1	Autosomal recessive	Similar to Type 1 HH but with accelerated iron loading and death by third decade from heart failure.	Roetto <i>et al</i> 2003
Type 3 or <i>TfR2</i> -related HH	604250	<i>TfR2</i>	7q22	Autosomal recessive	Chronic increase in iron absorption leading to iron deposition in the liver, joints, heart, skin and endocrine glands.	Camaschella <i>et al</i> 2000, Roetto <i>et al</i> 2001
Type 4 HH or Ferroportin disease	606069	<i>SLC40A1</i>	2q32	Autosomal dominant	Iron loading in reticuloendothelial macrophages leading to iron deposition in the liver, spleen.	Montosi <i>et al</i> 2001, Njajou <i>et al</i> 2001

1.4.2 Pathogenesis of hereditary haemochromatoses

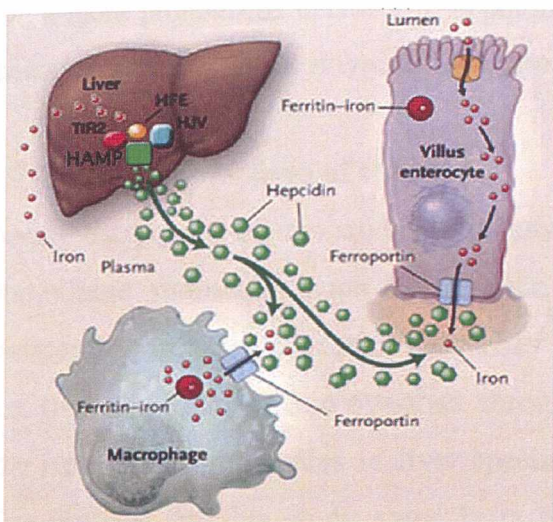
A switch in a single nucleotide resulting in a mutant HFE protein cannot possibly account for a disease with such a variable phenotype as HH. HFE neither binds nor transports iron, and the process by which it affects cellular iron uptake remains unclear. Findings of a physical interaction with TfR1 and more recently with TfR2 point out the implication of HFE in iron metabolism. Prior to the discovery of hepcidin it was thought that HH was the result of a defective HFE and a faulty HFE/TfR pathway that incorrectly signals crypt cells of an iron deficiency state despite increased saturation of circulating Tf with iron. The discovery of hepcidin, its implication in iron homeostasis and its interaction with FP1 has provided strong evidence of a molecular explanation of the regulation of iron absorption and its malfunction in HH. Mutations in HFE, TfR2, hepcidin and HJV lead to phenotypically similar forms of iron loading, suggesting that these proteins form part of the same regulatory pathway. Almost all types of HH (caused by mutations in HFE, TfR2, hepcidin and HJV) are characterised by lack of an appropriate hepcidin response to the iron burden (Bridle *et al* 2003, Gehrke *et al* 2003, Roetto *et al* 2003, Papanikolaou *et al* 2004, Nemeth *et al* 2005), with ferroportin disease being the only exception as it is the only type of HH where increased levels of serum prohepcidin in the early stages of the disease (Zoller *et al* 2005) and urinary hepcidin have been observed (Papanikolaou *et al* 2005). These observations suggest that HFE, TfR2 and HJV are regulators of hepcidin synthesis in the liver (Figure 1.7). Further reports of digenic inheritance of mutations in both *HFE* and *HAMP* (Merryweather-Clark *et al* 2003) and *HFE* and *TfR2* affecting the phenotype of the classic HH, has led to the hypothesis that JH is not a distinct monogenic disorder but could be genetically linked to the adult onset form of HH, with hepcidin being the common denominator in all forms of the disease (Pietrangelo *et al* 2005).

In this unifying pathogenic model for HH, HFE and TfR2 are considered minor regulatory proteins, since loss of function in each leads to the adult form of HH, while hepcidin and HJV are considered major regulators, since loss of function in these leads to the harsher juvenile form of HH (reviewed in Pietrangelo 2006). In the presence of functional hepcidin, HFE, HJV and TfR2, the amount of iron entering the plasmatic circulation is appropriate to the body iron needs as hepcidin communicates those needs between the liver, macrophages and the intestine (Figure

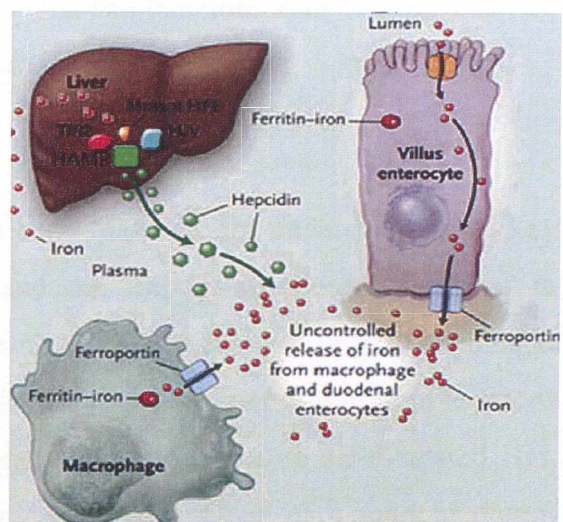
1.7A). Loss of HFE or Tfr2 will lead to an increased iron absorption from the intestine and into the portal circulation, however presence of the one minor regulator and the major regulator HJV, will aid in the maintenance of some hepcidin expression (Figures 1.7B and 1.7C). Mutations in the major regulator, HJV, will result to an increased efflux of iron into the plasma circulation as hepcidin fails to communicate body needs, resulting in a more severe phenotype (Figure 1.7D), while complete loss of hepcidin, even in the presence of functional HFE, Tfr2, and HJV, will lead to the uncontrolled release of iron and severe iron overload.

Studies in animal models and cell cultures have shed further light into the proposed role of these molecules in the development of HH however plenty remains to be explored before a full picture explaining the pathogenesis of HH can be drawn. Nicolas *et al* (2003) crossed *Hfe*^{-/-} mice with transgenic mice overexpressing hepcidin and found that hepcidin inhibited the iron accumulation normally observed in the *Hfe*^{-/-} mice. And studies by Laftah *et al* (2004), led to the suggestion that HFE acts either upstream of hepcidin or is involved in a hepcidin -independent regulatory pathway of iron absorption. Tfr2 and HJV are also proposed to act upstream of hepcidin, since expression of this important peptide in the liver has been shown to be significantly impaired in both Tfr2 and HJV KO mice. While Tfr2, which is predominantly expressed in the liver, has been proposed to act as a sensor of iron status, based on the observation that its levels are regulated by Tf saturation, such that receptor levels reflect Tf saturation (Robb and Wessling-Resnick 2004, Johnson and Enns 2004).

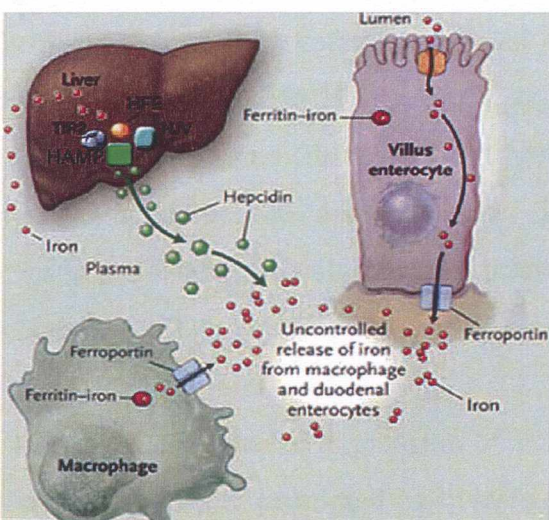
(A) Normal



(B) Type 1 or *HFE*-related HH



(C) Type 3 or *TfR2*-related HH



(D) Type 2A or *HJV*-related HH

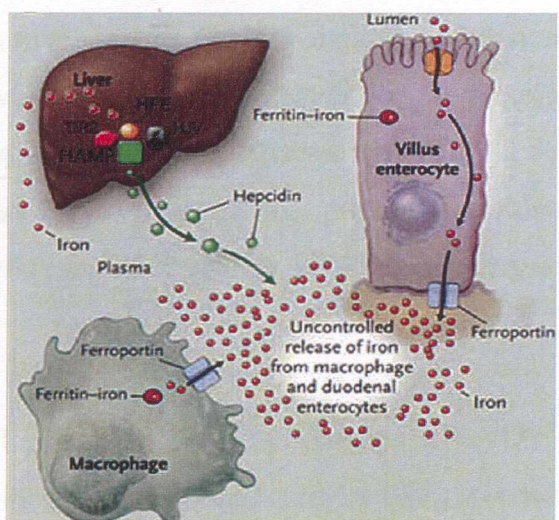


Figure 1.7 Unifying pathogenic model for the development of HH.

(Image adapted from Pietrangelo 2006)

(A) In the presence of functional HFE, HJV, Tfr2 and hepcidin, hepatic synthesis of hepcidin is attuned to body iron requirements. By regulating expression of FP1 on macrophages and intestinal cells, hepcidin controls dietary iron absorption and iron recycling. (B) Loss of HFE, which is considered a minor regulator of hepcidin, leads to inappropriately decreased hepcidin synthesis. Iron release from macrophages and intestinal cells proceeds without negative regulation leading to the iron loading phenotype that is recognised as type 1 HH. (C) Loss of Tfr2, which is also considered a minor regulator of hepcidin, has similar effects as loss of HFE, and leads to the iron loading phenotype recognised as type 3 HH. (D) Loss of a major regulator however, such as HJV, is associated

with a more pronounced decrease in hepcidin levels and therefore leads to a more severe phenotype as the one seen in type 2A HH, also known as JH.

1.5 Aims and objectives of the thesis

During the course of this study, leaps have been made in our understanding of key iron-related molecules such as hepcidin and the important role of the liver in maintaining iron homeostasis. The broad aim of this project was to gain an insight into the complexity of iron overload, through studying transcript and protein levels of key iron-related molecules in liver specimens from patients with *HFE*-related HH. The impetus for this study came from previous observations of a marked down-regulation in IRP1 protein levels in untreated HH patients and evidence of its expression in the nucleus of hepatocytes in treated patients, following immunohistochemistry. These observations prompted an investigation into the *ex vivo* expression of IRP1 in iron loaded HH patients, as well as its *in vitro* expression in protein extracts from cultured fibroblasts and human hepatoma cells loaded with iron, in an attempt to mimic the diseased state. The localisation of the protein was also investigated *in vitro* in cultured cells transiently transfected with an IRP1-GFP fusion protein.

Findings of a decreased expression of IRP1 protein in untreated patients with *HFE*-related HH, further prompted an investigation into transcript levels of this molecule in an attempt to elucidate the observed phenomenon. In addition to IRP1, liver hepcidin, TfR1, TfR2 and HJV transcript levels were also examined in order to determine their relative expression levels in untreated iron loaded patients as compared to control subjects. Transcript levels of all the studied genes were further examined in relation to clinical iron status parameters that included serum ferritin, serum iron, transferrin saturation and hepatic iron concentration. Available reagents also permitted an investigation into hepatic TfR2 protein expression levels in untreated as well as treated patients with *HFE*-related HH and the association of those levels with the aforementioned clinical iron parameters, as this molecule has recently been implicated in the molecular response of hepcidin to iron as an iron sensor in a pathway acting upstream of hepcidin. Studying the patterns of expression of these key iron-related molecules in normal and iron loaded states might provide an insight into this jigsaw known as iron homeostasis and its dysregulation in HH.

Chapter II

Materials and Methods

2.1 Materials

2.1.1 Liver tissue

Frozen liver specimens were kindly provided by Dr. Adrian Bomford, Institute of Liver Studies, King's College London, School of Medicine, King's College Hospital (KCH), Denmark Hill, U.K. Control liver samples included healthy liver that was donated to the department or from patients that had undergone liver biopsy for indications other than HH. Control specimens showed normal iron indices and liver histology and negative staining for iron by Perl's stain. Iron loaded liver tissue specimens were obtained either from routine liver biopsies (percutaneous needle biopsies) or from patients undergoing liver transplantation (explants), with prior consent from the patients. The majority of the cases were HH patients homozygous for the C282Y mutation (also referred to as YY) and were classified as grade of liver siderosis III or IV (pre-treatment). There were also single cases of iron overload ($HIC > 1500 \mu\text{g/g}$ dry wt) not due to homozygous mutations in the *HFE* gene and included a heterozygote for the C282Y mutation (referred to as CY), a case of pyruvate kinase deficiency (PKD), and a case of NH. Clinical iron indices of the specimens used in these studies were kindly provided by Dr. Kishor Raja (KCH). These were assessed using routine laboratory methods at KCH and included the HIC, SF, SI, TS and the TIBC. TS was expressed as the quotient of SI and TIBC $\times 100\%$. Reference ranges for these analytes are provided in Chapter I (Table 1.1). Tables summarising the clinical characteristics of each study group are provided in the beginning of respective chapters (Tables 3.1, 4.1 and 5.1). Appendix I contains a full list of relevant and clinical information on individual samples.

2.1.2 Cell lines

The human hepatocellular carcinoma cell line (HepG2), the human cervical carcinoma cell line (HeLa) and the African green monkey fibroblast-like cell line (COS) were all obtained from the European Collection of Animal Cell Culture (ECACC, Salisbury, U.K.).

2.1.3 Bacterial strains

The bacterial *Escherichia coli* (*E. coli*) strains INVαF' (Invitrogen, Paisley, U.K.) and NovaBlue Singles Competent cells (Novagen) were used for subcloning (sections 2.5.8.1 and 2.5.8.2).

2.2 Reagents and general equipment

2.2.1 Chemicals and reagents

General chemicals and reagents were purchased from Sigma-Aldrich (Dorset, U.K.) and BDH Laboratory Supplies (Poole, U.K.), unless stated otherwise. Molecular cloning reagents such as restriction endonucleases, DNA polymerases, reverse transcriptases, and accompanying buffers were from Promega (Southampton, U.K.) and New England Biolabs [(NEB), Hitchin, U.K.]. Bacteriological peptone, yeast extract and bacteriological agar were from Oxoid (Basingstoke, U.K.). Solutions were prepared in deionised water and autoclaved as appropriate.

2.2.2 Molecular weight markers

The 100bp DNA ladder, (100-1517bp), 1 kilo bp (Kbp) DNA ladder (0.5-10Kbp) and λ DNA, *Hind*III digest, (125-23130bp), (NEB) were used in estimating the size of DNA fragments. The pBluescript II SK+, *Hpa*II digest, 56-710bp in (1x) Tris Borate EDTA [(TBE); 0.045M Tris Borate; 0.001M EDTA] and (6x) agarose gel loading buffer [40% weight/volume (w/v) sucrose; 0.25% orange G; 0.25% xylene cyanol FF] was used for determining concentration of samples. The Prestained Protein Marker, Broad Range, [6.5-175kDa], the Broad Range Protein Marker (2-212kDa) (both NEB) and the Precision Plus Protein™ Standards, (10-250kDa) (Bio-Rad Laboratories Inc., Hemel Hempstead, U.K.) were used when estimating protein size.

2.2.3 Cell culture reagents

Cell culture media and reagents were also purchased from Sigma-Aldrich. Roswell Park Memorial Institute (RPMI) 1640 medium supplemented with fetal bovine serum (FBS) and antibiotics [10000 units (U) penicillin; 10mg streptomycin; in 0.9% NaCl] was commonly used. Phosphate buffer saline (PBS) (Oxoid) was calcium and magnesium chloride free.

2.2.4 Commonly used equipment

Centrifugation of solutions was carried out in a bench-top microfuge [eppendorf centrifuge (5415C)], a temperature controlled centrifuge [eppendorf (5148/5804R)], or in an ultracentrifuge (Beckman Floor Model L5-65, High Wycombe, Beckman Coulter Limited, U.K.), when speeds of up to 4000 or 20000 rounds per minute (rpm) were required, respectively. Absorbance of solutions was measured in a CECIL CE1021 spectrophotometer (Cecil Instruments Ltd, Cambridge, UK). The SE250 and SE600 Hoefer Mighty Small caster and electrophoresis units (Fisher Scientific, Loughborough, UK) were used for the electrophoretic runs of protein extracts. Electrophoresis of DNA was carried out in Hybaid tanks (Hybaid Ltd, Ashford, UK). For visualisation of DNA fragments agarose gels were placed under ultraviolet (UV) light, in the UVi transilluminator (Uvitex, Cambridge, UK) or the UVP BioDoc (UVP, Cambridge, UK).

2.3 Cell culture

2.3.1 Culturing of cell lines

Cells were cultured in full medium [RPMI-1640 medium supplemented with 10% volume/volume (v/v) FBS; 1% non-essential amino acids (NEAA); 1% antibiotics and 1% sodium pyruvate (100mM), the latter component included when culturing HepG2 cells], and grown in a humidified atmosphere of 5% CO₂, 95% air, at 37°C. Confluent populations of cells (at the plateau phase of exponential growth) were subcultured (passaged) with the aid of the proteolytic enzyme trypsin. To harvest the cultures, the monolayer of cells was washed with PBS and the cells were dislodged with a solution of 10% trypsin, 0.5mM EDTA, pH 8.0 in PBS by incubating at 37°C for 5 minutes (min). Once the cells were detached (additionally enforced by shaking, except in the case of HepG2 cells, which have a tendency to grow on top of each other and were therefore allowed to detach undisturbed) proteolysis was terminated by addition of 5 volumes of full medium. The cell suspension was then collected in 15mL-sterilin tubes, sedimented at 800rpm for 5min, and the cell pellet resuspended in full medium. An aliquot of the cell suspension (1mL) in a final volume of 10mL full medium was used for maintaining the cell lines, whereas other appropriate volumes of the cell suspension were used when a specific cell density was required. Cells were cultured in a Category II culture hood (HERA_{Safe}) and maintained in a cell

culture incubator (HERAcell) (Jencons, PLS, Leighton Buzzard, U.K.). Aseptic techniques were observed throughout when handling cells.

2.3.2 Counting cells with a haemocytometer

Cell density was determined by Trypan Blue exclusion using a haemocytometer (Neubauer). An aliquot of cells ($50\mu\text{L}$) was mixed with an equal volume of Trypan Blue solution (0.4%). The haemocytometer is a microscope slide with grids, forming nine large squares divided by triple lines. Each large square has an area of 1mm^2 . The depth of fluid in the slide chamber is 0.1mm, and therefore the total volume of fluid over each large square is $1 \times 1 \times 0.1 = 0.1\text{mm}^3 = 0.0001\text{cm}^3 = 0.0001\text{mL} = 10^{-4}\text{ mL}$. The cell suspension was transferred to the edge of the haemocytometer chamber, allowed to be drawn in under the coverslip and observed using an inverted microscope (Nikon eclipse TS100, Nikon UK Ltd, Surrey, U.K.). The number of unstained viable cells within the 1mm^2 area in both chambers was counted and an average of the 2 counts was calculated. The concentration [cells] and total number of cells were calculated using the following equations (Equation 2.1 and 2.2):

$$[\text{cells}] = \text{average cell count} \times 2 \times 10^4 = \alpha \text{ cells per mL of medium} \quad (\text{Equation 2.1})$$

$$\text{Total number of cells in plate/flask} = \alpha \times Z \quad (\text{Equation 2.2})$$

where Z is the total amount of solution used when harvesting the cells.

2.3.3 Cryopreservation of cells and revival of frozen stock

Cells to be preserved in liquid nitrogen were assessed for quality and confluency. Cells were trypsinised and resuspended in full medium. An aliquot was removed for counting, and the remaining cells centrifuged at 800rpm for 5min. The resulting cell pellet was resuspended in freeze medium [10% dimethylsulphoxide (DMSO); 90% FBS] and 1mL aliquots were placed in 1.2mL-cryovials (Nalgene) and left to cool slowly from room temperature to -80°C overnight before storing in a liquid nitrogen storage tank. To revive the frozen cells, a cryovial was removed from liquid nitrogen, and transferred to a 37°C water bath for a short period until almost all the cells had thawed out. The cells were then transferred, drop by drop, into tissue culture flasks containing pre-warmed full medium (at 37°C) and the cultures maintained as described under 2.3.1.

2.4 RNA and DNA preparations

2.4.1 Extraction of RNA from cultured cells or liver tissue

Total RNA was extracted from approximately 1×10^8 cells or 200mg of frozen liver tissue using the RNeasy midi kit (Qiagen Ltd., West Sussex, U.K.) and following the manufacturer's instructions. The exact composition of buffers supplied with this kit (buffers RLT, RW1 and RPE) was not provided by the manufacturer. To aid the initial steps of homogenising the cells and tissues, the Reacti Wear, microtissue grinder kit (PIERCE Chemical Company, Cramlington, U.K.) was used. Cells were harvested and the acquired pellet homogenised in 4mL of extraction buffer (buffer RLT - containing guanidine thiocyanate) supplemented with 1% (v/v) β -mercapto ethanol (β -Me). Frozen liver specimens were thawed out and incubated for 20min at 37°C in a water bath to dissolve any salts. The tissues were homogenised in buffer RLT (4mL) and lysates were centrifuged for 10min at 3500rpm at 20°C. Following centrifugation, the interphase was collected and the following steps were appropriate for the extraction of total RNA from either source of starting material.

An equal volume of 70% ethanol was added to the lysates and the samples were mixed vigorously by shaking. Each sample was applied to an RNeasy midi spin column, placed in a 15mL-centrifuge tube. Since the maximum loading volume of the column was 4mL, 3mL aliquots were loaded successively onto the RNeasy column, until all the lysate was applied to the column. The flow through was discarded each time. Buffer RW1 (4mL) was poured onto each column, the columns centrifuged at 3500rpm for 5min, and again the flow through discarded. Buffer RPE (2.5mL) (containing ethanol) was then added onto the columns and the columns centrifuged for 2min at 3500rpm. Another 2.5mL of buffer RPE were added onto each column, which was then centrifuged at 3500rpm for 5min, to dry the spin-column membrane and again the flow through discarded. To elute the RNA, the RNeasy columns were transferred to fresh 1.5mL-collection tubes. RNase-free H₂O (150 μ L for cell samples and 250 μ L for tissue samples) was pipetted directly onto each spin column membrane. The spin columns were left to stand for 1min, centrifuged for 3min at 3500rpm and the elution step was repeated by adding a second volume (250 μ L) of RNase-free H₂O. The acquired samples (approximately 500 μ L each) were then transferred to 1.5mL-eppendorf tubes and stored at -70°C.

The amount of total RNA in each sample was estimated spectrophotometrically (described in section 2.4.3). Expected average yields of total RNA isolated using this method and midi kit was 700 μ g and 950 μ g, when the source was tissue or cells, accordingly.

2.4.2 Purification of plasmid DNA from bacterial cells

2.4.2.1 Mini preparation of plasmid DNA from bacterial cells

A single bacterial colony was seeded in 3mL of lysogeny broth (LB) medium containing the appropriate antibiotics, and cultured overnight at 125rpm, at 37°C. The next day, 1.5mL of the culture was transferred to a 1.5mL-eppendorf tube and centrifuged at 12000rpm for 30seconds (s). The resulting bacterial pellet was washed with 0.5mL sodium tris ethylene-diamine-tetra-acetic acid (EDTA) [STE; 100mM NaCl; 10mM Tris, pH 8.0; 1mM EDTA] and then the cell pellet resuspended in 100 μ L glucose tris EDTA [GTE; 50mM glucose; 25mM Tris, pH 8.0; 10mM EDTA] with vigorous vortexing. 0.2mL of a solution of 1% (w/v) sodium dodecyl sulphate (SDS) and 0.2M sodium hydroxide (SDS/NaOH) was then added and contents mixed by inverting the tube rapidly five times. The solution was neutralised by adding 0.15mL of 3M potassium acetate and contents mixed by inverting the tube for 10s, which was then incubated on ice for 5min. The cells were then centrifuged at 12000rpm for 5min to sediment the cell debris and the supernatant was transferred to a 1.5mL-eppendorf tube. An equal volume of phenol:chloroform (v/v) was added and the contents mixed by vortexing. Following centrifugation at 12000rpm for 2min, the supernatant was transferred to a fresh 1.5mL-eppendorf tube. The double stranded (ds) DNA was precipitated by adding 2 volumes of 99% ethanol. The contents were mixed by vortexing and the mixture was allowed to stand for 2min at room temperature. The tubes were centrifuged at 12000rpm for 5min and the resulting pellet washed with 70% ethanol, by centrifugation at 12000rpm for 5min. The DNA pellet was air-dried for 10min and resuspended in 50 μ L TE (10mM Tris; 1mM EDTA, pH8.0) containing RNase A (10 μ g·mL⁻¹).

2.4.2.2 Maxi preparation of plasmid DNA from bacterial cells

Maxi preps of plasmid DNA were carried out using a plasmid maxi-prep kit (Qiagen) as per manufacturer's instructions. The desired colony was seeded in LB medium

(500mL) containing the appropriate antibiotics, and cultured overnight at 150rpm, at 37°C. An aliquot (200µL) of the bacterial culture was used to inoculate 500mL LB medium in a 2L-flask by incubating overnight at 150rpm, at 37°C. The culture was then centrifuged 50mL at a time in 50mL-sterilin tubes at 2500rpm, at 4°C for 10min. The resulting bacterial pellet was resuspended in 125mL buffer P1 (50mM Tris, pH 8.0; 10mM EDTA; 100µg·mL⁻¹ RNase A). Lysis buffer P2 (125mL) [200mM NaOH; 1%SDS (w/v)] was then added, mixed and incubated at room temperature for 5min. Ice-cold neutralisation buffer P3 (125mL) (3.0M potassium acetate, pH 5.5) was added, mixed immediately and the tube incubated on ice for 30 min. The solution was then centrifuged at 2500rpm, 4°C for 10min. In the meantime, a Qiagen-tip 10000 was equilibrated by applying 75mL QBT [750mM NaCl; 50mM 3-(N-Morpholino)-propanesulfonic acid (MOPS), pH 7.0; 15% isopropanol (v/v); 0.15% Triton X-100 (v/v)]. The supernatant from the centrifugation step was applied to the equilibrated tip and the tip was then washed with 300mL of buffer QC [1.0M NaCl; 50mM MOPS, pH 7.0; 15% isopropanol (v/v)]. The DNA was eluted with buffer QF (75mL) [1.25M NaCl; 50mM Tris, pH 8.5; 15% isopropanol (v/v)] and precipitated by adding 52.5mL of isopropanol. The mixture of DNA and isopropanol was centrifuged at 11000rpm for 30min at 4°C and following centrifugation, the supernatant was discarded. The DNA pellets were washed in 10mL 70% ethanol, by centrifugation at 11000rpm for 10min, were then air-dried, and the DNA redissolved in 0.5mL TE. The integrity of the isolated plasmid was verified by UV absorption and agarose gel electrophoresis (sections 2.4.3 and 2.5.6).

2.4.3 Spectrophotometric determination of the amount of RNA/DNA

Aliquots of the extracted nucleic acids were diluted and absorbance readings of the samples at wavelengths of 260 (A_{260}) and 280nm (A_{280}) were taken. The ratio of the readings at 260 and 280nm provides an estimate of the purity of the nucleic acid, with respect to contaminants that absorb in the UV, such as protein. Values of 1.8 and 2.0 correspond to pure preparations of DNA and RNA, respectively. An A_{260} of 1 corresponds to a concentration of 50µg·mL⁻¹ for dsDNA, and 40µg·mL⁻¹ for single-stranded DNA and RNA. The concentration (in µg·mL⁻¹) and yield (in µg) of DNA/RNA was calculated using equations 2.3 and 2.4, respectively:

$$\text{Concentration of nucleic acid} = [A_{260}] \cdot [X] \cdot [\text{Dilution factor}], \quad (\text{Equation 2.3})$$

where $X = 40\mu\text{g}\cdot\text{mL}^{-1}$ in the case of RNA or $50\mu\text{g}\cdot\text{mL}^{-1}$ in the case of DNA.

$$\text{Total yield} (\mu\text{g}) = \text{concentration} (\mu\text{g}\cdot\text{mL}^{-1}) \times \text{volume of sample} \quad (\text{Equation 2.4})$$

2.5 Standard methods involving DNA

2.5.1 Restriction enzyme digestions

Restriction digestions were performed by incubating dsDNA with an appropriate amount of restriction enzyme (RE) in its respective buffer as recommended by the supplier, and at the optimal conditions for that specific RE. Restriction digestions were generally carried out using 1U of RE per μg of DNA. Diagnostic digests (i.e. when evaluating progress of a digestion or insertion of a DNA fragment into a vector) had a final volume of 20 μL (small volume of RE and minimal DNA), while preparative digests (i.e. when isolating a DNA fragment from a plasmid for subcloning) were prepared to a final volume of 100 μL [large volume of RE and maximal amount of DNA (20 μg)]. To ensure complete digestion, the reactions were usually incubated for 3 hours (hrs) at the optimal temperature for enzyme activity (usually, 37°C). When necessary, more than one enzyme was included in the digest. These double digestions were only possible when both enzymes were active in the same buffer and at the same incubation temperature. When setting up the digests, an aliquot (5 μL) of the sample prior to the addition of the RE was transferred to another tube and incubated alongside to be used for comparison purposes when checking completion of the digestion by agarose gel electrophoresis.

2.5.2 'Fill in' reactions using Klenow Polymerase

RE digestion as described above often leads to the formation of sticky end fragments of DNA (either recessed or protruding 3' termini). For certain cloning purposes, however, it is often necessary to blunt these ends, which can be achieved using Klenow (DNA polymerase I) of *E. coli*, which possesses 5'→3' polymerase and 3'→5' exonuclease activity. Typical reactions were performed at room temperature for 30min and included for 1-5 μg of DNA fragment to be blunted, 1U of Klenow enzyme, in the presence of 10mM deoxyribonucleotide triphosphates (dNTPs)

(dATP, dCTP, dGTP and dTTP). To deactivate the enzyme, EDTA (0.25M) was added to the reaction which was then heated at 75°C for 10min.

2.5.3 Alkaline phosphatase treatment (dephosphorylation of cut vectors)

Alkaline phosphatase (calf intestinal) catalyses the removal of 5'-phosphate residues from DNA and other substrates such as RNA and dNTPs. Calf intestinal alkaline phosphatase (CIP) was used to remove 5'-phosphates from fragments of DNA, and in the case of linearised vectors to prevent self-ligation. Vector DNA was incubated with 5U CIP in 1xCIP buffer [0.1M Tris (pH 7.5 at 37°C); 0.1M MgCl₂] at 37°C for 1hr. Another 5U of CIP were added and incubated at 55°C for a further 1hr. To inactivate the CIP the sample was heated at 65°C for 1hr in the presence of 0.25M EDTA. The DNA was then precipitated as described under 2.5.5.

2.5.4 DNA ligation

Phosphodiester bonds between adjacent 3'-hydroxyl and 5'-phosphate termini in DNA can be joined (ligated) and T4 DNA ligase can catalyse the formation of these bonds using adenosine triphosphate (ATP) as an energy source. DNA ligase was thus used to join the linearised cloning vector with insert DNA (PCR product) carrying compatible cohesive termini (blunt ends). Typical ligations were performed by incubating ~100ng of linearised cloning vector with a five times molar excess of insert DNA in the presence of 1x ligase buffer [10x ligase buffer; 0.4M Tris, pH 7.8; 0.1M MgCl₂; 0.1M DTT; 5mM ATP] and 0.5U of T4 DNA ligase for 16hrs at 12°C, respectively for 2hrs at 25°C. In addition, control ligations were performed in the absence of insert DNA to determine the clones arising from self-ligation of inefficiently dephosphorylated vector. In the case of DNA fragments bearing sticky ends, ligations were prepared as described but incubated at 12°C. Efficacy of the ligation was assessed by agarose gel electrophoresis, by comparing the size of the original vector used prior addition of the insert to that of the generated vector following ligation.

2.5.5 Concentration of DNA by phenol extraction and ethanol precipitation

An equal volume of TE-buffered phenol was added to samples and agitated using a vortex genie for 1min. Samples were incubated on ice for 5min then spun for 3min at 13000rpm. The aqueous layer was transferred into a 0.5mL-eppendorf tube and

incubated on ice for 5min before being spun for 3min at 13000rpm. The aqueous layer was then transferred into a 1.5mL-eppendorf tube for ethanol precipitation. The DNA solution (1 volume) to be precipitated was mixed with 1/10th volume of 3M sodium acetate and 2.2 volumes ethanol (absolute or 99%) and incubated at 20°C for 1hr. The sample was then centrifuged at 12000rpm for 5min and the pellet washed in 500µL of 70% ethanol by centrifugation at 12000rpm for 5min. The pellet was finally air dried for 10min and dissolved in TE.

2.5.6 Agarose gel electrophoresis

Agarose gel electrophoresis was employed to separate, identify, and purify DNA fragments. Agarose gels were prepared depending on the size of the DNA fragment to be visualised (1.5% was used for separating DNA fragments smaller than 500bp, 1.0% for fragments between 500-800bp and 0.75% gels for DNA fragments bigger than 700bp). Samples to be electrophoresed were mixed with DNA sample buffer [40 % (w/v) glucose, 0.1 % (w/v) bromophenol blue (BPB), 0.1 M EDTA or the sample buffer described in section 2.2.2]. Gels were run in 0.5xTBE or 1xTAE buffer (0.04M Tris acetate; 0.001M EDTA) at 80-100V at room temperature. In addition, appropriate size markers were electrophoresed along with the DNA samples. DNA bands were visualised under UV light with the aid of the fluorescent dye ethidium bromide (Sharp *et al* 1973), which was added to the gel to a final concentration of 1µg·mL⁻¹.

2.5.7 Purification of DNA fragments from a low-melting point agarose gel

2.5.7.1 Purification of DNA fragments for subcloning

The digested DNA fragments were separated by agarose gel electrophoresis on a low-melting agarose gel (1%) and the DNA was visualised under a UV source over a glass plate. Using a razor, a slice of agarose containing the DNA band to be purified was cut, cutting as close to the DNA band as possible. The gel slice was placed into a 1.5mL-eppendorf tube, and heated at 65°C until all the agarose had dissolved (5-10min). The solution was then equilibrated at 37°C and purification proceeded using the Magic™ PCR Preps DNA Purification System (Promega). In brief, the melted agarose containing the desired DNA fragment was mixed thoroughly with 1mL of pre-warmed (37°C) PCR preps DNA purification resin (GTC). The resin/gel mixture

was then loaded onto a Magic™ Minicolumn using a 1mL syringe. The resin was washed twice with 80% isopropanol, and the column spun at 12000rpm for 30s to dry off the excess isopropanol. The purified DNA was eluted from the column by adding 50µL TE and then spinning at 12000rpm for 30s.

2.5.7.2 Purification of DNA fragments for use as standards and for sequencing

The GFX™ PCR DNA and Gel Band Purification Kit (Amersham Pharmacia Biotech UK Limited, Little Chalfont, U.K.) was also used for extracting the PCR products from low melting agarose gels. Bands were cut and placed in 1.5mL-eppendorf tubes with an appropriate amount of capture buffer (buffered solution containing acetate and chaotrope) to the size of the agarose slice containing the extracted bands (10µL of buffer for every 10mg of gel). The 1.5mL-eppendorf tube was vortexed and incubated at 60°C on a heat block until all the agarose was completely dissolved. The tube was then centrifuged at 14000rpm for 30s and the sample was transferred onto the GFX column (placed in a collection tube) and was incubated at room temperature for 1min. The GFX column was then centrifuged at 16000rpm for 30s. The flow through was discarded by emptying the collection tube and placing the GFX column back inside the collection tube. Wash buffer (TE) (500µL) was then added onto the column, which was centrifuged at 16000rpm for 30s. The collection tube was discarded and the GFX column was transferred to a fresh 1.5mL-eppendorf tube. The elution buffer (sequencing grade water) (50µL) was then applied directly on top of the glass fiber matrix in the GFX column. The column was left to incubate for 1min at room temperature and was then centrifuged at full speed for 1min to recover the purified DNA.

2.5.8 Transformation of bacteria

2.5.8.1 Transformation of competent cells

Bacterial transformation is the process by which bacterial cells take up naked DNA molecules. Competent cells were thawed on ice, gently mixed and aliquoted (50µL) into pre-chilled polypropylene tubes. 2.5µL of 0.5M β -Me were added to each aliquot of cells and mixed, before adding 2.5µL of the DNA solution (ligation mixture). The tubes were incubated on ice for 30min and then cells were heat shocked in a 42°C water-bath for 30s. The tubes were incubated on ice for 2min and then preheated

(42°C) LB broth (0.9mL) was added and the tubes were incubated at 225-250rpm, 37°C for 1hr in a shaking incubator. The transformation mixture (100µL) was plated on LB agar plates (90mm Petri dishes) containing the appropriate antibiotics. Once the fluid was taken up by the agar medium, plates were inverted and incubated overnight at 37°C.

2.5.8.2 Perfectly blunt cloning kit transformation

This method was commonly used for the insertion of PCR products into vectors pSTBlue-1 and pT7-Blue. The Perfectly Blunt cloning kit (Novagen) consisted of an initial end conversion reaction step, followed by ligation of the insert and the vector and subsequent transformation of the NovaBlue Singles competent cells. The end conversion reaction step was required to phosphorylate the PCR product for ligation. In a 0.7mL-eppendorf tube, 2µL of the PCR product were combined with 3µL H₂O and 5µL of end conversion mix and incubated at 22°C for 15min. The reaction was then inactivated by heating at 75°C for 5min, followed by cooling on ice for 2min and centrifugation at 6000rpm. The insert prepared in the end conversion reaction (10µL) was then combined with 50ng of the blunt vector and 4U of T4 DNA ligase and incubated at 22°C for 1-2hrs. The required number of cells (20µL) were thawed on ice and transferred into pre-chilled 1.5mL-polypropylene tubes. An aliquot (1µL) of the ligation reaction was added directly to the cells, the components were mixed, and the tubes placed on ice for 5min. A heat shock was performed by heating the tubes for exactly 30s in a 42°C water bath. The tubes were placed on ice for 2min. Room temperature SOC (80µL) was then added and the tubes incubated at 200-250rpm at 37°C for 30-60min in a shaking incubator. Transformations (50µL) were spread on LB agar plates containing the appropriate antibiotics. Following an overnight incubation at 37°C the desired colonies were used to inoculate further cultures for amplification of the constructed plasmids.

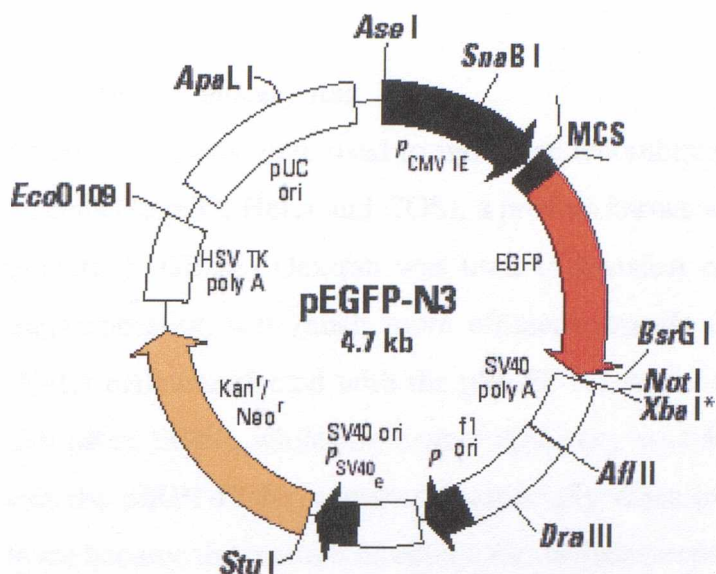
2.5.9 Antibiotic selection

Plasmids used for the cloning and manipulation of DNA have been engineered to harbour genes for antibiotic resistance. Bacterial transformations were plated onto media containing a certain antibiotic, and since only the bacteria which possessed the appropriate plasmid DNA would be able to metabolise the antibiotic and form

colonies, the bacterial cells containing the plasmid DNA were selected. Commonly used antibiotics were ampicillin ($1\mu\text{L}\cdot\text{mL}^{-1}$), tetracycline ($1.5\mu\text{L}\cdot\text{mL}^{-1}$) or kanamycin ($3\mu\text{L}\cdot\text{mL}^{-1}$), or a combination of the first two.

2.6 Plasmids

GFP is a 27kDa protein from the jellyfish *Aequorea victoria* that can be used as a fluorescent tag (cDNA for GFP has been cloned) and therefore as a localisation marker in living mammalian cells (Karlsson and Pines 1998). Clontech has modified GFP for brighter fluorescence (excitation maximum at 488 nm, emission maximum at 507 nm) and higher expression in mammalian cells and for insertion of proteins in frame at the N terminal of GFP. Rex is a 27kDa nucleocytoplasmic shuttle protein that predominantly localises to nucleoli. The pEGFP-N3 vector, depicted in Figure 2.1, was used to create the pIRP1-EGFP construct (gift from Dr. I Barjis) as well as the pRex-EGFP and pIRP2-EGFP constructs (Dr. K White). For the former construct, an *MscI* fragment of IRP1 was subcloned into *Ecl136II* in the multiple cloning site (MCS) of pEGFP-N3. The latter construct was created from a *SmaI-SnaBI* fragment of rat IRP2 cDNA (containing only the open reading frame) into *Eco47III* in the MCS of pEGFP-N3. The pRex-EGFP construct was created from a *PvuII-PmlII* fragment encoding Rex cDNA (containing no introns) from pSPRexHX5, fused into *SmaI* in the MCS of pEGFP-N3. pSPRexHX5 was created from a *HindIII-XmaI* fragment containing Rex cDNA (truncated form, N terminal 60 aa), presumably from pKCR27x, into the *HindIII-XmaI* sites of pSP72. The pKCR27x plasmid was constructed from pKCRH2. All constructs used were verified by DNA sequencing.



5'1 601 611 621 631 641 651 661 671
 GCT AGC GCT ACC GGA CTC **AGA** TCT CGA GCT CAA GCT TCG AAT TCT GCA GTC GAC GGT ACC GCG GGC CCG GGA TCC ATC GCC ACC **ATG** GTG
*Nhe*I *Eco*47 III *Bgl*II *Xba*I *Sac*I *Hind* III *Eco*R I *Pst*I *Sal*I *Kpn*I *Apa*I *Bsp*120 I *Bam*H I *Xba*I
*Ecl*36 II *Eco*RI *Hinc*II *Eco*R I *Pst*I *Sal*I *Kpn*I *Apa*I *Bsp*120 I *Bam*H I *Xba*I *Xcm*I
 EGFP

Figure 2.1 Diagrammatic representation of the pEGFP-N3 vector.

Diagram showing restriction map and multiple cloning site of pEGFP-N3. Unique restriction sites are shown in colour or bold. The *Not* I site follows the EGFP stop codon and the *Xba* I site (*) is methylated.

2.7 Cell manipulation

2.7.1 Transient transfection of eukaryotes

In this study two different methods were used to introduce recombinant vectors into cultured mammalian cells (HepG2, HeLa and COS), a process known as transfection. Initially, diethylaminoethyl (DEAE) Dextran was used to transfet cells, however, transfection with electroporation was much more efficient (transfection efficiency was up to 80% in HeLa cells transfected with the pEGFP-N3 vector and in HepG2 cells transfected with pRex-EGFP, while the lowest efficiency was 40% in HepG2 cells transfected with the pIRP1-EGFP construct), especially when examining GFP fluorescence and hence became the method of choice for the latter experiments.

2.7.1.1 Transfection of mammalian cells using DEAE-Dextran

The mechanism of action of DEAE-Dextran to promote uptake of DNA by cells is still unknown. It is thought that the polymer binds to DNA and inhibits nuclease activity and/or binds to cells and promotes endocytosis of the DNA (Lopata *et al* 1984). Cells at a density of $1\text{-}5 \times 10^5$ were plated out onto 9cm culture dishes 24 hrs prior transfection by which time the dishes would be 30-50% confluent. Cells at the required confluency for this procedure were washed three times in plain medium (RPMI-1640) prior to addition of the transfection mixture, after which they were incubated for 4hrs at 37°C. It was important that the transfection mixture contained the correct ratio of DNA to DEAE-Dextran, since if there were higher amounts of DNA than appropriate, the cationic charge on the DEAE-Dextran would have been neutralised or the complex may had become anionic and uptake by the cells would have been reduced. For each culture dish, a transfection mixture of $50\text{mg}\cdot\text{mL}^{-1}$ of DEAE-Dextran, molecular weight (M_r) ~500000Da (Pharmacia) with $10\mu\text{g}$ of plasmid DNA, in a solution of 0.05M Tris and plain medium in a final volume of 4mL was prepared. Following the 4hr incubation, the cells were washed twice with plain medium and a mixture containing chloroquine diphosphate was used to increase transfection efficiency. The cells were incubated for a further 3hrs in a mixture containing chloroquine (100 μM) in 3% plain and 7% full medium in a final volume of 10mL. The cells were finally washed twice with plain medium, and left to incubate in full medium. Transfection efficiency was analysed 48-72hrs later.

2.7.1.2 Transfection of mammalian cells by electroporation

Electroporation is a method in which cells are exposed to a brief, high-voltage electric impulse that creates rearrangement of the plasma membrane, thus making cells more permeable and allowing DNA to be taken up directly by diffusion (Chang 1992). Prior to transfection by electroporation, HeLa and HepG2 cells were seeded $1-5 \times 10^6$ per mL of full medium in 9cm culture dishes, aiming to achieve a confluence of 70-80% for HeLa cells and 80% for HepG2 cells on the day of transfection. Cells were harvested, counted, resuspended to 2.5×10^6 per mL in plain medium, and the cell suspension (0.4mL) was placed into a 0.2cm-electroporation cuvette containing plasmid DNA (10 or 40 μ g, depending on plasmid and type of cells transfected). Electroporation of HeLa cells was carried out using the pre-set protocol (160V, 500 μ F, exponential decay) in the GenePulser Xcell electroporation system (BioRad), whereas the electroporation protocol for HepG2 cells was optimised experimentally (optimum results obtained at 400V, 250 μ F, exponential decay) (Kumar *et al* 1994). The cells were pulsed once, immediately transferred to a culture dish, and cultured as described. Transient gene expression was assessed 24-48hrs following electroporation with a fluorescent inverted microscope (Olympus IX51, Olympus UK Ltd, Middlesex, UK). Transfected cells were usually fixed in 2% paraformaldehyde in PBS for 1hr at room temperature prior to observing GFP fluorescence.

2.7.2 Treatment of mammalian cells with ferric ammonium citrate

COS and HepG2 cells were seeded in 9cm culture dishes at 5.5×10^5 and 7×10^5 cells, respectively. Cultures were maintained for 7 days and iron loading was achieved by culturing the cells for a further 7 days in full medium containing 100 μ M ferric ammonium citrate (FAC; containing 16.5-18.5% Fe by weight), a chemical that is similar in its effects to NTBI and implicated in the development of iron overload (Batey *et al* 1980). Untreated cells, grown concomitantly for the same number of days, served as controls.

2.7.3 Atomic absorption spectrometry of iron

Paired cultures of cells growing in normal or iron-rich media were set up and maintained as described in 2.3.1 and 2.7.2. Cells were harvested as described in 2.3.1

(cell pellets from 4-5 plates were pooled together to achieve required cell volumes) and the acquired cell pellets were split into equal halves. To analyse the effect of iron treatment an aliquot (~200 μ L) from each set was mixed with an equal volume of 10mM HNO₃ in 1.5mL-eppendorf tubes. Digested samples were diluted up to 10mL with purite H₂O in 10mL-volumetric flasks for analysis by flame atomic absorption spectrometry in a SpectrAA 220 Atomic Absorption Spectrometer (Varian UK Ltd, Walton-on-Thames, U.K.). The flame type in the spectrometer was air acetylene and the lamp used was a hollow cathode lamp, Fe, P826 wavelength 248.3nm (Photron, Pty Ltd, manufactured in Australia). Iron concentration was determined by comparison with a calibration curve of 100 to 500mg Fe per mL (1-5 ppm) prepared from a standard solution of 1000mg·L⁻¹ (or 1000 ppm). Iron content was expressed as ppm and then converted to mg of Fe (Parkes and Templeton 1994). To estimate the amount of iron per μ g of protein, protein concentrations were measured using the Lowry assay (section 2.8.3.1), with a few modifications adapted from a protocol by Markwell *et al* (1978). Equal aliquots of the cells used for iron analysis were dissolved in PBS. The aliquot of the cells in PBS (50 μ L) was mixed with an equal volume of 1M NaOH and incubated at 37°C overnight. Following the overnight digestion, the protein content was measured using an aliquot of the dissolved pellet (20 μ L) and bovine serum albumin (BSA) at 0.1mg·mL⁻¹ to construct a standard curve. Standards and samples were prepared in duplicate and average values were used in generating the standard curve and estimating protein concentrations of samples. The uptake of iron from COS and HepG2 cells was expressed as the ratio of total μ g of Fe per total μ g of protein and experiments were performed six times. Atomic absorption of iron and protein concentrations of samples were measured in duplicate within each experiment and averaged values were expressed as mean \pm standard deviation (SD) from each experiment averaged between the six.

2.8 Protein extraction and Western blotting

Western blotting, also known as protein blotting or immunoblotting, evolved from DNA (Southern) blotting (Southern 1975) and RNA (Northern) blotting (Alwine *et al* 1977). The term Western blotting was coined by Burnette (1981) in keeping with the “geographic” naming tradition initiated by Southern, and involves the transfer of proteins from an SDS polyacrylamide gel onto an adsorbent membrane (Towbin *et al*

1979). The blotted membranes form a replica of the gel and the nitrocellulose bound proteins of interest can be detected with the use of specific antibodies raised against recognised epitopes of the protein of interest. The starting material and cellular localisation of the protein to be immunodetected determined the procedures that could be used in obtaining an extract that contained the protein in a soluble form. Different procedures and lysis buffers were therefore used for the preparation of appropriate protein extracts from cells and liver tissue specimens.

2.8.1 Protein extraction from cultured cells

2.8.1.1 Extraction of endogenous IRP1 and IRP1-GFP

To obtain cytoplasmic extracts of endogenously expressed proteins or following transfection, cells were harvested as described under 2.3.1, transferred into 15mL-sterilin tubes and the cell pellet washed in 10mL PBS. The pellet was then transferred to a 1.5mL-eppendorf tube and spun at 12000rpm for 1min. The pellet was resuspended in an equal volume of ice-cold 0.5% Triton X-100, 1mM phenyl methylsulphonyl fluoride (PMSF), 1mM pepstatin A in PBS and centrifuged again at 12000rpm for 1min. The acquired supernatant, containing the cytosolic proteins, was retained for use in further experiments.

2.8.1.2 Cytoplasmic, membrane and nuclear fractionation of IRP1-GFP

Cytoplasmic, membrane and nuclear fractionation of IRP1 and IRP1-GFP was carried out following slight adaptations to the protocol by Seiser *et al* (1995). Cells were cultured and harvested as described and the cell pellet resuspended in ice cold PBS and transferred to 1.5mL-eppendorf tubes to be centrifuged at 12000rpm for 1min. The resulting cell pellet was resuspended in 1 volume of ice cold hypotonic lysis buffer (10mM HEPES, pH 7.5; 40mM KCl; 3mM MgCl₂; 0.5% TX-100) and left on ice for 5min, then centrifuged at 12000rpm for 15s and the supernatant retained. The pellet was washed in 1 volume of lysis buffer and the combined supernatants were the cytoplasmic fraction. The pellet was then washed with 1 volume deoxycholate (DOC) buffer (lysis buffer with 0.5% DOC) and spun at 12000rpm for 1min. The supernatant was retained, the extraction with the DOC buffer repeated and the combined supernatants formed the membrane extract. Finally, 1 volume of nuclear extraction buffer (10mM HEPES, pH 7.5; 1.0M KCl; 3mM MgCl₂; 0.5% TX-100) was added to the pellet, which was grinded with a few

strokes of a hand homogeniser. The tube was placed on ice for 10min and then 20 μ L DNase1 (1mg·mL⁻¹) and 2 μ L RNase A (10mg·mL⁻¹), were added per 100 μ L extract. The tube was incubated at 37°C for 15-30min with occasional pipetting. Depending on the viscosity of the sample, after the 37°C incubation period, the sample was centrifuged at 12000rpm for 10min. The resulting supernatant was the nuclear solubilisate.

2.8.1.3 Extraction of TfR2

Cell lysates were prepared from HepG2 cells following the procedure described by Griffiths and Cox (2003). Cells were seeded at 1x10⁶ in 9cm culture dishes (minimum of two dishes) and harvested as previously either from confluent or following 7 day FAC treatment. The resulting cell pellet (pooled together) was resuspended in an equal volume of lysis buffer [0.02M Tris; 0.1M NaCl; 1mM EDTA; 1% Triton-X 100 (v/v), pH 6.8] with 1 μ L protease inhibitor cocktail per 100 μ L buffer and incubated at 4°C for 1hr with intermittent vortexing. The suspension was then centrifuged at 10000rpm for 15min at 4°C and the resulting supernatant containing TfR2 was stored at -20°C for use in further experiments.

2.8.2 Protein extraction from liver tissue

2.8.2.1 Extraction of IRP1 from liver tissue

Proteins were extracted from frozen liver biopsies (~200mg) by homogenising the tissue in an equal amount in volume of homogenizing buffer [HDG; 25mM HEPES buffer; 10% (v/v) glycerol; 15.4mM dithiothreitol (DTT); 17.4mM PMSF; 1mM pepstatin A] with the aid of the microtissue grinder and the Ultra Turrax T25 electric homogeniser (Labrotechnik, Staufen, Germany). Samples were homogenised in 15s bursts followed by intervals on ice. Samples were then transferred to 1.5mL-eppendorf tubes and centrifuged at 14000rpm for 20min, at 4°C. The liquid interphase was retrieved, transferred to fresh 1.5mL-eppendorf tubes and stored at -80°C for use in further experiments. Protein concentrations of the acquired protein extracts were determined by the method of Lowry (section 2.8.3.1).

2.8.2.2 Extraction of TfR2 from liver tissue

Proteins were extracted from 10mg of frozen human liver homogenised in 0.1mL lysis buffer for TfR2 as described under 2.8.1.3 (Griffiths and Cox 2003). Protein concentrations were determined using the total protein assay (BioRad) based on the Bradford method (section 2.8.3.2).

2.8.3 Determination of protein concentration

2.8.3.1 Determination of protein concentration by the Lowry method

Total protein concentration can be determined using the Folin phenol reagent by the procedure originally described by Lowry *et al* (1951). An aliquot (usually 20 μ L) of the sample to be assessed for protein concentration was diluted up to 400 μ L in H₂O. With a similar final volume, solutions to construct a standard curve were prepared by carrying out up to six dilutions of BSA (1mg·mL⁻¹) with a protein range from 0-1mg·mL⁻¹. All samples and standard solutions were prepared and assayed in duplicate. To each tube 2mL of Reagent C [25mL reagent A (2% Na₂CO₃ in 0.1M NaOH) and 0.5mL reagent B (0.5% CuSO₄·5H₂O in 1% sodium tartrate)] were added and the solution was allowed to stand for 10min. Then, 200 μ L of Reagent D (Folin-Ciocalteau's phenol reagent working solution) were added into each tube and the solutions were quickly mixed and allowed to stand for 30min. After 30min, the absorbance of each sample at 750nm was measured.

2.8.3.2 Determination of protein concentration by the Bradford method

This method is based on the binding properties of the dye Coomassie Brilliant Blue G-250 to proteins and cause of a shift in the absorbance maximum of the dye from 465nm to 595nm in acidic conditions, described by Bradford (1976). Generally, BSA (0.1mg·mL⁻¹) was used in generating a standard curve (protein range 0-16 μ g· μ L⁻¹) in standards with 800 μ L final volumes. This was the method of choice when minute amounts of samples could be spared (such in the case of samples from percutaneous liver biopsies). The assay required 1 μ L of unknown sample in 799 μ L H₂O, to which the BioRad reagent (200 μ L) was added and the solution incubated for 5min. Absorbance of solutions was measured at 595nm.

2.8.4 Separation of proteins using SDS-PAGE

2.8.4.1 Preparation of the samples for Western blotting

Prior to electrophoresis, the samples were diluted in buffer containing, SDS [$\text{CH}_3-(\text{CH}_2)_{10}\text{CH}_2\text{SO}_3^-\text{Na}^+$], an anionic detergent that binds strongly to and denatures the protein, and β -Me, which reduces any disulphide bonds stabilising the protein. The sample buffer also contained an ionisable tracking dye (BPB) and glycerol to give the sample solution density. Usually samples containing 20-100 μg of protein in a final volume of 20 or 40 μL in 2x SDS sample buffer [100mM Tris, pH 6.8; 4% SDS; 10% β -Me; 0.1%w/v BPB; and 20% glycerol] were prepared. Samples were then heated at 95°C for 2-5min to denature the proteins and expose the total length of the polypeptide chain to the detergent. After cooling, SDS polyacrylamide gel electrophoresis (SDS-PAGE) was performed, followed by immunoblotting with specific antibodies to detect the amount or presence of protein of interest in the samples.

2.8.4.2 Preparation of the SDS polyacrylamide gel

Discontinuous SDS-PAGE (Laemmli system) was employed for the separation of proteins in the homogenised liver samples or cell culture extracts. The term discontinuous refers to the difference in buffer ions and pH between the gel and the running buffer. In this method, a non-restrictive large pore gel, called the stacking gel was layered on top of a separating running gel and the proteins were separated according to their molecular weight. The position of a protein along the lane gave a good approximation of its size, and after staining the intensity of the band was an approximate indicator of the amount of protein present in the sample (Laemmli 1970).

2.8.4.3 Preparation and running of the SDS polyacrylamide gel

Discontinuous SDS-PAGE was set up by preparing a separating or running (bottom) gel [usually 7.5% acrylamide, unless stated otherwise, from a 30% (w/v) 29:1 acrylamide:bisacrylamide stock, AccuGel (National Diagnostics, Fradley, U.K.); 1.5M Tris, pH 8.8; 10% SDS; 100 μL 10% ammonium peroxodisulphate (APS) and 20 μL N,N,N',N'-tetramethylethylenediamine (TEMED), the two latter added just before pouring the gel] and a stacking (top) gel [4%acrylamide (from a 30%-0.8%

acrylamide:bisacrylamide stock; 0.1% SDS; 0.5M Tris, pH 6.8. with 10 μ L 10% APS and 10 μ L TEMED, added just before pouring)]. A separating gel of 7.5% can resolve proteins ranging between 36 to 94kDa (Sambrook *et al* 1989).

Samples were loaded into each well using a glass syringe (Scientific Glass Engineering Ltd), and the gel was run in running buffer (25mM Tris; 192mM glycine; 0.1% SDS) at a constant current of 10mA. Once electrophoresis was completed (indicated when the BPB colour marker had reached the end of the running gel) the gel was placed in tris buffered saline (TBS) (100mM Tris; 0.9% NaCl) for 2min. The TBS was replaced by Towbin transfer buffer (TTB) (25mM Tris; 192mM glycine; 20% methanol; 0.1% SDS) and the gel was left to equilibrate for 10min. The gel was then positioned on a nitrocellulose membrane (Hybond C+, Amersham, U.K.) and sandwiched between four pieces of blotter paper (Whatman, 3MM Chr). All membrane types were soaked in TTB for 2-5min before use. An overnight transfer was then carried out at a constant voltage of 10V, at 4°C.

2.8.4.4 Coomassie Brilliant Blue staining

To ensure equal loading between different lanes, gels were prepared and following SDS-PAGE were stained in Coomassie Brilliant Blue staining solution (80% methanol; 20% glacial acetic acid; 0.5g·L⁻¹ Coomassie Brilliant Blue R250) on a rocking platform for 60min. To visualise total protein bands the gels were placed in destaining solution (7% acetic acid, 5% methanol) overnight. If staining was of equal intensity between all lanes, that indicated that the concentration was correctly assessed and electrophoresis was repeated and followed by immunoblotting of the membranes. Total protein bands between different lanes were always of similar intensity indicating equal loading of proteins and when that was not the case the determination of protein concentration and staining of the gel were repeated.

2.8.5 Western blotting

Equal amounts of protein (usually 20-100 μ g per lane, as indicated in the respective figure legends) were separated by SDS-PAGE and transferred to nitrocellulose membranes as described. The membranes were pre-incubated in TBS and then incubated with blocking buffer, containing 5% non-fat milk in wash buffer [0.2%

polyoxyethylene-20-sorbitan-monolaurate (Tween-20) in TBS]. The length of the incubation in the blocking buffer and the subsequent steps of immunoblotting with a specific antibody varied between different experiments. All steps were carried out at room temperature and required constant shaking, except for the final colorimetric step, which after addition of reagents was allowed to proceed in the dark with minimal agitation.

2.8.5.1 Immunodetection of IRP1

The membrane was pre-incubated with blocking buffer for 30 min prior to incubation with the primary antibody for 2hrs. The primary antibodies used for detecting IRP1 have been well characterised and were rabbit anti-whole rat liver IRP1, rabbit anti-peptide A (VDFNRRADS¹³⁸LQKNQDLEFERNRC; residues 130-151) and rabbit anti-peptide B (NSYGS⁷¹¹RRGNDAVMARC; residues 707-721) of human IRP1 (gift of Dr. R. Eisenstein, Dept of Nutritional Sciences, University of Wisconsin, Madison, Wisconsin, 53706, U.S.A.) (Eisenstein *et al* 1993). Figure 3.1 (Chapter III) shows the position of the peptides on the IRP1 translated sequence. Primary antibodies were used diluted 1:1000 in blocking buffer. The secondary antibody was a biotin-SP-conjugated affinipure goat anti-rabbit IgG (Jackson ImmunoResearch Laboratories Inc., Soham, U.K.) that was diluted 1:2000 in blocking buffer and required a 1hr incubation. There was a further incubation of the membrane in streptavidin-alkaline phosphatase (strep-AP) diluted 1:1000 in 1% non-fat milk in wash buffer, for 1hr. In between all incubations, membranes were washed three times in wash buffer. Protein bands were visualised with the colorimetric method described under 2.8.5.4.

2.8.5.2 Immunodetection of TfR2

The antibody used in the immunodetection of TfR2 was a mouse monoclonal anti-human TfR2 antibody that was raised against the ectodomain of TfR2 (Clone 9F8 1C11, HyCult Biotechnology b.v., Uden, Netherlands). The membrane was pre-incubated with blocking buffer for 2hrs prior to incubation with the primary antibody diluted 1:1000 in blocking buffer for a further 2hrs. The secondary antibody, a biotin-SP-conjugated donkey anti-mouse IgG (Jackson ImmunoResearch Laboratories Inc.) was diluted 1:2000 in blocking buffer and incubated for 1hr. There was a further incubation in strep-AP diluted 1:2000 in 1% non-fat milk in wash

buffer, for 1hr. In between all incubations, membranes were washed three times (5min each wash) in wash buffer. Protein bands were visualised with the colorimetric method described under 2.8.5.4.

2.8.5.3 Immunodetection of GFP and actin

For the detection of GFP, the membrane was pre-incubated with blocking buffer for 30min prior to incubation with the primary antibody for 2hrs. The primary antibody, a rabbit polyclonal anti-GFP anti-serum (AbCam, Cambridge, U.K.), raised against a highly purified recombinant GFP made in *E. coli*, was used diluted 1:2500 and was followed by incubation with the secondary antibody (biotin-SP-conjugated affinipure goat anti-rabbit IgG), diluted 1:2000 in blocking buffer and incubated for 1hr. Membranes were then incubated for 1hr in strep-AP diluted 1:1000 in 1% non-fat milk in wash buffer followed by development of bands with the colorimetric method (2.8.5.4). In between all incubations, membranes were washed three times in wash buffer. Similarly for the immunodetection of actin, a rabbit anti-actin anti-serum diluted 1:1000 was used and all incubation and detection steps were as described above.

2.8.5.4 Colorimetric detection

The final step of the immunodetection was the incubation of membranes in AP substrate. The technique utilises the fact that an AP reporter enzyme is attached to the secondary antibody via a biotin-avidin link. Biotin is conjugated to both the secondary antibody and the enzyme used for visualisation. Relying on the specific binding properties of biotin and avidin, a complex of streptavidin and biotynilated AP is added to the membrane. Because streptavidin will bind more than one molecules of biotin, the amount of enzyme at each specific protein location will be amplified. Membranes were incubated with 5-bromo 4-chloro 3-indoylphosphate [BCIP, 50mg·mL⁻¹ in 100% dimethylformamide (DMF)] and nitro blue tetrazolium (NBT, 50mg·mL⁻¹ in 70% DMF) substrate diluted in AP buffer [100mM Tris, pH 9.5; 100mM NaCl; 100mM MgCl₂] for 1hr. Once the bands appeared, the membranes were washed in water to quench the staining.

2.9 First strand synthesis and real-time polymerase chain reaction

Different protocols for the optimal reverse transcription of RNA were used depending on the type of Polymerase Chain Reaction (PCR) (nested PCR or real-time PCR) that was to follow. PCR primers were designed using "Primer 3", which is available at <http://www-genome.wi.mit.edu/cgi-bin/primer/primer3.cgi>.

2.9.1 Synthesis of cDNA strand for nested PCR analysis

Total RNA (1 μ g) from cells was reverse transcribed in a final volume of 40 μ L using ImPromII Reverse Transcriptase (RT) as follows: initially, total RNA (1 μ g) was diluted up to 15 μ L with the appropriate amount of RNase free H₂O and heat denatured at 70°C for 5min. Pre-incubated (70°C for 5min) primers (25 μ M dT₁₅) were added to the diluted RNA and the solution incubated first at 70°C for 5min, and then chilled on ice for 5min. The following reverse reaction components were then added before adding the ImProm-II RT: 0.75x RT-buffer [250mM Tris-HCl (pH 8.3 at 25°C); 375mM KCl; 50mM DTT], 1.5mM MgCl₂, 0.25mM dNTPs and RNasin. The volume was made up to 40 μ L with diethylpyrocarbonate H₂O. At this point an RT negative sample was prepared before adding 1U of ImProm-II RT to the remaining mixture. Reverse transcription was initiated by annealing the primers at 25°C for 5min, chain extension of first strand at 37°C for 60min and a heat inactivation of ImPromII-RT at 70°C for 15min.

2.9.2 Synthesis of cDNA Strand for real-time PCR analysis

Total RNA (1 μ g) extracted from liver tissue was reverse transcribed into single-stranded complementary DNA (cDNA) using avian myeloblastosis virus reverse transcriptase (AMVRT). Initially, 1 μ g of RNA was made up to 10.5 μ L in RNase free water and incubated at 65°C for 3min. The following reaction components were added: 1x RT-buffer (250mM Tris-HCl; 250mM KCl; 50mM MgCl₂; 2.5mM spermidine; 50mM DTT), 1mM dNTPs, 2.5mM DTT, 15U RNase inhibitor, 150U AMVRT and random decamer primers 2 μ g· μ L⁻¹ (Promega) to a final volume of 20 μ L and reactions were incubated at 42°C for 90min. RNase free H₂O (20 μ L) was then added to the reactions, which were incubated at 100°C for 5min. A control RNA reaction without the RT was included in order to check for genomic DNA contamination.

2.9.3 Nested PCR

Nested PCR comprised two rounds, a first, outer round using primers spanning exons 1 and 21 of IRP1 and a second, inner round, using primers spanning exons 4 and 18. Reaction components of the first round were 10x ThermoPol buffer, 0.5mM primers, 0.2mM dNTPs, 2mM MgSO₄, appropriate amount of H₂O and 1U Taq polymerase in a volume of 40µL, followed by the addition of template cDNA (10µL) to a final volume of 50µL. The reactions were overlaid with mineral oil and cycling conditions were 30 cycles of denaturation at 95°C for 1min, primer annealing at 58°C for 1min, extension at 72°C for 3min and a final cycle of extension at 72°C for 10min. For the second round, the reaction component concentrations were similar to those used in the first round of PCR and the main difference was the amount and nature of the template. In the second round only 1µL of template was used, which was the PCR product of the first round. Cycling conditions were 1 cycle of denaturation at 95°C for 3min, followed by 30 cycles of denaturation at 95°C for 1min, primer annealing at 58°C for 1min, extension at 72°C for 2min and a final cycle of extension at 72°C for 10min. PCR product identity was confirmed via agarose gel electrophoresis and sequencing. Primers used for nested PCR were from EUROGENETEC Ltd (Romsey, U.K.). First round primer set (IRP1ex) was as follows: forward CTGCTTGGGTCAGGTCG, reverse CCCACCATTCTAGCTT CCAA, giving rise to a 1899bp product corresponding to the full length of IRP1. And the second round primer set (IRP1s) was: forward GTCTGCCCTGCTGATCT TGT and reverse GATTCCCCAGAAGGCAGAT. Appendix II contains the IRP1 sequence and highlights positions recognised by the primers used.

2.9.4 Real-time quantitative PCR

Quantitative real-time PCR (qRT-PCR) experiments were performed using a Light Cycler™, (LightCycler ID: 4250) (Roche Diagnostics, East Sussex, U.K.) at the Molecular Biology Unit (MBU), School of Biomedical Sciences, King's College London, U.K. and all required reagents and consumables were also from Roche Diagnostics. The LightCycler instrument allowed amplification and detection in the same tube based on the simultaneous measurement of the fluorescence of SYBR Green I, which has a maximum emission wavelength at 520nm and binds specifically to the minor groove of dsDNA (Morrison *et al* 1998). The LightCycler-FastStart

DNA Master SYBR Green I kit was used for the amplification of the cDNAs in 10 μ L reaction volumes set up in glass microcapillary tubes and was monitored after each elongation step, by SYBR Green I dye binding to amplified products. Table 2.1.1 indicates the primers used, the expected size of the amplicon and the exons spanned on the corresponding cDNA sequence. Table 2.1.2 indicates the optimum MgCl₂ and acquisition temperature for each primer set, while table 2.2 lists the cycling conditions for each gene explicitly. Primers used were from EUROGENETEC Ltd, except for the IRP1 (GENSET SA, Paris, France) and β -actin set of primers (gift from Dr. Yas Heidari, Randal Centre for Molecular Mechanisms of Cell Function, King's College London, U.K.).

Table 2.1.1 Sequences of primers, orientation, size of amplicon and regions amplified for quantification of genes in qRT-PCR

Human Gene Symbol	GenBank Accession Number	Position of Sequence	Forward Primer 5' → 3'	Reverse Primer 5' → 3'	Size of Amplicon (bp)
<i>HAMP</i>	AF309489	Exons 2-4	CCTGACCAGTGGCTCTGTT	CAGGGCAGGTAGGTTCTACG	180
<i>HJV/HFE2</i>	AK092682	Exon 4	AACCATGTGGAGATCCAAGC	TTATAGCTCCCCGACGATTG	202
<i>IRP1/ACO1</i>	Z11559	Exons 16-18	AAGCTGGAATGCCTTAGCAA	CTCGTGGAGTTAGGCCTCTG	252
<i>TfR1/TFRC</i>	X01060	Exons 11-13	AAAATCCGGTGTAGGCACAG	TTAAATGCAGGGACGAAAGG	179
<i>TfR2/HFE3</i>	AF067864	Exons 1-2	TGGGGTCTATTCCAGAGAGC	TTCCTCTCCTCCTCCAGGT	110
<i>ACTB</i>	X00351	Exons 3-4	AGAAAATCTGGCACCAACACC	TGATCTGGGTCATCTTCTCG	120

Table 2.1.2 Optimal cycling conditions for quantification of HAMP, HJV, IRP1, TfR1, TfR2 and β-actin in qRT-PCR
Acquisition temperature refers to the temperature at which fluorescence measurements were taken.

Human Gene Symbol	MgCl ₂ Concentration (mM)	Cycle Conditions		
		Annealing Temp (°C)/Time (s)	Extension Temp (°C)/Time (s)	Acquisition Temp (°C)/Time (s)
<i>HAMP</i>	4			86/5
<i>HJV</i>	5			86/5
<i>IRP1</i>	5		72/10	82/5
<i>TfR1</i>	5	55/10		86/5
<i>TfR2</i>	5			84/5
<i>β-actin</i>	4		72/7	87/5

2.9.4.1 Optimisation of real-time PCR runs

In order to achieve optimal real-time PCR conditions the optimum magnesium chloride concentration, annealing temperature and acquisition time for each primer set had to be established. For each primer combination, the optimum MgCl₂ concentration and annealing temperature were determined experimentally in a trial run on control samples using MgCl₂ concentrations ranging from 1-5mM (Figure 2.2A). For most primer pairs a MgCl₂ concentration of 5mM and an annealing temperature of 55°C was most optimal, while for *β-actin* and *HAMP* an optimal MgCl₂ concentration of 4mM was determined to obtain a specific and efficient amplification (Tables 2.1.2 and 2.2). Once the optimum MgCl₂ concentration for each set of primers was established by melting curve analysis (Figure 2.2B) and by running the PCR products on a gel (Figure 2.2C), the bands were cut out and purified (as described under section 2.5.7.2) (Figure 2.2D). The concentration of the pure product containing the amplicon sequence was determined by comparison to a marker with bands of known concentration expressed in fg·μL⁻¹.

Each dsDNA has its own specific melting temperature (T_m), which is defined as the temperature at which 50% of the DNA becomes single stranded, and 50% remains double stranded, and checking the T_m of the PCR products can be compared with analysing a PCR product by length in agarose gel electrophoresis (Figures 2.2B and 2.2.C). Performing a melting curve analysis after a trial run differentiated the product of interest from other non-specific products (such as primer-dimers) formed. Non specific products are also dsDNA and therefore bind SYBR Green I dye, however tend to give a lower T_m (Figure 2.2E). Once the T_m of the PCR product was known, the specificity of the reaction was increased further by running the samples again and measuring the fluorescence at 1°C below the T_m . Since non-specific products melt at lower temperatures than the T_m of the specific product, the only fluorescence measured at that temperature, referred to as the acquisition temperature was that generated by the product (Table 2.1.1 and Figure 2.2F). The optimisation steps described here increased sensitivity and specificity of the experiment, resulting in a melting curve that showed a single peak relating to the specific product (Figure 2.2E).

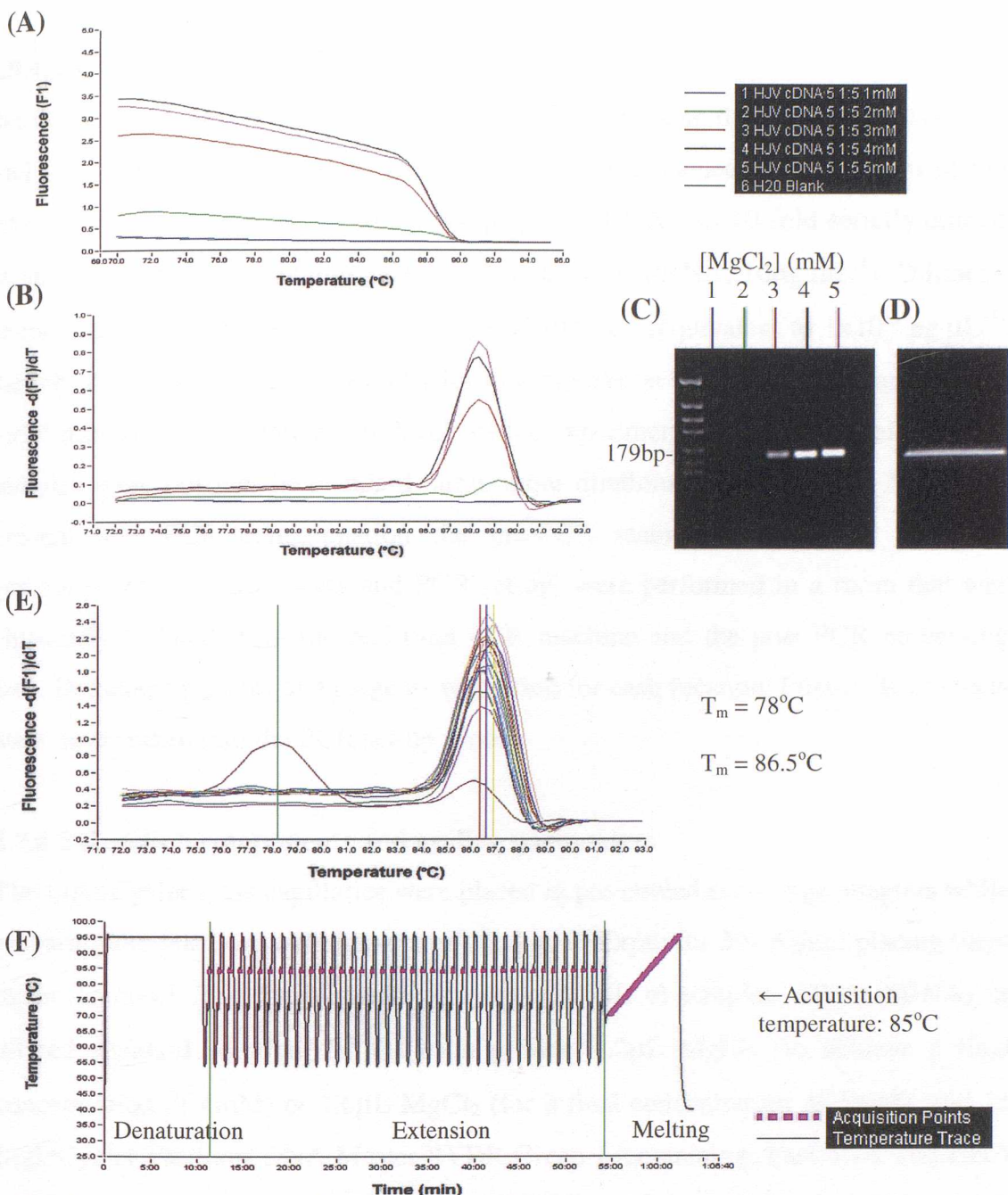


Figure 2.2 Real-time PCR optimisation via magnesium chloride titration and use of appropriate acquisition temperature (T_m).

(A) Detection of HJV amplified in the presence of magnesium concentrations that ranged from 1-5mM. Plot of SYBR Green I fluorescence versus temperature and (B) plot of the negative derivative of fluorescence ($-dF/dT$) versus temperature. (C) Optimum magnesium concentration established at 4mM by agarose gel electrophoresis analysis of the amplified products, which were then pooled and once purified served as standards (D). (E) Standards and unknowns generated a specific melting peak characterised by the same melting temperature ($T_m = 86.5^\circ\text{C}$). Non-specific products or primer-dimers had a lower T_m (78°C). (F) Plot of fluorescence versus time indicated acquisition temperature for the specific amplification of the HJV transcript based on its T_m .

2.9.4.2 Preparation of standards

Standards were prepared by amplification purification using the PCR products of the trial run (2.9.4.1). Standards of known concentration enabled the estimation of the levels of expression in the unknown samples. The DNA was 10-fold serially diluted in nuclease-free H₂O containing carrier transfer RNA (tRNA; 10µg·mL⁻¹). Dilutions of the standards were usually in the range of 10⁻³-10⁻⁸ (equivalent to 1x10⁻³ pg·µL⁻¹) though often reached 10⁻¹² especially for low expression transcripts. The range of the serial dilutions had to fall within levels of the experimental samples, therefore when samples were outside the standard curve more dilutions were included. Finally, to prevent any PCR contamination the pre-PCR manipulations (DNA isolation, generation of standard curves and PCR set-up) were performed in a room that was physically isolated from the real-time PCR machine and the post-PCR processing area. Dedicated pipettes and reagents were used for each location. Post-PCR products were never taken into the PCR set-up room.

2.9.4.3 Reaction components and cycling parameters

The LightCycler glass capillaries were placed in pre-cooled centrifuge adapters while preparing the reactions and then centrifuged at 2000rpm for 30s before placing them in the carousel. The 20µL reactions contained 1µL of template DNA (cDNA) or diluted standard solution, 0.5µM each primer, 1.2µL MgCl₂ (to achieve a final concentration of 4mM) or 1.6µL MgCl₂ (for a final concentration of 5mM), and 1x LightCycler FastStart DNA Master SYBR Green I (containing: Fast Start Taq DNA polymerase, reaction buffer, dNTP mix, SYBR Green I dye and 10mM MgCl₂). Each run along with the unknown samples contained a series of at least 6 standard dilutions, a control reaction containing H₂O instead of template and RT negative controls, to detect possible contamination of the mastermix or genomic contamination. The cycling protocol after an initial denaturation step (95°C for 600s), followed 40 cycles of a four-segment amplification and quantification program (denaturation, annealing, elongation, acquisition) with a single fluorescence measurement, 1 melting cycle (65°C to 95°C at 0.1°C·s⁻¹ and continuous fluorescence measurements) and a final cooling cycle down to 40°C (Table 2.2). The required elongation time was calculated by dividing the length of the product by 25 (Roche

Diagnostics. LightCycler FastStart DNA Master SYBR Green I. Instruction manual, version 6, 2002).

Table 2.2 Specific cycling conditions for quantification of HAMP, HJV, IRP1, TfR1, TfR2 and β-actin in qRT-PCR

Human Gene Symbol	Denaturation ¹	Amplification			Melting ³	Cooling
		Annealing Segment 1	Segment 2	Elongation ²		
	Temp (°C)/Time (s)	Temp (°C)/Time (s)	Temp (°C)/Time (s)	Temp (°C)/Time (s)	Temp (°C)/Time (s)	Temp (°C)/Time (s)
<i>HAMP</i>	95/600	95/15	55/10	72/10	70/30	40/45
<i>HJV</i>	95/600	95/15	55/10	72/10	70/30	40/45
<i>IRP1</i>	95/600	95/15	55/10	72/10	70/30	40/60
<i>TfR1</i>	95/600	95/15	55/10	72/10	70/30	40/45
<i>TfR2</i>	95/600	95/15	55/10	72/10	70/30	40/45
<i>β-actin</i>	95/600	95/15	55/10	72/7	75/30	40/45

¹ Pre-incubation time to activate the Fast-Start Taq DNA polymerase.

² The elongation time was calculated by dividing the length of the product (bp) by 25.

³ Melting from 65°C to 95°C at 0.1°C per sec.

2.9.4.4 Confirmation of PCR product identity

Confirmation of PCR product identity was achieved via melting curve analysis, followed by purification and sequencing of the products. During the melting cycle, fluorescence of SYBR Green I dye bound to the dsDNA drops as the fragment becomes denatured, and the turning point of that plot (Figure 2.3B) gives rise to the melting peak (Figure 2.3C and 2.3D). The T_m of the melting curve generated by amplification of the transcript in the unknown samples (Figure 2.3D) was compared to the T_m generated by the standards (Figure 2.3C) and was always of similar value (values provided in Chapter IV), therefore confirming product identity. The PCR products were pooled and subjected to 1.5% low melting agarose gel electrophoresis, which resulted in a single band with the desired length (Figure 2.2D). Purified products (Figures 4.1 and 4.2) were sequenced using their corresponding primers and following the dideoxy or chain termination method in an automatic sequencer ABI Prism 3100 Genetic Analyser at the MBU, King's College London, UK. Amplified sequences had 95-99% identity with their expected corresponding human sequences as determined by BLAST analysis.

2.10 Data acquisition and evaluation

2.10.1 LightCycler data acquisition

Real-time PCR quantitative analysis was performed using the fit points method of the LightCycler Software data analysis (version 3.5.28). The SYBR Green I signal of each sample was plotted versus the number of cycles (Figure 2.3A). Baseline fluorescence may vary from sample to sample, therefore, using the LightCycler analysis software, background fluorescence was removed by setting a noise band. For data acquisition in all runs the noise band was positioned at a point where the line crossed all sample curves at the lower part of the log-linear phase (when fluorescence was plotted against cycle number), excluding all background noise (Figure 2.3E). The upper border of the log-linear phase was then set by selecting the number of fit points and selection of the fit points was restricted to the linear phase of the PCR curve (Figure 2.3E, top panel). The fluorescence threshold set was then used to determine cycle numbers or crossing points (C_p), which indicated where the signal curve crossed an arbitrary threshold intersecting the signal curves in their exponential phases. The C_p values are proportional to the logarithms of the initial target concentrations (Figure 2.3E, bottom panel). A calibration curve of the C_p

values of the standard dilution series versus the concentrations of the unknowns was calculated and used to determine the concentrations of the unknowns, based on their C_p values, which was done automatically by the software (Figure 2.3F).

Real-time PCR efficiencies for each run were calculated from the given slopes generated by the software. The corresponding real-time PCR efficiency (E) of one cycle in the exponential phase was calculated according to equation 2.5:

$$E = 10\left(\frac{-1}{slope}\right)^{-1} \quad (\text{Equation 2.5})$$

The correlation coefficient (r) of all standard curves was -1.000, showing a linear relationship between the efficiency of target amplification and the slope, and the error for all runs was less than 0.2. (Roche Molecular Biochemicals, Technical Note No LC12/2000)

2.10.2 Calculation of copy numbers

Real-time PCR runs were performed two to three times to account for inter-assay variability and concentrations (generated as above) between runs were compared and an average value for each sample and transcript calculated. Since the length of the PCR products was known, the average concentration of each sample was used in estimating copy numbers per μL of cDNA for each transcript that was calculated using equation 2.6.

$$\text{Copy number} = \text{mg DNA} \times \left(\frac{\text{pmol}}{660 \text{ pg}}\right) \times \left(\frac{10^6 \text{ pg}}{1 \mu\text{g}}\right) \times \left(\frac{1}{\text{No. bp}}\right) \quad (\text{Equation 2.6})$$

where No. bp is the size of the amplicon, and 660 is the mean molar mass of a base pair

The suitability of the chosen housekeeping gene (β -actin) in terms of stability was checked by ensuring that the levels of β -actin remain comparable between controls and iron loaded samples. Values (in $\text{fg} \cdot \mu\text{L}^{-1}$) from a minimum of two runs were averaged and copy numbers calculated and normalised to β -actin. Any samples that demonstrated strange amplification kinetics or had different T_m were excluded from any further statistical analysis.

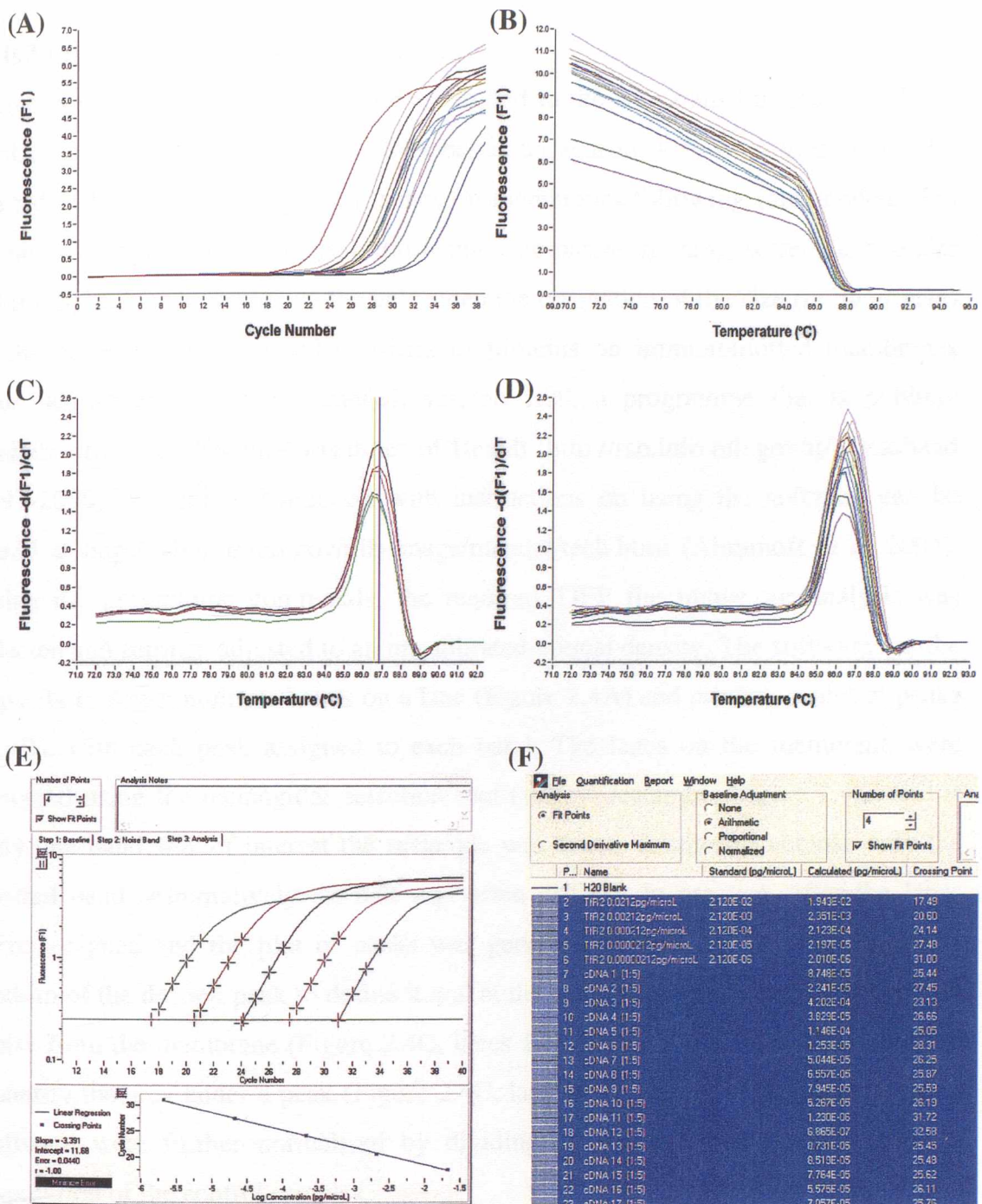


Figure 2.3 Real-time PCR of TfR2 mRNA levels in human liver tissue.

(A) Baseline plot showing increase in fluorescence during amplification of the target transcript. (B) Plot of the negative derivative of fluorescence ($-dF/dT$) versus temperature. (C) Fluorescence of the SYBR Green I dye bound to the dsDNA drops as the fragment is denatured. The turning point of curve B results into a melting peak. (D) The melting peak was used to confirm PCR product identity as the T_m of the standards matched the T_m of the unknowns therefore confirming specificity of the amplification. (E) Plot of the standard curve generated from the readings on the top panel. (F) Calculated and actual values for the standards (2-6) and calculated concentrations of unknowns (7-23).

2.10.3 Image acquisition and processing

Images were acquired with the camera attached to the UVi transilluminator or UVP BioDoc and saved as TIFF files. DNA bands on agarose gels were visualised with the aid of UV light, while protein bands on membranes following immunodetection or on SDS polyacrylamide gels following Coomassie staining were taken under natural light. Marker bands on the gels aided the estimation of the size (in bp or kDa) of the observed bands. Band densities of proteins on immunoblotted membranes were semi-quantified using ImageJ, version 1.29, a programme that is publicly available from the National Institutes of Health (<http://rsb.info.nih.gov/ij/>) (Rasband 1997-2006). An online handbook with instructions on using the software can be found at <http://rsb.info.nih.gov/nih-image/manual/tech.html> (Abramoff *et al* 2004). Using the programme commands, the required TIFF file image for analysis was selected and settings adjusted to an uncalibrated optical density. The software has the capacity to detect multiple bands on a lane (Figure 2.4A) and produce a plot of peaks (2.4B), with each peak assigned to each band. The lanes on the membrane were assigned using the rectangular selection tool (yellow rectangle, Figure 2.4E) and if only one band was of interest the rectangle was drawn smaller to enclose only the desired band. Alternatively, as that was often difficult in practice, after the lanes were assigned and the plot of peaks was generated, a line was drawn across the bottom of the desired peak to define it and at the same time exclude any background noise from the membrane (Figure 2.4C, lanes 1-4). The wand tool was then used to quantify the area under a peak (Figure 2.4C, lane 4). The values obtained using this software were further normalised by dividing all values by the mean value of expression of the control samples.

To ensure that the immunoblotting technique could respond to and that ImageJ could detect increasing amounts of protein, immunodetection using anti-IRP1 anti-serum was carried out on increasing protein concentrations (2, 4, 6 and 8 µg) of a single sample (control liver protein extract) (Figure 2.4D). The lanes were assigned with the rectangular tool (Figure 2.4E) and a plot of peaks was generated (Figure 2.4C). The area under the peak was measured by clicking inside the area defined by the base line with the wand tool (example shown in Figure 2.4C, lane 4). A curve of IRP1 protein expression (in arbitrary units) versus protein concentration (µg) was constructed with a significant positive correlation ($r=0.998$, $P=0.002$) (Figure 2.4F).

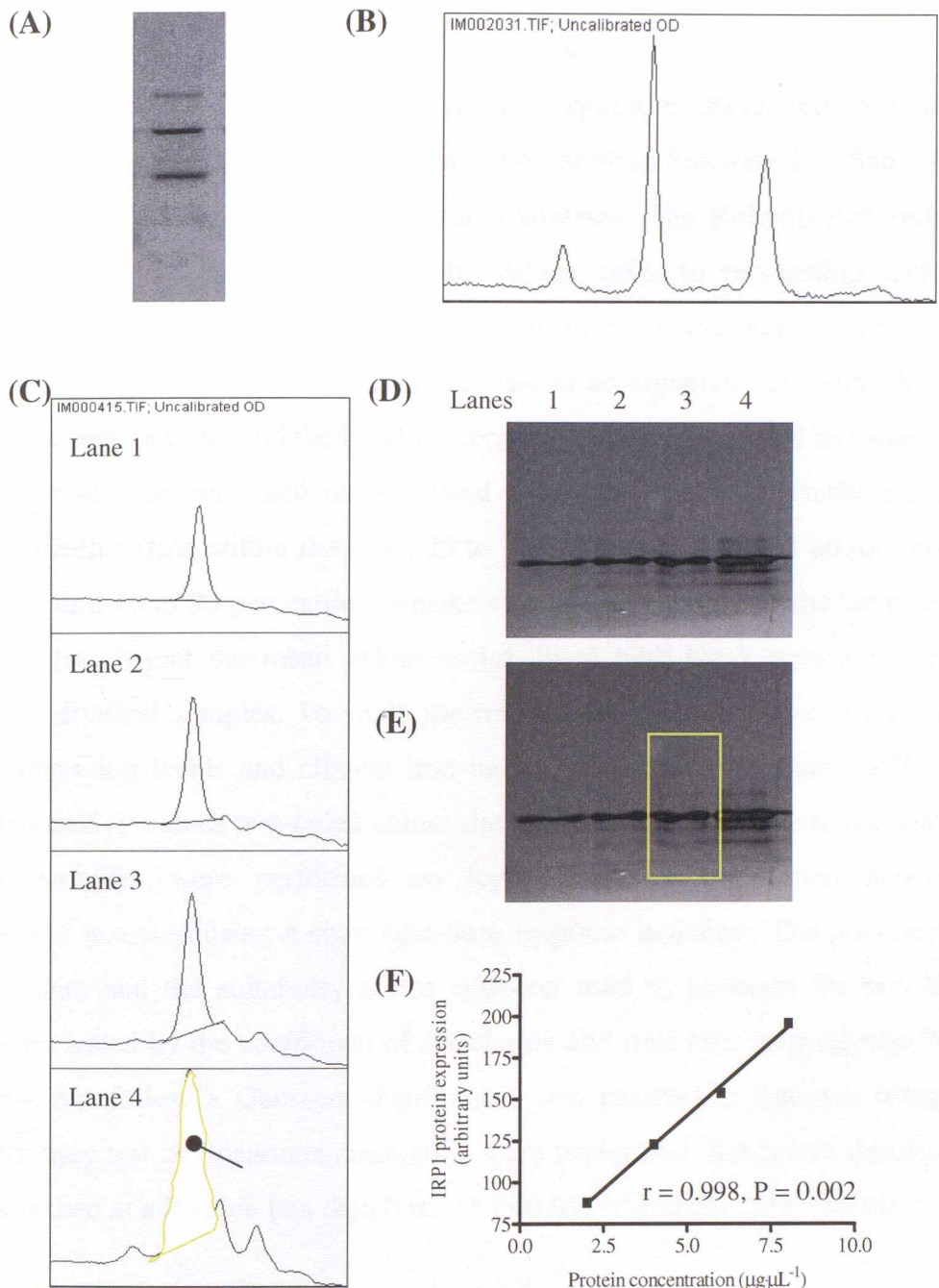


Figure 2.4 Analysis of immunoblotted membranes using ImageJ.

ImageJ can detect multiple bands on a lane (A) and generate a plot of peaks (B), using higher peaks to denote more intense bands. The lanes on the membrane can be assigned using the rectangular selection tool (E) and the generated peaks can be defined by drawing a line across their bases (C). To test that the Western blotting technique and the subsequent quantification with ImageJ can respond to increasing amounts of protein, immunodetection using anti-IRP1 was carried out on 2, 4, 6 and 8 μg of a control liver protein extract (D). The lanes were assigned (E) and the areas under the peaks were measured using the wand tool (C, lane 4). A curve of IRP1 protein expression (in arbitrary units) versus protein concentration was constructed with a significant positive correlation (F).

2.10.4 Statistical analysis

A computer spreadsheet (Excel 2003, Microsoft Corporation, Redmond, WA) and a statistical program GraphPad Prism version 4.0 (GraphPad Software Inc, San Diego, CA, U.S.A.) were used to perform the present analyses. The Kolmogorov-Smirnov test was used to test the normality of the values, prior to proceeding with the appropriate analyses. To determine the significance of the results differences between groups were analysed with a paired t test or an unpaired t test with Welch's correction, as appropriate, and the P value reported. Data are presented as mean \pm SD and all P values are two-sided unless stated otherwise. Box and whiskers graphs depict the median (line within the box), 25 to 75 percentiles (top and bottom border of the box), and 10 to 90 percentiles (whiskers). Column bars depict the mean \pm SD, while dot plots depict the mean values (solid lines) with black dots representing values of individual samples. To study the relationship (linear) between mRNA or protein expression levels and clinical iron indices, Pearson correlation coefficients were calculated (P values two-tailed unless stated otherwise). Non-linear associations between variables were performed on logarithmically transformed dependent variables and assessed using a sigmoidal-dose response equation. The goodness-of-fit of the data and the suitability of the equation used to generate the non linear curves were tested by the coefficient of correlation and runs test, respectively. When values did not follow a Gaussian distribution, non parametric analyses using the Mann-Whitney test or Spearman correlation were performed. Statistical significance was established at a P value less than 0.05. (* P<0.05, ** P<0.01, *** P<0.001)

Chapter III

Expression of liver IRP1 protein in hereditary haemochromatosis

3.1 Introduction

3.1.1 IRP1 protein expression

IRP1 has been purified and cloned from a variety of mammalian tissues and cells (Rouault *et al* 1990, Yu *et al* 1992) and since then its important role in iron homeostasis as an IRE-binding protein has been well described (section 1.3.1). The RNA-binding activity of IRP1 involves the insertion or extrusion of a 4Fe-4S cluster, while more recent evidence suggests that additional mechanisms controlling IRP1 function exist. The functional orthologue of IRP1, IRP2, was identified shortly after IRP1 (Samaniego *et al* 1994) however the significance of the existence of two IRPs is only now starting to emerge. Studies on IRP1 (Meyron-Holtz *et al* 2004a) and IRP2 (Cooperman *et al* 2005, Galy *et al* 2005) KO mice suggest that IRP2, rather than IRP1 is the main regulator of mammalian iron homeostasis. While IRP2 KO mice develop microcytic anaemia and adult onset neurodegeneration, mice with homozygous deletions in IRP1 develop no abnormalities. Mice lacking both copies of IRP2 and one copy of IRP1 develop more severe anaemia and neurodegeneration than the IRP2 KO mice, while mice lacking both copies of IRP1 and IRP2 do not survive gestation (Smith *et al* 2006). IRP1 is now thought to respond to stimuli other than iron or iron-related (Meyron-Holtz *et al* 2004b) and is believed to become important in pathologic situations, especially in the presence of oxidants that when produced in high concentrations can destabilise the Fe-S cluster (reviewed in Rouault 2002).

Numerous studies have demonstrated a reduction in the RNA binding activity of IRP1 in the presence of excess iron, attributed to the presence of the 4Fe-4S cluster. The idea that this reduction can, under extreme conditions, be accompanied by a reduction in the levels of the protein has not been extensively explored. Early studies on the effect of iron manipulations on IRP1 activity and levels in several cell lines have shown that a decrease in the activity of IRP1 was not accompanied by a decrease in the levels of the protein (Tang *et al* 1992, Samaniego *et al* 1994, Henderson and Kuhn 1995, Guo *et al* 1995). However, studies showing the

translation-independent degradation of IRP1 by haem in iron loaded rabbit fibroblast cells (Goessling *et al* 1992, 1994) as well as the decrease of IRP1 protein levels in liver extracts from heavily iron loaded HH patients (Flanagan *et al* 1995) suggest that alternative regulatory pathways may exist.

In agreement with the latter studies, down-regulation of IRP1 has been observed in both human and mouse iron loaded liver using both immunohistochemistry and Western blotting (Cunninghame Graham 1998). Immunohistochemical staining of paraffin-embedded human liver sections from both normal subjects and patients with *HFE*-related HH provided information not only on the levels of expression of this protein but also on its intracellular localisation. Immunostaining of normal human liver and from HH patients following phlebotomy treatment revealed a nuclear signal for IRP1 in addition to the cytoplasmic staining. Western blotting experiments in the same study further revealed the existence of extra bands in addition to the main IRP1 band as predicted from its cDNA sequence. Taken together these observations prompted an investigation into the nuclear localisation of IRP1 and the possibility of the existence of alternatively spliced forms of the protein.

3.1.2 Subcellular distribution and alternatively spliced forms of IRP1

IRP1, due to its important role in regulating expression of TfR1 and ferritin, has been the focus of many studies and is widely considered to be a cytoplasmic protein. As there have been reports of cytoplasmic proteins that shuttle between the nucleus and the cytoplasm (Mohamed *et al* 2000), observations of a nuclear signal of IRP1 following immunohistostaining of human liver raised the question of whether that is also the case for IRP1. Active transport of proteins across the nuclear envelope occurs through the nuclear pore complexes and the cut-off size regarding the transport of macromolecules through that complex is 40-50kDa. Proteins larger than 60kDa enter the nucleus only if they contain import signals, such as the nuclear localisation signal (NLS), which in the majority of mammalian proteins consists of a few positively charged residues, mainly arginine and lysine. Based on sequence analysis of the human IRP1 sequence, the location of a putative NLS (KLKYIKKY; residues 328-336) on the surface of the protein has been described (Cunninghame Graham 1998), which further supports the possibility of a nuclear function for the protein.

Most mammalian genes contain non-coding sequences that need to be removed in order to generate a functional message, a process known as mRNA splicing. Splicing occurs in the nucleus, together with the other modifications to the pre-mRNAs such as addition of the cap structure to the 5' end of transcripts, and the poly(A) tail to the 3' end. Splicing is not only responsible for removing introns from the pre-mRNA transcript but also for the generation of different mRNAs from the same gene by alternative splicing. Recent discoveries indicate that alternative splicing influences not only the primary sequence of proteins, but also the time, efficiency, and place of protein expression (reviewed in Dreyfuss *et al* 2002). In iron-related proteins, alternative spliced isoforms have been described for ferritin, DMT1, and HFE. The presence of these different forms often has a bearing on the cellular location of the transcript and expression of the isoforms has been reported to be regulated by iron. The possibility of a nuclear presence and existence of alternatively spliced forms of IRP1 is reminiscent of systems where an RNA-binding protein regulates or controls splicing of the mRNA transcript according to cellular needs. A paradigm of RNA binding proteins that are known to shuttle between the cytoplasm and the nucleus to perform such function are members of the embryonic lethal abnormal vision family of proteins that regulate mRNA expression of AU-rich element containing mRNAs (Brennan *et al* 2000). In this case shuttling of the binding proteins between the cytoplasm and the nucleus is thought to be regulated by phosphorylation.

The aim of the work presented in this chapter was to reinforce the observed down-regulation of IRP1 in the liver of patients with *HFE*-related HH as compared to control livers and investigate whether the results could be replicated in different cell lines following iron loading. A human hepatoma cell line was of particular interest seeking to examine the suitability of the cell line as a model for the human disease. A further aim was to investigate the extra bands that have been previously observed, following Western blotting with anti-IRP1 anti-sera, in addition to the main IRP1 band and determine whether they relate to potential alternatively spliced products of IRP1. And finally in order to reinforce and further investigate initial observations of a nuclear localisation of IRP1, cell lines overexpressing a chimeric protein of IRP1 containing GFP were also created.

3.2 Results

3.2.1 Down-regulation of liver IRP1 protein in iron overload

3.2.1.1 Evaluation of IRP1 protein levels in the liver of HH patients

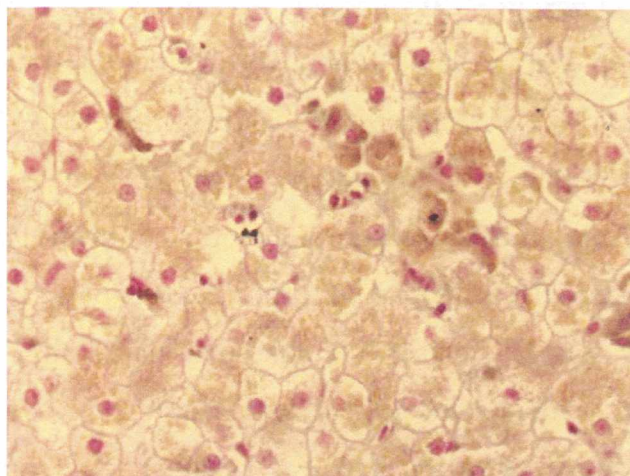
The characteristics and clinical iron indices of the study groups used in this chapter are given in Table 3.1, while individual information on samples can be found in Appendix I. Expression of liver IRP1 protein was initially characterised by immunohistochemistry using paraffin embedded iron loaded HH liver sections (Cunningham Graham 1998). A representative example is shown in Figure 3.1, where an iron loaded section from an untreated HH patient, prior to treatment, showed no IRP1 staining following immunostaining with chicken anti-whole rat liver IRP1 anti-serum (Figure 3.1A). In contrast, in a section taken from the same patient following phlebotomy treatment, there was a clearly defined purple signal for IRP1 with a cytoplasmic and plasma membrane staining pattern, as well as evidence of nuclear staining (Figure 3.1B). Both the plasma and nuclear membranes of the hepatocytes were clearly defined and the stained nuclei had apparent distinct nucleolar staining. The evidence presented suggested that in hepatocytes there is an inverse relationship between the levels of IRP1 and the extent of iron deposits.

Table 3.1 Clinical characteristics and iron indices of study groups in Chapter III

	Control group n=3	Untreated HH group n=3
Age at diagnosis, (years)*	36 ± 8 (27 - 42)	59 ± 12 (51 - 73)
Sex, (male/female)	3/0	3/0
SF, ($\text{ng} \cdot \text{mL}^{-1}$)*	73.67 ± 33.50 (50 - 112)	2471 ± 1820 (458 - 4001)
SI, ($\mu\text{moles} \cdot \text{L}^{-1}$)*	18.33 ± 4.041 (14 - 22)	35.33 ± 8.327 (26- 42)
TIBC, ($\mu\text{moles} \cdot \text{L}^{-1}$)*	62.67 ± 6.429 (58 - 70)	46 ± 10.58 (38 - 58)
TS, (%)*	29 ± 8 (23 - 38)	82 ± 32 (45 - 100)
HIC, ($\mu\text{g Fe/g dry wt}$)*	182.7 ± 195.2 (28 - 402)	13017 ± 12868 (2378 - 27320)

* Range (mean ± SD) (min-max)

(A)



(B)

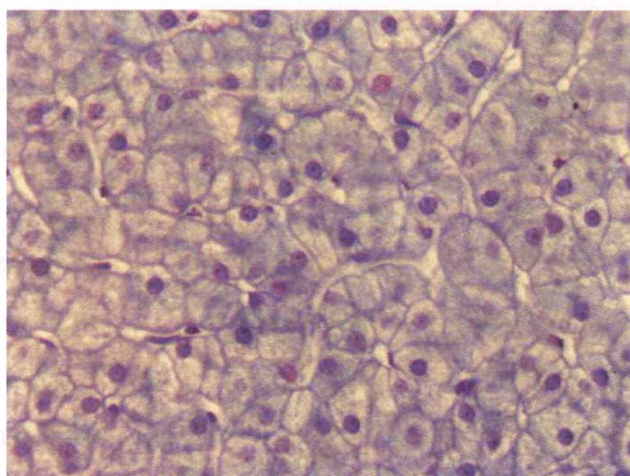


Figure 3.1 Expression of IRP1 protein in liver sections from an HH patient before and after phlebotomy treatment.

(A) IRP1 was detected by immunohistochemical staining using a polyclonal anti-IRP1 anti-serum (Cunningham Graham 1998). There was barely detectable IRP1 expression in the iron-loaded section. (B) In contrast, there was strong expression of IRP1 in the section taken post-treatment, following the removal of 60 units of whole blood from the patient, when iron levels had returned to normal. In addition to the cytoplasmic staining there was also evidence of nuclear IRP1 staining (Magnification 400x).

The initial observation of a down-regulation of IRP1 in iron loaded liver was further investigated by Western blotting using a polyclonal antibody raised in rabbits against purified rat IRP1 that demonstrated the expression of human IRP1 protein at ~98kDa. In agreement with the evidence from the immunohistochemistry, IRP1 protein levels were lower in cytoplasmic protein extracts from liver specimens taken from untreated HH patients when compared to controls (Neonaki *et al* 2002) when an anti-peptide A (Figure 3.2) or anti-peptide B (Figure 3.3) anti-serum was used in the immunoblotting. A total of 6 liver specimens from 3 controls, 1 mild iron loaded CY patient and 2 heavily iron loaded YY patients were examined and although the results of the immunohistochemistry showed a complete absence of IRP1 in the iron loaded sections prior treatment, Western blotting analysis showed a reduction in IRP1 protein levels of 50-60% in the iron loaded samples as compared to controls (Figures 3.2C and 3.3C).

As previously described by Cunningham Graham (1998) and Gracia Sancho (2003), in addition to the main IRP1 protein band recognised at approximately 98kDa in human liver, the anti-sera used in these experiments immunoreacted with extra bands of higher (upper bands) and lower molecular weight (lower bands) as evident in Figure 3.2A and to a less extent in Figure 3.3A. An upper band of ~118kDa and lower bands of ~86kDa and ~75kDa were evident as indicated in both figures. Evidence for the presence of extra forms of IRP1 has been further documented in cytoplasmic COS and HepG2 cell extracts in section 3.2.1.2 and in the literature (Oliveira and Drapier 2000, Henderson *et al* 1993, Patino and Walden 1992) and is discussed in more detail in sections 3.2.4 and 3.3.2.

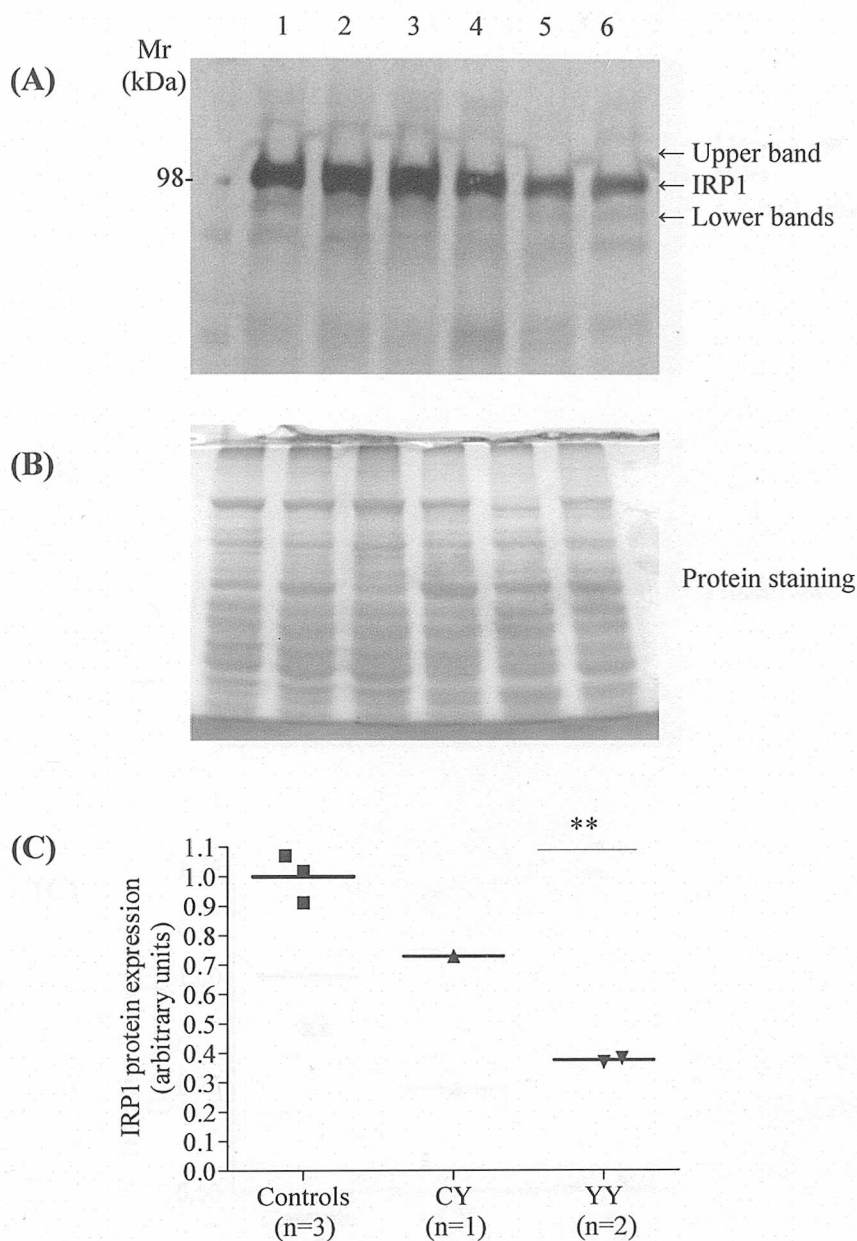


Figure 3.2 Western blotting analysis of IRP1 in human liver using an anti-peptide A of IRP1 anti-serum.

(A) Liver protein extracts (25 μ g) were subjected to SDS-PAGE and transblotted onto a nitrocellulose membrane. IRP1 was detected using polyclonal anti-peptide A of IRP1 anti-serum and migrated as a 98kDa protein. Expression of the protein was weaker in iron loaded patients homozygous for the C282Y mutation (lanes 5, 6) as compared to controls (lanes 1-3) ($P=0.006$). A case of mild iron overload (CY) is shown (lane 4) with levels of IRP1 expression lower than controls but higher than in the YY group. (B) Coomassie Brilliant Blue stained gel demonstrating equal protein loading. (C) Graphical representation of experimental data shown in A. Western blotting and quantification of band densities and analysis was carried out as described in Chapter II.

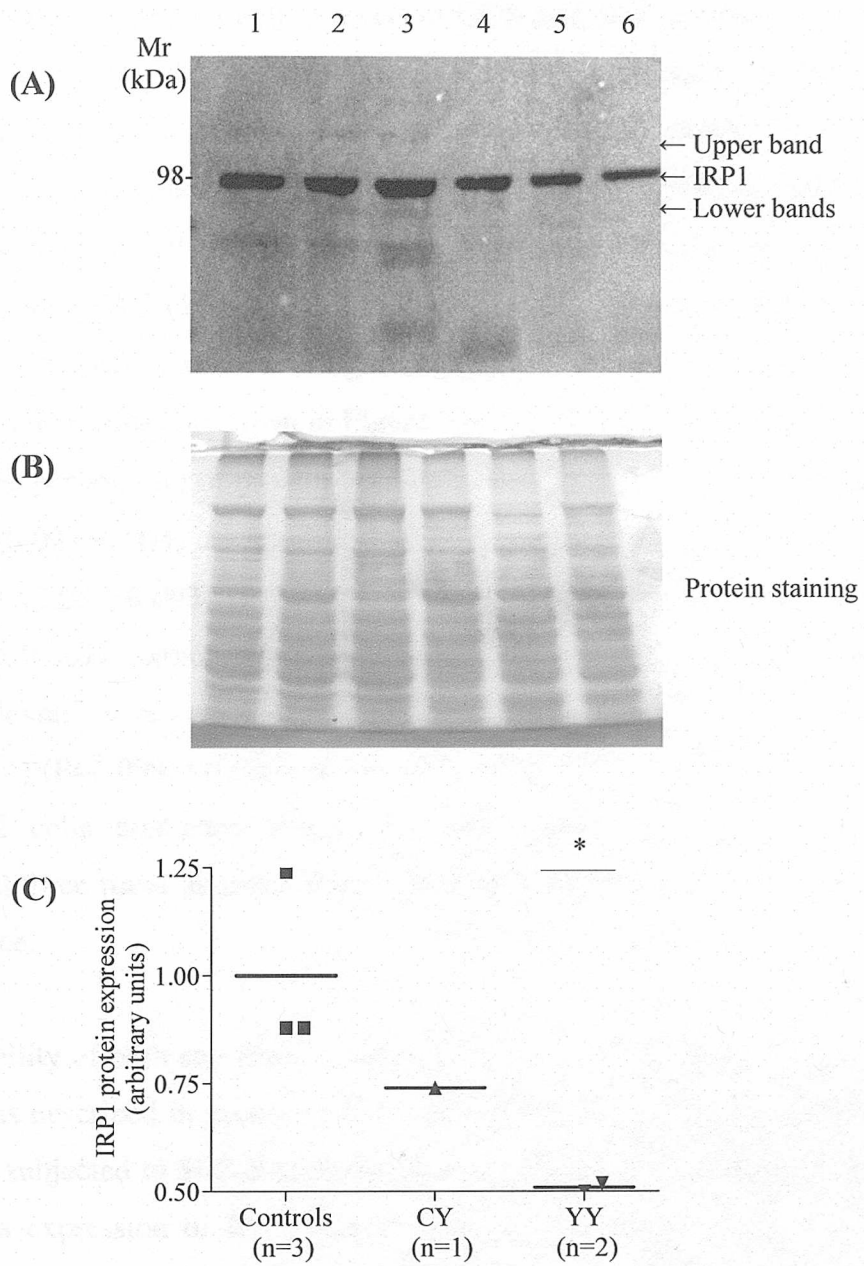


Figure 3.3 Western blotting analysis of IRP1 in human liver using anti-peptide B of IRP1 anti-serum.

(A) Liver protein extracts ($25\mu\text{g}$) were subjected to SDS-PAGE and transblotted onto a nitrocellulose membrane. IRP1 was detected using a polyclonal anti-peptide B of IRP1 anti-serum and migrated as a 98kDa protein. Expression of the protein was weaker in iron loaded patients homozygous for the C282Y mutation (lanes 5, 6) as compared to controls (lanes 1-3) ($P=0.05$). A case of mild iron overload is shown (lane 4) with levels of IRP1 expression lower than controls but higher than in the YY group. (B) Coomassie Brilliant Blue stained gel demonstrating equal protein loading. (C) Graphical representation of experimental data in A. Western blotting and quantification of band densities and analysis was carried out as described in Chapter II.

3.2.1.2 Evaluation of IRP1 protein levels in COS and HepG2 cells

To further investigate the observation of the down-regulation in IRP1 protein expression, two different cell lines were used to investigate changes in levels of the protein induced by iron loading. Prior to investigating IRP1 protein levels an initial experiment to ensure that the cells are capable of taking up iron was set up. Cells were treated with FAC (100 μ M) and the amount of iron in untreated as compared with treated cells was examined using atomic absorption spectroscopy as described under 2.7.3. The results are shown in Figure 3.4. The amount of iron expressed as the total μ g of Fe per total μ g of protein was increased about 5-fold in COS cells treated with FAC (0.022 ± 0.004) as compared with the amount present in the untreated control cells (0.004 ± 0.003) ($P<0.0001$) (Figure 3.4A). Similarly, untreated HepG2 cells (0.002 ± 0.001) contained comparable amounts of iron to the untreated COS cells, and levels increased 18-fold when HepG2 cells were treated with FAC (0.036 ± 0.011) ($P=0.0005$) (Figure 3.4B). It is interesting to note that untreated COS and HepG2 cells contained almost the same amount of iron, yet the latter accumulated three times as much iron when they were exposed to the same amount of iron source.

Once the ability of both cell lines to take up iron was established, cells were treated with FAC as described in section 2.7.2. Cell extracts were prepared as described in 2.8.1.1 and subjected to SDS-PAGE and immunoblotting with anti-IRP1 anti-serum. Endogenous expression of IRP1 was evident in cytoplasmic extracts of both cell lines (Figures 3.5 and 3.6 for COS, and 3.7 and 3.8 for HepG2). In COS cells, IRP1 migrated as a band of the expected molecular weight of 98kDa (Figures 3.5 and 3.6, lanes 1-4 and 1-6, respectively) and a similar signal was evident in HepG2 cells (3.7 and 3.8, lanes 1-4 and 1-6 and 1-5, respectively). COS cells treated with FAC (Figures 3.5 and 3.6, lanes 5-8 and 7-12, respectively) displayed a reduction in IRP1 protein levels (Figures 3.5A, 3.6A and 3.6B) of about 48%. The reduction was evident when the cell extracts were immunoblotted using anti-peptide A of IRP1 (Figures 3.5A and 3.5C), anti-peptide B (Figures 3.6A and 3.6D) or anti-whole IRP1 (Figures 3.6B and 3.6E) anti-serum. Amongst up to six samples of HepG2 cells treated with FAC (Figures 3.7 and 3.8), IRP1 protein was barely detectable in only one sample when immunoblotting with anti-peptide A (Figures 3.7A, lane 5), but undetectable in any other cell extract when immunoblotted either with anti-peptide A

(Figures 3.7A and 3.7C; lanes 6-8), anti-peptide B (Figures 3.8A and 3.8D; lanes 7-12) or anti-whole IRP1 (Figures 3.8B and 3.8E; lanes 6-10) anti-serum.

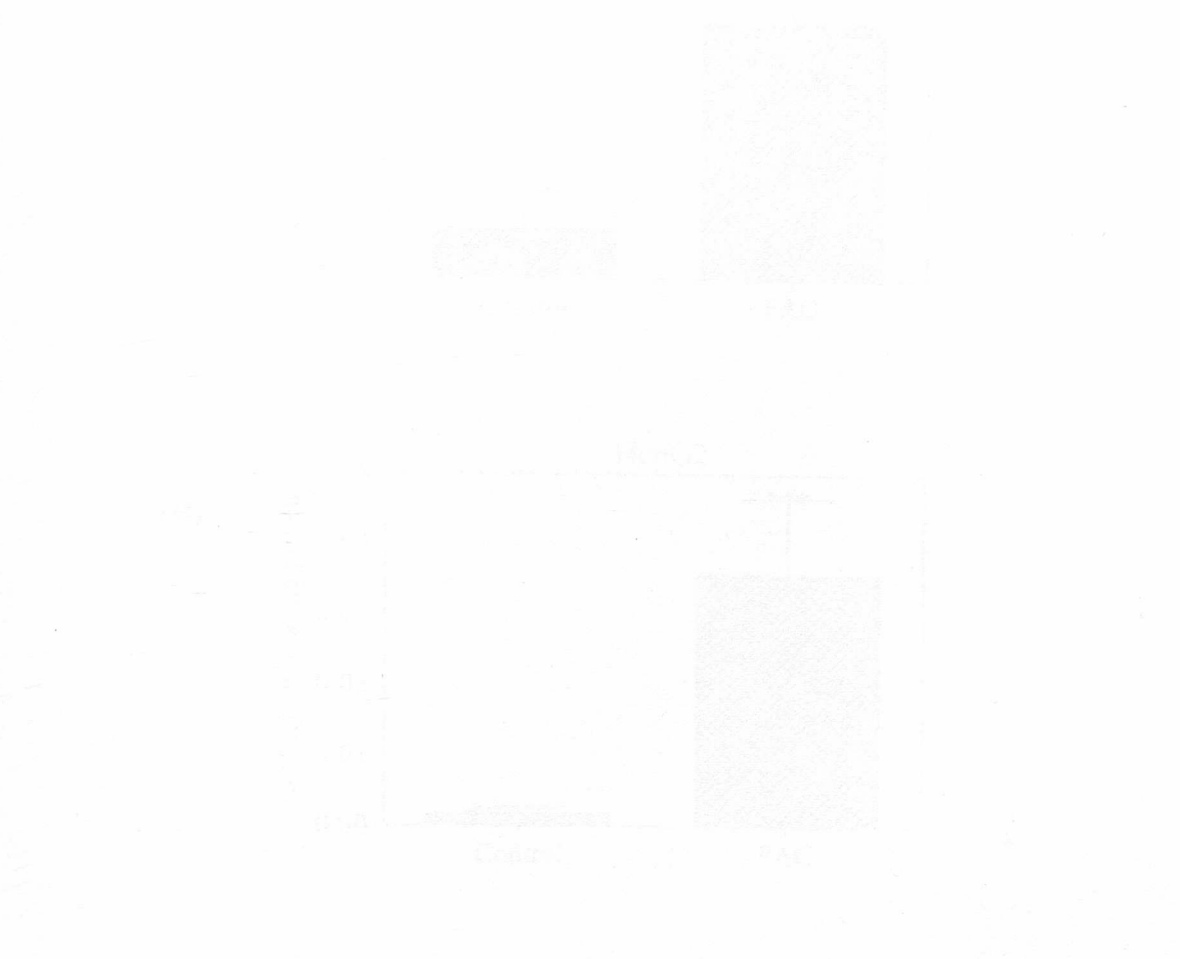


Figure 3.7 Effect of pre-binding antiserum on IRP and lymphoma cells.

IRP1 cells, either treated with 100μg/ml for 1 hour and washed off or remained untreated during the growth experiments as described in Chapter 3. The cells were lysed by adding 100 μl of lysis buffer to the treated cell of protein and approximately 50μg of the total protein was resolved on 10% acrylamide gel (0.5 mm thickness) impregnated with 0.05% bromophenol blue and 0.05% SDS and the gels of the different lanes were stained and scanned as described in Chapter 3. The ratio of protein to anti IRP1, anti peptide A and anti peptide B antibodies applied to the PAA membrane is indicated in parentheses.

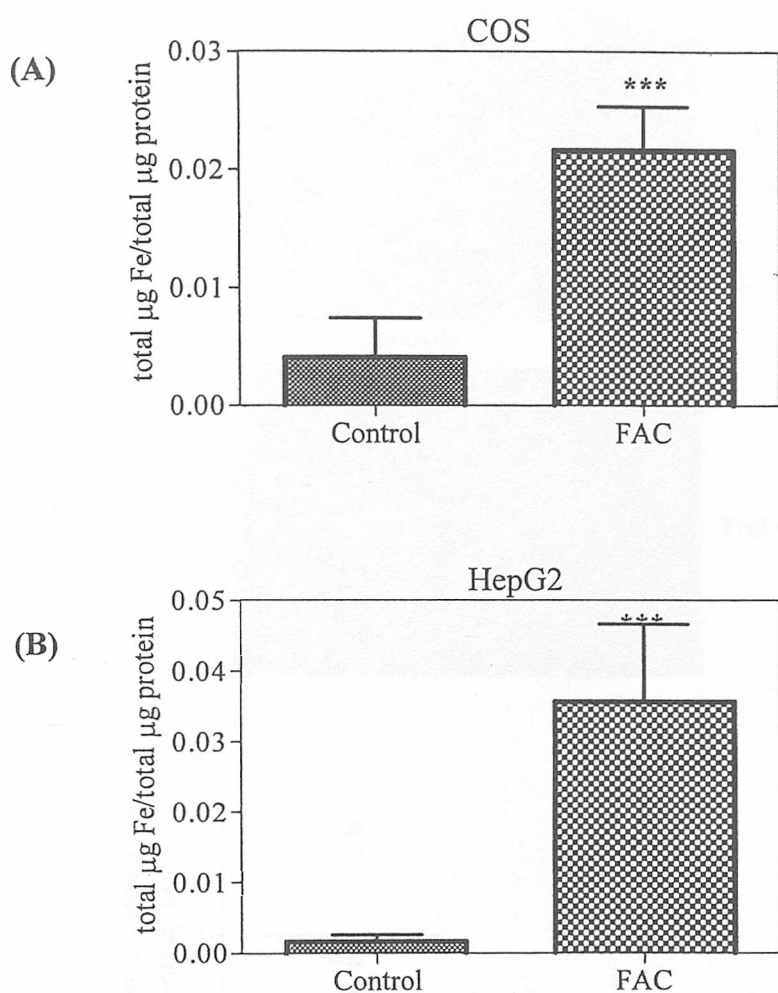


Figure 3.4 Effect of iron loading treatment on COS and HepG2 cells.

(A) COS cells were treated with 100µM FAC for 7 days and levels of iron measured using atomic absorption spectrometry as described in Chapter II. The ratio of the total µg of iron relative to the total µg of protein was significantly higher in the FAC treated cells as compared to untreated cells ($P<0.0001$). (B) Similarly, HepG2 cells were cultured and treated with FAC for 7 days and levels of iron measured using atomic absorption spectrometry as described in Chapter II. The ratio of the total µg of iron relative to the total µg of protein was significantly higher in the FAC treated cells as compared to untreated cells ($P=0.0005$).

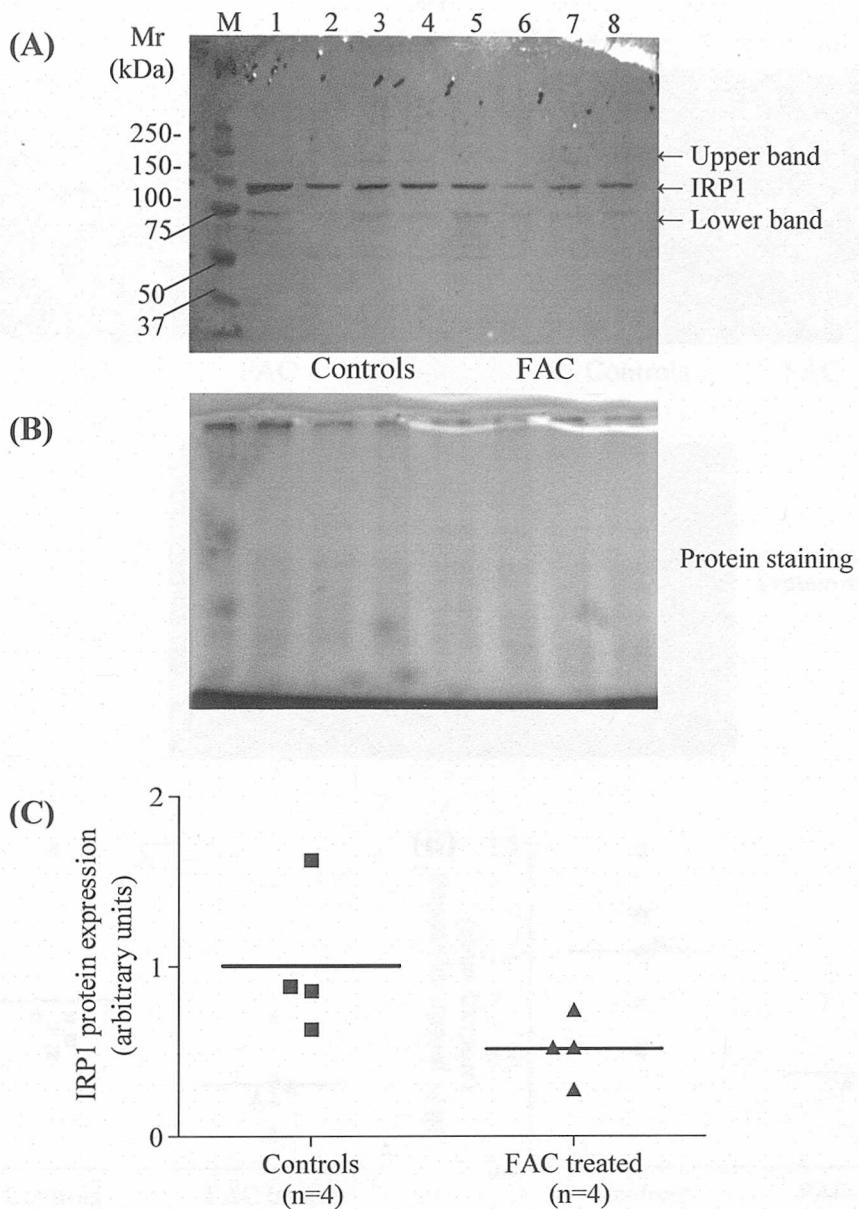


Figure 3.5 Effect of iron loading on IRP1 protein levels in COS cells as assessed by Western blotting using polyclonal anti-peptide A of human IRP1 anti-serum.

(A) COS cells were grown to confluence and then left untreated or cultured in the presence of iron (FAC, 100 μ M) for a further 7 days. Cytoplasmic protein extracts (50 μ g) were subjected to SDS-PAGE and transblotted onto a nitrocellulose membrane. Endogenous IRP1 was detected with polyclonal anti-peptide A of IRP1 anti-serum and migrated as a 98kDa protein. Iron treatment caused a decrease but did not significantly affect IRP1 expression in untreated (lanes 1-4) and iron treated (lanes 5-8) COS cells ($P=0.111$). (B) Coomassie Brilliant Blue stained gel demonstrating equal protein loading. (C) Graphical representation of experimental data in A. Iron loading of cells, Western blotting and quantification of band densities and analysis was carried out as described in Chapter II.

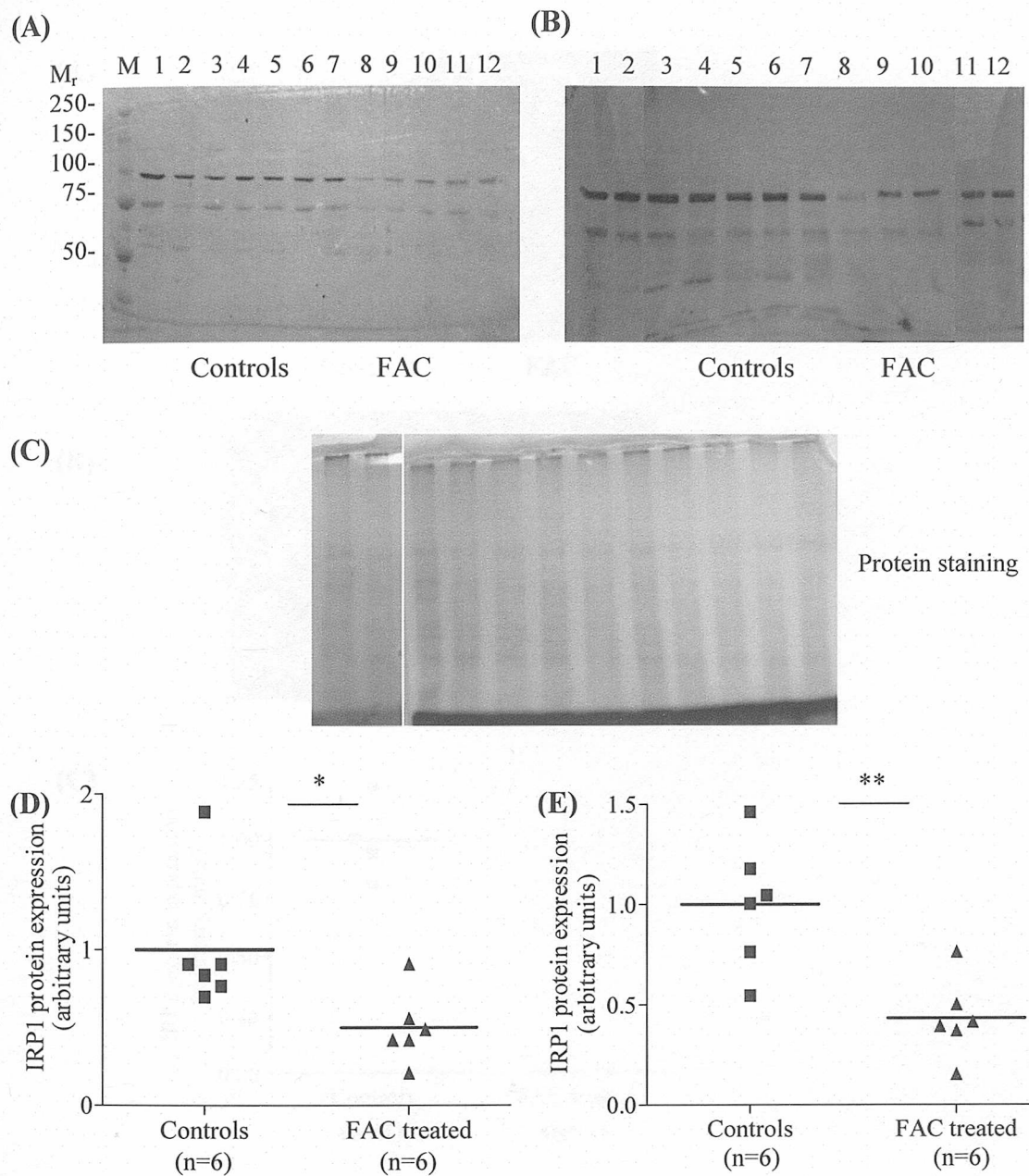


Figure 3.6 Effect of iron loading on IRP1 protein levels in COS cells as assessed by Western blotting using anti-peptide B and anti-whole human IRP1 anti-serum.

(A), (B) COS cells were grown to confluence and then left untreated or cultured in the presence of iron (FAC, 100µM) for a further 7 days. Cytoplasmic protein extracts (50µg) were subjected to SDS-PAGE and transblotted onto a nitrocellulose membrane. IRP1 was detected with a polyclonal anti-peptide B (A) and anti-whole (B) of IRP1 anti-serum and migrated as a 98kDa protein. Iron loading decreased IRP1 protein expression in treated (lanes 1-6) as compared to untreated (lanes 7-12) COS cells. (C) Coomassie Brilliant Blue stained gel demonstrating equal protein loading. (D, E) Graphical representation of experimental data in A and B, respectively. Use of anti-peptide B of IRP1 anti-serum detected a down-regulation in IRP1 of marginal significance ($P=0.043$) (D), while use of anti-whole of IRP1 anti-serum a strong one ($P=0.006$) (E).

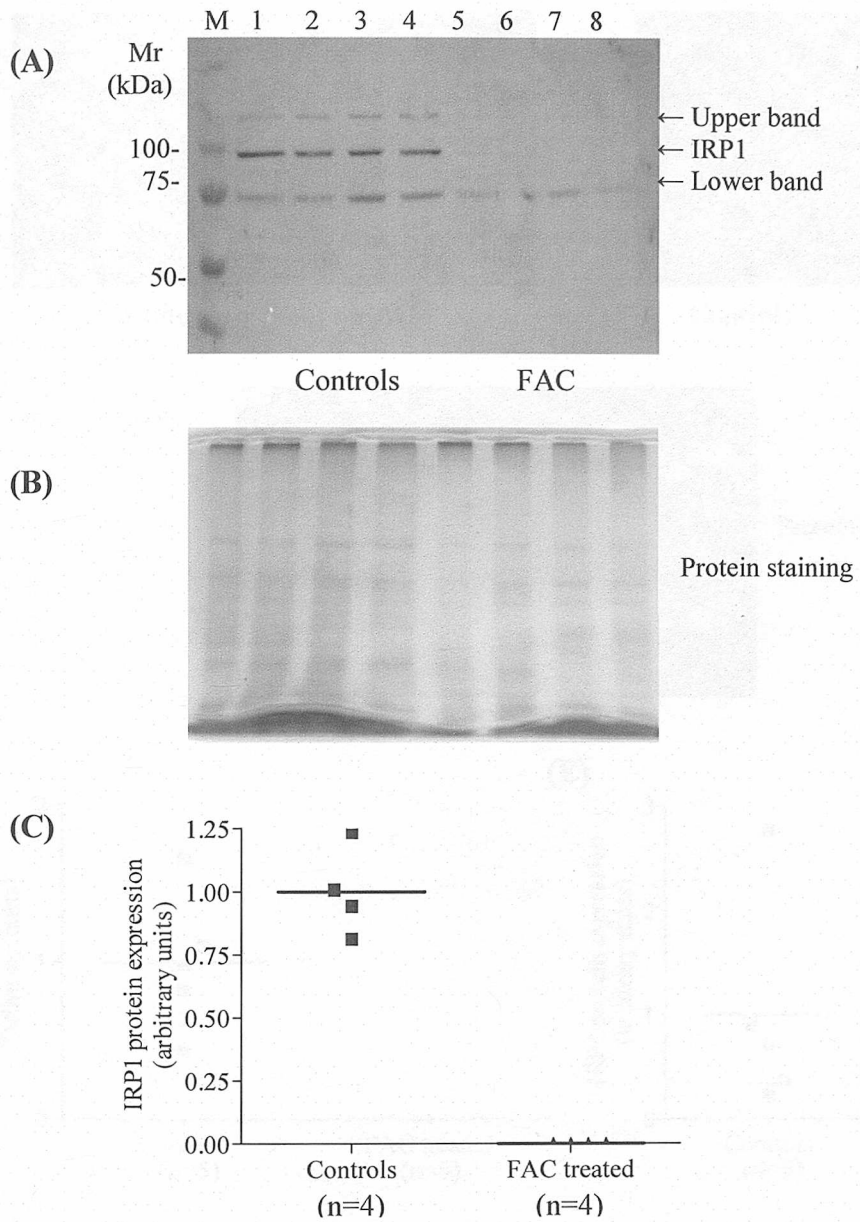


Figure 3.7 Effect of iron loading on IRP1 protein levels in HepG2 cells as assessed by Western blotting using polyclonal anti-peptide A human IRP1 anti-serum.

(A) HepG2 cells were grown to confluence and then left untreated or cultured in the presence of iron (FAC, 100 μ M) for a further 7 days. Cytoplasmic protein extracts (25 μ g) were subjected to SDS-PAGE and transblotted onto a nitrocellulose membrane. Endogenous IRP1 was detected using a polyclonal anti-peptide A of IRP1 anti-serum and migrated as a 98kDa protein. Untreated HepG2 cells expressed endogenous IRP1 (lanes 1-4), however following iron treatment IRP1 was not detectable in extracts from treated cells (lanes 5-8).

(B) Coomassie Brilliant Blue stained gel demonstrating equal protein loading. (C) Graphical representation of experimental data in A. Iron loading of cells, Western blotting and quantification of band densities and analysis was carried out as described in Chapter II.

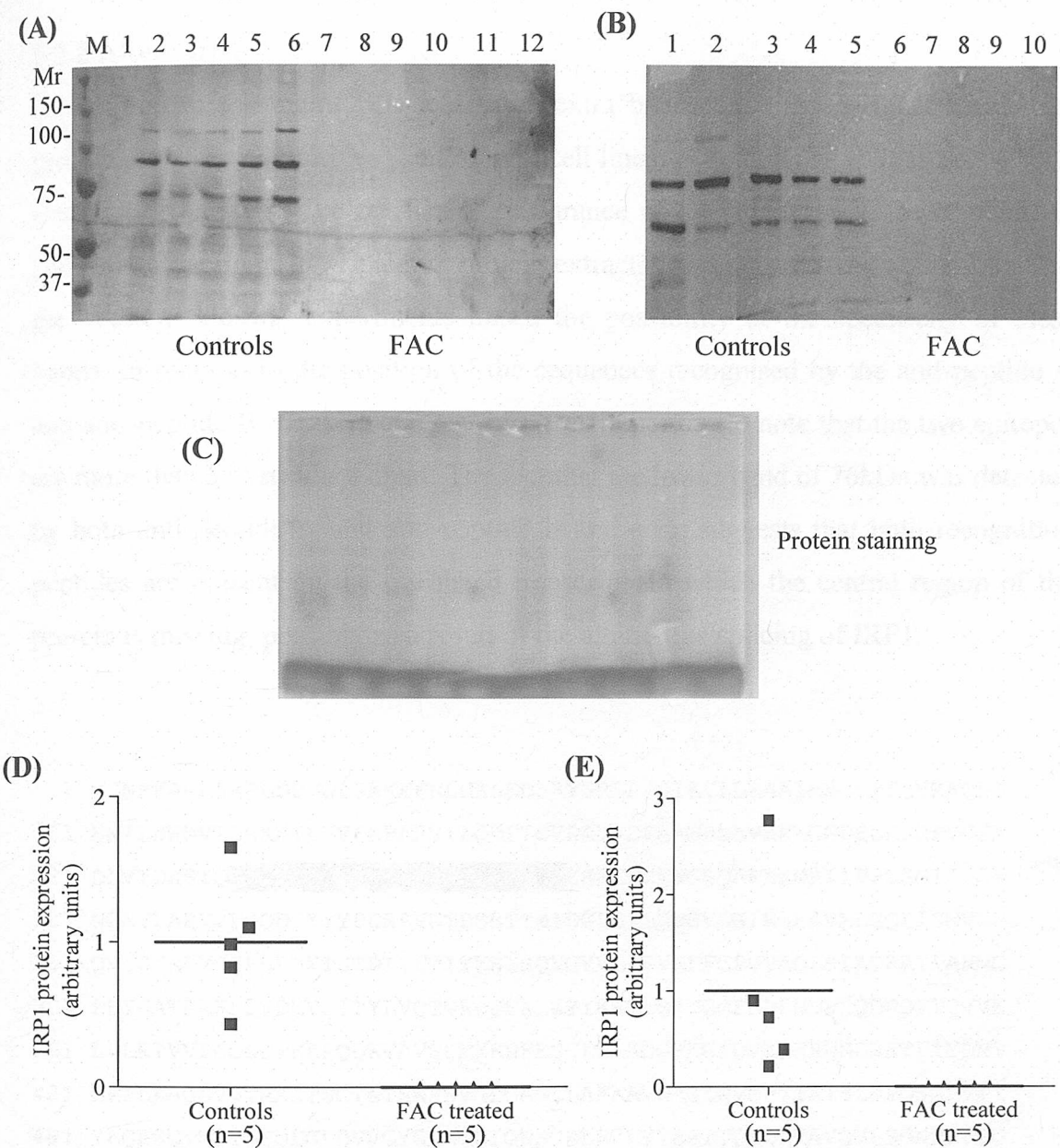


Figure 3.8 Effect of iron loading on IRP1 protein levels in HepG2 cells as assessed by Western blotting using anti-peptide B and anti-whole human IRP1 anti-serum.

(A), (B) HepG2 cells were grown to confluence and then left untreated or cultured in the presence of iron (FAC, 100 μ M) for a further 7 days. Cytoplasmic protein extracts (25 μ g) were subjected to SDS-PAGE and transblotted onto a nitrocellulose membrane. IRP1 was detected using a polyclonal anti-peptide B (A) and anti-whole (B) of IRP1 anti-serum and migrated as a 98kDa protein. Endogenous IRP1 protein expression was evident in untreated (lanes 1-6 in A; lanes 1-5 in B) HepG2 cells. IRP1 was undetectable following iron loading in the FAC treated cells (lanes 7-12 in A; lanes 6-10 in B). (C) Coomassie Brilliant Blue stained gel demonstrating equal protein loading. (D), (E) Graphical representation of experimental data in A and B, respectively. Iron loading of cells, Western blotting and quantification of band densities and analysis was carried out as described in Chapter II.

3.2.2 Alternative splicing of IRP1

In addition to the main IRP1 band, the extra bands observed in the human liver protein extracts were also evident in both cell lines, in controls as well as in the FAC treated cell extracts. The consistent appearance of extra upper and lower bands in addition to the main IRP1 band in protein extracts from human liver and cell lines in the Western blotting experiments raised the possibility of the specificity of these bands. In relation to the position of the sequences recognised by the anti-peptide A and anti-peptide B anti-sera (Figure 3.9), it is important to note that the two epitopes are more than 550 residues apart. The fact that the lower band of 76kDa was detected by both anti-peptide A and anti-peptide B anti-sera, suggests that both recognition peptides are present on the translated transcript, in which the central region of the protein is missing, possibly as a result of the alternative splicing of IRP1.

1 MSNPFAHLAEPLDPVQPGKKFFNLNKLEDSRYGRLPFSIRVLLEAIRNCDEFLVKKQDI
61 ENILHWNVTQHKNIEVPFKPARVILQDFTGVPAVVDFAAMRDAVKLGGDPEKINPVC
121 DLVIDHSIQVDFNRRADS₁₃₈LQKNQDLEFERNRERFEFLKGWSQAFHNMRIIPPGSIIHQV
peptide A
181 NLEYLARVVFDQDGYYYPDSLVGTDSDHTTMIDGLGILGWGVGGIEAEAVMLGQPISMVLP
241 QVIGYRLMGKPHPLVTSTDIVLTITKHLRQVGVVGKFVEFFGPVVAQLSIADRATIANMC
301 PEYGATAAFFPVDEVSITYLVQTGRDEEKLKYIKKYLQAVGMFRDFNDPSQDPDFTQVVE
361 LDLKTVVPCSGPKRPQDKVAVSDMKKDFESCLGAKQGFQVVAPEHHNDHKTFIYDNT
421 EFTLAHGSVVIAAITSCTNTSNPSVMLGA₄₄₁GLLAKKAVDAGLNMPYIKTSLSPGSGVVTY
481 YLQESGVMPYLSQLGFDVVGYGCMTCIGNSGPLPEPVVEAITQGDLVAVGVLSGNRNFEG
541 RVHPNTRANYLASPPLVIAYAIAGTIRIDFEKEPLGVNAKGQQVFLKDIWPTRDEIQAVE
601 RQYVIPGMFKEVYQKIETVNESWNALATPSDKLFFWNSKSTYIKSPPFFENLTLDLQPPK
661 SIVDAYVLLNLGDSVTTDHISPAGNIARNSPAARYLTNRGLTPREFNSYGSRRGNDAVMA
721 RGTTFANIRLLNRFLNKQAPQTIHLPSEILDVFDAEERYQQAGLPLIVLAGKEYGAGSSR
781 DWAAKGP₇₉₁FLLGIKAVLAESYERIHRSNLVGMGVIPLEYLPGENADALGLTGQERYTIIIP
841 ENLKPKQMVKVQVKLDTGKTFQAVMRFDTDVELTYFLNGGILNYMIRKMAK
peptide B

Figure 3.9 Location of peptides on IRP1 sequence recognised by anti-peptide A and anti-peptide B anti-sera.

Exons are shown in alternating text colour and in red is the residue overlap splice site. Residues 130-151 (VDFNRRADS¹³⁸ LQKNQDLEFERNR) represent peptide A and are recognised by the anti-peptide A anti-serum, while the anti-peptide B anti-serum recognises residues 707-721 (NSYGS⁷¹¹RRGNDAVMARC) of human IRP1 (Eisenstein *et al* 1993).

With regards to the presence of the extra bands, two striking differences were evident between the two cell lines: the prominent presence of the lower band (75kDa) and the absence of the upper band (118kDa), irrespective of iron treatment, in COS cells. In HepG2 cells, iron treatment resulted in the disappearance of not only the main IRP1 band but also of both the lower (75kDa) and upper (118kDa) bands. Interestingly, the lower band (75kDa) was still evident in the iron treated HepG2 cells immunoblotted with anti-peptide A of IRP1 anti-serum (Figure 3.7A), but both upper and lower bands disappeared along with the main IRP1 band in the membranes that were immunoblotted with anti-peptide B (Figure 3.8A) and anti-whole (Figure 3.8B) IRP1 anti-sera. Absence of a signal of the lower band in the human liver (Figure 3.3) and in HepG2 cells (Figures 3.7A, 3.8A and 3.8B) suggests a form of control exerted on both the main protein as well as putative spliced forms. While absence of the upper band (118kDa) in COS cells could be attributed to a cell specific expression of a spliced form of IRP1, further experiments would need to be conducted before reaching such conclusions. The second lower band of 86kDa observed in the human liver extracts was not evident in either of the two cell lines. The structure of IRP1 was examined for splicing patterns that would maintain the protein reading frame and Table 3.2 lists the different possibilities based on exon (intron phase) prediction.

Table 3.2 Alternative splicing patterns of IRP1

Transcript	5' Exons	3' Exons	Length of peptide (amino acids)	Peptide size (kDa)	Expected size of PCR product (bp)	
					IRP1s5 IRP1s3	IRPex1 IRPex21
Full length	1 - 11	12 - 21	889	105	1898	2973
Δ8-17	1 - 7	18 - 21	455	50	597	1672
Δ6-16	1 - 5	17 - 21	394	44	417	1492
Δ6-15	1 - 5	16 - 21	429	47	522	1597
Δ6-13	1 - 5	14 - 21	523	57	804	1879
Δ7-14	1 - 6	15 - 21	532	59	830	1905
Δ5-12	1 - 4	13 - 21	529	58	817	1892
Δ7-11	1 - 6	12 - 21	659	73	1072	2147
Δ9-14	1 - 8	15 - 21	637	71	1132	2207

To examine the possibility of the presence of alternatively spliced products of IRP1 in the liver, a nested PCR approach on reverse transcribed total RNA from HepG2 cells was employed as described under 2.9.1 and 2.9.3. The nested PCR strategy indicated the presence of at least 3 alternative products of IRP1 splicing. In addition to the full length transcript of 1.9kbp (Figure 3.10, lanes 1-3, 6-8, 10-12), three smaller bands of 710bp (lane 3), 550bp (lane 7) and 500bp (lane 2), were amplified in HepG2 cells. All three amplicons were purified as described under 2.5.7.2 and sequenced (2.9.4.4) and sequence alignments of each transcript with IRP1 are included in Appendix III. The nested PCR protocol was extensively optimised and tested previously and further spliced products had been identified, with the 500bp spliced product also amplified in FAC treated HepG2 cells (Folch Codera 2004).

According to sequence comparison between the ~550bp transcript and human IRP1 (Appendix III, transcript 1), alignment started at exon 15, indicating that exons 5 to 14 (inclusive) were absent in the transcript. Analysis of exon ends indicated that the Δ5-14 splice form would not have the IRP1 reading frame maintained and therefore it is unlikely that this transcript has any biological function. Sequence comparison of the ~500bp amplicon (Appendix III, transcript 2) revealed that the transcript aligned with exons 7 and 18 of IRP1, with bases 871-2265 excised (IRP1 sequence provided in Appendix II). The reading frame is maintained in this transcript but whether it is a functional spliced form of IRP1 remains to be explored. Finally, based on sequence comparison of the ~710bp amplicon (Appendix III, transcript 3), the amplicon's sequence aligned with exons 14 to 17 of IRP1. If based on exon prediction, the transcript was missing exons 5 and 13, the expected size using the IRP1s set of primers would be 732bp. Analysis of exon ends indicated that the Δ5-13 splice form would not have had the IRP1 reading frame maintained and the transcript is therefore unlikely to have a significant biological function.

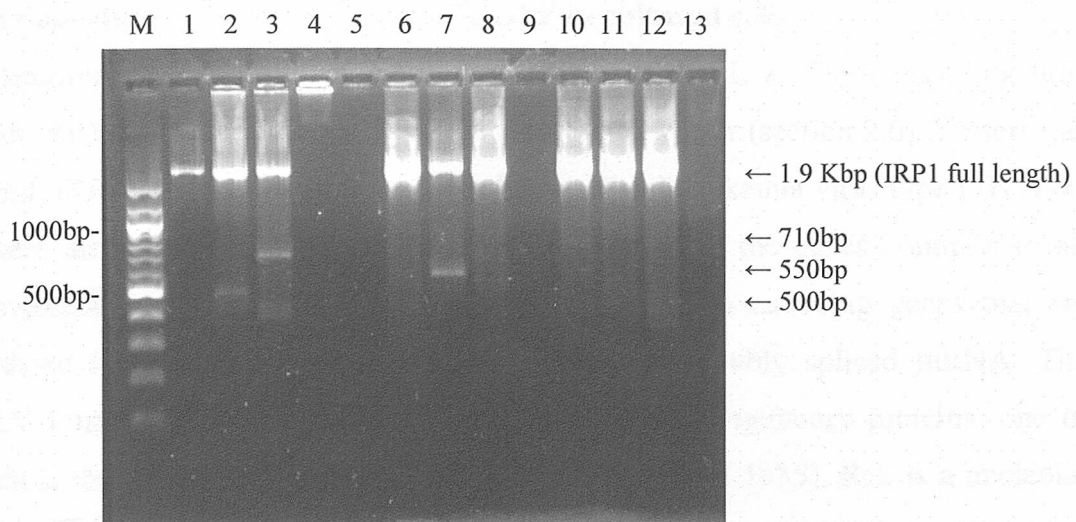


Figure 3.10 Electrophoretic analysis of Nested PCR products derived from HepG2 cells.

Nested PCR resulted in the amplification of full length IRP1 (1.9Kbp) in untreated HepG2 cells (lanes 2-4, 6-8), in FAC treated cells (lanes 10-12) and in the positive control (plasmid containing full length IRP1 sequence) (lane 1). Smaller products were also amplified in untreated cells (lanes 2, 3 and 7) of ~710bp (lane 3), ~550bp (lane 7), and ~500bp (lane 2). No amplification was observed in the negative controls (lanes 5, 9 and 13). Nested PCR and product analysis were as described in Chapter II.

3.2.3 Subcellular distribution of IRP1-GFP in cultured cells

To determine the subcellular distribution pattern of IRP1, a cDNA encoding full-length IRP1 was fused into a pEGFP-N3 expressing vector (section 2.6). To serve as control, IRP2 and the Rex protein of the human T-cell leukemia virus type I (HTLV-1) were also fused into the same vector. In addition to the genes common to all retroviruses the HTLV-1 genome contains a pX region encoding genes that are translated into two different reading frames from a doubly spliced mRNA. The HTLV-1 transcripts code for at least two *trans*-acting regulatory proteins, one of which is the 27kDa Rex phosphoprotein (Kiyokawa *et al* 1985). Rex is a nucleolar protein that is required for the expression of the viral structural proteins *gag* and *env* and facilitates the transport of unspliced or singly spliced mRNAs from the nucleus to the cytoplasm. Similar to the IRE/IRP system, viral mRNA contains a Rex-responsive element (RXRE), a sequence near the 3' terminus that mediates Rex responsiveness.

Cells were transiently transfected as described under 2.7.1.1 and examined for GFP fluorescence after 48hrs, prior to collecting the cells and preparing the fractionated cell extracts as described in 2.8.1.2. After an initial experiment on COS cells transiently transfected with pIRP1-EGFP, pIRP2-EGFP, pRex-EGFP or the pEGFP-N3 vector alone, cell extracts were prepared as described under 2.8.1.1 and subjected to SDS-PAGE followed by immunoblotting with the anti-GFP anti-serum (Figure 3.11Ai). Western blotting demonstrated the expression of IRP1-GFP protein at the expected size of about 125kDa (Figure 3.11Ai, lane 1), and of IRP2-GFP protein at 132kDa (Figure 3.11Ai, lane 2). When cell extracts of pIRP1-EGFP transfected COS cells were immunoblotted with anti-peptide A of IRP1 anti-serum, both endogenous IRP1 (~98kDa) as well as IRP1-GFP (~125kDa) protein were detected (Figure 3.11Aii). Protein bands corresponding to Rex-GFP and GFP protein, from pRex-EGFP and pEGFP-N3 transfected cells accordingly, resolved at the bottom of the membrane in Figure 3.11A (i), as the resolution of the gel was not appropriate to their molecular size, especially for the latter construct. To ensure that the pRex-EGFP and pEGFP-N3 transfected cells express proteins of the expected size constructs, experiments were repeated and in the case of cell extracts from pRex-EGFP transfected cells, the gel was allowed to run longer, thus enabling a better resolution of the Rex-GFP protein, which was detected at its predicted size of 54kDa

(Figure 3.11B). Similarly when cell extracts of pEGFP-N3 transfected cells were run on a 12% gel and immunoblotted with anti-GFP anti-serum, the expected 27kDa band was evident as indicated (Figure 3.11C).

COS cells were then transiently transfected with pIRP1-EGFP as above and the cell extracts fractionated as described in 2.8.1.2. to investigate the subcellular distribution of the IRP1-GFP protein. Untransfected COS cells served as controls (Figure 3.12A, lanes 1-3 and 8). Western blotting with anti-serum against the peptide A of IRP1 allowed detection of both endogenous IRP1 (~98kDa) and the IRP1-GFP product (~105kDa) in a cytoplasmic fraction of COS cells (prepared as described in 2.8.1.1) (Figure 3.12A, lane 4), as well as in cytoplasmic (Figure 3.12A, lane 5), membrane (Figure 3.12A, lane 6) and nuclear fractions (Figure 3.12A, lane 7). The presence of both endogenous IRP1 protein and the IRP1-GFP product was more evident in the two cytoplasmic fractions (Figure 3.12A, lanes 4 and 5) and less evident in the membrane and nuclear fractions (Figure 3.12A, lanes 6 and 7). Untransfected cells strongly expressed endogenous IRP1 protein (Figure 3.12A, lanes 1-3 and 8). When the same extracts were immunoblotted using an anti-actin anti-serum, all fractions displayed a band of the expected size for actin (~42kDa) (Figure 3.12B). In the membrane fraction a faint band for actin (Figure 3.12B, lane 6) was evident, while in the nuclear fraction (Figure 3.12B, lane 7) no signal was observed. Immunoblotting for actin was not expected to be informative particularly with respect to the nuclear fraction as this protein is primarily a cytoplasmic one, although reports on the intranuclear location of actin are now starting to emerge (reviewed in Pederson and Aebi 2003). Immunoblotting using anti-GFP anti-sera on the same cell extracts was also attempted however was not successful.

To exclude the possibility that the observed nuclear presence of IRP1-GFP protein in the transiently transfected cells is an artefact due to the consequences of over-expression of the pIRP1-EGFP construct, the subcellular distribution of endogenous IRP1 protein expression in untransfected COS cells was investigated alongside the subcellular fractions of the pIRP1-EGFP transfected cells. COS cells transfected with the pRex-EGFP construct were also sub-fractionated and all cell extracts were subjected to SDS-PAGE with subsequent immunoblotting using anti-peptide A of IRP1 anti-serum. Endogenous IRP1 was detected in both the cytoplasmic and

membrane fractions of the untransfected COS cells (Figure 3.12C, lanes 1 and 2), however was not evident in the nuclear fraction (Figure 3.12C, lane 3). In pIRP1-EGFP transfected cells, both endogenous IRP1 and the IRP1-GFP product were evident in all three subcellular fractions as previously (Figure 3.12C; lane 4, cytoplasmic; lane 5, membrane; lane 6, nuclear). Interestingly, endogenous IRP1 protein was evident in all three subcellular fractions of pRex-EGFP transfected cells (Figure 3.12C; lane 7, cytoplasmic; lane 8, membrane; lane 9, nuclear). Western blotting using anti-GFP anti-serum on the same cell extracts was again attempted however was unsuccessful. The absence of a signal of endogenous IRP1 expression in the nuclear fraction of untransfected cells does not rule out the presence of IRP1 in the nucleus as it could have been the result of low levels of IRP1 expression, however its presence in the nuclear fraction of pRex-EGFP transfected cells was puzzling and hence results were not conclusive.

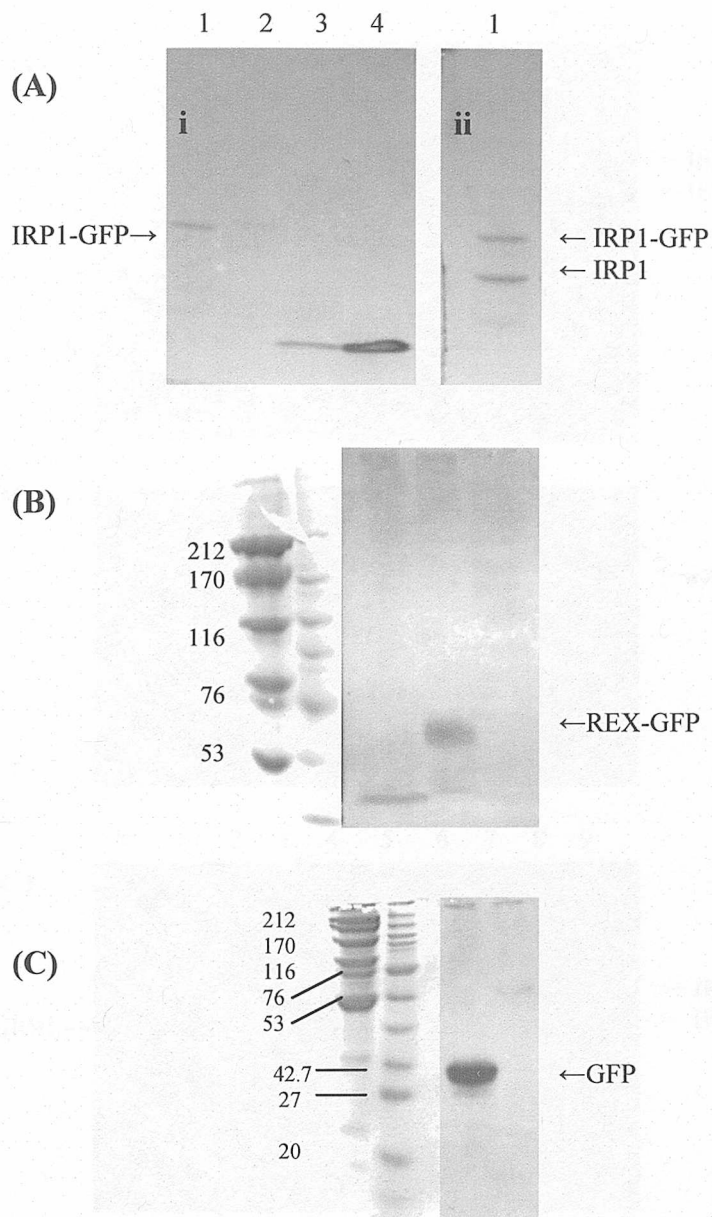


Figure 3.11 Transient expression of IRP1-GFP and Rex-GFP constructs in COS cells.

(A) (i) Western blotting of cytoplasmic extracts of COS cells transfected with the pIRP1-EGFP (lane 1), pIRP2-EGFP (lane 2), pRex-EGFP (lane 3) construct or the pEGFP-N3 vector alone (lane 4). The membrane was immunoblotted with anti-GFP anti-serum and a band of the expected size for IRP1-GFP (~125kDa) was evident as indicated in lane 1. (ii) Cytoplasmic COS cells extracts (50 μ g), transiently transfected with the pIRP1-EGFP construct were subjected to SDS-PAGE. Following immunoblotting with anti-peptide A of IRP1 anti-serum, both endogenous IRP1 (~98kDa) and IRP1-GFP (~125kDa) immunoreacted and were evident as indicated (lane 1). (B) Cell extracts from COS cells transfected with the pRex-EGFP vector were subjected to SDS-PAGE on a 12% gel. A band of the expected size was evident (~54kDa). (C) Cell extracts from COS cells transfected with the pEGFP-N3 vector alone were subjected to SDS-PAGE on a 12% gel and a band of the expected size was evident (~27kDa).

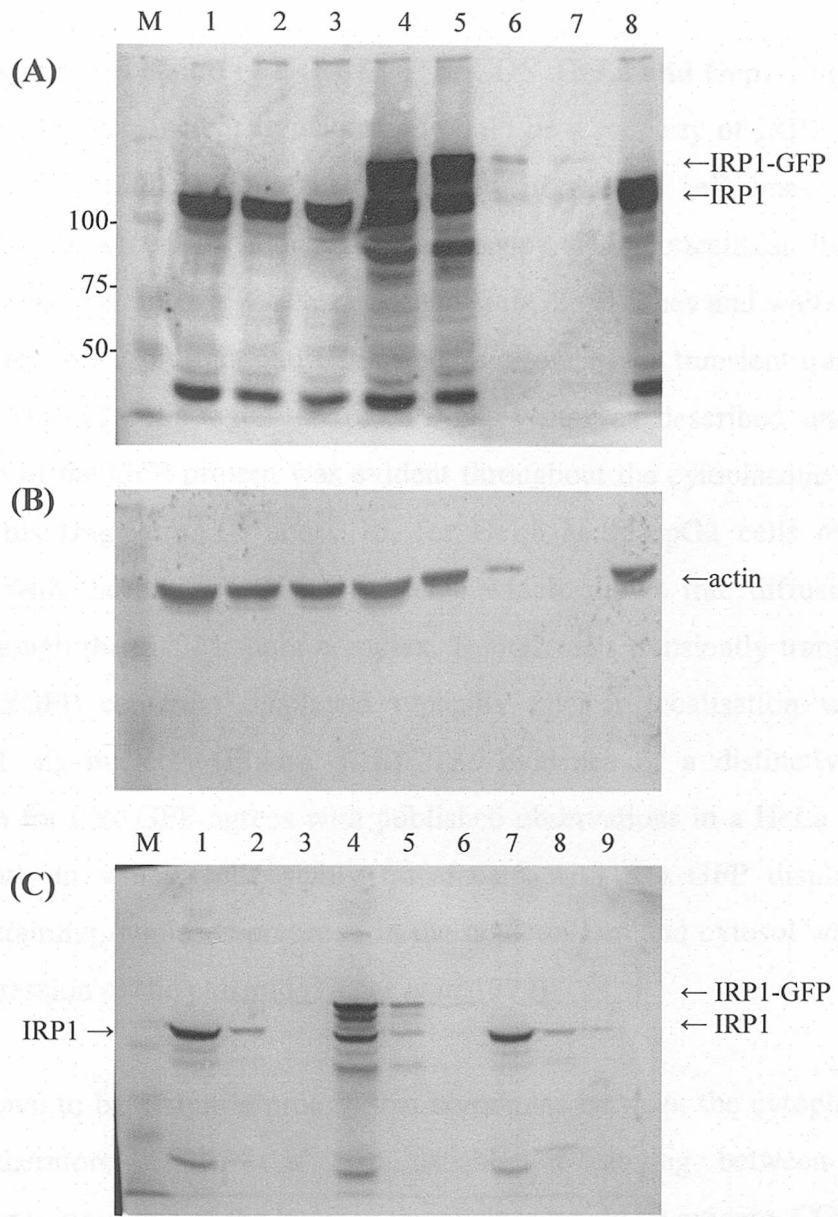


Figure 3.12 Subcellular distribution of IRP1 in COS cells.

(A) Crude cytoplasmic extracts of untransfected COS cells (lanes 1-3, 8) were subjected to Western blotting alongside a cytoplasmic extract of pIRP1-EGFP transiently transfected cells (lane 4) and subcellular fractions of pIRP1-EGFP transfected cells (lane 5, cytosol; lane 6, membrane; lane 7, nuclear). (B) A replica of the gel shown in A was subjected to Western blotting (12%) using rabbit anti-actin anti-serum. (C) COS cells were transiently transfected with pIRP1-EGFP or pRex-EGFP, and fractionated cell extracts were subjected to SDS-PAGE alongside fractionated cell extracts from untransfected COS cells (lane 1, cytosol; lane 2, membrane; lane 3, nuclear). Following immunoblotting with anti-peptide-A of IRP1 anti-serum, both IRP1-GFP and endogenous IRP1 immunoreacted and were evident as indicated in the subcellular fractions of cells transfected with the pIRP1-EGFP (lane 4, cytosol; lane 5, membrane; lane 6, nuclear) and pRex-EGFP (lane 7, cytosol; lane 8, membrane; lane 9, nuclear) constructs.

3.2.4 Transient expression of IRP1-GFP in COS, HeLa and HepG2 cells

To examine whether nuclear translocation could be a property of IRP1, the cellular localisation of the IRP1-GFP fusion protein in several cell lines was further investigated by confocal or fluorescent microscopy. The intracellular distribution of IRP1-GFP was examined in COS, HeLa and HepG2 cell lines and was compared to that of the Rex-GFP product and GFP alone. Following the transient transfection of HeLa and HepG2 cells with the pEGFP-N3 vector as described under 2.7.1.2, distribution of the GFP protein was evident throughout the cytoplasmic and nuclear compartments (Figures 3.13 and 3.15, for HeLa and HepG2 cells respectively), consistent with the size of GFP of 27kDa which allows free diffusion into the nucleus through the nuclear pore complex. HepG2 cells transiently transfected with the pRex-EGFP construct displayed typically nuclear localisation with distinct staining of the nucleoli (Figure 3.16). The evidence of a distinctive nucleolar localisation for Rex-GFP agrees with published observations in a HeLa derived cell line (HLtat), in which cells stably transfected with Rex-GFP displayed strong nucleolar staining, while its presence in the nucleoplasm and cytosol was attributed to overexpression of the plasmid (Heger *et al* 1999).

Rex is known to be a shuttle protein that commutes between the cytoplasm and the nucleus, therefore if IRP1 is also capable of moving between these two compartments, presence of the latter in the nucleus would be evident. COS cells were transiently transfected with the pIRP1-EGFP construct and fluorescence was observed using confocal microscopy (Figure 3.18). Fluorescence was evident in the cytoplasm and the nucleus, excluding the nucleoli as evident in Figure 3.18C. The IRP1-GFP fusion protein localised in the cytoplasm and perinuclear regions of HeLa and HepG2 cells transiently transfected with the respective construct, and to a less extent in the nucleus of these cells (Figures 3.14 and 3.17, for HeLa and HepG2 respectively). Evidence of the expression of IRP1-GFP in the nucleus therefore came from all studied cell lines, COS (Figure 3.19A), HeLa (Figure 3.19B) and HepG2 (Figure 3.19C), and often displayed exclusion of staining in the nucleoli as evident in Figure 3.19B.

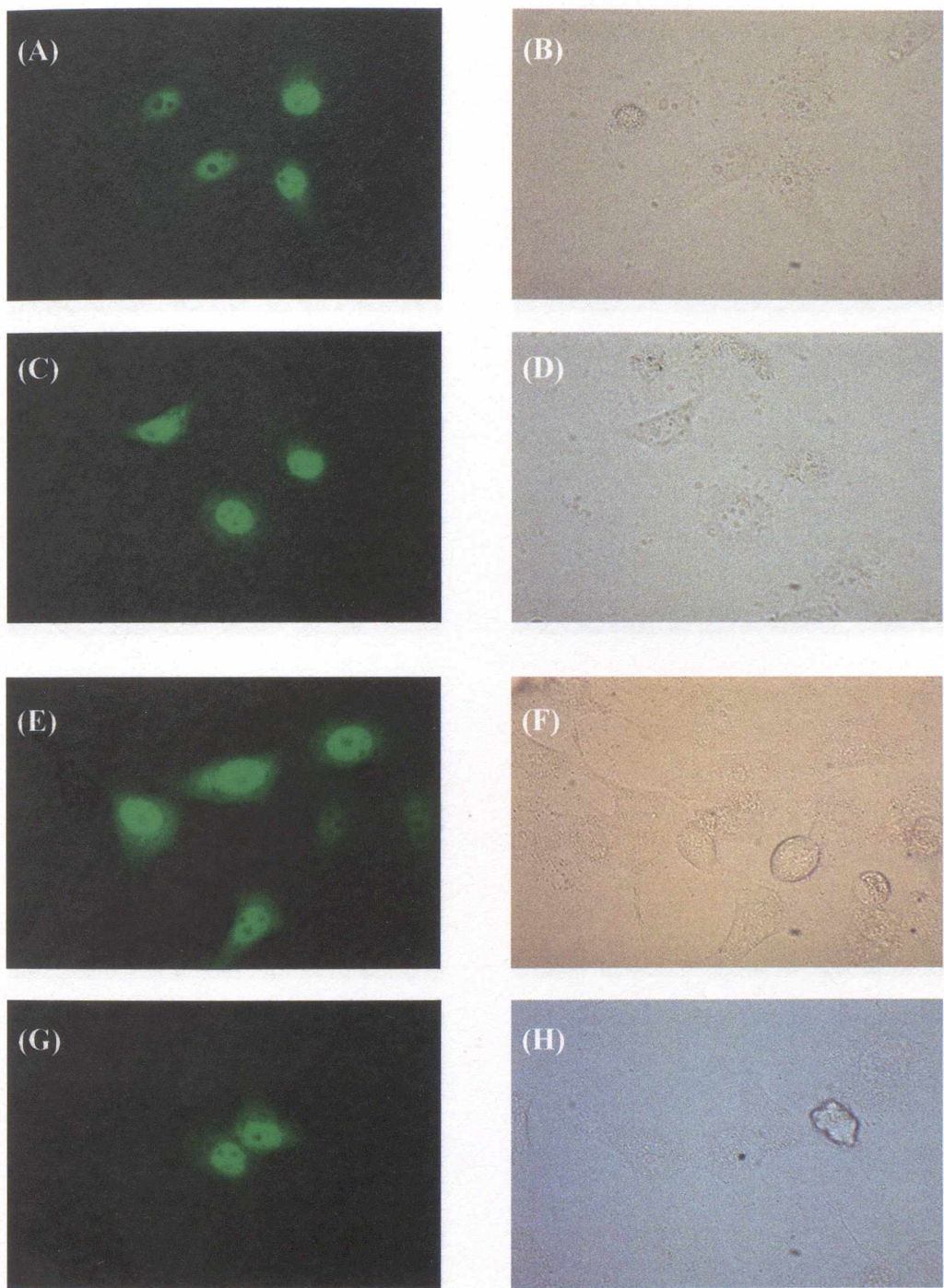


Figure 3.13 Fluorescence microscopy of GFP protein in HeLa transfected cells.

(A), (C), (E), (G) 400x image showing distribution of the GFP product in transiently transfected HeLa cells. Fluorescence is evident throughout the nucleus, excluding the nucleoli. (B), (D), (F), (H) phase contrast image of cells in A, C, E, G, respectively.

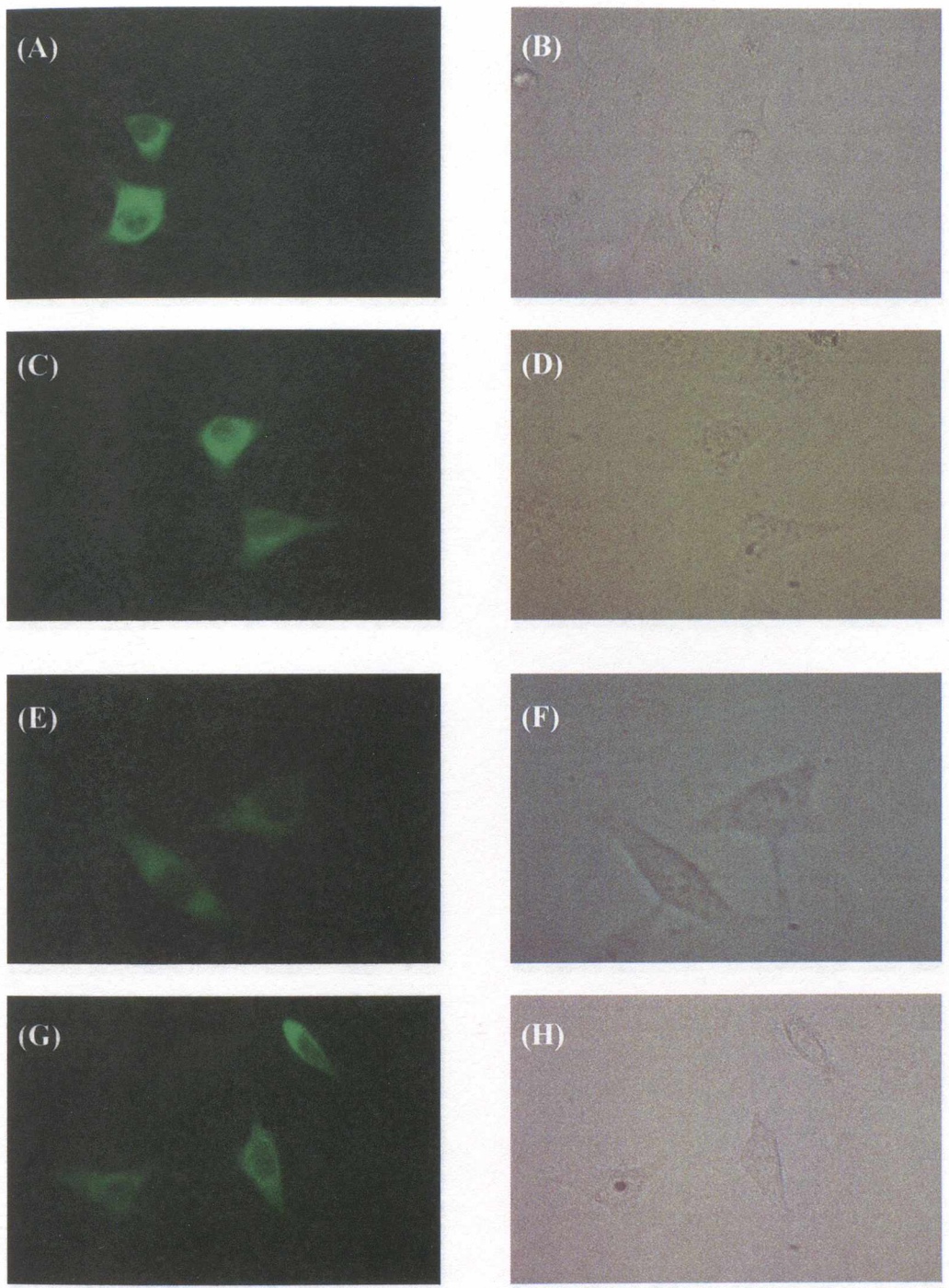


Figure 3.14 Fluorescence microscopy of IRP1-GFP protein in transfected HeLa cells.

(A), (C), (E), (G) 400x image of cells showing distribution of the IRP1-GFP product in transiently transfected HeLa cells. Fluorescence is evident in the cytoplasm with strong perinuclear staining as shown in A. (B), (D), (F), (H) phase contrast image of cells in A, C, E, G, respectively.

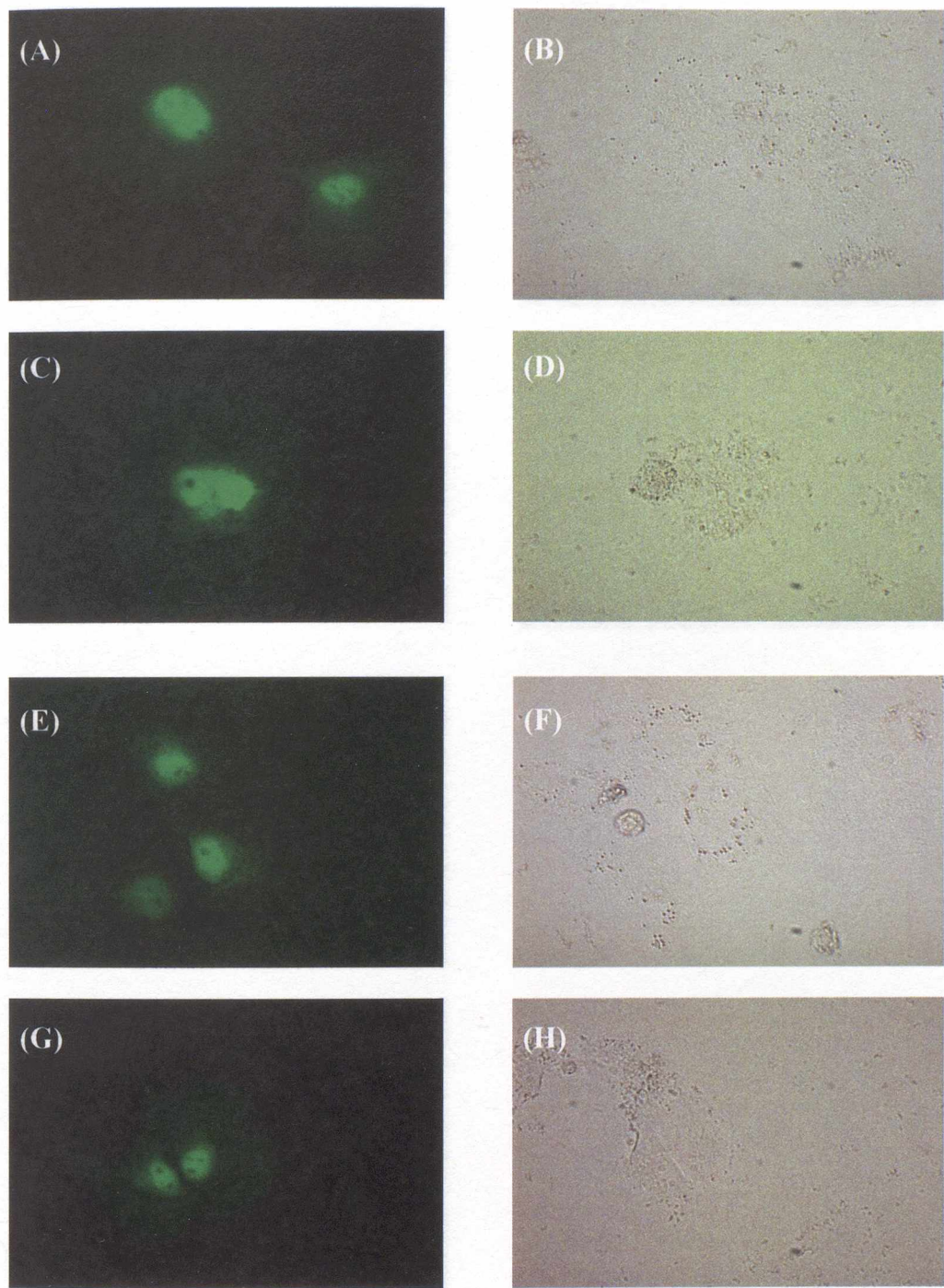


Figure 3.15 Fluorescence microscopy of GFP protein in transfected HepG2 cells.

(A), (C), (E), (G) 400x image showing distribution of the GFP product in transiently transfected HepG2 cells. Fluorescence is evident in the nucleus, excluding the nucleoli, with some cytoplasmic signal. (B), (D), (F), (H) phase contrast image of cells in A, C, E, G, respectively.

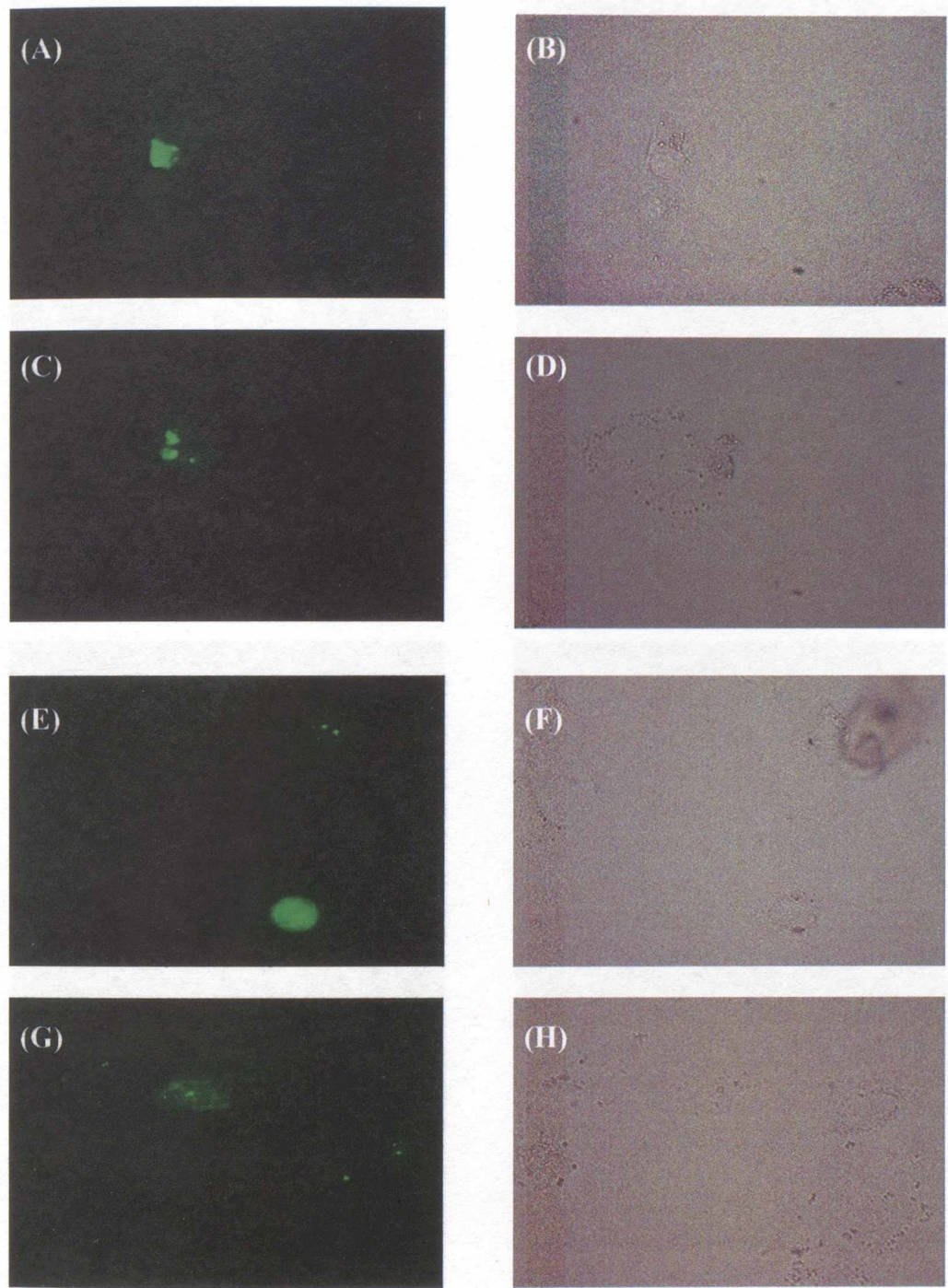


Figure 3.16 Fluorescence microscopy of Rex-GFP protein in HepG2 cells.

(A), (C), (E), (G) HepG2 cells transiently transfected with the pRex-EGFP vector showing distribution of the Rex-GFP product. Fluorescence is evident in the nucleus with intense nucleolar staining. (C) Fluorescence in this cell is strong in the nucleoli with less staining of the nucleus as is the case in some cells in (E) and (G). (B), (D), (F), (H) phase contrast image of cells in A, C, E, G, respectively. (400x images)

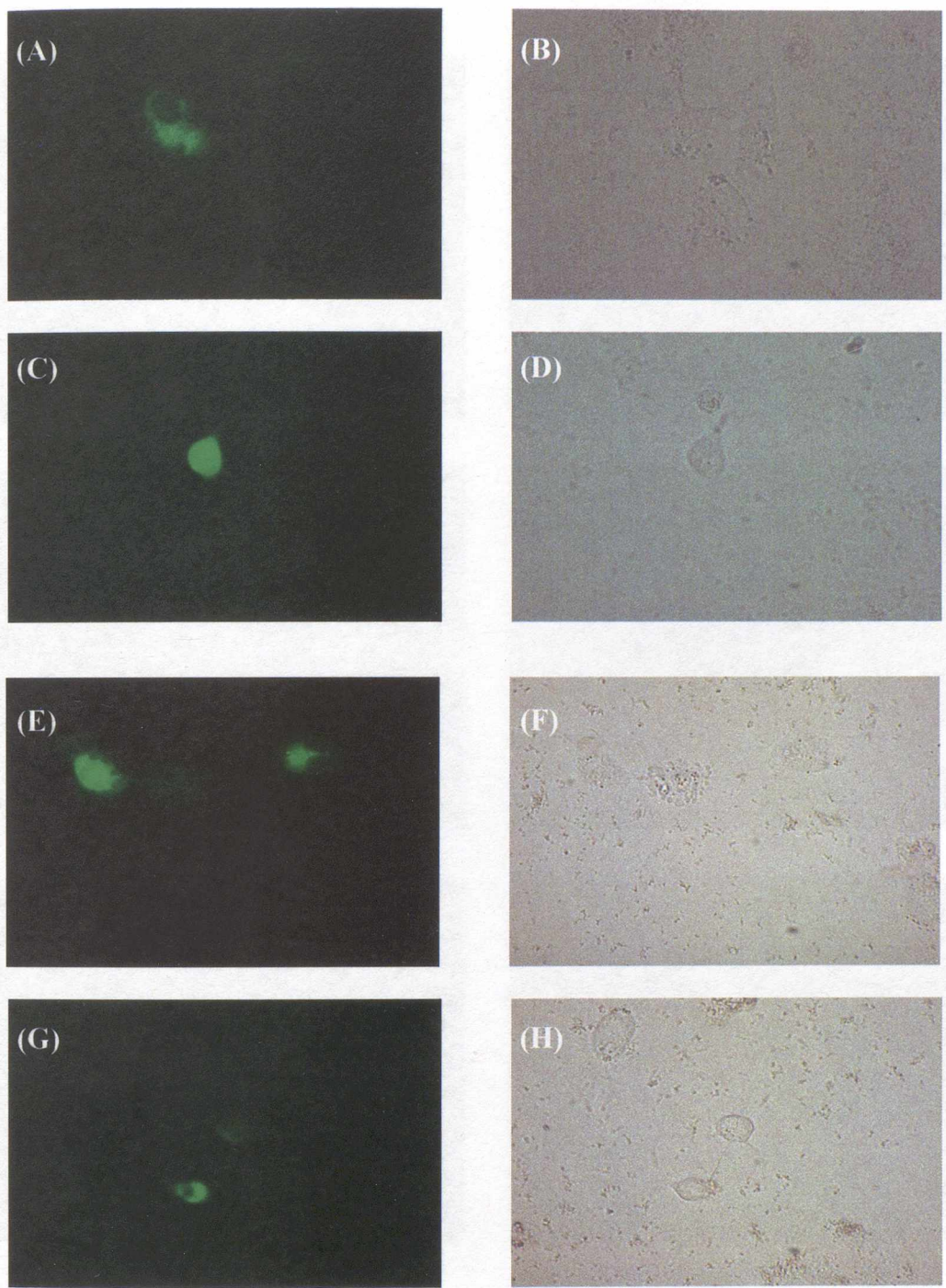


Figure 3.17 Fluorescence microscopy of IRP1-GFP protein in HepG2 cells.

(A), (G) HepG2 cells transiently transfected with the pIRP1-EGFP construct showing distribution of the IRP1-GFP product in the cytoplasm, often intense (E), with some expression in the nucleus, excluding the nucleoli as evident in A. (C) Fluorescence is evident throughout a non-fully formed hepatocyte. (B), (D), (F), (H) phase contrast image of cells in A, C, E, G, respectively. (400x images)

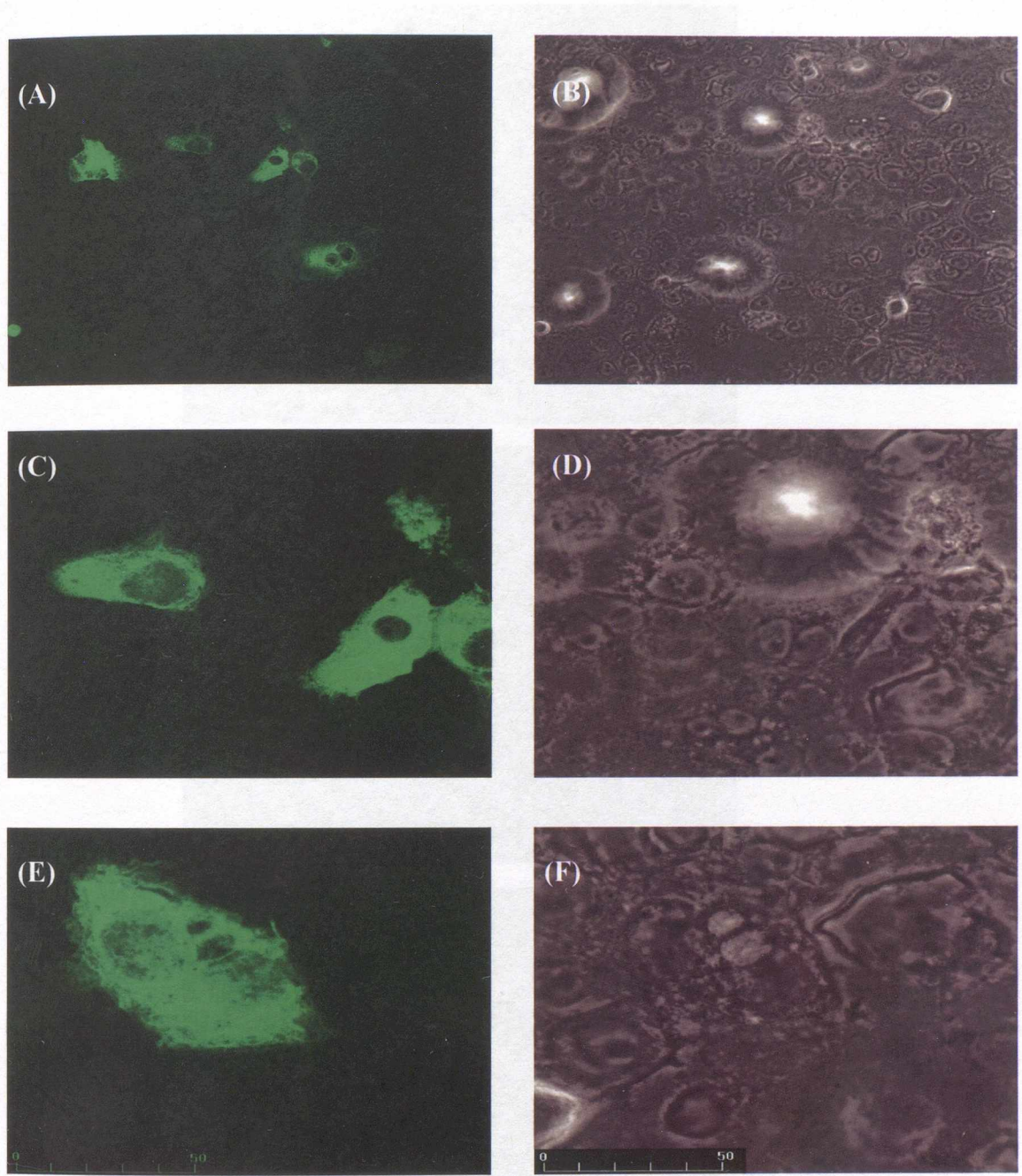


Figure 3.18 Confocal microscopy of IRP1-GFP protein in transfected COS cells.

(A), (C), (E) Cells showing distribution of the IRP1-GFP product in transiently transfected COS cells. Fluorescence is evident in the cytoplasm with some staining of the nucleus, excluding the nucleoli as evident in C. (B), (D), (F) phase contrast image of cells in A, C, E respectively.

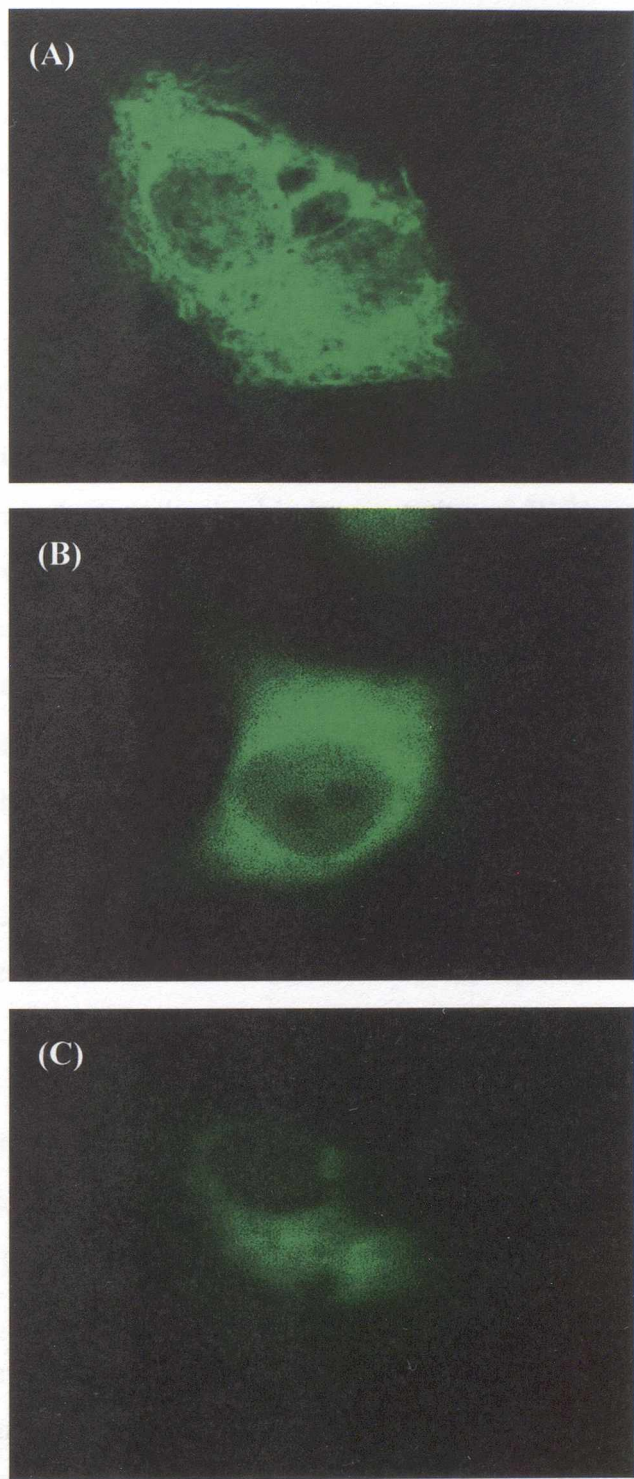


Figure 3.19 Evidence of IRP1-GFP protein expression in the nucleus.

Cells showing distribution of the IRP1-GFP product in transfected COS (A), HeLa (B) and HepG2 (C) cells. Fluorescence is evident in the cytoplasm with strong perinuclear staining, and in the nucleus. Nuclear staining excludes the nucleoli as more evident in B.

3.3 Discussion

3.3.1 Hepatic IRP1 is down-regulated in response to iron loading

IRP1 is an RNA binding protein that post-transcriptionally modulates the expression of mRNAs encoding for proteins involved in iron homeostasis. It has been well established that the RNA binding activity of IRP1 is regulated post-translationally by the insertion or extrusion of a 4Fe-4S cluster, without changes in IRP1 protein levels. However, the possibility of an alternative mechanism of regulation of this protein was suggested from findings that under extreme iron loading conditions, as in HH, the levels of the protein decreased. And while there is a substantial body of evidence concerning the reduction in the binding activity of IRP1 under normal conditions, whether this reduction is accompanied by a reduction in the levels of the protein, under extreme conditions, has attracted less attention. Early studies have suggested that a decrease in the activity of IRP1 was not accompanied by a decrease in the levels of the protein. RNA band-shift analysis in many studies showed that increased levels of iron led to a reduction in RNA binding activity, while decreased iron levels resulted in increased binding activity (Tang *et al* 1992, Haile *et al* 1992). These findings led to the proposal of the iron-mediated regulation of IRP1 binding activity through the Fe-S mechanism (Haile *et al* 1992) (Chapter I, section 1.3.1).

Most of these earlier studies were carried out on cultured cells, in which iron levels were manipulated *in vitro* by adding a source of iron (such as FAC) or haem (such as hemin). Western blotting analysis showed that IRP1 levels were unchanged, despite a decrease in the binding activity of the protein, in H/TRE-BP-1 cells [stable transformants of mouse fibroblast (B6) cells which express a myc epitope-tagged chimeric human-mouse IRP1], rabbit skin fibroblasts (Rab9) and human erythroleukemia (K562) cells (Tang *et al* 1992); in mouse fibroblasts (Ltk⁻) and mouse F1 melanoma (B16F1) cells (Henderson and Kuhn 1995); and in rat hepatoma (FTO2B), and HeLa cells (Guo *et al* 1995). Subsequent studies from different groups however, showed that protein levels of IRP1 diminished under conditions of iron loading (Table 3.3). A reduction in IRP1 binding activity with concomitant decrease in protein levels was first noted in Rab9 cells treated with almost twice the amount of FAC (Goessling *et al* 1992) as compared to the studies mentioned above and later in liver extracts from iron loaded HH patients (Flanagan *et al* 1995). Further evidence of a reduction in IRP1 binding activity that was accompanied by a decrease in the

protein levels in response to iron came from observations using recombinant human IRP1 bearing a phosphomimetic mutation in serine at position 138 and endorsed the possibility of a degradation of IRP1 in response to iron. IRP1 activity and levels were reduced in B6 and human embryonic kidney 293 (HEK293) cells in the presence of hemin (Fillebeen *et al* 2003).

The results presented in this Chapter are in agreement with the latter studies and particularly with those of Flanagan *et al* (1995), demonstrating decreased IRP1 protein expression in the liver of patients with *HFE*-related HH. In iron loaded HepG2 cells a similar but stronger reduction in the levels of the protein was evident, while the disappearance of IRP1 seen in HepG2 cells was not as marked in iron treated COS cells, exemplifying the suitability of iron loaded HepG2 cells as a model to mimic *in vitro* iron overload. HepG2 cells represent a well-differentiated hepatocellular carcinoma cell line that maintains most hepatic functions (Aden *et al* 1979, Hann *et al* 1990) and cells were cultured for 7 days prior to iron treatment to ensure that they exhibit the adult phenotype (Kelly and Darlington 1989). IRP1 protein expression after iron treatment was more evidently absent in HepG2 cells that perhaps by virtue of their origin contain a number of iron uptake mechanisms and hence become more iron loaded than COS cells, as indicated by the atomic iron absorption experiments, leading to a much more marked reduction in the levels of IRP1. The FAC treatment that was used to mimic the *ex vivo* clinical human HH samples, is similar in its effects to NTBI (Kaplan *et al* 1991, Randell *et al* 1994) and is important for the development of iron overload (Hershko *et al* 1978, Batey *et al* 1980, Harrison *et al* 1996). In some of the earlier studies that did not report a decrease in the protein expression of IRP1, such as the one carried out by Henderson and Kuhn (1995), the iron treatment was performed on iron depleted cells, and hence cellular levels of iron may have not greatly exceeded normal levels. The choice of cell line and iron treatment therefore may account for the inconsistencies in the literature regarding the concomitant loss of IRP1 activity and protein levels under iron loading.

The findings presented thus far suggest an impaired adaptive response to the iron accumulation in the liver of HH patients and suggest that when iron levels are increased, to the point that ferritin stores are saturated, there is a decrease in the

levels of IRP1 protein. The molecular mechanism of this observed decrease in IRP1 protein levels was further investigated and the results are presented in Chapter IV and further discussed in Chapter VI. It is interesting to note that the intracellular production of ROS was found to be increased in iron “overloaded” HepG2 cells (Cabrita *et al* 2005), which raises the possibility of the implication of oxidative stress in the regulation of the protein. Oxidative stress has also been implicated in the increase in iron absorption in rats fed on a fish oil rich diet. IRP1 activity as well as expression of IRP1 was up-regulated in the liver of rats on the fish oil rich diet compared to rats on a control diet (Miret *et al* 2003). While a recent study by Clarke *et al* (2006) in mice deficient in superoxide dismutase 1 (SOD1) (*Sod1*^{-/-}), further reported that IRP1 protein abundance can be iron regulated. IRP1 protein levels as well as binding activity were down-regulated in the liver of *Sod1*^{-/-} mice and led the authors to conclude that the increase in oxidative stress observed in these mice can promote damage to the Fe-S clusters, causing IRP1 to be irreversibly as well as reversibly controlled.

With respect to the binding activity and expression of IRP1 in tissues other than the liver, a high IRP1 activity has been observed in the duodenum of HH patients (Pietrangelo *et al* 1995, Recalcati *et al* 2006) and in reticuloendothelial macrophages (Cairo *et al* 1997). Flanagan *et al* (1995) in addition to liver IRP1 investigated the intestinal expression of IRP1 and found little effect of iron overload. Similarly the down-regulation of IRP1 seen in human haemochromatotic liver has not been observed in the duodenum of the same patients or mice, which may reflect the absence of a significant change in iron levels in the duodenum of HH patients (Lombard *et al* 1990, Flanagan *et al* 1995, Cunningham Graham 1998).

Table 3.3 Expression of IRP1 in response to iron

IRP1 binding activity	IRP1 protein levels	Material	Iron source	Other observations or comments	Respective studies
Decreased	No change	B6, H/IRE-BP-1, K562, Rab-9	Hemin (100µM)		Tang <i>et al</i> 1992
Decreased	No change	FTO2B, HeLa	FAC (50µM)		Guo <i>et al</i> 1995
Decreased	No change	Ltk ⁻ , B16F1	FAC (60µM)		Henderson and Kuhn 1995
Decreased	Decreased	Rab-9	FAC (100µM) haem		Goessling <i>et al</i> 1992
Decreased	Decreased	Human liver	Iron loading due to HH	Activity inversely correlated with HIC	Flanagan <i>et al</i> 1995
Decreased	Decreased	B6, HEK293	Hemin (100µM)	Recombinant human IRP1-mutation in Ser-138	Fillebeen <i>et al</i> 2003
Decreased	Decreased	HEK, <i>Abcb7</i> KO mice, <i>Sod1</i> ^{-/-} mice liver	Hemin (100µM)		Clarke <i>et al</i> 2006
Increased	Increased	Rat liver	Fish oil rich diet	Decrease in non-haem iron stores in liver	Miret <i>et al</i> 2003

3.3.2 Smaller forms of IRP1

Evidence for the presence of smaller forms of IRP1 came mainly from the Western blotting experiments and is well in agreement with several reports in the literature. Patino and Walden (1992) observed the extra bands in various rabbit tissue extracts using a mouse anti-rabbit IRP1 anti-serum. In particular extra bands were present in the kidney and liver extracts (~100kDa, ~66kDa, and ~50kDa) but not in lung or brain extracts, and were attributed to degradation of IRP1 protein. Henderson *et al* (1993), using two different anti-sera developed in rabbits raised against amino acids 1-13 and 670-683 (exon 17) of human IRP1, observed a smaller band of ~46kDa that immunoreacted with the former anti-serum in mouse spleen, liver, lymph node but not in lung, intestine, brain, kidney, muscle, heart; while the latter anti-serum did not detect the smaller band in the tissue survey even though the mouse sequence is identical to the human sequence, however it did pick up a higher band of ~150kDa in the liver. Oliveira and Drapier (2000) detected the smaller band of ~46kDa in RAW 264.7 macrophages using an anti-serum raised against the N-terminal peptide of human IRP1 (Henderson *et al* 1993). While the more recent studies by Popovic and Templeton (2005), detected extra bands of ~111kDa and ~95kDa in HepG2 using a commercial anti-IRP1 antibody.

The positions of the peptides recognised by two of the antibodies used in this study are located towards the C and N terminal sides of IRP1, as indicated in Figure 3.9. The consistent presence of the extra bands in membranes immunoblotted with anti-peptide A or anti-peptide B anti-sera, suggests that both antibodies immunoreacted with the recognised epitopes and therefore both peptides are present in what could be alternatively spliced forms of IRP1 lacking central exons. According to the predicted transcripts listed in Table 3.2, the splicing patterns that could account for the lower band of 75kDa are those of transcripts Δ 7-11 and Δ 9-14. Sequence analysis of the nested PCR products supported the idea of missing exons in the alternatively spliced transcripts of IRP1 that were identified (Δ 5-14, Δ 6-17 and Δ 5-13), however the results need to be confirmed and whether these are functional forms of IRP1 has not been examined. Moreover, the sequence alignments did not match any of the predicted variants, which need to be further examined for cryptic splice sites, and therefore conclusions could not be drawn.

3.3.3 Intracellular localisation of IRP1

The intracellular distribution of IRP1 was then investigated in cultured cells. Western blotting experiments revealed the presence of IRP1-GFP in nuclear fractions of COS cells, however further experiments are necessary before firm conclusions can be drawn. Since the target mRNAs of IRP1 are both cytosolic (ferritin) and membrane (TfR1) associated, a signal was expected as evident for both cytosolic and membrane fractions. The predominant presence of IRP1 in cytoplasmic fractions agrees with a study by Patton *et al* 2005 carried out on rat liver. This study also found IRP1 in the membrane fraction and concluded that the localisation of IRP1 to the membranes involves phosphorylation and is responsive to cellular iron status. In terms of the current findings, the observations need to be repeated and reinforced with the use of anti-GFP as well as an antibody raised against a nuclear protein so that the nuclear fraction is examined for the presence of proteins. To exclude the possibility that the observed nuclear localisation in the transfected cells is an artefact due to the consequences of over-expression of IRP1-GFP, the localisation of IRP1 in other cell lines needs to be further addressed if it can localise in the nucleus of endogenously expressing cells. The results of confocal and fluorescence microscopy further supported the observations from the subcellular fractions as fluorescence was evident in the nucleus of IRP1-GFP transiently transfected COS, HeLa and HepG2 cells. In agreement with the Western blotting experiments, the amount of fluorescence was less evident in the nucleus as compared to the expression of the protein in the cytoplasm or perinuclear regions. The localisation of IRP1 in the perinuclear region agrees with a study by Patton *et al* (2005) that however did not observe IRP1 expression in the nucleus of NIH3T3 cells.

Preliminary data suggesting that the mainly cytoplasmic IRPs might be also present in the nucleus to a smaller extent and under certain conditions, comes in accordance with a functional study carried out by Zolotukhin *et al* (1994). Zolotukhin *et al* (1994) showed that the IRE/IRP system can rescue nuclear RNA from a human immunodeficiency virus type 1 (HIV-1) instability (INS) sequence, similar to the activity of the Rev/Rev Responsive Element (Rev/RRE) system. Although this was not the main emphasis of the study the data clearly indicated the nuclear activity of IRP1. Both HIV-1 and HTLV-1 use a post-transcriptional regulatory system, involving both cytoplasmic and nuclear events to control expression of their

structural proteins (Zolotukhin *et al* 1994). In these systems, the presence of elements decreasing mRNA expression (also known as *cis*-acting repressors, CRS) is counteracted by the interaction of regulatory proteins with specific mRNA sites. One well studied instability/inhibitory element is that of HIV-1 called INS-1, the down-regulatory effects of which are antagonised by the interaction of the Rev regulatory protein (in the case of HTLV-1 the regulatory protein is Rex) with a distinct element located on the viral mRNA termed Rev Responsive Element (RRE) [RXRE in the case of HTLV-1] (Zolotukhin *et al* 1994). Zolotukhin *et al* (1994) hypothesise that since Rev and Rex systems can overcome viral and cellular posttranscriptional regulatory elements, they may represent mRNA rescue systems permitting efficient expression of a variety of heterologous 'defective' or unstable mRNAs. Rev in particular is thought to chaperone RRE-containing mRNAs through the entire pathway from the nucleus to the cytoplasm, which is supported by findings of Rev shuttling.

The presence of a putative NLS on IRP1 and the observations of a nuclear localisation of IRP1 and IRP1-GFP taken together with the finding by Zolotukhin *et al* (1994) that the IRE/IRP system can rescue nuclear RNA from an HIV instability (INS) sequence prompt for a closer examination of this regulatory system. It would be exciting to investigate possible novel functions of these mainly considered cytoplasmic proteins as well as of the IRE/IRP interactions in the nucleus. IRPs present in the nucleus may bind to the IREs present on the mRNA precursors of iron related transcripts and regulate their alternative splicing. This regulatory mechanism could possibly be affected by iron stores, since under high iron conditions IRPs cannot bind IREs. This would lead to the intron containing the IRE becoming accessible for excision, resulting in the accumulation of messages without IREs.

Alternative splicing of genes involved in iron transport and storage has been reported for ferritin, TfR2 and DMT1, and more recently for HFE (Thénié *et al* 2000, Furnham *et al* 2004). Alternative splicing forms of ferritin have been reported in *Drosophila melanogaster*, with or without an IRE in their 5' UTR (Georgieva *et al* 1999, Lind *et al* 1998). And interestingly, ferritin has been detected by immunocytochemistry in the nucleus of hepatocytes of iron overloaded mice (Smith *et al* 1990) and by immunofluorescence and confocal microscopy in K562

cells (Pountney *et al* 1999). Two forms have been described for TfR2, an alpha (α) and a beta (β) form; α is the full length transcript and is the main mRNA as judged by Northern blotting, while β is missing exons 1 to 3 and has a longer version of exon 4, encoding an intracellular form that is more widely expressed in tissues than the α form (Kawabata *et al* 1999). Neither form contains any IREs however. In mammalian cells two isoforms of DMT1 result from alternate splicing of a single gene product. A splice variant in human Nramp2 originally described by Lee *et al* (1998) and later by Tabuchi *et al* (2002) showed that alternative splicing regulates DMT1 localisation in the cell. The IRE containing form is predominantly expressed in epithelial cell lines while the non-IRE form in blood cell lines. And the non-IRE form has also been found to localise in the nuclei of neuronal cells or of neuronal origin (Roth *et al* 2000). The tissue specific expression of the DMT1 isoforms is thought to be regulated by erythropoiesis (Tchernitchko *et al* 2002). The existence of IRE and non-IRE containing isoforms of iron-related molecules and the evidence of a nuclear IRP1 presence prompts for an investigation into the interaction between IRP1 and any of these transcripts in the nucleus.

3.3.4 Future directions

Prior to carrying out any future work based on the outcomes of the presented studies, it is imperative that some of the experimental evidence be verified using appropriate controls that were not available at the time. Although the anti-IRP1 antibodies have been extensively used by others previously, it is important to illustrate their specificity. That could be achieved using synthetic peptides corresponding to the sequence of amino acids recognised by the aforementioned antibodies. Incubating the antibody with the peptide prior to carrying out the Western blotting experiments would block any antibody activity. The expected outcome would be an absence of the main IRP1 band, as well as of the upper and lower bands (provided that the proposed hypothesis holds and they are specific products). A further control to illustrate the specificity of the anti-IRP1 antibodies would be the use of a cell line not expressing IRP1. And finally, whilst immunodetection for actin did not prove to be an appropriate control (the levels of α -actin are thought to be influenced by iron), another housekeeping gene needs to be identified, such as β -actin or tubulin, that will

corroborate the use of equal amounts of protein between samples when carrying out the Western blotting experiments.

Additional evidence on the nested PCR approach examining the alternatively spliced forms of IRP1 could be obtained by performing 2D protein electrophoresis followed by microsequencing of the extra bands and again alignment with the IRP1 sequence. To take the observations of the nuclear presence of IRP1 further, site-directed mutagenesis of the putative NLS could be attempted aiming to observe exclusion of a signal from the nucleus. Further experiments could also involve using leptomycin B, a metabolite of *Streptomyces* that is an exportin 1 (CRM1)-inactivating antibiotic, which blocks nuclear export (Kudo *et al* 1998). Treatment with leptomycin B, would reveal whether IRP1-GFP shuttles between the cytoplasm and the nucleus, as it would cause the chimera to accumulate in the nucleus if that is the case.

Further experiments could also involve examination of the subcellular distribution of IRP1 and IRP1-GFP in response to iron. Stable cells expressing IRP1-GFP would be needed in order to achieve the latter, while expression of endogenous IRP1 could be revisited by optimising ways to achieve stronger expression and if that is achievable by examining expression following iron treatment. Attempts were made in creating stable cell lines expressing IRP1-GFP, by incubating transfected cells in a medium supplemented with the antibiotic Geneticin (G418) followed by individual clone isolation using cloning cylinders, however were not fruitful. The stable transfection of HepG2 cells with pEGFP-N3 has been reported, with selection achieved by using a medium with $800\mu\text{g}\cdot\text{mL}^{-1}$ G418 for 2 weeks (Moh *et al* 2003).

Chapter IV

Hepatic mRNA levels of HAMP, HJV, TfR1, TfR2 and IRP1 in HH

4.1 Introduction

The observation of a down-regulation in IRP1 protein levels in the liver of HH patients in Chapter III prompted an investigation into the transcript levels of this regulatory protein in an attempt to explore the molecular mechanism behind this phenomenon. Transcript levels of HAMP, as well as of TfR1, TfR2 and HJV in the liver of HH patients were also of interest as these molecules are strongly implicated in iron absorption and homeostasis and although the causative genes have been discovered, the pathogenesis of HH remains elusive. It is only in the last years that some clues are beginning to surface and the uncontrolled iron accumulation seen in these disorders is now widely believed to be due to lack of an appropriate hepcidin response to the increasing iron burden. The cellular iron exporter FP1 is thought to be hepcidin's main target, which in the case of HH fails to receive the message and stop egress of iron into the circulation. What's more, hepcidin expression is now thought to be under the dual control of HJV and TfR2, although the exact ways and links remaining to be established. In the study presented in this chapter, the mRNA expression of the key iron-related molecules IRP1, HAMP, HJV, TfR1, and TfR2 was measured in the liver of iron loaded patients. The expression levels of these transcripts were evaluated in relation to serum iron indices and iron deposition in the liver.

The overall aim of the study presented in this chapter was to examine the mRNA levels of key iron-related transcripts in physiological and iron loading conditions. An evaluation of IRP1 mRNA levels in HH patients as compared to control subjects would provide an insight into the observed down-regulation in hepatic IRP1 protein levels in HH and point to either a transcriptional or post-transcriptional underlying mechanism. Levels of the hepcidin transcript in the liver have been the focus of numerous studies, but none provide a picture of all five molecules in the face of HH. A further aim was to study the relationship between these molecules and clinical iron parameters in an attempt to elucidate possible cues to which these molecules respond, if at all, at the level of transcription.

4.2 Results

4.2.1 Clinical characteristics of study groups

Using quantitative real-time PCR, transcript levels of iron-related genes *HAMP*, *HJV*, *IRP1*, *TfR1* and *TfR2* were determined in 7 controls, 5 iron loaded patients homozygous for the C282Y mutation in the *HFE* gene (YY genotype group) as well as in patients with hepatic iron levels higher than 1500 μ g Fe per g dry weight, irrespective of their genotype (iron loaded phenotype group, n=7). The latter group consisted of the 5 patients homozygous for the C282Y mutation, a heterozygote for the same mutation (CY), and a case of PKD. The characteristics and clinical iron parameters of the subject groups used in this study, including age, gender, serum ferritin, serum iron, transferrin saturation, total iron binding capacity and hepatic iron concentration are summarised in Table 4.1. Control subjects showed normal iron indices and had no evidence of disturbances in the body iron status. Characteristics including date of birth, age at year of biopsy and clinical indices (SF, SI, TS, TIBC, HIC and grade of siderosis) for individual samples is provided in Appendix I (Tables A and B).

Table 4.1 Clinical characteristics and iron indices of study groups in chapter IV

	Control group n=7	YY genotype group n=5	Iron loaded phenotype group n=7
Age at diagnosis, (years)*	45 ± 12 (27 - 60)	53 ± 12 (41 - 73)	50 ± 13 (31 - 73)
Sex, (male/female)	7/0	4/1	6/1
SF, (ng·mL⁻¹)*	269.4 ± 218.3 (98 - 625)	3035 ± 1635 (950 - 5165)	2801 ± 1724 (458 - 5165)
SI, (μmoles·L⁻¹)*	18.14 ± 2.478 (14 - 21)	41.52 ± 4.031 (37 - 46)	39.66 ± 6.925 (26 - 46)
TIBC, (μmoles·L⁻¹)*	53.29 ± 5.678 (46 - 62)	44.02 ± 7.114 (38 - 56)	46.01 ± 7.853 (38 - 58)
TS, (%)*	34 ± 3.266 (30 - 39)	95 ± 7.463 (83 - 100)	88 ± 20.30 (45 - 100)
HIC, (μg Fe/g dry wt)*	768.7 ± 288.3 (319 - 1114)	15854 ± 10796 (3974 - 27320)	15949 ± 11887 (2378 - 30000)

* Range (mean ± standard deviation) (min-max)

4.2.2 Real-time PCR efficiency

HAMP, HJV, IRP1, TfR1, and TfR2 mRNA levels were analysed by qRT-PCR (primers used and exons amplified shown in Chapter II, Table 2.1.1) and PCR reactions were checked by both melting curve and gel analysis (Figures 4.1 and 4.2). qRT-PCR resulted in single product specific melting temperatures and a single band on the gel of the expected size based on the nucleotide sequence of each respective transcript for HAMP (Figure 4.1A), HJV (Figure 4.1B), TfR1 (Figure 4.1C), IRP1 (Figure 4.2A), and TfR2 (Figure 4.2B) and β -actin (Figure 4.2C). The melting peak of the unknowns matched that of the standards confirming product specificity. The T_m of standards and unknowns were 89.046°C and 88.978°C for *HAMP*, 88.578°C and 88.328°C for *HJV*, 84.963°C and 84.675°C for *TfR1*, 83.29°C and 83.418°C for *IRP1*, 86.663°C and 86.571°C for *TfR2*, and 89.672°C and 89.641°C for β -actin. Furthermore, investigated transcripts showed high real-time PCR efficiency rates with high linearity (Pearson correlation coefficient $r=-1.000$) as calculated using Equation 2.5, Chapter II. Real-time PCR efficiencies (E_s) were 1.948, 1.870, 1.898, 1.896, 1.969, 1.928 for *HAMP*, *HJV*, *IRP1*, *TfR1*, *TfR2* and β -actin, respectively. Finally, levels of β -actin mRNA were comparable between controls and iron loaded patients (YY genotype group or iron loaded phenotype group), thus validating the use of β -actin as a suitable housekeeping gene in this set of experiments.

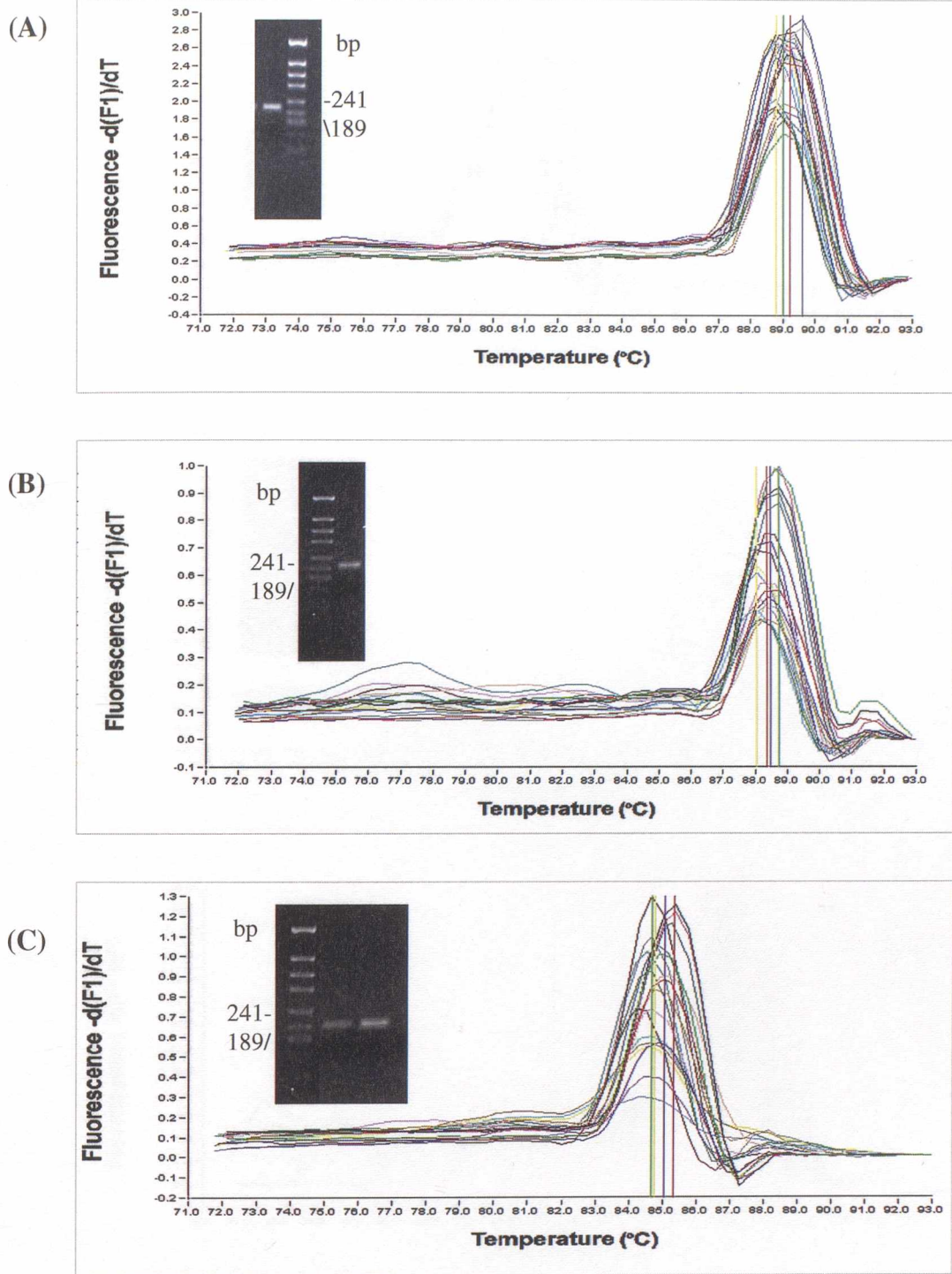


Figure 4.1 Melting curve and gel analysis of the HAMP, HJV and TfR1 transcripts.

Amplicon melting temperatures were determined by calculating the derivatives of the curve with the LightCycler software and visualised by plotting the negative derivatives against temperature. Single melting peaks showing specific amplification of (A) HAMP at $\sim 89^{\circ}\text{C}$, (B) HJV at $\sim 88.4^{\circ}\text{C}$, and (C) TfR1 at $\sim 84.8^{\circ}\text{C}$, were obtained. Real-time PCR products were run on 1.5% agarose gels and the expected amplicon sizes for (A) HAMP $\sim 180\text{bp}$, (B) HJV $\sim 202\text{bp}$ and (C) TfR1 $\sim 179\text{bp}$, were evident.

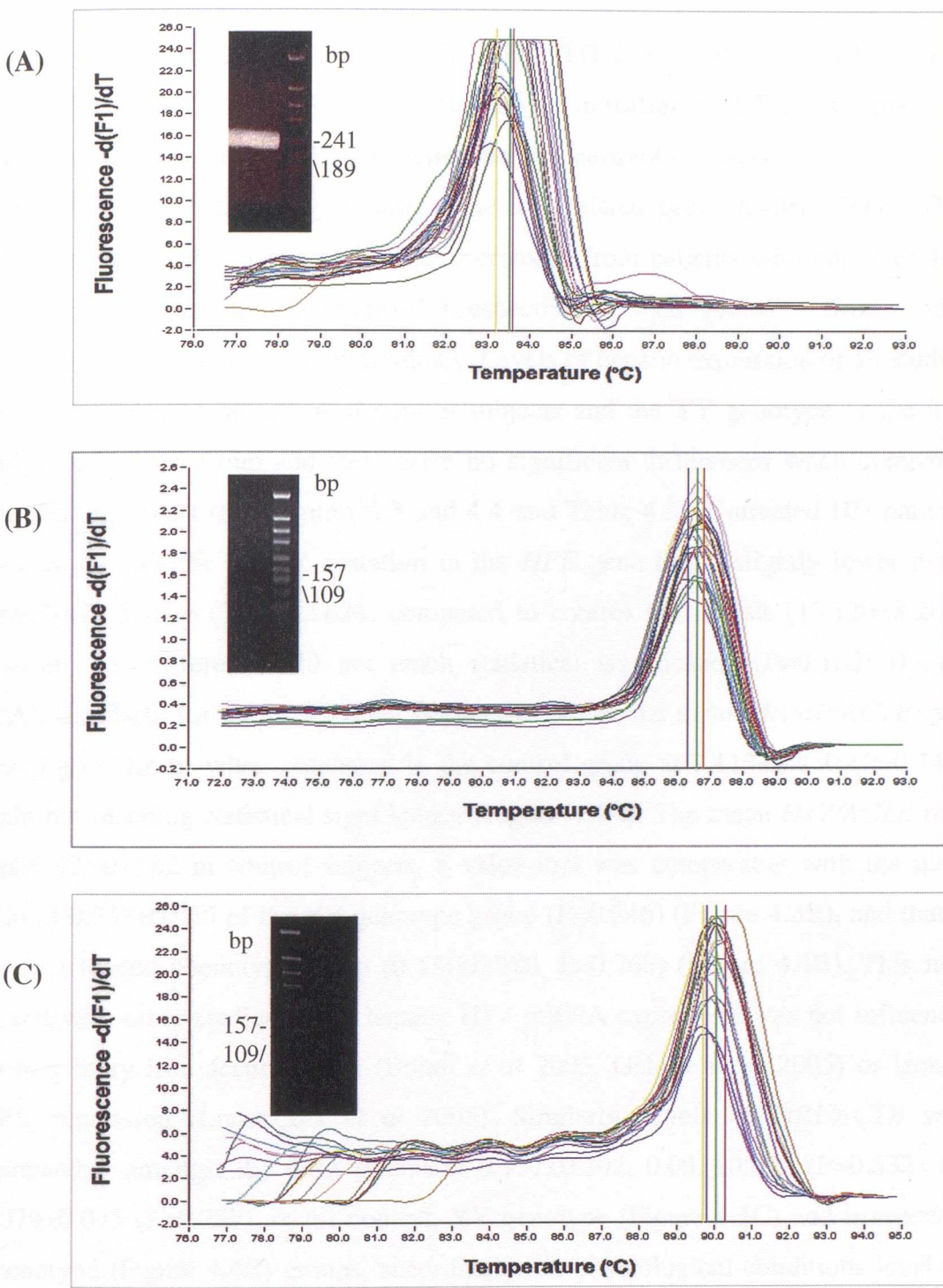


Figure 4.2 Melting curve and gel analysis of the IRP1, TfR2, and β -actin transcripts.

Amplicon melting temperatures were determined by calculating the derivatives of the curve with the LightCycler software and visualised by plotting the negative derivatives against temperature. Single melting peaks showing specific amplification of (A) IRP1 at $\sim 83^{\circ}\text{C}$, (B) TfR2 at $\sim 86.6^{\circ}\text{C}$, and (C) β -actin at $\sim 89.6^{\circ}\text{C}$, were obtained. Real-time PCR products were run on 1.5% agarose gels and the expected amplicon sizes for (A) IRP1 $\sim 251\text{bp}$, (B) TfR2 $\sim 110\text{bp}$ and (C) β -actin $\sim 120\text{bp}$, were evident.

4.2.3 Levels of hepatic HAMP, HJV, TfR1, TfR2 and IRP1 mRNA in iron loaded HH patients homozygous for the major mutation in *HFE*, patients with iron overload irrespective of their genotype and control subjects

Using qRT-PCR, hepatic expression of the iron-related genes *HAMP*, *HJV*, *TfR1*, *TfR2*, and *IRP1*, were analysed in liver specimens from patients with untreated HH (YY genotype group), iron overload irrespective of their genotype (iron loaded phenotype group), and control individuals. Levels of hepatic expression of all studied genes were comparable amongst control subjects and the YY genotype or the iron loaded phenotype group and there were no significant differences when compared with the unpaired t test (Figures 4.3 and 4.4 and Table 4.2). Untreated HH patients homozygous for the C282Y mutation in the *HFE* gene had a slightly lower mean *HAMP/ACTB* ratio (7.474 ± 2.624) compared to control individuals (13.120 ± 8.284), however this difference did not reach statistical significance ($P=0.160$) (Figure 4.3A). Similarly for the iron loaded phenotype group, the mean *HAMP/ACTB* ratio was slightly lower when compared to the control group at 7.113 ± 2.430 ($P=0.147$), again not reaching statistical significance (Figure 4.4A). The mean *HJV/ACTB* ratio was 0.375 ± 0.282 in control subjects, a value that was comparable with the mean ratio of 0.352 ± 0.055 of the YY genotype group ($P=0.846$) (Figure 4.3B), and that of the iron loaded phenotype group (0.431 ± 0.380 , $P=0.768$) (Figure 4.4B). This is in accord with other studies where hepatic HJV mRNA expression was not influenced by hereditary iron accumulation (Bondi *et al* 2005, Gehrke *et al* 2005) or lack of *HFE* expression (Ludwiczek *et al* 2005). Similarly, levels of *TfR1/ACTB* were comparable amongst the three groups at 0.137 ± 0.102 , 0.092 ± 0.092 ($P=0.532$) and 0.079 ± 0.075 ($P=0.287$), in the control, YY genotype (Figure 4.3C) and iron loaded phenotype (Figure 4.4C) groups, accordingly. At physiological conditions levels of *TfR2/ACTB* were 1.285 ± 1.224 , comparable to 1.277 ± 0.579 ($P=0.988$) of the YY genotype group (Figure 4.3D), and 1.254 ± 0.620 ($P=0.957$) of the iron loaded phenotype group (Figure 4.4D). Similarly TfR2 mRNA levels in the livers of *HFE* KO mice and controls were found to be equally abundant (Fleming *et al* 2000, Muckenthaler *et al* 2003). Finally, levels of *IRP1/ACTB* were 3.492 ± 2.162 , 2.790 ± 1.938 ($P=0.597$) and 3.105 ± 1.601 ($P=0.719$), in the control, YY genotype (Figure 4.3E), and iron loaded phenotype (Figure 4.4E) groups, respectively.

Hepatic expression of the mentioned genes was also measured in one treated HH patient, homozygous for the major mutation in *HFE*, and in one case of NH (Table 4.2). HAMP mRNA expression in the iron-depleted HH patient was found to be notably low (0.989) compared to all other samples (comparison of the mean ratios with the t test cannot be performed in this case since the test requires at least two values per group). This finding agrees with studies by Bridle *et al* (2003) and Gehrke *et al* (2005), who have found a significant down-regulation in hepatic hepcidin expression in treated HH patients compared to a control group or an untreated YY genotype group. TfR1 levels in the treated HH patient were comparable to the mean ratios of all study groups, but interestingly, TfR2 levels were higher (5.300). Levels of IRP1 were also higher in this case (6.951), and a slight increase was also observed in the levels of HJV (1.272). Similarly, HAMP levels in the liver of the NH case were very low (0.960), while levels of TfR1 (0.150) were comparable to the mean value of each of the study groups. Levels of IRP1 (0.791), TfR2 (0.341) and HJV (0.144) however, were somewhat lower in the NH case when compared with the mean value of each study group.

Table 4.2 Summary of mRNA expression levels of studied genes

	HAMP	HJV	TfR1	TfR2	IRP1
Control group	13.12 ± 8.284	0.375 ± 0.282	0.137 ± 0.102	1.285 ± 1.224	3.492 ± 2.162
YY group	7.474 ± 2.624	0.352 ± 0.055	0.092 ± 0.092	1.277 ± 0.579	2.790 ± 1.938
[iron] group	7.113 ± 2.430	0.431 ± 0.380	0.079 ± 0.075	1.254 ± 0.620	3.105 ± 1.601
Treated HH	0.989	1.272	0.133	5.300	6.951
Neonatal H	0.960	0.144	0.150	0.341	0.791

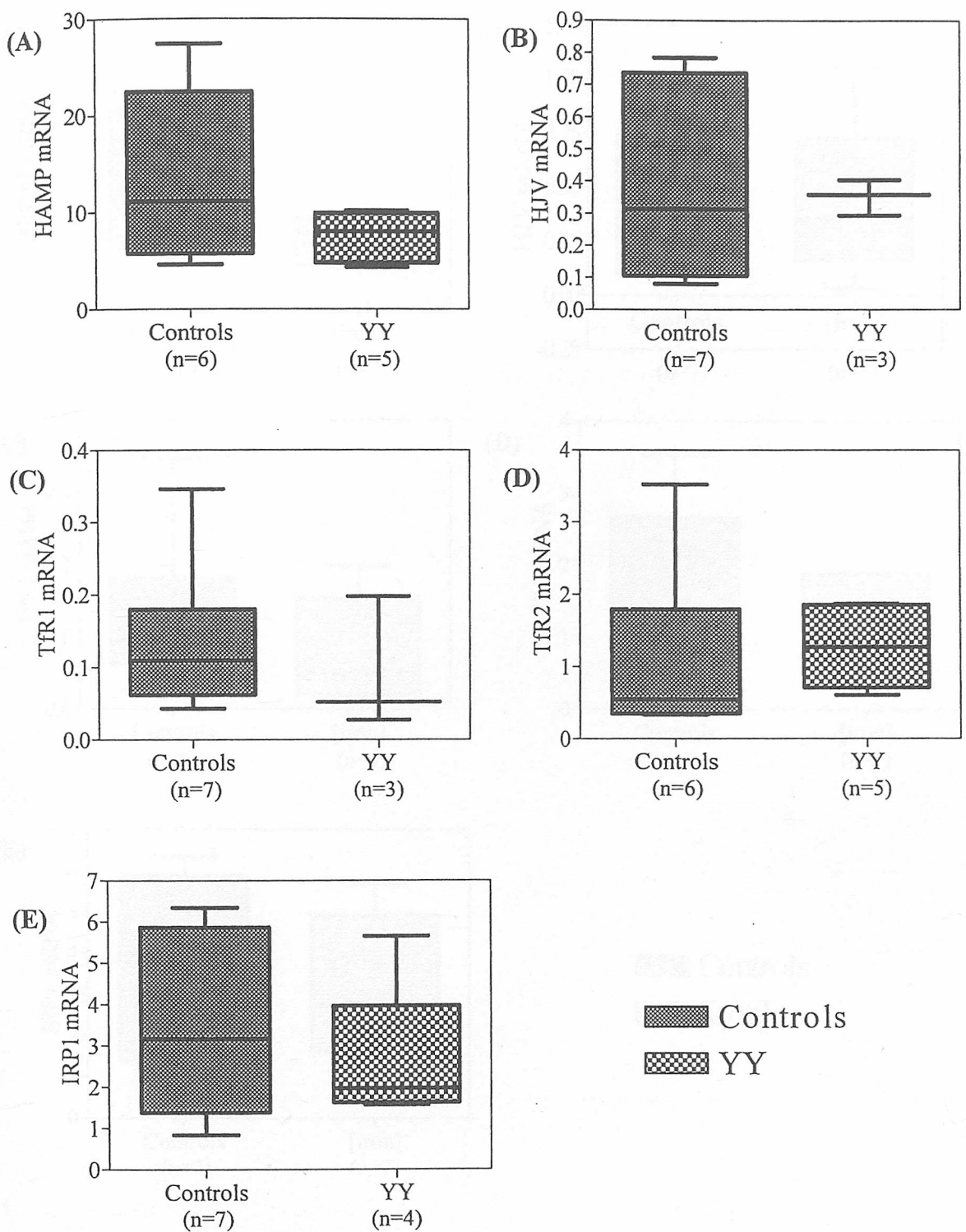


Figure 4.3 Hepatic mRNA expression of HAMP, HJV, TfR1, TfR2 and IRP1 in HH patients homozygous for the C282Y mutation and control individuals.

There were no significant differences in the expression of (A) HAMP ($P=0.160$), (B) HJV ($P=0.846$), (C) TfR1 ($P=0.532$), (D) TfR2 ($P=0.988$) or (E) IRP1 ($P=0.597$) between the control and the YY group, as analysed with the unpaired t test (two-tailed).

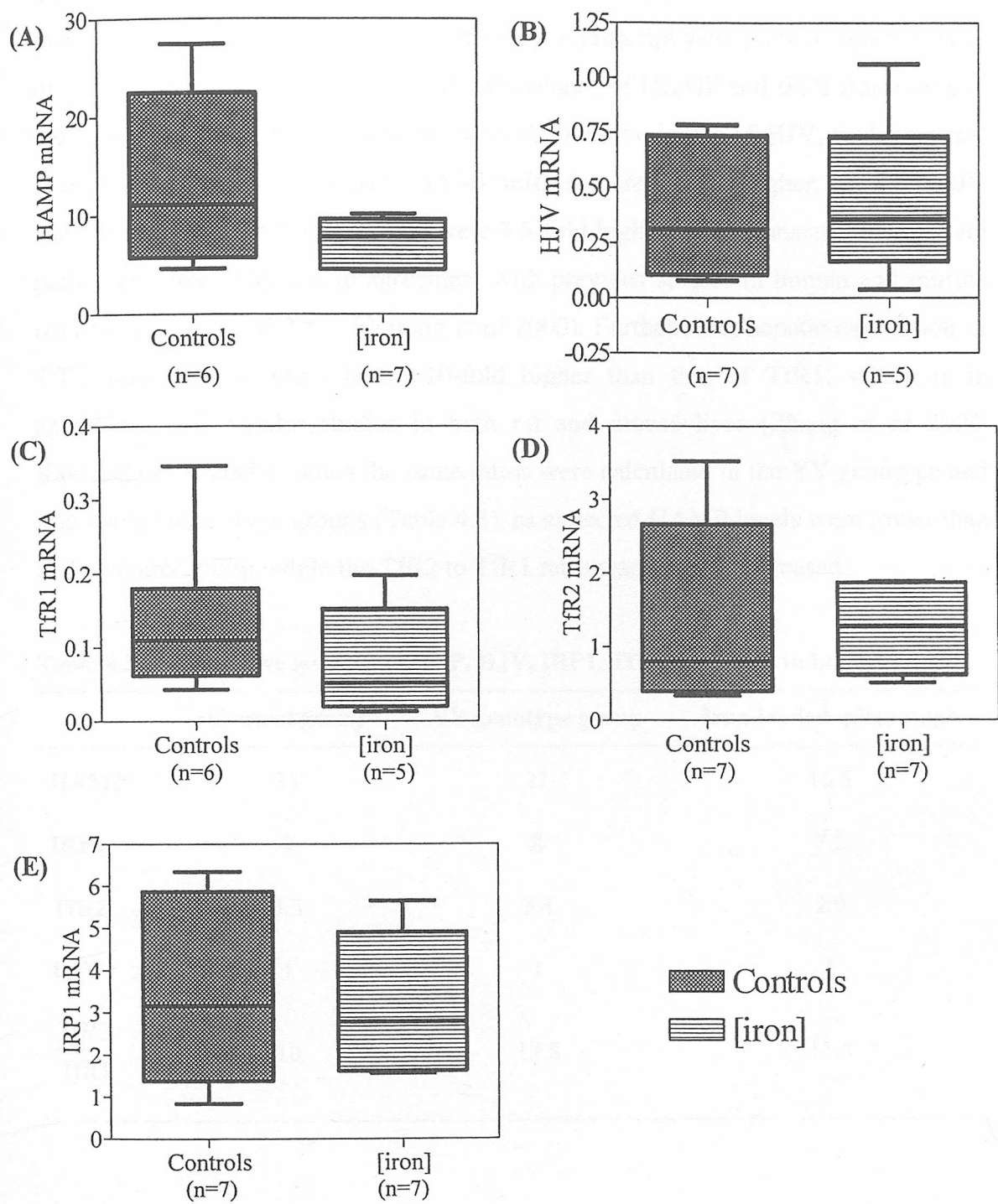


Figure 4.4 Hepatic mRNA expression of HAMP, HJV, TfR1, TfR2 and IRP1 in patients with iron overload irrespective of genotype and control individuals.

There were no significant differences in the expression of (A) HAMP ($P=0.147$), (B) HJV ($P=0.768$), (C) TfR1 ($P=0.287$), (D) TfR2 ($P=0.957$) or (E) IRP1 ($P=0.719$) between the control and the iron loaded group, as analysed with the unpaired t test (two-tailed).

4.2.4 Abundance of HAMP and IRP1 mRNA in human liver

When relative mRNA amounts for each studied transcript were plotted collectively in one graph (Figures 4.5A and 4.5B), the abundance of HAMP and IRP1 transcripts in the liver became evident. Compared with the relative levels of HJV, under normal iron conditions, levels of hepatic HAMP mRNA were 35-fold higher, those of IRP1 were 9-fold higher and TfR2 levels were 3.5-fold higher. TfR1 transcript levels were particularly low, which is in agreement with previous studies in human and murine liver (Kawabata *et al* 2001, Fleming *et al* 2000). Furthermore, hepatic expression of TfR2 mRNA was found to be 10-fold higher than that of TfR1, which is in agreement with similar studies in both rat and mouse liver (Zhang *et al* 2004, Kawabata *et al* 2000). When the same ratios were calculated in the YY genotype and iron loaded phenotype groups (Table 4.3), as expected HAMP levels were lower than in the control group, while the TfR2 to TfR1 ratio was slightly increased.

Table 4.3 Comparative levels of HAMP, HJV, IRP1, TfR1 and TfR2 in human liver

	Control group	YY genotype group	Iron loaded phenotype
HAMP	35	21	16.5
IRP1	9	8	7.2
TfR2	3.5	3.4	2.9
HJV	1	1	1
$\frac{TfR2}{TfR1}$	10	13.8	15.8

Figure 4.5 Comparative levels of HAMP and IRP1 mRNA expression in human liver
Relative expression of HAMP mRNA was 35-fold higher
in IRP1 and TfR2 were 9-fold and 3.5-fold higher
HJV expression of HAMP mRNA was 10-fold higher
in TfR2 mRNA levels were 10-fold higher than
the TfR1 mRNA levels were as under study.

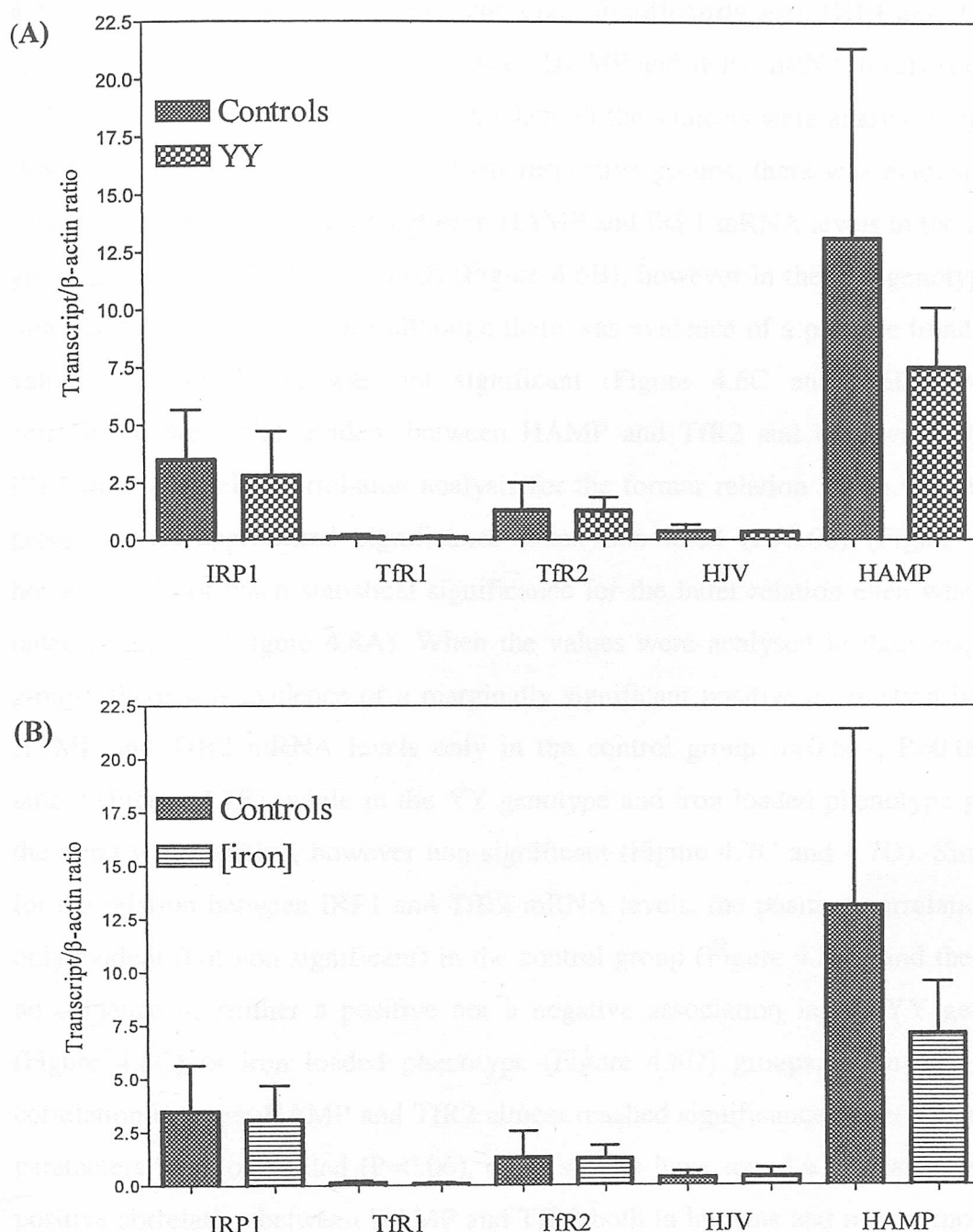


Figure 4.5 Abundance of HAMP and IRP1 mRNA expression in the liver.

Hepatic expression of HAMP mRNA was 35-fold higher than that of HJV, while expression of IRP1 and TfR2 was 9-fold and 3.5-fold higher than HJV, accordingly, in the control study group. Expression of HAMP mRNA was 21-fold higher than HJV in the YY genotype group (A) and 16.5-fold in the iron loaded phenotype group (B). Expression of IRP1, TfR1, TfR2 and HJV mRNA levels were of similar abundance in all three groups (A and B).

4.2.5 Hepatic HAMP mRNA levels correlate significantly with IRP1 and TfR2

A positive, significant correlation between HAMP and IRP1 mRNA levels ($r=0.648$, $P=0.023$) was observed (Figure 4.6A), when all the subjects were analysed together. When the values were analysed in their respective groups, there was evidence of a significant positive correlation between HAMP and IRP1 mRNA levels in the control group ($r=0.754$, $P=0.04$ one-tailed) (Figure 4.6B), however in the YY genotype and iron loaded phenotype groups although there was evidence of a positive trend in the values, the correlation was not significant (Figure 4.6C and 4.6D). Positive correlations were also evident between HAMP and TfR2 and between TfR2 and IRP1 mRNA levels. Correlation analysis for the former relation in the whole study group almost approached significance when one-tailed ($P=0.06$) (Figure 4.7A), however did not reach statistical significance for the latter relation even when one-tailed ($P=0.085$) (Figure 4.8A). When the values were analysed in their respective groups, there was evidence of a marginally significant positive correlation between HAMP and TfR2 mRNA levels only in the control group ($r=0.692$, $P=0.06$ one-tailed) (Figure 4.7B), while in the YY genotype and iron loaded phenotype groups, the trend was negative, however non-significant (Figure 4.7C and 4.7D). Similarly, for the relation between IRP1 and TfR2 mRNA levels, the positive correlation was only evident (but non-significant) in the control group (Figure 4.8B), and there was no evidence of neither a positive nor a negative association in the YY genotype (Figure 4.8C) or iron loaded phenotype (Figure 4.8D) groups. Even though the correlation between HAMP and TfR2 almost reached significance when the analysis parameters were one-tailed ($P=0.06$), other studies have found a similar significant positive correlation between HAMP and TfR2 both in humans and mouse models of HH (Gehrke *et al* 2003, 2005). Gehrke *et al* (2005) further observed a correlation between hepatic levels of HAMP and HJV in HH patients, which however was not evident in the presented data. No other correlations were evident in any of the possible combinations between the studied genes.

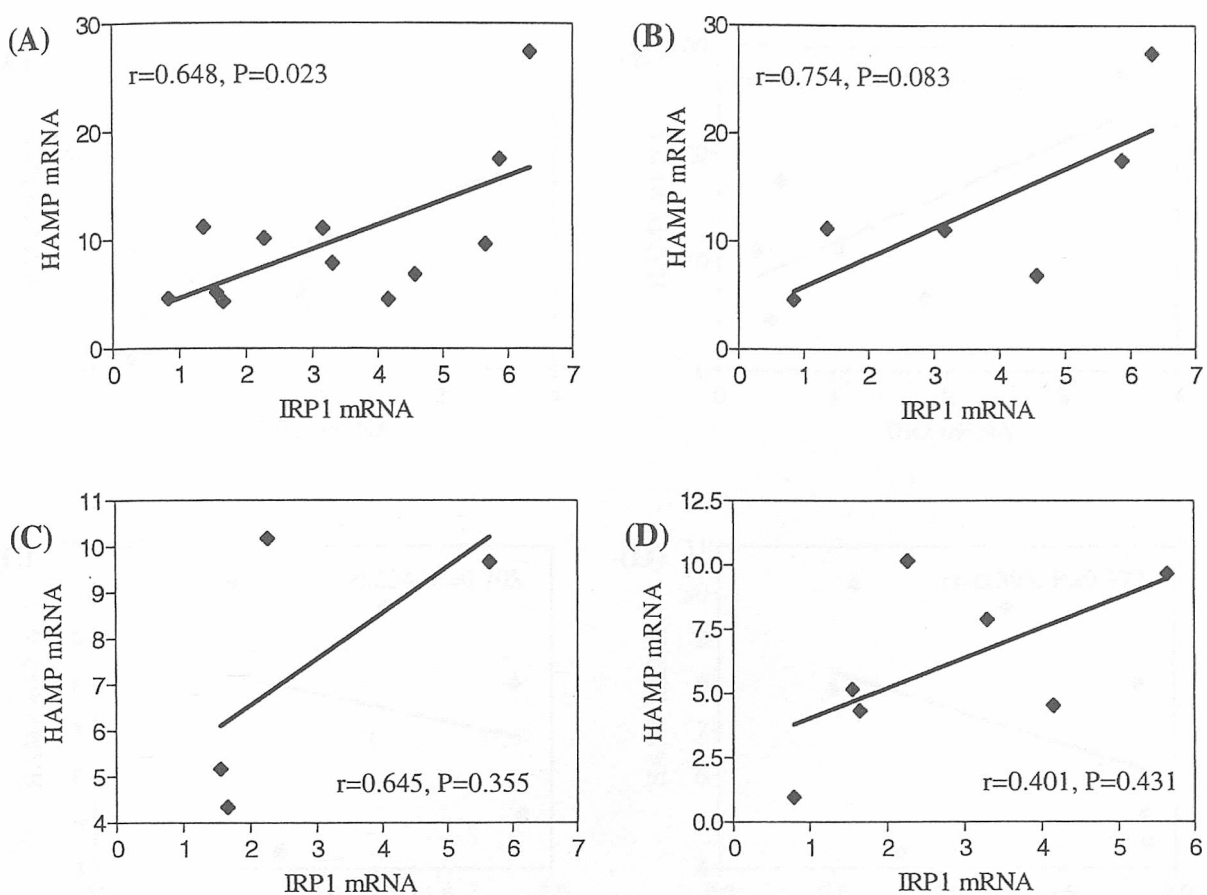


Figure 4.6 Linear regression analysis of the correlation between hepatic HAMP and IRP1 mRNA expression.

(A) Hepatic HAMP and IRP1 mRNA levels were significantly correlated in the study group as a whole. (B) The relationship remained positive, however did not reach significance (unless one-tailed) in the control group. The positive trend of an association between HAMP and IRP1 mRNA levels was evident but not significant in the YY genotype group (C) as well as the iron loaded phenotype group (D).

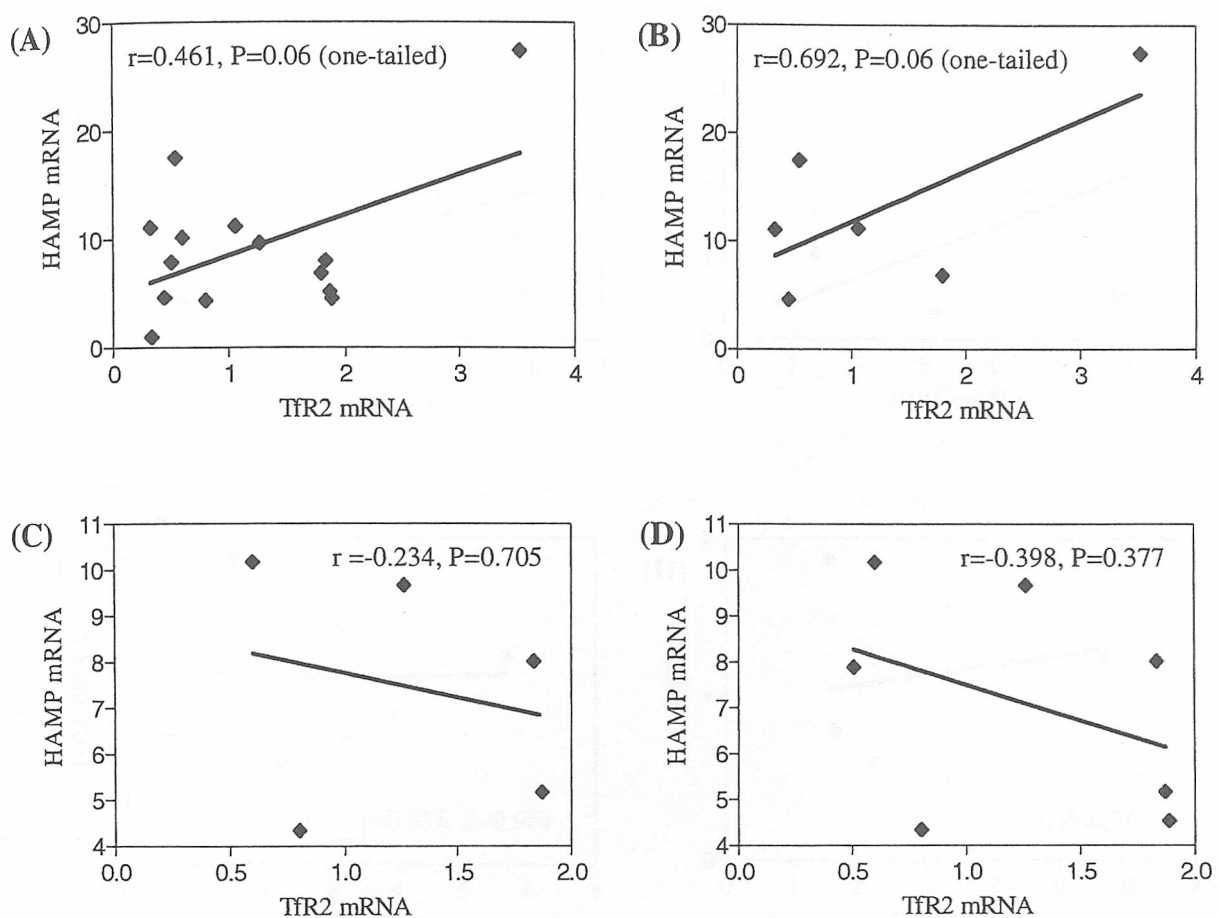


Figure 4.7 Linear regression analysis of the correlation between hepatic HAMP and TfR2 mRNA expression.

(A) Hepatic HAMP and TfR2 mRNA levels were nearly significantly correlated in the study group as a whole. (B) The relationship remained evidently positive, however did not reach significance in the control group. The association between HAMP and TfR2 mRNA levels displayed a non significant evidently negative trend in the YY genotype group (C) as well as in the iron loaded phenotype group (D).

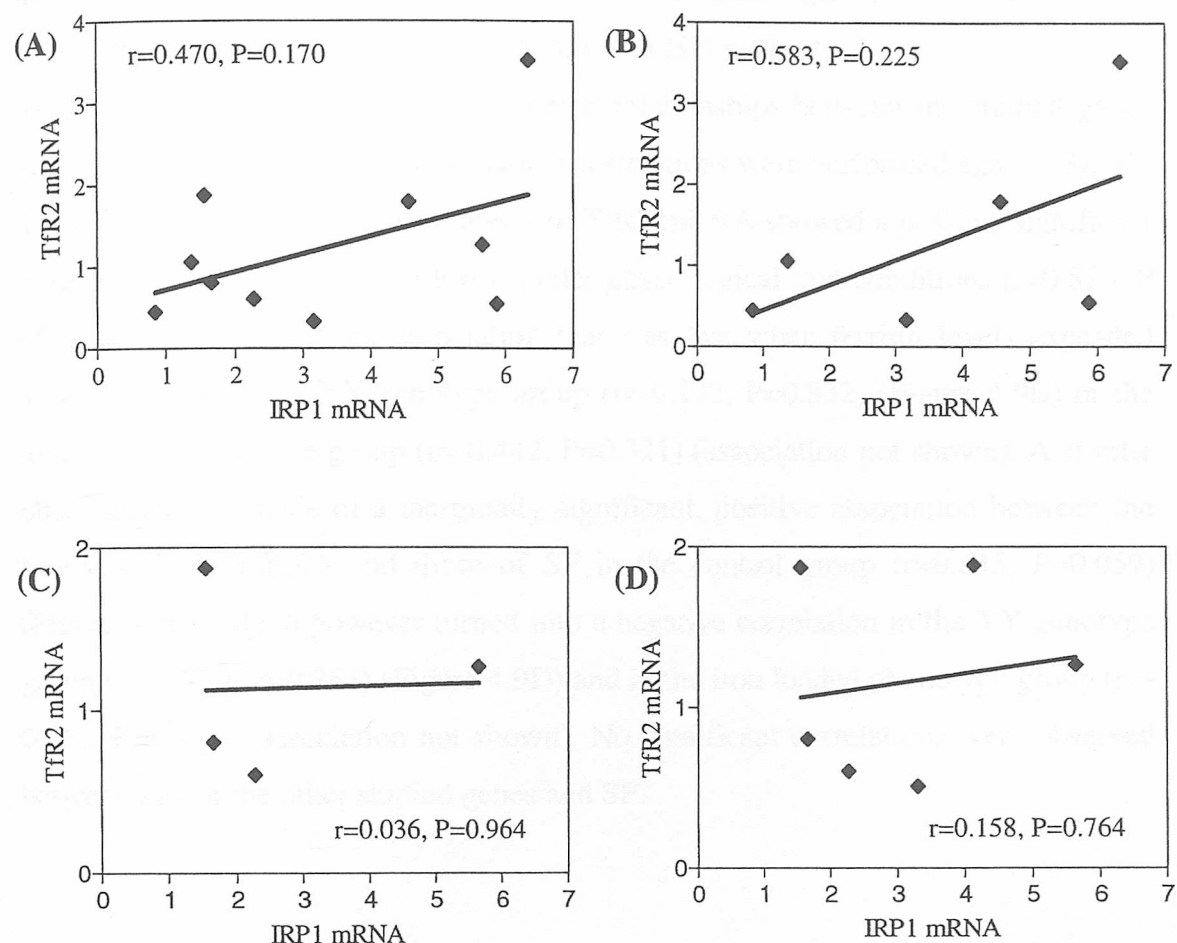


Figure 4.8 Linear regression analysis of the correlation between hepatic TfR2 and IRP1 mRNA expression.

Hepatic TfR2 and IRP1 mRNA levels were evidently positive but non-significantly correlated in the study group as a whole (A) and in the control group (B). While a trend of any nature in that relationship was not evident in the YY genotype group (C) or the iron loaded phenotype group (D).

4.2.6 Hepatic TfR2 and IRP1 mRNA levels correlate significantly with levels of serum ferritin in the control group but not in HH patients

To gain a further insight into the potential relationships between the studied genes and clinical iron status indices, statistical correlations were performed against SI, SF, TS, TIBC, and the HIC. Hepatic levels of TfR2 mRNA showed a positive significant correlation with serum ferritin levels under physiological iron conditions ($r=0.820$, $P=0.045$) (Figure 4.9A), an association that was lost when ferritin levels exceeded normal ranges, in the YY genotype group ($r=-0.132$, $P=0.832$) (Figure 4.9B) or the iron loaded phenotype group ($r=-0.442$, $P=0.321$) (association not shown). A similar observation was made of a marginally significant, positive association between the levels of IRP1 mRNA and those of SF in the control group ($r=0.645$, $P=0.059$) (Figure 4.9C), which however turned into a negative correlation in the YY genotype group ($r=-0.739$, $P=0.261$) (Figure 4.9D) and in the iron loaded phenotype group ($r=-0.667$, $P=0.148$) (association not shown). No significant correlations were observed between any of the other studied genes and SF.

Figure 4.9 shows scatter plots illustrating the correlation between serum ferritin and hepatic mRNA expression of TfR2 and IRP1 respectively.

Figure 4.9A TfR2 mRNA was significantly correlated with serum ferritin in control subjects and in HH patients with a YY genotype (no homozygosity locus of TfR2 was significantly correlated with serum ferritin in control subjects but no significant correlation was evident in the YY genotype group).

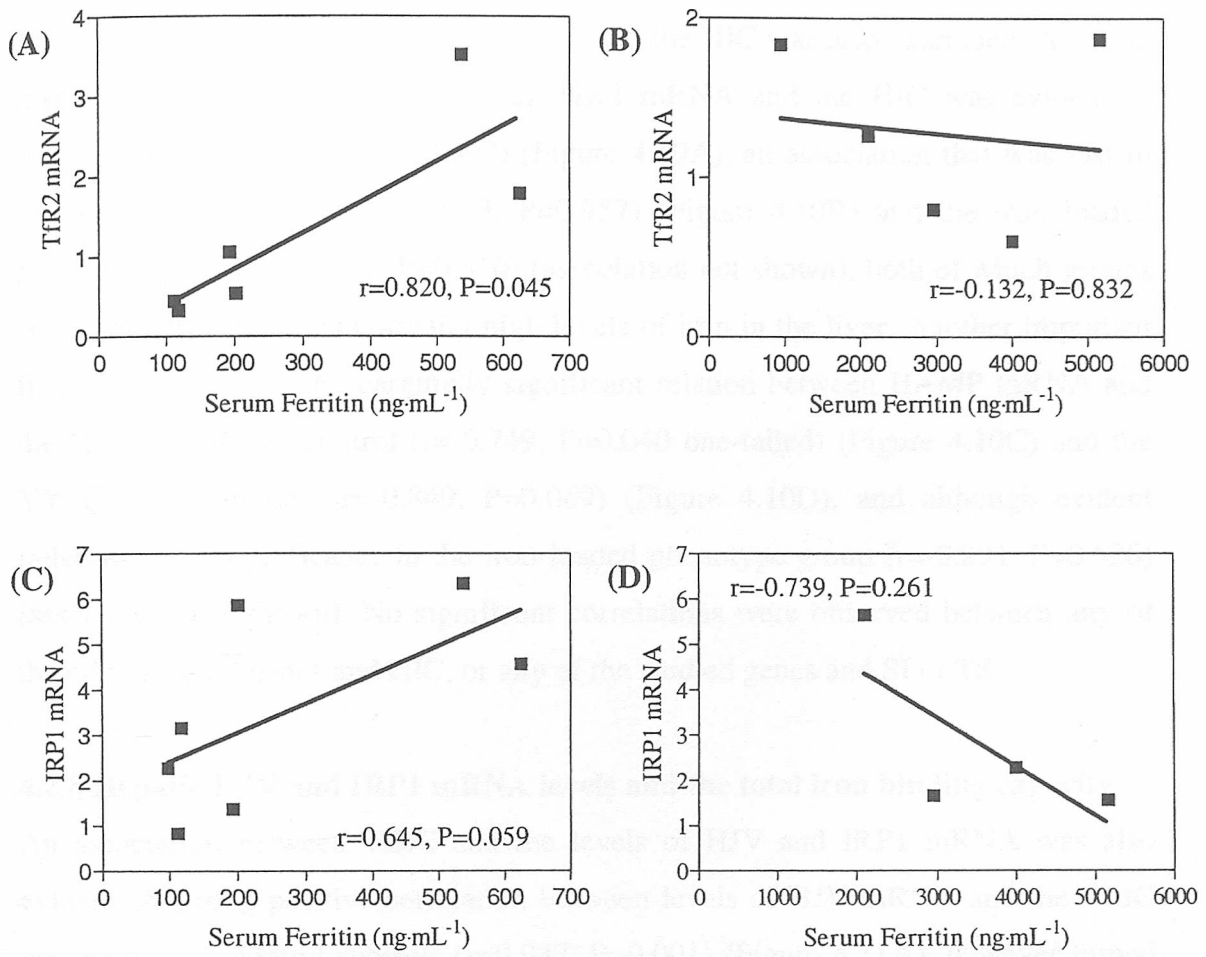


Figure 4.9 Linear regression analysis of the correlation between serum ferritin and hepatic mRNA expression of the IRP1 and Tfr2 transcripts.

Hepatic levels of Tfr2 mRNA were significantly correlated with serum ferritin in control subjects (A), but not in HH patients with a YY genotype (B). Similarly, levels of IRP1 mRNA were positively correlated with serum ferritin in controls (C), but an inverse non-significant correlation was evident in the YY genotype group (D).

4.2.7 Hepatic HAMP and TfR2 mRNA levels and the hepatic iron concentration

The association between the studied genes and the HIC was also examined. A strong inverse correlation between levels of TfR2 mRNA and the HIC was evident in control subjects ($r=-0.920$, $P=0.009$) (Figure 4.10A), an association that was lost in the YY genotype group ($r=-0.033$, $P=0.957$) (Figure 4.10B) and the iron loaded phenotype group ($r=-0.451$, $P=0.310$) (association not shown), both of which groups are characterised with abnormally high levels of iron in the liver. Another important finding was an inverse, marginally significant relation between HAMP mRNA and the HIC in both the control ($r=-0.749$, $P=0.040$ one-tailed) (Figure 4.10C) and the YY genotype groups ($r=-0.849$, $P=0.069$) (Figure 4.10D), and although evident failed to reach significance in the iron loaded phenotype group ($r=-0.291$, $P=0.526$) (association not shown). No significant correlations were observed between any of the other studied genes and HIC, or any of the studied genes and SI or TS.

4.2.8 Hepatic HJV and IRP1 mRNA levels and the total iron binding capacity

An association between TIBC and the levels of HJV and IRP1 mRNA was also evident. A strong positive correlation between levels of HJV mRNA and the TIBC was evident in control subjects ($r=0.947$, $P=0.001$) (Figure 4.11A), however turned negative but non-significant in the iron loaded phenotype group ($r=-0.417$, $P=0.485$) (Figure 4.11B). Interestingly, a marginally significant positive relation was evident between IRP1 mRNA levels and the TIBC in both the YY genotype ($r=0.938$, $P=0.062$) (Figure 4.11D) and the iron loaded phenotype groups ($r=0.867$, $P=0.027$), however there was no evidence of either a positive nor a negative association in the control group ($r=-0.156$, $P=0.738$) (Figure 4.11C). Finally, to rule out the possibility that the observed associations were not truly linear, values of clinical iron indices were logarithmically transformed and relations between those values and levels of gene expression were re-examined via a non-linear regression model. A non-linear analysis was not appropriate in any of the possible combinations.

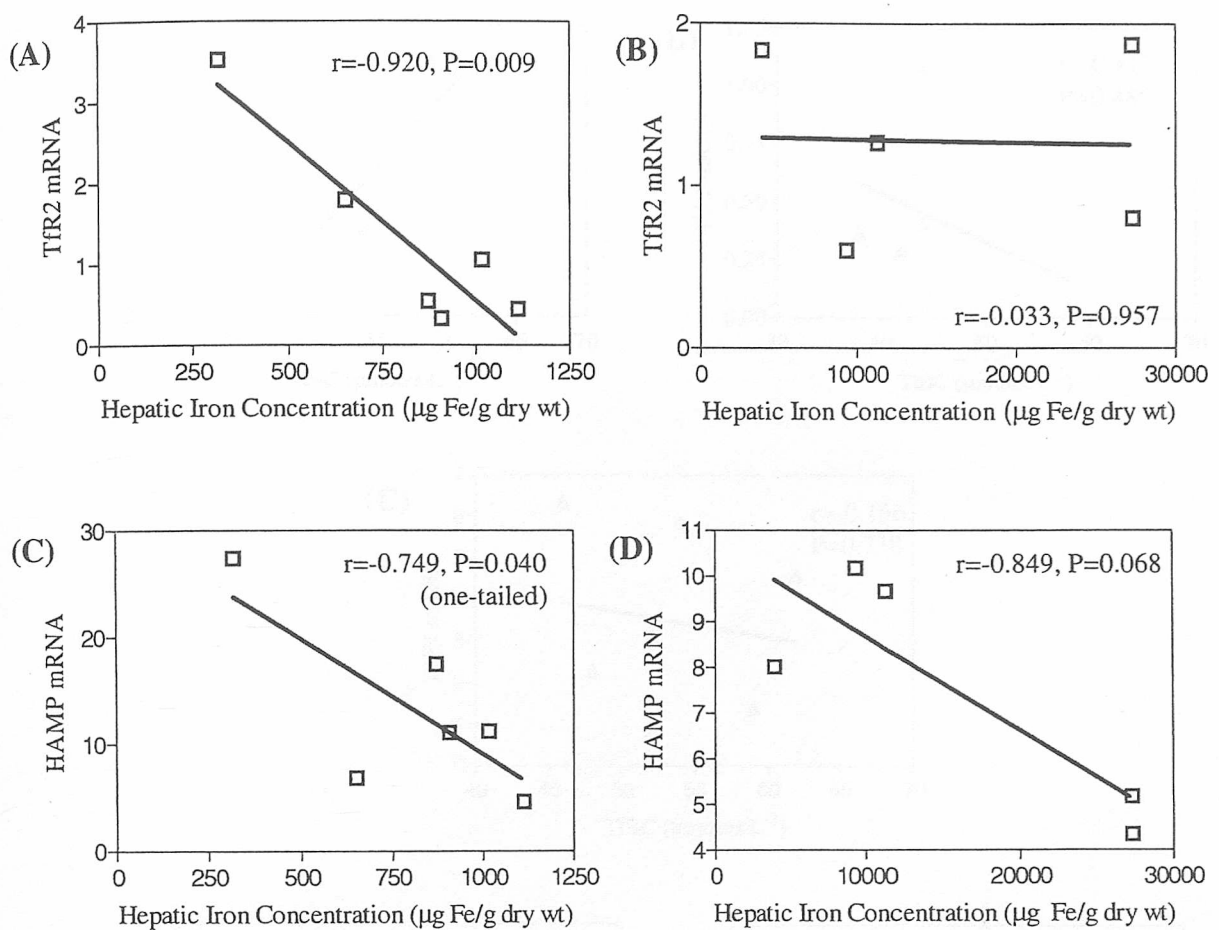


Figure 4.10 Linear regression analysis of the correlation between the hepatic iron concentration and hepatic mRNA expression of the Tfr2 and HAMP transcripts.

Hepatic levels of Tfr2 mRNA were significantly inversely correlated with the hepatic iron concentration in control subjects (A), but not in HH patients with a YY genotype (B). Similarly, hepatic levels of HAMP mRNA were inversely correlated with the hepatic iron concentration in controls (C), and similarly (though only marginally significant when one-tailed) in the YY genotype group (D).

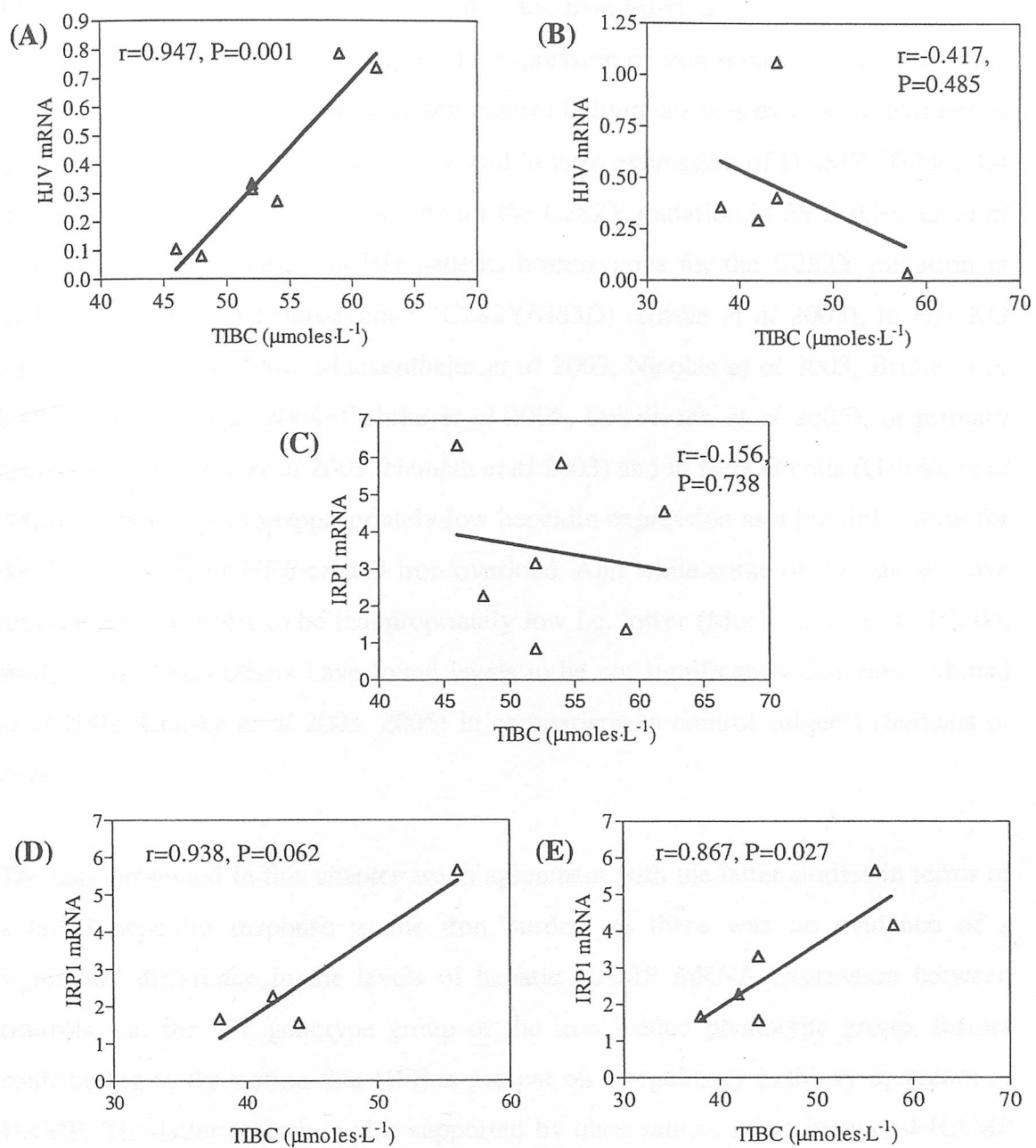


Figure 4.11 Linear regression analysis of the correlation between TIBC and hepatic mRNA expression of the HJV and IRP1 transcripts.

Hepatic levels of HJV mRNA were significantly correlated with TIBC in control subjects (A), but not in HH patients with a YY genotype (B). There was no evidence of a correlation between TIBC and hepatic IRP1 mRNA levels in the control group (C), however a positive association (significant when one-tailed) was evident in the YY genotype group (D) and a significant one in the iron loaded phenotype group (E).

4.3 Discussion

4.3.1 Hepatic hepcidin fails to respond to the iron burden

In the study presented in this chapter the expression of iron-related transcripts in the liver of patients with iron overload and control individuals was evaluated. Numerous groups have examined both the *ex vivo* and *in vitro* expression of HAMP (Tables 4.4 and 4.5), in HH patients homozygous for the C282Y mutation in *HFE* (Gehrke *et al* 2003, Gehrke *et al* 2005), in HH patients homozygous for the C282Y mutation in *HFE* and compound heterozygotes (C282Y/H63D) (Bridle *et al* 2003), in *Hfe* KO mice (Ahmad *et al* 2002, Muckenthaler *et al* 2003, Nicolas *et al* 2003, Bridle *et al* 2003, Hermann *et al* 2004, Gehrke *et al* 2005, Ludwiczek *et al* 2005), in primary hepatocytes (Gehrke *et al* 2003, Nemeth *et al* 2003) and in HepG2 cells (Gehrke *et al* 2003), all pointing to inappropriately low hepcidin expression as a possible cause for the development of *HFE*-related iron overload. And while some of the studies have found HAMP mRNA to be inappropriately low i.e. lower (Muckenthaler *et al* 2003, Bridle *et al* 2003) others have found levels to be not significantly different (Ahmad *et al* 2002, Gehrke *et al* 2003, 2005) in comparison to control subjects (humans or mice).

The data presented in this chapter are in agreement with the latter studies in terms of a failed hepcidin response to the iron burden, as there was no evidence of a significant difference in the levels of hepatic HAMP mRNA expression between controls and the YY genotype group or the iron loaded phenotype group, further contributing to the notion that *HFE* is present on a regulatory pathway upstream of HAMP. The latter remark is also supported by observations of an increased HAMP mRNA expression in patients with secondary iron overload (Gehrke *et al* 2005) and in *Hfe*^{+/+} mice injected with Fe-dextran (Muckenthaler *et al* 2003). The *HFE* related or dependent control of hepcidin expression was further evident in the presented data through the observation of low HAMP mRNA expression in the treated HH patient, regardless of the seemingly iron normal phenotype with respect to the clinical iron indices.

Table 4.4 Hepatic mRNA expression of iron-related genes in studies using material from human subjects and cell lines

	HAMP	TfR2	Other observations and comments	Respective studies
Patients with type I-HH	No change. Positive correlation with SF in controls, inverse correlation with SF in HH. Strong correlation with TfR2 (in whole study group and in controls and HH separately).	No change	TfR1 mRNA levels decreased in HH. No change in DMT1 and Cp.	Gehrke <i>et al</i> 2003
	Decreased (5.4-fold)		Increased FP1	Bridle <i>et al</i> 2003
	No change. Strong correlation with TfR2 and HJV.	No change	No change in HJV. HAMP increased in secondary iron overload.	Gehrke <i>et al</i> 2005
Primary human hepatocytes (iron loaded)	Decreased (50%)			Nemeth <i>et al</i> 2003
HepG2 (iron loaded)		Increased	Holo-Tf up-regulates TfR2 protein levels	Deaglio <i>et al</i> 2002
	Down-regulated in response to non-Tf bound ferric iron but not in response to Fe ₂ -Tf.			Gehrke <i>et al</i> 2003
		No change. Holo-Tf up-regulates protein levels.	Response not similar in K562	Robb and Wessling-Resnick 2004

Table 4.5 Hepatic mRNA expression of iron-related genes in the animal model of HH

	HAMP	HJV	TfR1	TfR2	Other observations	Respective studies
<i>Hfe</i> ^{-/-}			Undetectable	No change	TfR2 abundant	Fleming <i>et al</i> 2000
	No change				HAMP levels were 5-fold higher in wild-type mice on iron supplemented diet compared to <i>Hfe</i> KO on the same diet	Ahmad <i>et al</i> 2002
	Decreased (P=0.03)				Increased FP1	Bridle <i>et al</i> 2003
	Low levels				HAMP positively (but weak) correlates with HIC	Nicolas <i>et al</i> 2003
	Decreased	Decreased	No change		HAMP increased in <i>Hfe</i> ^{+/+} mice injected with Fe-dextran	Muckenthaler <i>et al</i> 2003
	No change					Herrmann <i>et al</i> 2004
	Strong correlation with TfR2 and HJV	No change			HAMP correlates with HIC in <i>Hfe</i> ^{+/+}	Gehrke <i>et al</i> 2005
	Decreased (4-fold)	No change		Reduced when fed iron rich diet	HAMP correlates with hepatic FP1. Decreased Hp.	Ludwiczek <i>et al</i> 2005
				Up-regulated protein levels	Similar observation in <i>Hbb</i> ^{th-1} mice and rats on Fe rich diet	Robb and Wessling-Resnick 2004

Levels of hepatic HJV, IRP1, TfR1 and TfR2 mRNA were not influenced by hereditary iron accumulation. In accord with the studies of Gehrke *et al* (2003, 2005) no significant changes were evident in the expression of TfR2 in untreated HH patients (YY genotype group) or in iron loaded patients irrespective of their genotype (phenotype group) as compared to controls. Similar findings in murine liver of *Hfe* KO mice exist for TfR2 mRNA levels (Fleming *et al* 2000, Muckenthaler *et al* 2003) and *in vitro* iron loading of HepG2 cells has no bearing on the transcript's levels either (Robb and Wessling-Resnick 2004). Similarly, levels of the HJV transcript were comparable in the liver of untreated HH patients (YY genotype group) and in iron loaded patients (phenotype group) as compared to controls. This observation is also in accord with studies in human (Gehrke *et al* 2005) as well as murine liver (Gehrke *et al* 2005, Ludwiczek *et al* 2005).

Transcriptional regulation of IRP1 and TfR1 has not been studied in great detail, however previous studies have observed a decrease in TfR1 mRNA in untreated HH patients (Gehrke *et al* 2003), as well as in *Hfe*^{-/-} mice (Fleming *et al* 2000, Muckenthaler *et al* 2003, Herrmann *et al* 2004). The presented data, however suggest that hepatic expression of both the IRP1 and TfR1 transcripts was not influenced by iron overload or mutations in the *HFE* gene. With reference to the down-regulation of IRP1 at the protein level demonstrated in Chapter III, this observation points to a post-transcriptional level of control of this iron-regulator in response to excess iron in the liver. The underlying mechanism of this post-transcriptional control has not been further explored however evidence in the literature suggests that it could involve the degradation of IRP1 after destabilisation of its 4Fe-4S cluster. Recent studies in mice lacking superoxide dismutase 1 (SOD1), a deficiency in which is known to promote oxidative damage, an 80% reduction in the levels of hepatic IRP1 was observed in the SOD1^{-/-} mice as compared to wild-type mice, while this reduction was accompanied by only a 30-40% decrease in the mRNA levels (Starzyński *et al* 2005). The authors concluded that less efficient transcription of the *IRP1* gene or decreased stability of the mRNA could only partially account for the observed down-regulation in IRP1 protein levels in the SOD1^{-/-} mice and proposed that it could also be due to proteolytic degradation of the protein after destabilisation of its 4Fe-4S cluster by O₂⁻.

4.3.2 Abundance and correlation of HAMP and IRP1 mRNA in the human liver

qRT-PCR analysis of the relative gene expression of HAMP, HJV, IRP1, TfR1 and TfR2 transcripts in the liver suggests that levels of the HAMP and IRP1 transcripts are higher compared to the other studied transcripts with TfR1 and HJV being expressed at the lowest levels. A 10-fold higher expression of the TfR2 transcript was evident compared to TfR1, which is in agreement with a study by Zhang and colleagues (2004), who found that isolated rat hepatocytes had 10-fold lower TfR1 mRNA levels than TfR2. It is also in accord with other studies by Kawabata *et al* (2001) and Fleming *et al* (2000) who observed that TfR2 mRNA and protein levels were more abundant than TfR1 mRNA and protein levels in murine liver and immature erythroid precursors. Hepcidin is proving to be an iron-regulatory protein, much like IRP1, therefore copies of this transcript perhaps need to be present in ample amounts for translation when the protein is needed to exert its control.

A further finding was a correlation between hepatic levels of HAMP mRNA and those of IRP1 and TfR2. The latter finding of a correlation between HAMP and TfR2 confirms the results of previous studies both in humans (Gehrke *et al* 2003, 2005) and mice (Gehrke *et al* 2005). In contrast to those studies however, that have observed the relation irrespective of a mutation in the *HFE* gene, the aforementioned correlation was significant only when the subjects were examined as a whole group and in the control study group, but not in the two iron-loaded groups. A relation between HAMP and IRP1 has not been examined previously and based on the observations presented in this chapter, it probably occurs irrespective of *HFE*. There was also an evident, however non-significant association between TfR2 and IRP1, when the subjects were analysed as a whole group and in the control group.

4.3.3 Hepatic HAMP and TfR2 transcripts correlate with the HIC

Transcript levels were evaluated in relation to serum iron markers and histological iron deposition in the liver. A further finding was that of an association between the hepatic levels of IRP1 and TfR2 mRNA with SF. In both cases, a strong positive relation could only be observed in control subjects and was abrogated in HH patients (YY genotype). These findings suggest that both IRP1 and TfR2 transcript levels respond (to a small extend) to elevated levels of iron under physiological conditions, a control mechanism that perhaps is lost in HH. Similar observations in response to

SF have also been reported for the HAMP transcript by Gehrke *et al* (2003), strengthening the notion of a link between the three molecules. Moreover an inverse correlation between levels of TfR2 mRNA and the HIC was evident in control subjects. This relationship, which was not evident in HH patients with a YY genotype, suggests that when hepatic iron concentrations start reaching upper physiological levels, levels of the TfR2 transcript are kept fairly low, a mechanism that perhaps is abrogated in HH. In that case, mRNA levels between the two groups would be no different due to the fact that at lower physiological levels there would be high levels of TfR2 transcript, therefore pulling the mean values of the two groups closer. Another important finding was an inverse relation between HAMP mRNA and HIC, which suggests that the lowest levels of HAMP mRNA relate to the more severe phenotype of the disease. This finding is in agreement with Gehrke *et al* (2003) who found a strong inverse correlation between HAMP and SF in untreated HH patients, since levels of serum ferritin and the HIC are known to be associated (Beaumont *et al* 1980). It is, however, in contrast with other studies that have found positive correlations between HAMP and HIC in untreated HH (Bridle *et al* 2003) as well as mouse models of this disease (Nicolas *et al* 2003, Gehrke *et al* 2005). Finally, there was evidence of a correlation between HJV and the TIBC in the absence of iron overload, while IRP1 correlated with TIBC in the presence of iron overload. The TIBC is a measure of the total amount of iron with which plasma can combine, mostly due to Tf. The TIBC is not as an informative iron status parameter as SF or TS are and thus no firm conclusions could be drawn from these observations.

4.3.4 Duodenal expression of molecules implicated in iron import and export

The studies presented in this thesis were focused on the liver as this is the organ most prominently affected in HH. A review of the literature focusing on transcript levels of molecules expressed in the intestine in relation to HH might also prove insightful. A number of studies on the expression levels of duodenal transporters of iron in HH patients (Zoller *et al* 2001 and 2003, Byrnes *et al* 2002, Stuart *et al* 2003) and mouse models of the disease (Griffiths *et al* 2001, Ludwiczek *et al* 2005) have reported an increased iron absorption in HH (Tables 4.6 and 4.7, accordingly). The mRNA expression levels of DMT1 at the luminal membrane (Zoller *et al* 2001 and 2003, Rolfs *et al* 2002, Byrnes *et al* 2002, Stuart *et al* 2003) and of FP1 at the basolateral membrane (Rolfs *et al* 2002, Stuart *et al* 2003) have been found to be increased in

HFE-related HH. The expression of Dcytb has also been reported to be increased both in humans (Zoller *et al* 2001) and *Hfe* KO mice (Muckenthaler *et al* 2003, Herrmann *et al* 2004, Ludwiczek *et al* 2005). No modulation in Hp mRNA or protein levels has been observed in HH (Zoller *et al* 2001, 2003, Rolfs *et al* 2002, Stuart *et al* 2003), while Zoller *et al* (2003) observed an increase in TfR1 mRNA levels. Overall, in the intestine of HH patients mRNA expression of DMT1 and FP1 are increased, while Hp remains unchanged. The fate of Dcytb levels in HH is debatable as only one study has found increased levels of this reductase (Zoller *et al* 2001), while later studies by the same group have observed no changes in the levels of the transcript (Zoller *et al* 2003, Stuart *et al* 2003) or of the protein (Zoller *et al* 2003).

When compared to the outcomes of the human studies, data obtained from *Hfe* KO mice have provided some contrasting results. For DMT1, an increase both in the mRNA levels and the protein levels of this transporter has been reported (Fleming *et al* 1999, Griffiths *et al* 2001, Ludwiczek *et al* 2005), however others have failed to make similar observations (Muckenthaler *et al* 2003, Herrmann *et al* 2004). Levels of FP1 in the human studies were found to be increased however none of the animal studies came to the same conclusion (Muckenthaler *et al* 2003, Herrmann *et al* 2004). Dcytb transcript levels have been reported to be increased, while levels of TfR1 have been found to be unchanged or even decrease in animal models. The unaffected level of Hp expression in HH has been the only agreeable outcome in both human and animal studies.

As care should be taken when extrapolating evidence from the animal models to the human situation, and thus based on the findings emerging from the human studies, the phenotype of intestinal cells in HH seems to be identical to those in a state of iron deficiency. Hepcidin fails to signal the intestine to stop iron absorption and instead levels of DMT1, Dcytb, and FP1 in the duodenum are up-regulated, enhancing iron efflux into the intestinal cell and iron egress into the portal circulation. The study by Dupic *et al* (2002), on normal mice fed on an iron rich diet (i.e. not a mutant or mouse model of HH), illustrates what could be the expected response to the increasing iron burden from the diet; a decrease in the mRNA levels of DMT1, Dcytb, FP1 and TfR1.

Table 4.6 Duodenal mRNA expression of iron-related genes in patients with HFE associated HH

DMT1	Dcytb	FP1	Hp	TfR1	Other observations and comments	Respective studies
Increased mRNA and protein levels	Increased		No change			Zoller <i>et al</i> 2001
Increased mRNA (DMT1-IRE)		Increased	No change in mRNA or protein levels		Inverse correlation between DMT1 and TS, SF in controls	Rolfs <i>et al</i> 2002
	No change in mRNA or protein levels		No change in mRNA or protein levels	Increased. No correlation with DMT1, FP1, Dcytb, Hp or SF, TS	No differences between treated and untreated HH	Zoller <i>et al</i> 2003
Positive correlations between Dcytb, Hp, FP1, DMT1, irrespective of HFE						
Increased mRNA and protein levels					HFE expression	Byrnes <i>et al</i> 2002
Increased mRNA (IRE)					Positive correlation between DMT1 and FP1 in the whole study group, and in HH and non-HH groups separately	Stuart <i>et al</i> 2003
Negative correlation with SF	No change	Increased	No change			

Table 4.7 Duodenal mRNA expression of iron-related genes in animal models of HH and mice on iron rich diet

	DMT1	Dcytb	FP1	Hp	TfR1	Other observations and comments	Respective studies
<i>Hfe</i> ^{-/-}	No change in mRNA or protein levels	Increased	No change	No change	No change	No correlation between expression and HIC	Herrmann <i>et al</i> 2004
	Increased mRNA levels and protein	Increased	No change	No change	Decreased mRNA but no reduction in protein levels	Increased IRP1 protein	Ludwiczek <i>et al</i> 2005
	No change	Increased	Decreased	No change			Muckenthaler <i>et al</i> 2003
	Increased						Griffiths <i>et al</i> 2001
<i>β2m</i> ^{-/-}	Increased		Increased		No change		Muckenthaler <i>et al</i> 2004
<i>Usf2</i> ^{-/-}	Increased protein levels	Increased protein levels	Increased protein levels				Viatte <i>et al</i> 2005
	DMT1-IRE increased					no change in DMT1-non-IRE	Fleming <i>et al</i> 1999
Mice on Fe rich diet	Decreased	Decreased	Decreased	No change	Decreased		Duplic <i>et al</i> 2002

4.3.5 Future directions

The mechanism of regulation of *HAMP* gene expression in response to iron status is not clearly understood, however it is thought that iron *per se* is not directly involved in inducing an effect. That has been suggested by the absence of increased *HAMP* mRNA in primary mouse hepatocytes exposed to iron-citrate (Pigeon *et al* 2001), and by observations of decreased *HAMP* mRNA expression in human hepatocytes exposed to FAC or diferric-Tf (Nemeth *et al* 2003) and in HepG2 cells incubated with non-Tf-bound ferric iron (Gehrke *et al* 2003). The latter finding suggesting that down-regulation of hepcidin is restricted to NTBI. An increase in the LIP of the hepatocyte, leading to the subsequent production of ROS might have some bearing on the regulation of hepcidin, perhaps through the production of cytokines, such as IL-6, which has been found to have an inducing effect on *HAMP* mRNA (Nemeth *et al* 2003). As already mentioned in Chapter I, some aspects of the molecular control of *HAMP* mRNA might implicate C/EBPa, which was found to influence synthesis of *HAMP* mRNA in mice (Courselaud *et al* 2002). In addition to the binding motifs for C/EBP, the hepcidin gene promoter has been found to also contain binding sites for the signal transducer and activator of transcription (STAT). Interestingly, a binding site for STAT proteins has also been identified in the promoter region of the *IRP1* gene and control via STAT has been implicated in the nitric oxide dependent control of *IRP1* gene expression (Starzynski *et al* 2006). It would be useful to compare promoter regions in these molecules and investigate whether they could be under a common regulatory pathway. Finally, to obtain further insights into the complex phenomenon of iron homeostasis and its misregulation in HH, it would prove useful to compare protein levels of hepcidin and HJV in the liver of controls and patients with mutations in the *HFE* gene, which was impeded in the current studies due to the lack of appropriate antibodies and suitable assays. Expression of TfR2 at the protein level was examined in patients with *HFE*-related HH and the findings are presented in Chapter V.

Chapter V

Expression of liver TfR2 protein in hereditary haemochromatosis

5.1 Introduction

TfR2 was discovered as a molecule that had amino acid homology to the classic Tf receptor protein, TfR1. TfR2 is expressed predominantly in the liver (Kawabata *et al* 1999), but also in the intestine (Griffiths and Cox 2003) and to a less extent in erythroid cells (Kawabata *et al* 1999), although there have been reports of an absence of TfR2 protein expression in normal erythroid cells (Calzolari *et al* 2004). TfR1 on the other hand is expressed in a wider range of tissues (Gatter *et al* 1983). Studies by Kawabata *et al* (2000), showed that human TfR2- α interacts with human apo-Tf at pH 6 and with human Fe³⁺-Tf at a physiological pH, however with a 25-30 times lower affinity than that of TfR1 (Kawabata *et al* 2000, West *et al* 2000). Observations that led to the conclusion that TfR2- α is a second Tf receptor that can mediate cellular iron transport. And based on the relative abundance of the two transcripts in the liver, Fleming *et al* (2000) proposed that TfR2 continues to mediate uptake of Tf-bound iron by the liver after TfR1 is down-regulated by iron overload in HH, and thus may account for the increased susceptibility of the liver to iron loading.

Unlike TfR1, TfR2 lacks an IRE element and hence is not thought to be under post-transcriptional control via the IRPs, an observation that has led many to conclude that TfR2- α expression does not depend on iron status but rather varies due to the different stages of the cell cycle (Kawabata *et al* 2000). Moreover, although the IRE/IRP system is the well known regulatory mechanism for TfR1, Tong *et al* (2002) demonstrated the transcriptional up-regulation of TfR1 in iron-depleted cells transfected with an IRE-lacking TfR1 construct. The same group failed to induce a similar observation using a TfR2 construct under the same conditions, supporting the hypothesis of a differential regulation of these two members of the TfR family. In line with these observations, studies to date have reported that transcript levels of TfR2 are unaffected by iron status, in the mouse model of HH (Fleming *et al* 2000, Muckenthaler *et al* 2003) and in the liver of HH patients (Gehrke *et al* 2003, 2005), a finding that agrees with the results presented in Chapter IV. Studies of the receptor at the protein level, however, have been confined to cell lines and animal models and

therefore the goal of the study presented in this chapter was to investigate whether TfR2 protein expression in the liver of HH patients is altered in response to hepatic iron overload. A further aim was to correlate levels of hepatic TfR2 protein expression with clinical iron status parameters such as serum iron, serum ferritin, transferrin saturation, hepatic iron concentration and total iron binding capacity in HH patients compared with control subjects.

5.2 Results

5.2.1 TfR2 protein expression in human liver

TfR2 protein levels were compared in livers of control and iron loaded HH patients by Western blotting. The study groups used in this set of experiments and a summary of their clinical iron status parameters is given in Table 5.1. Of the 8 iron loaded specimens, 7 were homozygous for the C282Y mutation in the *HFE* gene (YY) and 1 was a C282Y/H63D compound heterozygote (CY). Expression of TfR2 protein was also investigated in the livers of two YY patients, who had received phlebotomy treatment (grade of siderosis III and IV, pre-treatment).

Table 5.1 Clinical characteristics and iron indices of study groups in Chapter V

	Control group n=12	Untreated HH group n=8	Treated HH group n=2
Age at diagnosis, (years)*	39 ± 8 (23 - 53)	49 ± 7 (41 - 60)	53, 67
Sex, (male/female)	10/0	8/0	2/0
SF, ($\text{ng} \cdot \text{mL}^{-1}$)*	111.8 ± 56.5 (50 - 223)	1801 ± 1184 (458 - 4001)	49.00 ± 16.97 (37 - 61)
SI, ($\mu\text{moles} \cdot \text{L}^{-1}$)*	18.25 ± 4.808 (12 - 30)	31.81 ± 7.964 (20 - 42)	33.00 ± 7.071 (28 - 38)
TIBC, ($\mu\text{moles} \cdot \text{L}^{-1}$)*	59.17 ± 6.506 (48 - 70)	48.75 ± 9.036 (38 - 65)	45.00 ± 1.414 (44 - 46)
TS, (%)*	30 ± 6.394 (21 - 38)	68 ± 25 (31 - 100)	72 ± 16 (61 - 84)
HIC, ($\mu\text{g Fe/g dry wt}$)*	291.2 ± 200.0 (28 - 628)	6791 ± 8659 (1967 - 27320)	211.0 ± 107.5 (135 - 287)

* Range (mean \pm standard deviation) (min-max)

TfR2 migrated as a band of approximately 100kDa, as measured in the early stages of staining development following immunoblotting, whilst the marker was still visible (Figure 5.1A, lane M), which is in agreement with the expected M_r of the molecule of 105kDa, under reducing conditions. Levels of the protein were initially analysed in 4 controls (lanes 1-4) and 4 iron loaded HH patients (lanes 5-8), of which 1 was a CY (lane 5) (Figure 5.1B). TfR2 protein levels were significantly up-regulated in the iron loaded samples as compared with controls ($P=0.005$) (Figure 5.1B and 5.1D). The increase in TfR2 protein was further observed in another set of samples when Western blotting was performed in livers from 3 controls (lanes 1-3), 4 untreated (lanes 4-7) and 1 treated (lane 8) HH patient, where the up-regulation in untreated HH patients was again found to be significant ($P=0.041$) (Figure 5.2A and 5.2B). Initial experiments were repeated up to six times using a different combination of the order of samples used in figures 5.1A and 5.2A and with the inclusion of a further 5 control samples and 1 treated HH. Across the whole cohort of samples, levels of hepatic TfR2 were significantly up-regulated in iron loaded HH (2.971 ± 0.918) compared with controls (0.971 ± 0.437), ($P=0.0003$) (Figure 5.2C). TfR2 protein levels in the two treated HH patients were also markedly increased (arbitrary units were 1.765 and 3.088, respectively), however because of the size of the cohort, the results failed to reach statistical significance.

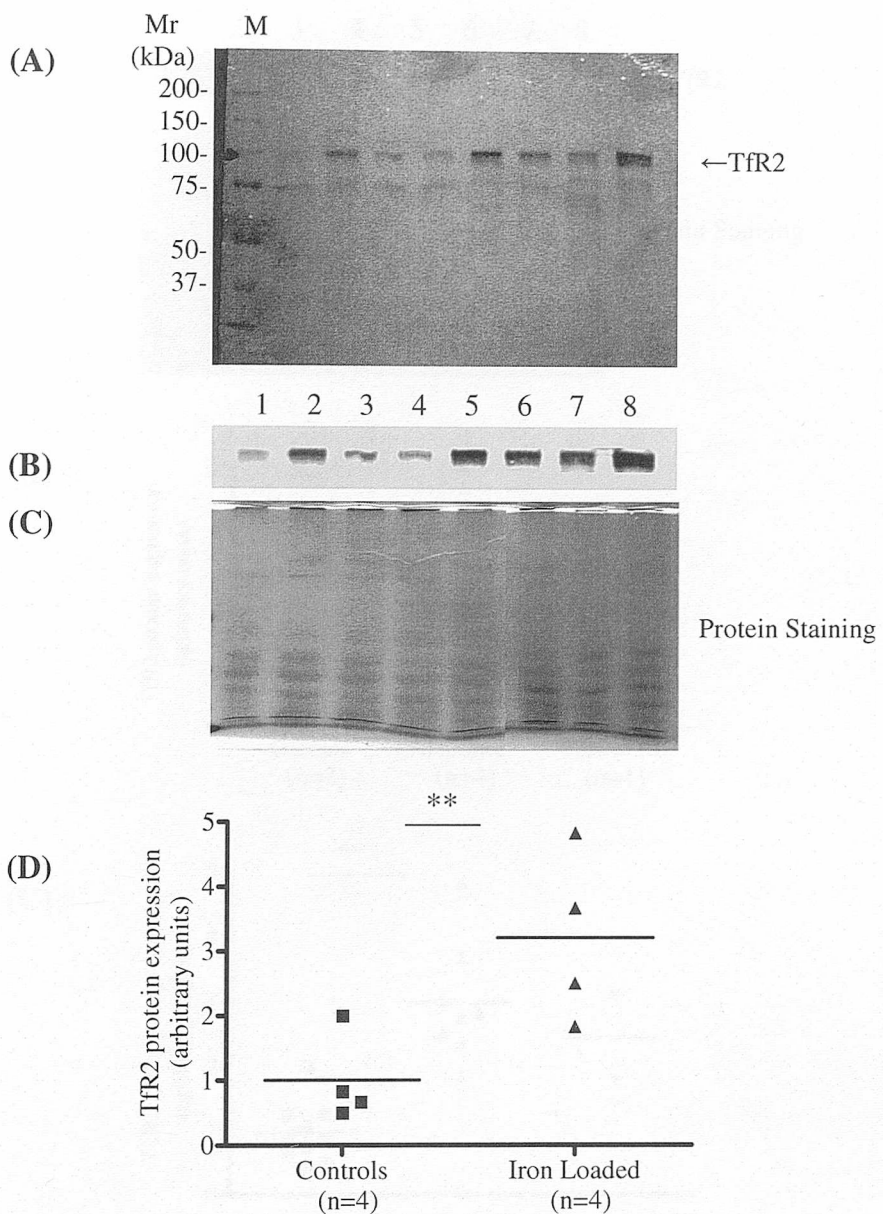


Figure 5.1 Western blotting analysis of TfR2 in human liver.

(A) Western blotting analysis was performed in liver biopsy specimens from 4 controls (lanes 1-4) and 4 iron loaded patients (lanes 5-8). Liver protein extracts ($80\mu\text{g}$) were subjected to SDS-PAGE and transblotted onto a nitrocellulose membrane. TfR2 was detected using a mouse monoclonal anti-TfR2 anti-serum and migrated as a 100kDa protein. (B) Iron loaded HH patients (lanes 5-8) had a significant increase in TfR2 protein levels as compared with control subjects (lanes 1-4) ($P=0.005$). (C) Coomassie Brilliant Blue stained gel demonstrating equal protein loading. (D) Graphical representation of experimental data shown in B. Western blotting and quantification of band densities and analysis was carried out as described in Chapter II.

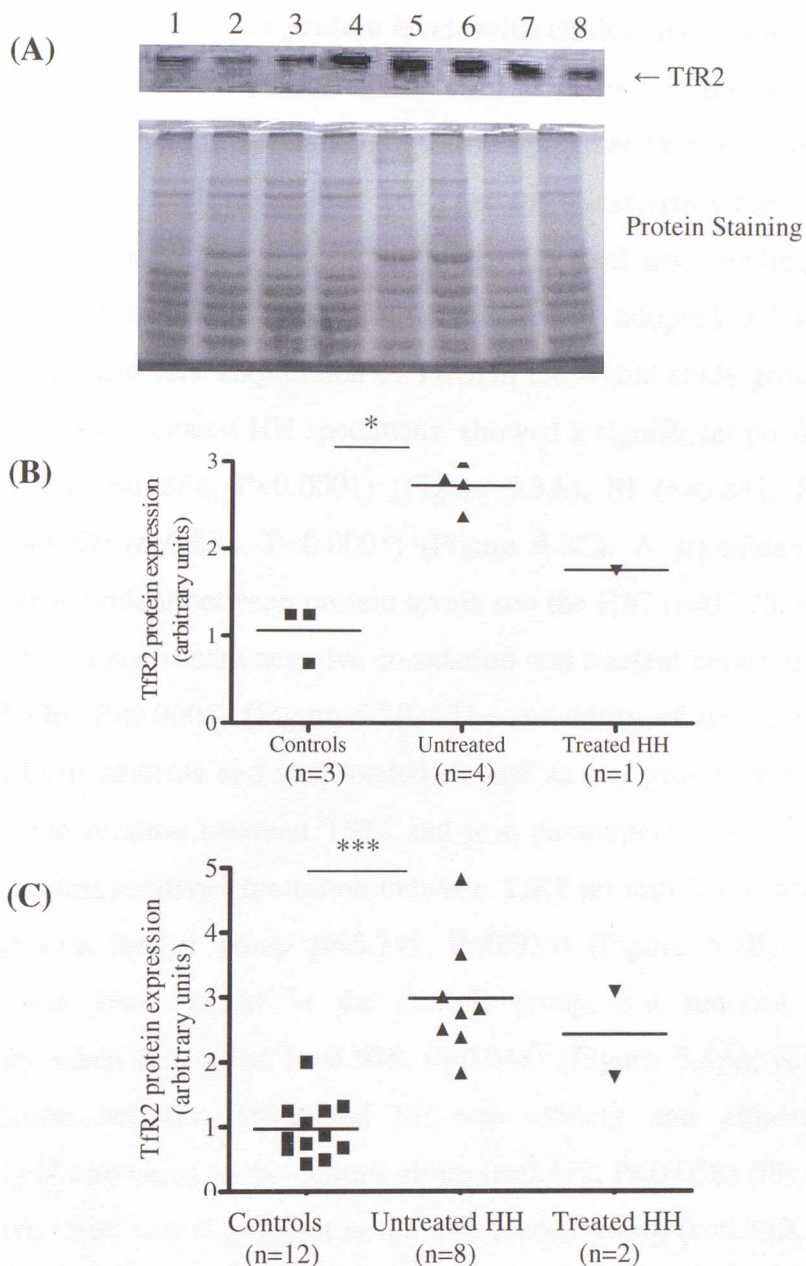


Figure 5.2 Western blotting analysis of TfR2 in untreated and treated HH patients.

(A) TfR2 was detected in the liver of 3 control subjects (lanes 1-3), 4 untreated HH (lanes 4-7) and 1 treated HH (lane 8) patient. Liver protein extracts (80 μ g) were subjected to SDS-PAGE and transblotted onto a nitrocellulose membrane and TfR2 was detected using a mouse monoclonal anti-TfR2 anti-serum. Equal protein loading using Coomassie Brilliant Blue is also shown. (B) Band intensity in A is shown in the dot plot diagram. TfR2 protein was significantly up-regulated in untreated HH patients as compared with control subjects ($P=0.041$). (C) Dot plot showing quantitative determination of TfR2 protein expression from the complete cohort of patients determined in 3 independent experiments. Untreated HH patients had a significant increase in TfR2 protein expression compared with control subjects ($P<0.001$). Expression of TfR2 in treated subjects was also evidently higher than in the control group, but lower than in the untreated group.

5.2.2 Correlation of hepatic TfR2 protein levels with clinical iron indices

To further investigate the observed up-regulation of TfR2 protein levels in HH, the relations between amounts of protein and clinical iron parameters were examined. As the nature of the possible relation between TfR2 and the transferrin saturation, serum iron, serum ferritin, hepatic iron concentration and the total iron binding capacity was unknown two approaches to modelling the data were adopted, a linear and a non-linear regression analysis. Expression of TfR2 in the whole study group ($n=20$), with the exception of the treated HH specimens, showed a significant positive linear correlation with TS ($r=0.888$, $P<0.0001$) (Figure 5.3A), SI ($r=0.881$, $P<0.0001$) (Figure 5.3B) and SF ($r=0.892$, $P<0.0001$) (Figure 5.3C). A significant positive correlation was also evident between protein levels and the HIC ($r=0.773$, $P<0.0001$) (Figure 5.3D), while a significant negative correlation was evident between TfR2 and the TIBC ($r=-0.736$, $P<0.0001$) (Figure 5.3E). The suitability of the grouping (i.e. expression data from controls and iron loaded studied as one group) was examined by investigating the relation between TfR2 and iron parameters in the two groups individually. A strong positive correlation between TfR2 protein levels and TS was observed in the iron loaded group ($r=0.749$, $P=0.035$) (Figure 5.4B), while the positive trend was also evident in the control group, but reached statistical significance only when one-tailed ($r=0.506$, $P=0.048$) (Figure 5.4A). Similarly, a positive correlation between TfR2 and SF was evident and almost reached significance only if one-tailed in the control group ($r=0.477$, $P=0.058$) (Figure 5.4C), while the positive trend was significant in the iron loaded group ($r=0.820$, $P=0.013$) (Figure 5.4D). Strong positive correlations were also evident between TfR2 and HIC in both study groups, controls ($r=0.630$, $P=0.028$) (Figure 5.4E) and untreated HH patients ($r=0.919$, $P=0.001$) (Figure 5.4F). A positive association between TfR2 and SI, was more evident in the iron loaded group ($r=0.539$, $P=0.168$) (Figure 5.5B) than in the control group ($r=0.110$, $P=0.733$) (Figure 5.5A), however failed to reach statistical significance in either group. Finally, the negative trend depicting the relationship between TfR2 and TIBC was evident in both groups with the iron loaded group reaching significance when the correlation was one-tailed ($r=-0.653$, $P=0.04$) (Figure 5.5C), and the control group not quite reaching significance even when one-tailed ($r=-0.435$, $P=0.08$) (Figure 5.5D).

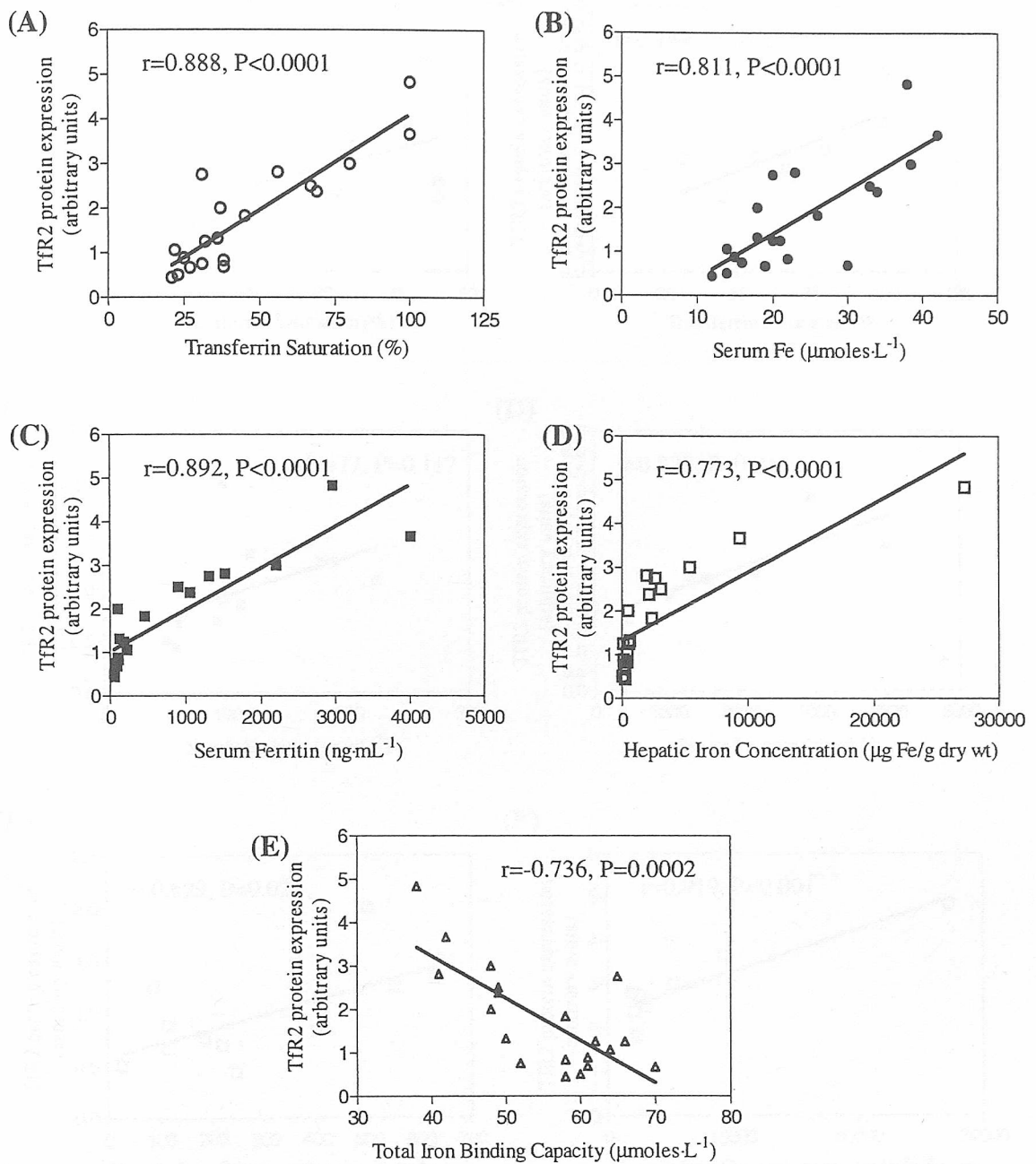


Figure 5.3 Linear regression analysis of the correlation between hepatic TfR2 protein expression and clinical iron status indices in the whole study group.

TfR2 protein levels correlated significantly with the transferrin saturation (A), serum iron (B), serum ferritin (C) and the hepatic iron concentration (D) in the whole study group (12 controls and 8 untreated HH patients) ($n=20$). An inverse significant correlation was evident between TfR2 protein levels and the total iron binding capacity (E).

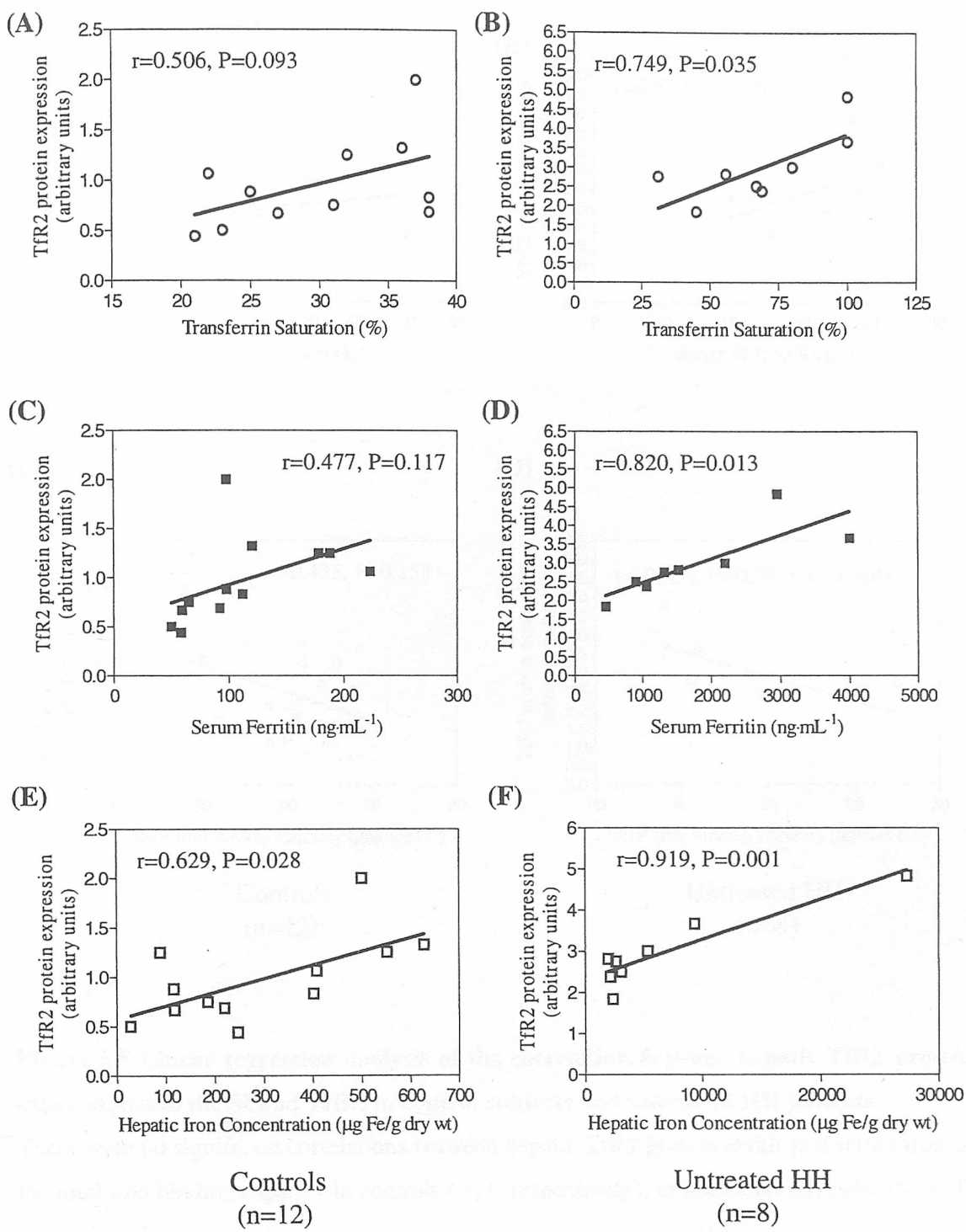


Figure 5.4 Linear regression analysis of the correlation between hepatic TfR2 protein expression and the TS, SF and the HIC in control subjects or untreated HH patients.

TfR2 protein levels correlated significantly with the transferrin saturation and serum ferritin in untreated HH patients (B, D respectively), while significance for that relationship was marginal when one-tailed in controls (A, C respectively). TfR2 protein levels correlated significantly with the hepatic iron concentration in controls (E) as well as in untreated HH patients (F).

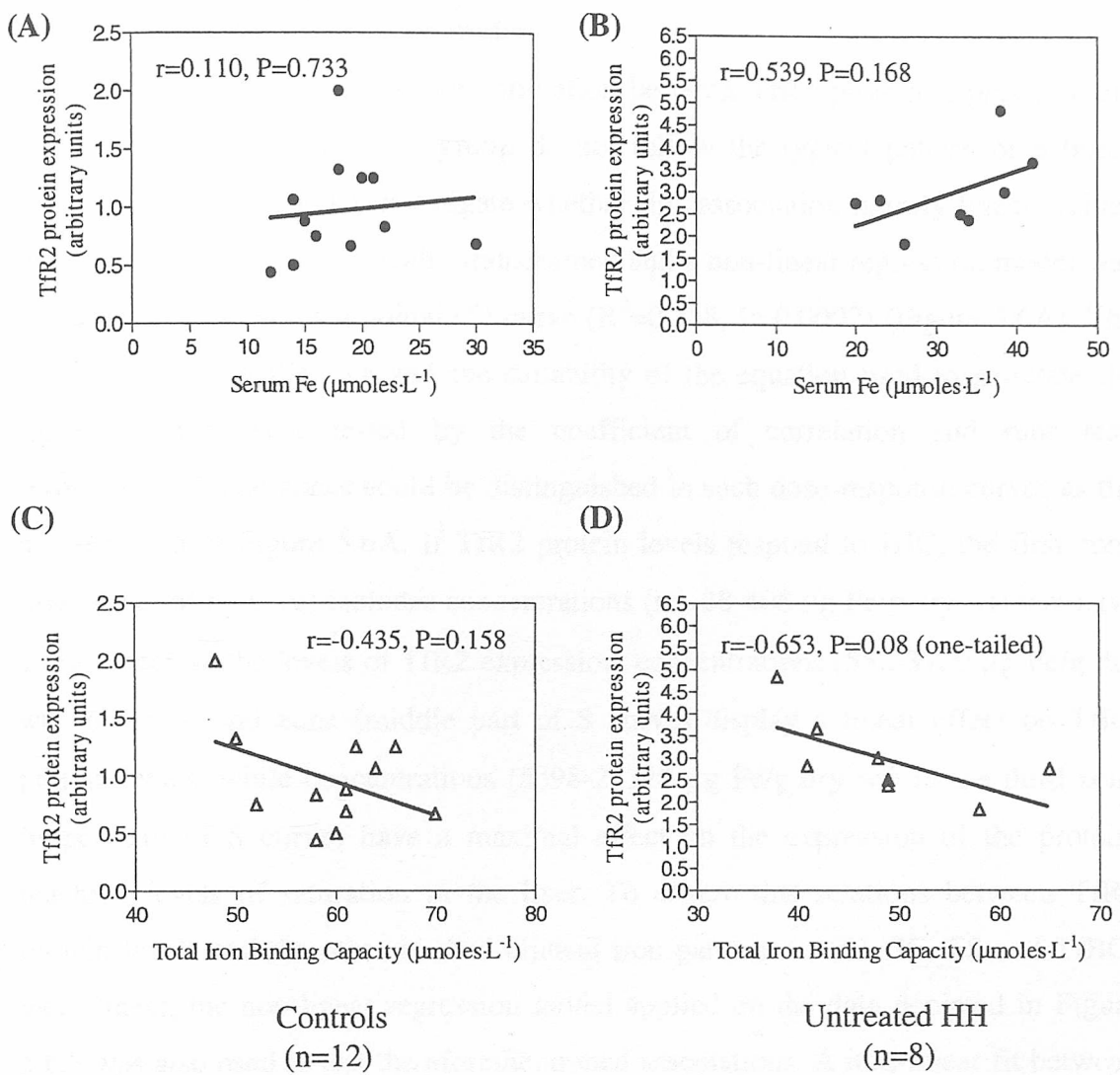


Figure 5.5 Linear regression analysis of the correlation between hepatic TfR2 protein expression and the SI and TIBC in control subjects and untreated HH patients.

There were no significant correlations between hepatic TfR2 protein levels and serum iron or the total iron binding capacity in controls (A, C respectively), or untreated HH patients (B, D respectively).

5.2.3 Non-linear regression analysis of the associations between hepatic TfR2 protein levels and clinical iron indices

The points depicting the positive correlation between TfR2 protein expression and the HIC evident in the heavy group do not follow the typical pattern of a linear relation (Figure 5.4F). To investigate whether this association is truly linear, values for the HIC were logarithmically transformed and a non-linear regression model was applied that yielded a sigmoidal (S) curve ($R^2=0.758$, $P=0.0002$) (Figure 5.6A). The goodness-of-fit of the data and the suitability of the equation used to generate the sigmoid curve were tested by the coefficient of correlation and runs test, respectively. Three zones could be distinguished in such dose-response curves as the one depicted in Figure 5.6A. If TfR2 protein levels respond to HIC, the first zone (lower part of S curve) includes concentrations (i.e. 28-408 $\mu\text{g Fe/g dry wt}$) that have a low effect on the levels of TfR2 expression, concentrations (552-3109 $\mu\text{g Fe/g dry wt}$) in the second zone (middle part of S curve) display a linear effect on TfR2 protein levels, while concentrations (5398-27320 $\mu\text{g Fe/g dry wt}$) in the third zone (upper part of S curve) have a maximal effect on the expression of the protein, reaching levels of saturation in the liver. To ensure that relations between TfR2 protein levels and the other studied clinical iron parameters (SI, SF, TS and TIBC) were linear, the non-linear regression model applied on the data depicted in Figure 5.6A was also used to test the aforementioned associations. A non-linear fit between TfR2 protein levels and the logarithmically transformed values of TS (Figure 5.6B), SI (Figure 5.6C), SF (Figure 5.6D) or TIBC (Figure 5.6E), however did not prove appropriate as the statistical software used was unable to find any best fit curves, further confirming the linearity of these associations.

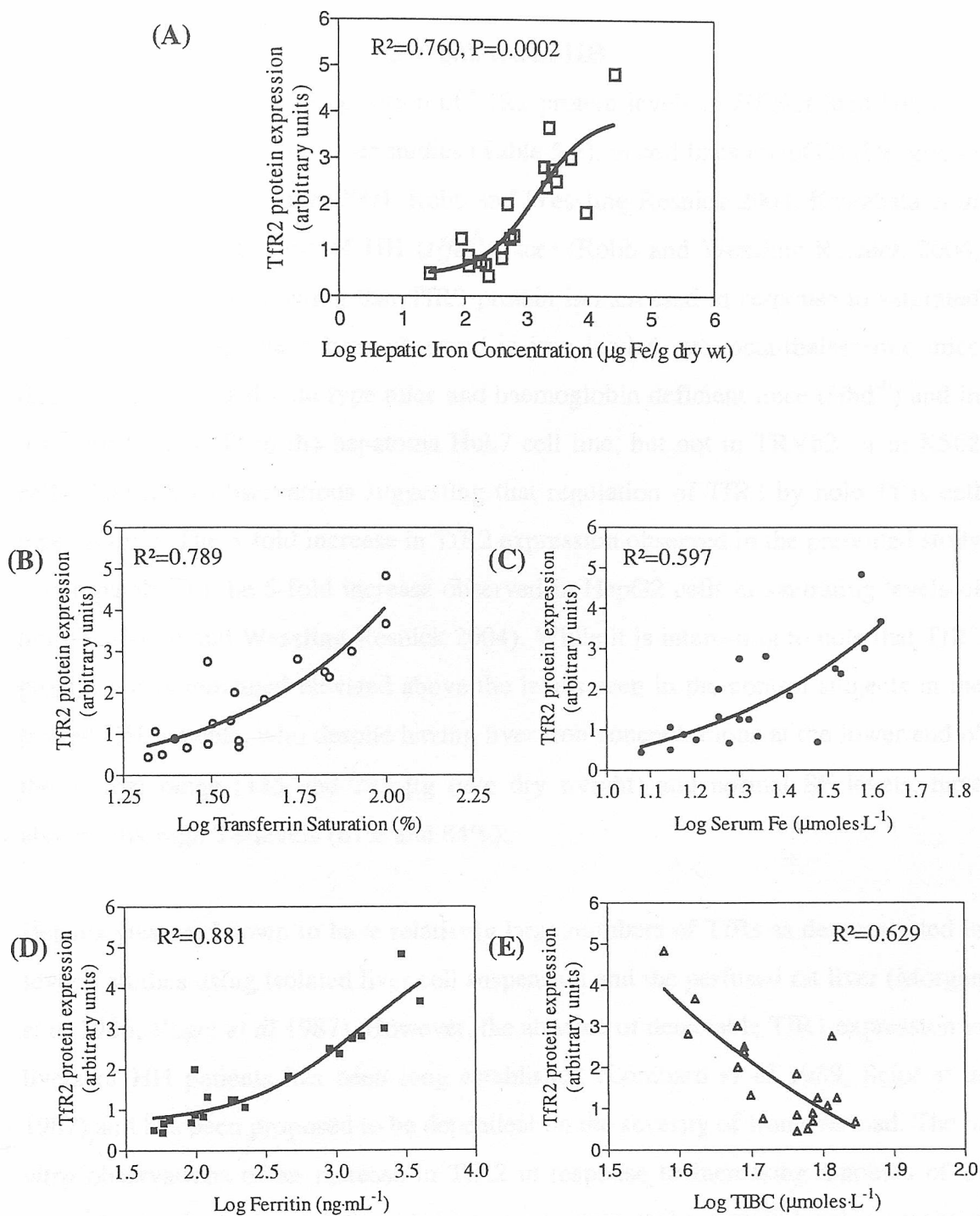


Figure 5.6 Non-linear regression analysis of the correlation between the hepatic Tfr2 protein expression and clinical iron status indices in the whole study group.

The non-linear regression analysis of the correlation between Tfr2 protein expression and the log of the hepatic iron concentration in controls and untreated HH patients ($n=20$) yielded a sigmoidal curve (A). The non-linear approach was not appropriate to depict the associations between Tfr2 and the log of transferrin saturation (B), serum iron (C), ferritin (D) and total iron binding capacity (E).

5.3 Discussion

5.3.1 Hepatic TfR2 protein is up-regulated in HH

The observation of an up-regulation of TfR2 protein levels in *HFE*-related HH is in agreement with numerous other studies (Table 5.2), in cell lines (HepG2) (Deaglio *et al* 2002, Johnson and Enns 2004, Robb and Wessling-Resnick 2004, Kawabata *et al* 2005) and animal models of HH (*Hfe*^{-/-} mice) (Robb and Wessling-Resnick 2004, Wilkins *et al* 2006) showing that TfR2 protein is increased in response to saturated Tf. Similar findings have been observed in iron loaded rats, beta-thalassemic mice (Hbb^{th-1}), iron loaded wild type mice and haemoglobin deficient mice (Hbd^{-/-}) and in response to holo-Tf in the hepatoma Huh7 cell line, but not in TRVb2, or in K562 cells. The latter observations suggesting that regulation of TfR2 by holo-Tf is cell type specific. The 3-fold increase in TfR2 expression observed in the presented study is comparable to the 5-fold increase observed in HepG2 cells at saturating levels of holo-Tf (Robb and Wessling-Resnick 2004). While it is interesting to note that TfR2 protein levels remained elevated above the levels seen in the control subjects in the treated HH patients, who despite having liver iron concentrations at the lower end of the normal range (135 and 285 µg Fe/g dry weight) and normal SF levels, have abnormally high TS levels (61% and 84%).

Hepatocytes are known to have relatively large numbers of TfRs as demonstrated in several studies using isolated liver cell suspension and the perfused rat liver (Morgan *et al* 1986, Vogel *et al* 1987). However, the absence of detectable TfR1 expression in livers of HH patients has been long established (Lombard *et al* 1989, Sciot *et al* 1987) and has been proposed to be dependent on the severity of iron overload. The *in vitro* observations of an increase in TfR2 in response to increasing amounts of Tf supports a reciprocal regulation of the two receptors at the protein level in response to iron. With respect to other iron-related molecules and their expression in the liver, IRP1 has also been found to be down-regulated in HH in Chapter III, and more recently FP1 protein expression has been found to be increased in the liver of C282Y homozygous HH patients (Adams *et al* 2003). In the intestine DMT1 protein expression was unchanged in mouse models of HH (Cannone-Hergaux *et al* 2001). In all cases, with TfR1 being the only exception although not evident in the data presented in Chapter III, it is interesting to note that a change in the levels of the

protein was not accompanied by a change in the mRNA levels of the respective transcript.

Table 5.2 Hepatic TfR2 protein expression in cell lines and animal models

	TfR2	TfR1	Other observations and comments	Respective studies
HepG2	Increased by holo-Tf		Similar finding on TfR2 protein in K562. No change in TfR2 protein levels in the presence of apo-Tf.	Deaglio <i>et al</i> 2002
	Increased by holo-Tf. Increase in half-life of protein.	Increased by holo-Tf	Similar findings on TfR2 protein levels in Huh7 cell line, but not in TRVb2 or K562.	Johnson and Enns 2004
	Increased by holo-Tf		No change in TfR2 protein levels in the presence of apo-Tf or NTBI. No change in TfR2 protein levels in K562, HeLa expressing exogenous TfR2 or HEK293T cells.	Robb and Wessling-Resnick 2004
	Increased by holo-Tf		TfR2 mRNA levels unchanged. No change in TfR2 protein levels in K562.	Kawabata <i>et al</i> 2005
Hfe ^{-/-}	Up-regulated		Also increased in <i>Hbd</i> ^{-/-} mice, <i>Hbb</i> ^{th-1} , but decreased in <i>hpx</i> mice.	Wilkins <i>et al</i> 2006
	Up-regulated	Decreased	Levels of TfR2 also up-regulated in rats on iron rich diet, <i>Hbb</i> ^{th-1} , but decreased in <i>hpx</i> mice.	Robb and Wessling-Resnick 2004

5.3.2 Saturable expression of liver TfR2 protein in HH

The finding of a direct correlation between hepatic TfR2 protein levels and the degree of TS seen in this chapter are in further agreement with the results of the *in vitro* studies indicating that diferric-Tf increases TfR2 expression by prolonging the half-life of the protein (Robb and Wessling-Resnick 2004, Johnson and Enns 2004). Moreover, increased expression of TfR2 was found in those livers with a high iron concentration with the relationship yielding a sigmoid curve when TfR2 protein expression was plotted as a function of the logarithm of HIC, with TfR2 expression saturating at high levels of liver iron. In chapter IV, hepatic TfR2 mRNA levels were shown to be comparable between iron loaded and control groups, which is in agreement with recent studies by Gehrke *et al* (2003, 2005), but does not agree with findings of decreased levels in the mouse model of HH (*Hfe*^{-/-}) (Ludwiczek *et al* 2005). Relying on the findings presented in Chapter IV and those of the studies using human liver in the experimental protocol, it could be concluded that up-regulation of TfR2 is a post-transcriptional event possibly elicited by the levels of TS, reflecting the systemic iron availability. Bearing in mind that TfR2 is a membrane protein receptor that binds a ligand carrying iron, binding of diferric-Tf to TfR2 would be the most upstream regulatory event in the cascade leading to the production of HAMP.

5.3.3 Future directions

HepG2 cells express TfR2 (Kawabata *et al* 1999, Deaglio *et al* 2002, Vogt *et al* 2003, Calzolari *et al* 2004), but also synthesise and secrete Tf (Knowles *et al* 1980). Treatment of HepG2 cells with holo-Tf (25μM) was attempted in order to examine the response on the levels of the TfR2 protein, however time did not permit optimisation of the Western blotting technique and hence no results could be obtained. Further experiments that were attempted and are worth pursuing include examining TfR1 protein levels both *in vitro* and *ex vivo*. Experiments were carried out on HeLa and HepG2 cell lines and human liver using the mouse anti-human TfR1 anti-serum (Zymed Laboratories Inc) which has been used successfully by Le and Richardson (2003). However no results were obtained and with regards to the *in vitro* experiments that could perhaps be attributed to the presence of TfR1 in a truncated form and therefore cruder extracts, for instance from cells that have been detached in the absence of trypsin, may have proved a more appropriate approach.

Chapter VI

Conclusions

6.1 Down-regulation of IRP1 protein in HH is a post-transcriptional event

The results presented in Chapter III, show that IRP1 protein expression is down-regulated in iron overload. The levels of the protein were decreased both in the *ex vivo* as well as in the *in vitro* investigations, with the decrease being less marked in the monkey fibroblast cell line, pointing possibly towards a cell specific response. The underlying mechanism of the down-regulation of IRP1 in the liver, is limited to two possibilities, inhibition of transcription or post-transcriptional regulation (either through increased turnover of protein or inhibition of translation), and was further investigated by examining transcript levels of the protein *ex vivo*. The results presented in Chapter IV indicate that IRP1 mRNA was unaffected by iron overload, which rules out a transcriptional control and is in favour of a post-translational mechanism that remains to be elucidated. It could be hypothesised that the marked down-regulation in hepatic IRP1 protein levels, is the result of an excessive accumulation of iron in these cells, since as seen in Chapter I they possess several mechanisms for acquiring not only iron from the circulation, but also haem and ferritin. Excess iron, especially in the non-Tf bound form, is known to promote oxidative stress which in turn stimulates production of ROS, resulting perhaps in the observed instability of IRP1.

The appearance of extra bands in addition to the main IRP1 band and the possibility of a nuclear presence of IRP1 in hepatocytes of patients with *HFE*-related HH, in cultured fibroblasts and in human cervical carcinoma and hepatoma cells, points towards the possibility of the existence of alternatively spliced forms of IRP1 with novel functions in the nucleus. The presence of extra bands on a nitrocellulose membrane following immunoblotting could be due to several factors other than alternative splicing. The presence of bands that are lower than the main band be the result of a degradation product, a cleaved fragment, a different member of the same family, or a cross reaction to a non-related protein. While upper bands could be dimers or other oligomers of the protein, a phosphorylated, or post translationally modified product, or a cross reaction to a non-related protein. The existence of

alternatively spliced forms of transcripts that are implicated in iron homeostasis has been documented in the literature with ferritin being the first identified, followed by DMT1 and TfR2, and more recently HFE. Further experiments would need to be conducted before any conclusions can be drawn, however if the extra bands were found to be IRP1 products, then it could be speculated that a dual presence of IRP1 in the cytoplasm and the nucleus, or the shuttling of the protein between the two compartments, could point to an as yet undefined regulatory role. Perhaps to exert its well-established binding control on IRE-containing transcripts in the nucleus or to alter the splicing patterns of these molecules, scenarios that are not too far-fetched according to studies that suggest that translation could occur in the nucleus (Iborra *et al* 2001).

6.2 Transcript levels of iron-related molecules expressed in the liver are not affected by iron overload

The mRNAs of iron related proteins were measured in the livers of untreated patients with *HFE*-related HH and controls. The data presented in Chapter IV suggest that hepatic levels of HAMP, HJV, TfR1, TfR2 and IRP1 mRNA were comparable in HH patients as compared to controls. A positive relation was observed between hepatic transcript levels of HAMP, IRP1 and TfR2 that suggests a possible connection between these molecules. Mutations in the HAMP and TfR2 genes cause a similar phenotype of HH suggesting that the products of these two genes perhaps share a common pathway of iron homeostasis. Under physiological conditions, expression of TfR2 mRNA in the liver exceeded that of TfR1, while transcript levels of HAMP exceeded those of all other studied transcripts, with IRP1 being the second highest. It could be hypothesised that the HAMP, IRP1 and TfR2 transcripts, which might be members of the same or distinct pathways that regulate iron homeostasis, need to be present in ample amounts ready to be translated when the protein is required by the cell. At physiological levels of iron, transcript levels of hepatic IRP1 and TfR2 correlated with serum ferritin concentrations suggesting that perhaps IRP1 and TfR2 could be transcribed in response to iron levels, a relation however that was not evident in the presence of excess iron stores due to mutations in HFE.

6.3 Saturability of hepatic TfR2 protein expression in HH

The results presented in Chapter V, revealed that TfR2 protein expression in the liver of patients with *HFE*-related HH was up-regulated as compared to control subjects. Since transcript levels of this molecule were unchanged as shown in Chapter IV, the observed increase in the levels of TfR2 protein must be the result of a post-transcriptional phenomenon. Although not directly tested in the presented studies, evidence from other relevant studies suggests that the half-life of TfR2 is prolonged in response to increased amounts of diferric-Tf. In accord with these observations, the up-regulation of TfR2 was saturable in response to increasing amounts of hepatic iron as indicated by the sigmoid curve that is characteristic of signal transduction pathways. Even under physiological conditions uptake of Tf-bound iron by the liver can be mediated by TfR2 since this receptor is highly expressed in this tissue. Increased levels of TfR2 in the liver of patients with *HFE*-related HH, combined perhaps with a non-functional HFE, might be causing the excessive accumulation of iron observed in this disorder. In addition, as increased dietary iron uptake continues to burden the circulation of iron, more Tf becomes saturated and more free iron is present in the plasma in the form of NTBI. Since hepatocytes are equipped with several iron uptake mechanisms, uptake of NTBI from the circulation adds another pathway contributing to the increased hepatic iron overload. An increase in NTBI causes an increase in the LIP of the hepatocyte, which in turn will lead to oxidative stress via production of ROS. Oxidative stress will perhaps cause the degradation of IRP1 as seen in Chapter III, causing the dysregulation of the control mechanisms that could be exerted by this molecule.

6.4 Summary of observations

The challenge posed following any study is to define the activities and relationships between the molecules of interest based on the findings. Any proposed model aiming to elucidate the function of hepcidin, HJV, TfR2, TfR1 and IRP1 in iron metabolism and their deregulation in HH has to consider the pattern of expression of the molecules along with the biochemical evidence. The studies presented throughout this thesis do not provide sufficient evidence to fully account for the iron loaded phenotype that is characteristic of HH. Some conclusions can be drawn however, based on the presented findings and a review of the relevant literature. Mutations in hepcidin, HFE, HJV or TfR2 lead to haemochromatosis, with mutations in hepcidin

and HJV leading to a more severe phenotype of the disorder, suggesting that these are key molecules in the control of iron homeostasis. The findings presented in this thesis reflect the importance of hepcidin, IRP1 and TfR2 as iron-regulatory molecules whose expression is deregulated in *HFE*-related HH. Moreover, the possibility of a link between IRP1, the intracellular iron regulator, and hepcidin in the liver raises the prospect of a link between intracellular and systemic iron homeostasis.

Transcript levels of hepcidin, IRP1 and TfR2 were expressed with highest abundance in the livers of controls, homozygous YY patients with *HFE*-related HH as well as iron loaded individuals irrespective of their genotype. Expression of each transcript correlated strongly with the other when all subjects were studied as a whole group, however the positive relation between HAMP and TfR2 mRNA levels in the control group was lost in the face of iron overload. Indeed hepcidin failed to respond to the increased iron burden and remained at levels comparable to those observed under physiological iron conditions, while levels of TfR2 increased in the face of increasing circulating iron carrying Tf. The results of the studies presented in Chapters III, IV and V suggest that transcript levels of molecules do not reflect protein levels of expression, since there were decreased IRP1 and increased TfR2 protein levels in the liver of patients with *HFE*-related HH, while transcript levels were unchanged. IRP1 and TfR2, and perhaps other molecules that have not yet been studied at the protein level, such as hepcidin and HJV, are therefore subject to post-transcriptional mechanisms of control, the details of which remain to be explored.

Recent hypotheses point to the liver as a regulatory organ in sensing and controlling iron absorption via hepcidin. When levels of iron are high (Figure 6.1A), hepcidin synthesis is thought to be regulated in response to TS by a signal cascade triggered possibly by HFE, HJV or TfR2 in response to levels of diferric-Tf. TfR2 and HJV have been proposed as hepcidin activators or modulators *in vivo* since patients with TfR2 or HJV mutations have low or undetectable urinary levels of hepcidin (Nemeth *et al* 2005). In addition, Wallace *et al* (2005) have demonstrated that TfR2 KO mice fail to up-regulate HAMP mRNA or pro-hepcidin protein in response to increased iron stores. Loss of TfR2 in these mice leads to significantly less hepatic expression of HFE and HJV mRNA compared to controls, which suggests that TfR2 may act

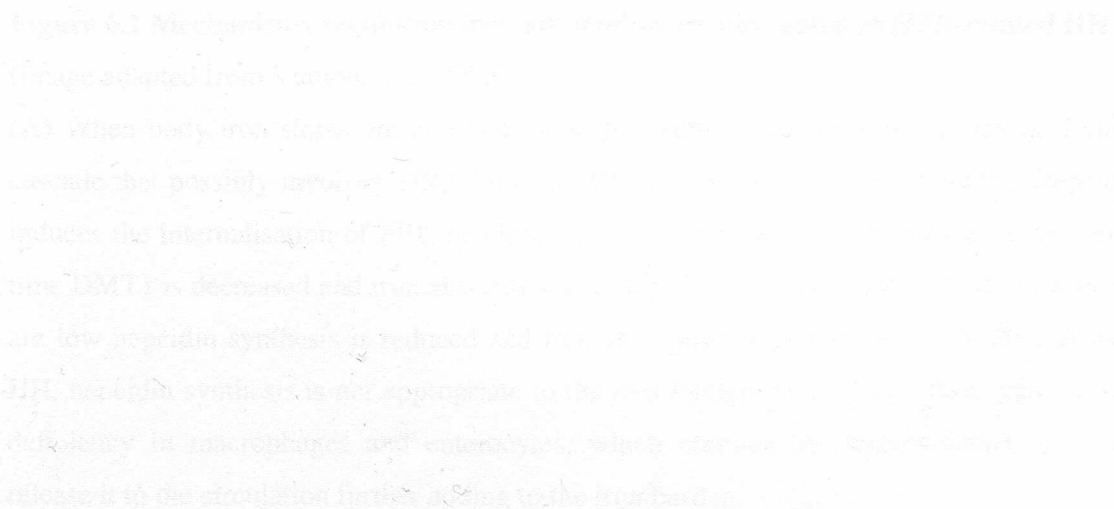
upstream of HFE and HJV in the iron signalling pathway. Relevant published studies discussed in Chapter IV, suggest that there is an inverse correlation between the expression of hepcidin in the liver and the expression of iron transporters in the gut. Therefore, while hepcidin expression is increased, expression of DMT1, Dcytb, and FP1 in the duodenum decreases. Less dietary iron enters the enterocyte and hepcidin promotes internalisation of FP1, leading to decreased efflux of iron into the plasma circulation. When levels of iron are low (Figure 1.6B) on the other hand, hepcidin synthesis is less marked and hence expression of molecules in the duodenum promote the uptake of dietary iron and the efflux of ferrous iron into the circulation.

In patients with *HFE*-related HH (Figure 6.1C), evidence of an increased hepatic expression of TfR2 could possibly represent an attempt to drive hepcidin production by hepatocytes. Although hepcidin production was not appropriate to the iron burden in this form of HH, there were basal levels of expression as in the model presented in Chapter I (Figure 1.7), as TfR2 could perhaps partly compensate for the loss of HFE function. Expression of TfR2 reflected levels of saturated Tf and reached saturable levels at upper levels of excess iron. A failure to stimulate hepcidin will result in the impairment of hepcidin mediated FP1 degradation, leading to increased iron export from intestinal absorptive cells and from macrophages, therefore leading to the observed iron deficiency in these cell types that is characteristic of the disorder. Levels of DMT1 and Dcytb remain elevated leading to increased dietary iron absorption, while IRP1 expression in the duodenum is also increased, in contrast to the levels of the protein in the hepatocytes of these patients.

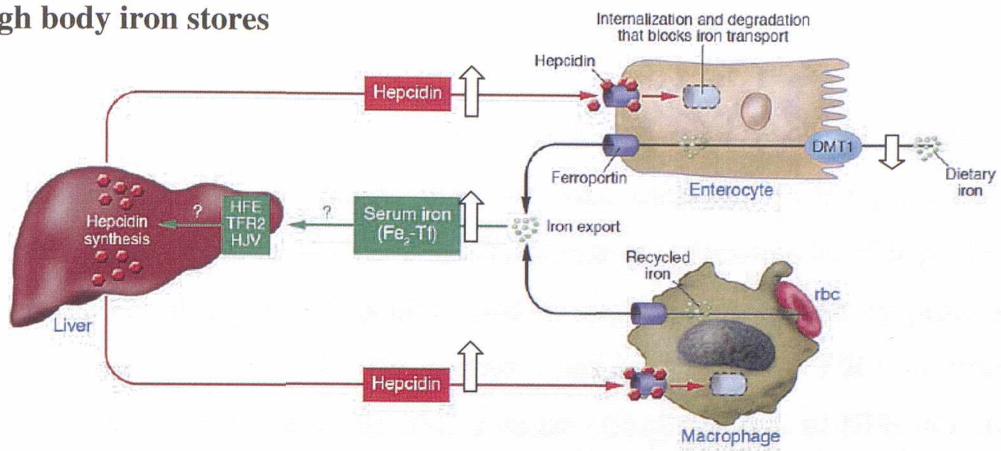
The studies presented in this thesis measured mRNA expression of iron-related molecules using whole liver extracts and there was no separation of expression in hepatocytes from that of Kupffer cells. Studies on Kupffer cells (Lou *et al* 2005, Montosi *et al* 2005) and macrophages (Montosi *et al* 2005), suggest that these two cell types are not involved in up-regulating hepcidin in response to iron. A plasma factor present in Tf-saturated serum therefore signals the hepatocyte to express hepcidin and whether the presence of functional HFE is crucial in this signalling remains to be explored. Disabling mutations in TfR2 cause iron overload with an adult-onset phenotype, characterised again by hepcidin deficiency and there is evidence that the converse situation holds, where HFE partially compensates for the

loss of function of this transferrin receptor isoform. It is not clear however whether HFE in hepatocytes is required for the activation of hepcidin synthesis although lack of functional HFE might be the reason for inappropriate hepcidin up-regulation in *HFE*-related HH. Whether TfR2 and HFE act in the same or distinct regulatory pathways of hepcidin synthesis, or whether HFE is part of a hepcidin -independent pathway of iron homeostasis, remains unclear.

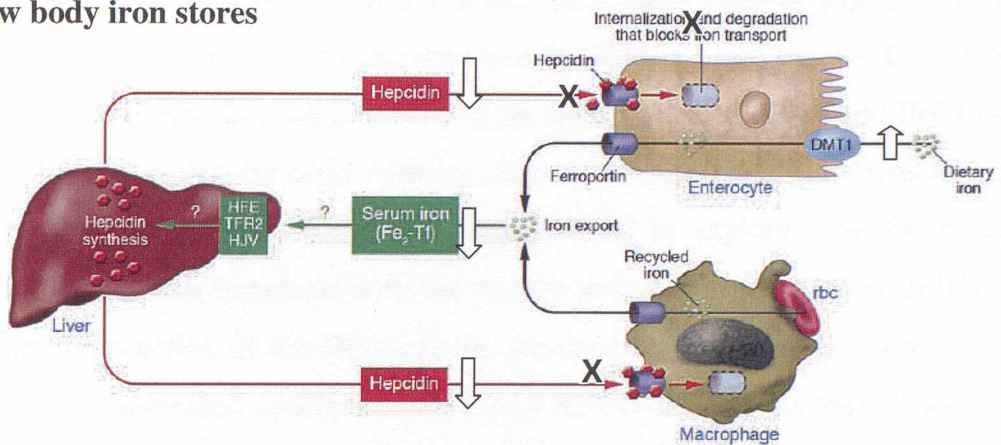
In a recent study presenting a compartmental model of iron regulation in the mouse (Lao and Kamei 2006), it was predicted that even in the presence of a functional HFE, increased iron uptake alone would be sufficient to cause a dysregulation of iron homeostasis. According to the simulated model, in the setting of iron overload that is characteristic of *HFE*-related HH, when levels of NTBI were increased and started approaching micromolar amounts, a response that ultimately down-regulated hepcidin was elicited with diferric-Tf as the link between the erythroid compartment and the iron regulatory mechanism. Iron absorption by the duodenum was increased and there was a lack of adequate hepcidin synthesis to decrease iron absorption to match the iron excretion rate. An increase in the presence and uptake of saturated Tf via TfR2, which has been found to be up-regulated in the liver of these patients, leading to increased levels of NTBI, might be the reason behind the halt in hepcidin synthesis and the consequences of that vicious cycle that patients with HH are caught up in.



(A) High body iron stores



(B) Low body iron stores



(C) HFE-related HH

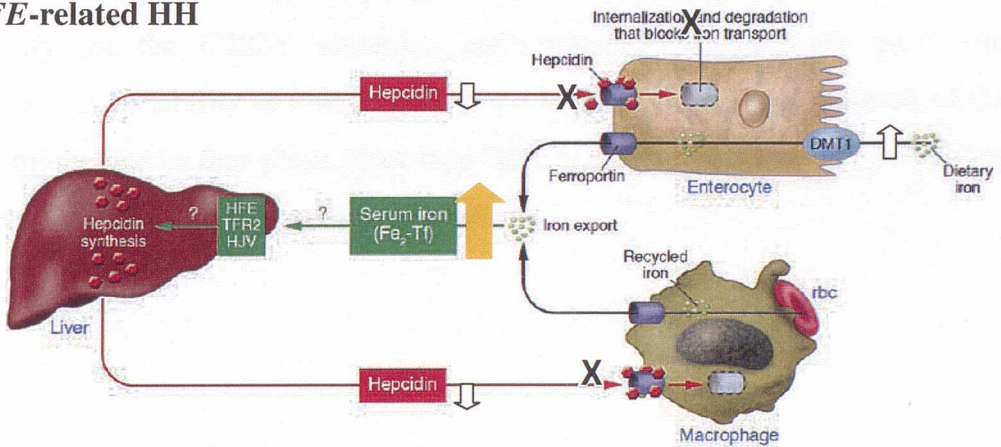


Figure 6.1 Mechanisms regulating iron absorption are abrogated in HFE-related HH.

(image adapted from Vaulont *et al* 2005)

(A) When body iron stores are elevated, hepcidin synthesis by the liver is increased via a cascade that possibly involves TfR2, HFE or HJV and diferric-Tf as the stimulus. Hepcidin induces the internalisation of FP1, blocking egress of iron into the circulation. At the same time DMT1 is decreased and iron absorption is reduced. (B) When levels of body iron stores are low hepcidin synthesis is reduced and iron absorption is increased. (C) In HFE-related HH, hepcidin synthesis is not appropriate to the iron burden, leading to a false state of iron deficiency in macrophages and enterocytes, which continue to absorb dietary iron and release it to the circulation further adding to the iron burden.

6.5 Remaining issues

The post-transcriptional mechanisms regulating levels of IRP1 and TfR2 protein expression in response to iron loading have not been addressed in the presented studies and therefore remain to be explored. The regulatory mechanisms of hepcidin synthesis and the possibility that hepcidin could be another iron regulatory protein are equally unresolved issues. As the precise roles of HFE and TfR2 in iron metabolism remain uncertain, other remaining issues include the role of HFE in iron homeostasis and the significance of its interaction with either TfR1 or TfR2, as well as whether TfR2 serves more functions, than merely Tf-bound iron uptake. Does the mutation in the HFE protein have any bearing on the activities of IRP1 and IRP2 as iron-sensors for low molecular iron? Although there is evidence that mutations in the HFE protein lead to HH, and there is a clear rational to explain how the main mutation, C282Y, which interferes with the mutant protein's association with β 2m, could disrupt the function of the HFE protein, the mechanism by which the C282Y mutation leads to increased absorption of dietary iron remains a mystery. There is considerable variation in the penetrance of HFE mutations, and in addition to homozygosity for the C282Y mutation, environmental factors have also been "blamed" for the variability in iron accumulation and the clinical presentation of the disease. It might also be that genes other than HFE or the presence of more mutations in HFE could be causing this phenotypic variation.

References

- ABBOUD, S. & HAILE, D. J. (2000) A novel mammalian iron-regulated protein involved in intracellular iron metabolism. *J Biol Chem*, 275, 19906-12.
- ABRAMOFF, M. D., MAGELHAES, P. J., & RAM, S. J. (2004) Image processing with ImageJ. *Biophotonics International*, 11, 36-42.
- ADAMS, P. C., BARBIN, Y. P., KHAN, Z. A. & CHAKRABARTI, S. (2003) Expression of ferroportin in hemochromatosis liver. *Blood Cells Mol Dis*, 31, 256-61.
- ADDESS, K. J., BASILION, J. P., KLAUSNER, R. D., ROUAULT, T. A. & PARDI, A. (1997) Structure and dynamics of the iron responsive element RNA: implications for binding of the RNA by iron regulatory binding proteins. *J Mol Biol*, 274, 72-83.
- ADEN, D. P., FOGEL, A., PLOTKIN, S., DAMJANOV, I. & KNOWLES, B. B. (1979) Controlled synthesis of HBsAg in a differentiated human liver carcinoma-derived cell line. *Nature*, 282, 615-6.
- AHMAD, K. A., AHMANN, J. R., MIGAS, M. C., WAHEED, A., BRITTON, R. S., BACON, B. R., SLY, W. S. & FLEMING, R. E. (2002) Decreased liver hepcidin expression in the Hfe knockout mouse. *Blood Cells Mol Dis*, 29, 361-6.
- AISEN, P. (2004) Transferrin receptor 1. *Int J Biochem Cell Biol*, 36, 2137-43.
- AISEN, P., ENNS, C. & WESSLING-RESNICK, M. (2001) Chemistry and biology of eukaryotic iron metabolism. *Int J Biochem Cell Biol*, 33, 940-59.
- ALWINE, J. C., KEMP, D. J. & STARK, G. R. (1977) Method for detection of specific RNAs in agarose gels by transfer to diazobenzyloxymethyl-paper and hybridization with DNA probes. *Proc Natl Acad Sci U S A*, 74, 5350-4.
- ANDREWS, N. C. (1999) Disorders of iron metabolism. *N Engl J Med*, 341, 1986-95.
- ANDREWS, N. C. (2000) Iron homeostasis: insights from genetics and animal models. *Nat Rev Genet*, 1, 208-17.
- ANDREWS, N. C. (2005a) Understanding heme transport. *N Engl J Med*, 353, 2508-9.
- ANDREWS, N. C. (2005b) Molecular control of iron metabolism. *Best Pract Res*

Clin Haematol, 18, 159-69.

- ARREDONDO, M., MARTINEZ, R., NUNEZ, M. T., RUZ, M. & OLIVARES, M. (2006) Inhibition of iron and copper uptake by iron, copper and zinc. *Biol Res*, 39, 95-102.
- ARREDONDO, M., MUÑOZ, P., MURA, C. V. & NUNEZ, M. T. (2003) DMT1, a physiologically relevant apical Cu⁺ transporter of intestinal cells. *Am J Physiol Cell Physiol*, 284, C1525-30.
- AZIZ, N. & MUNRO, H. N. (1987) Iron regulates ferritin mRNA translation through a segment of its 5' untranslated region. *Proc Natl Acad Sci U S A*, 84, 8478-82.
- BABITT, J. L., HUANG, F. W., WRIGHTING, D. M., XIA, Y., SIDIS, Y., SAMAD, T. A., CAMPAGNA, J. A., CHUNG, R. T., SCHNEYER, A. L., WOOLF, C. J., ANDREWS, N. C. & LIN, H. Y. (2006) Bone morphogenetic protein signaling by hemojuvelin regulates hepcidin expression. *Nat Genet*, 38, 531-9.
- BACON, B. R. (2001) Hemochromatosis: diagnosis and management. *Gastroenterology*, 120, 718-25.
- BARTON, J. C., McDONNELL, S. M., ADAMS, P. C., BRISSOT, P., POWELL, L. W., EDWARDS, C. Q., COOK, J. D. & KOWDLEY, K. V. (1998) Management of hemochromatosis. Hemochromatosis Management Working Group. *Ann Intern Med*, 129, 932-9.
- BASILION, J. P., ROUAULT, T. A., MASSINOPLE, C. M., KLAUSNER, R. D. & BURGESS, W. H. (1994) The iron-responsive element-binding protein: localization of the RNA-binding site to the aconitase active-site cleft. *Proc Natl Acad Sci U S A*, 91, 574-8.
- BASTIN, J. M., JONES, M., O'CALLAGHAN, C. A., SCHIMANSKI, L., MASON, D. Y. & TOWNSEND, A. R. (1998) Kupffer cell staining by an HFE-specific monoclonal antibody: implications for hereditary haemochromatosis. *Br J Haematol*, 103, 931-41.
- BATEY, R. G., LAI CHUNG FONG, P., SHAMIR, S. & SHERLOCK, S. (1980) A non-transferrin-bound serum iron in idiopathic hemochromatosis. *Dig Dis Sci*, 25, 340-6.
- BEARD, J. L., & DAWSON, H. D. (1997) Iron. In: B. L. O'DELL & R. A. SUNDE, (Eds). *Handbook of nutritionally essential mineral elements*. New York,

Marcel Dekker. pp 275-334.

- BEAUMONT, C., SIMON, M., SMITH, P. M. & WORWOOD, M. (1980) Hepatic and serum ferritin concentrations in patients with idiopathic hemochromatosis. *Gastroenterology*, 79, 877-83.
- BEUTLER, E., FELITTI, V. J., KOZIOL, J. A., HO, N. J. & GELBART, T. (2002) Penetrance of 845G-->A (C282Y) HFE hereditary haemochromatosis mutation in the USA. *Lancet*, 359, 211-8.
- BEZWODA, W. R., BOTHWELL, T. H., CHARLTON, R. W., TORRANCE, J. D., MACPHAIL, A. P., DERMER, D. P. & MAYET, F. (1983) The relative dietary importance of haem and non-haem iron. *S Afr Med J*, 64, 552-6.
- BIASOTTO, G., ROETTO, A., DARAIO, F., POLOTTI, A., GERARDI, G. M., GIRELLI, D., CREMONESI, L., AROSIO, P. & CAMASCHELLA, C. (2004) Identification of new mutations of hepcidin and hemojuvelin in patients with HFE C282Y allele. *Blood Cells Mol Dis*, 33, 338-43.
- BINDER, R., HOROWITZ, J. A., BASILION, J. P., KOELLER, D. M., KLAUSNER, R. D. & HARFORD, J. B. (1994) Evidence that the pathway of transferrin receptor mRNA degradation involves an endonucleolytic cleavage within the 3' UTR and does not involve poly(A) tail shortening. *Embo J*, 13, 1969-80.
- BODMER, J. G., PARHAM, P., ALBERT, E. D. & MARSH, S. G. (1997) Putting a hold on "HLA-H". The WHO Nomenclature Committee for Factors of the HLA System. *Nat Genet*, 15, 234-5.
- BOMFORD, A. (2002) Genetics of haemochromatosis. *Lancet*, 360, 1673-81.
- BOMFORD, A. & WILLIAMS, R. (1976) Familial iron storage disease in two sisters. *Proc R Soc Med*, 69, 806-7.
- BONDI, A., VALENTINO, P., DARAIO, F., PORPORATO, P., GRAMAGLIA, E., CARTURAN, S., GOTTARDI, E., CAMASCHELLA, C. & ROETTO, A. (2005) Hepatic expression of hemochromatosis genes in two mouse strains after phlebotomy and iron overload. *Haematologica*, 90, 1161-7.
- BOURDON, E., KANG, D. K., GHOSH, M. C., DRAKE, S. K., WEY, J., LEVINE, R. L. & ROUAULT, T. A. (2003) The role of endogenous heme synthesis and degradation domain cysteines in cellular iron-dependent degradation of IRP2. *Blood Cells Mol Dis*, 31, 247-55.
- BRADFORD, M. M. (1976) A rapid and sensitive method for the quantitation of

- microgram quantities of protein utilizing the principle of protein-dye binding. *Anal Biochem*, 72, 248-54.
- BRENNAN, C. M., GALLOUZI, I. E. & STEITZ, J. A. (2000) Protein ligands to HuR modulate its interaction with target mRNAs in vivo. *J Cell Biol*, 151, 1-14.
- BRIDLE, K. R., FRAZER, D. M., WILKINS, S. J., DIXON, J. L., PURDIE, D. M., CRAWFORD, D. H., SUBRAMANIAM, V. N., POWELL, L. W., ANDERSON, G. J. & RAMM, G. A. (2003) Disrupted hepcidin regulation in HFE-associated haemochromatosis and the liver as a regulator of body iron homoeostasis. *Lancet*, 361, 669-73.
- BRITTON, R. S., FLEMING, R. E., PARKKILA, S., WAHEED, A., SLY, W. S. & BACON, B. R. (2002) Pathogenesis of hereditary hemochromatosis: genetics and beyond. *Semin Gastrointest Dis*, 13, 68-79.
- BURNETTE, W. N. (1981) "Western blotting": electrophoretic transfer of proteins from sodium dodecyl sulfate-polyacrylamide gels to unmodified nitrocellulose and radiographic detection with antibody and radioiodinated protein A. *Anal Biochem*, 112, 195-203.
- BUTT, J., KIM, H. Y., BASILION, J. P., COHEN, S., IWAI, K., PHILPOTT, C. C., ALTSCHUL, S., KLAUSNER, R. D. & ROUAULT, T. A. (1996) Differences in the RNA binding sites of iron regulatory proteins and potential target diversity. *Proc Natl Acad Sci U S A*, 93, 4345-9.
- BYRNES, V., BARRETT, S., RYAN, E., KELLEHER, T., O'KEANE, C., COUGHLAN, B. & CROWE, J. (2002) Increased duodenal DMT-1 expression and unchanged HFE mRNA levels in HFE-associated hereditary hemochromatosis and iron deficiency. *Blood Cells Mol Dis*, 29, 251-60.
- CABRITA, M., PEREIRA, C. F., RODRIGUES, P., CARDOSO, E. M. & AROSA, F. A. (2005) Altered expression of CD1d molecules and lipid accumulation in the human hepatoma cell line HepG2 after iron loading. *Febs J*, 272, 152-65.
- CADENAS, E. (1989) Biochemistry of oxygen toxicity. *Annu Rev Biochem*, 58, 79-110.
- CAIRO, G., RECALCATI, S., MONTOSI, G., CASTRUSINI, E., CONTE, D. & PIETRANGELO, A. (1997) Inappropriately high iron regulatory protein activity in monocytes of patients with genetic hemochromatosis. *Blood*, 89, 2546-53.

- CALZOLARI, A., DEAGLIO, S., SPOSI, N. M., PETRUCCI, E., MORSILLI, O., GABBIANELLI, M., MALAVASI, F., PESCHLE, C. & TESTA, U. (2004) Transferrin receptor 2 protein is not expressed in normal erythroid cells. *Biochem J*, 381, 629-34.
- CAMASCHELLA, C., ROETTO, A., CALI, A., DE GOBBI, M., GAROZZO, G., CARELLA, M., MAJORANO, N., TOTARO, A. & GASPARINI, P. (2000) The gene TFR2 is mutated in a new type of haemochromatosis mapping to 7q22. *Nat Genet*, 25, 14-5.
- CAMASCHELLA, C., ROETTO, A. & DE GOBBI, M. (2002) Genetic haemochromatosis: genes and mutations associated with iron loading. *Best Pract Res Clin Haematol*, 15, 261-76.
- CANONNE-HERGAUX, F., FLEMING, M. D., LEVY, J. E., GAUTHIER, S., RALPH, T., PICARD, V., ANDREWS, N. C. & GROS, P. (2000) The Nramp2/DMT1 iron transporter is induced in the duodenum of microcytic anemia mk mice but is not properly targeted to the intestinal brush border. *Blood*, 96, 3964-70.
- CANONNE-HERGAUX, F., LEVY, J. E., FLEMING, M. D., MONTROSS, L. K., ANDREWS, N. C. & GROS, P. (2001) Expression of the DMT1 (NRAMP2/DCT1) iron transporter in mice with genetic iron overload disorders. *Blood*, 97, 1138-40.
- CARELLÀ, M., D'AMBROSIO, L., TOTARO, A., GRIFA, A., VALENTINO, M. A., PIPERNO, A., GIRELLI, D., ROETTO, A., FRANCO, B., GASPARINI, P. & CAMASCHELLA, C. (1997) Mutation analysis of the HLA-H gene in Italian hemochromatosis patients. *Am J Hum Genet*, 60, 828-32.
- CARPENTER, C. E. & MAHONEY, A. W. (1992) Contributions of heme and nonheme iron to human nutrition. *Crit Rev Food Sci Nutr*, 31, 333-67.
- CASEY, J. L., HENTZE, M. W., KOELLER, D. M., CAUGHMAN, S. W., ROUAULT, T. A., KLAUSNER, R. D. & HARFORD, J. B. (1988) Iron-responsive elements: regulatory RNA sequences that control mRNA levels and translation. *Science*, 240, 924-8.
- CASEY, J. L., KOELLER, D. M., RAMIN, V. C., KLAUSNER, R. D. & HARFORD, J. B. (1989) Iron regulation of transferrin receptor mRNA levels requires iron-responsive elements and a rapid turnover determinant in the 3' untranslated region of the mRNA. *Embo J*, 8, 3693-9.

- CHANG, D. C. (1992) *Guide to electroporation and electrofusion*, Academic Press.
- CHENG, Y., ZAK, O., AISEN, P., HARRISON, S. C. & WALZ, T. (2004) Structure of the human transferrin receptor-transferrin complex. *Cell*, 116, 565-76.
- CLARKE, S. L., VASANTHAKUMAR, A., ANDERSON, S. A., PONDARRE, C., KOH, C. M., DECK, K. M., PITULA, J. S., EPSTEIN, C. J., FLEMING, M. D. & EISENSTEIN, R. S. (2006) Iron-responsive degradation of iron-regulatory protein 1 does not require the Fe-S cluster. *Embo J*, 25, 544-53.
- CONRAD, M. E., BENJAMIN, B. I., WILLIAMS, H. L. & FOY, A. L. (1967) Human absorption of hemoglobin-iron. *Gastroenterology*, 53, 5-10.
- CONRAD, M. E., UMBREIT, J. N. & MOORE, E. G. (1999) Iron absorption and transport. *Am J Med Sci*, 318, 213-29.
- CONSTABLE, A., QUICK, S., GRAY, N. K. & HENTZE, M. W. (1992) Modulation of the RNA-binding activity of a regulatory protein by iron in vitro: switching between enzymatic and genetic function? *Proc Natl Acad Sci USA*, 89, 4554-8.
- COOPERMAN, S. S., MEYRON-HOLTZ, E. G., OLIVIERRE-WILSON, H., GHOSH, M. C., MCCONNELL, J. P. & ROUAULT, T. A. (2005) Microcytic anemia, erythropoietic protoporphyrina, and neurodegeneration in mice with targeted deletion of iron-regulatory protein 2. *Blood*, 106, 1084-91.
- CORRADINI, E., FERRARA, F. & PIETRANGELO, A. (2004) Iron and the liver. *Pediatr Endocrinol Rev*, 2 Suppl 2, 245-8.
- COURSELAUD, B., PIGEON, C., INOUE, Y., INOUE, J., GONZALEZ, F. J., LEROYER, P., GILOT, D., BOUDJEMA, K., GUGUEN-GUILLOUZO, C., BRISSOT, P., LOREAL, O. & ILYIN, G. (2002) C/EBPalpha regulates hepatic transcription of hepcidin, an antimicrobial peptide and regulator of iron metabolism. Cross-talk between C/EBP pathway and iron metabolism. *J Biol Chem*, 277, 41163-70.
- COX, T. M. & KELLY, A. L. (1998) Haemochromatosis: an inherited metal and toxicity syndrome. *Curr Opin Genet Dev*, 8, 274-81.
- CRICHTON, R. R. & BOELAERT, J. R. (2001) *Inorganic biochemistry of iron metabolism: from molecular mechanisms to clinical consequences*, Chichester, Wiley.
- CRICHTON, R. R., WILMET, S., LEGSSYER, R. & WARD, R. J. (2002) Molecular and cellular mechanisms of iron homeostasis and toxicity in

- mammalian cells. *J Inorg Biochem*, 91, 9-18.
- CUNNINGHAME GRAHAM, D. S. (1998) The regulation of the Iron Regulatory Protein (IRP1) in iron loaded liver. Ph.D. thesis. University of London.
- CUTHBERT, J. A. (1997) Iron, HFE, and hemochromatosis update. *J Investig Med*, 45, 518-29.
- DE FREITAS, J. M. & MENEGHINI, R. (2001) Iron and its sensitive balance in the cell. *Mutat Res*, 475, 153-9.
- DE SOUSA, M., REIMAO, R., LACERDA, R., HUGO, P., KAUFMANN, S. H. & PORTO, G. (1994) Iron overload in beta 2-microglobulin-deficient mice. *Immunol Lett*, 39, 105-11.
- DEAGLIO, S., CAPOBIANCO, A., CALI, A., BELLORA, F., ALBERTI, F., RIGHI, L., SAPINO, A., CAMASCHELLA, C. & MALAVASI, F. (2002) Structural, functional, and tissue distribution analysis of human transferrin receptor-2 by murine monoclonal antibodies and a polyclonal antiserum. *Blood*, 100, 3782-9.
- DEICHER, R. & HORL, W. H. (2006) New insights into the regulation of iron homeostasis. *Eur J Clin Invest*, 36, 301-9.
- DONOVAN, A., BROWNIE, A., ZHOU, Y., SHEPARD, J., PRATT, S. J., MOYNIHAN, J., PAW, B. H., DREJER, A., BARUT, B., ZAPATA, A., LAW, T. C., BRUGNARA, C., LUX, S. E., PINKUS, G. S., PINKUS, J. L., KINGSLEY, P. D., PALIS, J., FLEMING, M. D., ANDREWS, N. C. & ZON, L. I. (2000) Positional cloning of zebrafish ferroportin1 identifies a conserved vertebrate iron exporter. *Nature*, 403, 776-81.
- DRAPIER, J. C., HIRLING, H., WIETZERBIN, J., KALDY, P. & KUHN, L. C. (1993) Biosynthesis of nitric oxide activates iron regulatory factor in macrophages. *Embo J*, 12, 3643-9.
- DREYFUSS, G., KIM, V. N. & KATAOKA, N. (2002) Messenger-RNA-binding proteins and the messages they carry. *Nat Rev Mol Cell Biol*, 3, 195-205.
- DUPIC, F., FRUCHON, S., BENSAID, M., BOROT, N., RADOSAVLJEVIC, M., LOREAL, O., BRISSOT, P., GILFILLAN, S., BAHRAM, S., COPPIN, H. & ROTH, M. P. (2002) Inactivation of the hemochromatosis gene differentially regulates duodenal expression of iron-related mRNAs between mouse strains. *Gastroenterology*, 122, 745-51.
- DUPUY, J., DARNAULT, C., BRAZZOLOTTO, X., KUHN, L. C., MOULIS, J.

- M., VOLBEDA, A. & FONTECILLA-CAMPS, J. C. (2005) Crystallization and preliminary X-ray diffraction data for the aconitase form of human iron-regulatory protein 1. *Acta Crystallograph Sect F Struct Biol Cryst Commun*, 61, 482-5.
- DUPUY, J., VOLBEDA, A., CARPENTIER, P., DARNAULT, C., MOULIS, J. M. & FONTECILLA-CAMPS, J. C. (2006) Crystal structure of human iron regulatory protein 1 as cytosolic aconitase. *Structure*, 14, 129-39.
- EDWARDS, C. Q., GRIFFEN, L. M., GOLDGAR, D., DRUMMOND, C., SKOLNICK, M. H. & KUSHNER, J. P. (1988) Prevalence of hemochromatosis among 11,065 presumably healthy blood donors. *N Engl J Med*, 318, 1355-62.
- EISENSTEIN, R. S. (2000) Iron regulatory proteins and the molecular control of mammalian iron metabolism. *Annu Rev Nutr*, 20, 627-62.
- EISENSTEIN, R. S. & BLEMINGS, K. P. (1998) Iron regulatory proteins, iron responsive elements and iron homeostasis. *J Nutr*, 128, 2295-8.
- EISENSTEIN, R. S., TUAZON, P. T., SCHALINSKE, K. L., ANDERSON, S. A. & TRAUGH, J. A. (1993) Iron-responsive element-binding protein. Phosphorylation by protein kinase C. *J Biol Chem*, 268, 27363-70.
- ERLITZKI, R., LONG, J. C. & THEIL, E. C. (2002) Multiple, conserved iron-responsive elements in the 3'-untranslated region of transferrin receptor mRNA enhance binding of iron regulatory protein 2. *J Biol Chem*, 277, 42579-87.
- FEDER, J. N., GNIRKE, A., THOMAS, W., TSUCHIHASHI, Z., RUDDY, D. A., BASAVA, A., DORMISHIAN, F., DOMINGO, R., JR., ELLIS, M. C., FULLAN, A., HINTON, L. M., JONES, N. L., KIMMEL, B. E., KRONMAL, G. S., LAUER, P., LEE, V. K., LOEB, D. B., MAPA, F. A., MCCLELLAND, E., MEYER, N. C., MINTIER, G. A., MOELLER, N., MOORE, T., MORIKANG, E., PRASS, C. E., QUINTANA, L., STARNES, S. M., SCHATZMAN, R. C., BRUNKE, K. J., DRAYNA, D. T., RISCH, N. J., BACON, B. R. & WOLFF, R. K. (1996) A novel MHC class I-like gene is mutated in patients with hereditary haemochromatosis. *Nat Genet*, 13, 399-408.
- FEDER, J. N., PENNY, D. M., IRRINKI, A., LEE, V. K., LEBRON, J. A., WATSON, N., TSUCHIHASHI, Z., SIGAL, E., BJORKMAN, P. J. &

- SCHATZMAN, R. C. (1998) The hemochromatosis gene product complexes with the transferrin receptor and lowers its affinity for ligand binding. *Proc Natl Acad Sci U S A*, 95, 1472-7.
- FILLEBEEN, C., CHAHINE, D., CALTAGIRONE, A., SEGAL, P. & PANTOPOULOS, K. (2003) A phosphomimetic mutation at Ser-138 renders iron regulatory protein 1 sensitive to iron-dependent degradation. *Mol Cell Biol*, 23, 6973-81.
- FLANAGAN, P. R., HAJDU, A. & ADAMS, P. C. (1995) Iron-responsive element-binding protein in hemochromatosis liver and intestine. *Hepatology*, 22, 828-32.
- FLEMING, M. D., ROMANO, M. A., SU, M. A., GARRICK, L. M., GARRICK, M. D. & ANDREWS, N. C. (1998) Nramp2 is mutated in the anemic Belgrade (b) rat: evidence of a role for Nramp2 in endosomal iron transport. *Proc Natl Acad Sci U S A*, 95, 1148-53.
- FLEMING, M. D., TRENOR, C. C., 3RD, SU, M. A., FOERNZLER, D., BEIER, D. R., DIETRICH, W. F. & ANDREWS, N. C. (1997) Microcytic anaemia mice have a mutation in Nramp2, a candidate iron transporter gene. *Nat Genet*, 16, 383-6.
- FLEMING, R. E., AHMANN, J. R., MIGAS, M. C., WAHEED, A., KOEFFLER, H. P., KAWABATA, H., BRITTON, R. S., BACON, B. R. & SLY, W. S. (2002) Targeted mutagenesis of the murine transferrin receptor-2 gene produces hemochromatosis. *Proc Natl Acad Sci U S A*, 99, 10653-8.
- FLEMING, R. E., MIGAS, M. C., HOLDEN, C. C., WAHEED, A., BRITTON, R. S., TOMATSU, S., BACON, B. R. & SLY, W. S. (2000) Transferrin receptor 2: continued expression in mouse liver in the face of iron overload and in hereditary hemochromatosis. *Proc Natl Acad Sci U S A*, 97, 2214-9.
- FLEMING, R. E., MIGAS, M. C., ZHOU, X., JIANG, J., BRITTON, R. S., BRUNT, E. M., TOMATSU, S., WAHEED, A., BACON, B. R. & SLY, W. S. (1999) Mechanism of increased iron absorption in murine model of hereditary hemochromatosis: increased duodenal expression of the iron transporter DMT1. *Proc Natl Acad Sci U S A*, 96, 3143-8.
- FOLCH CODERA, G. (2004) Putative alternative splicing forms in human iron regulatory protein 1. B.Sc. dissertation. London Metropolitan University.
- FORBES, J. R. & GROS, P. (2003) Iron, manganese, and cobalt transport by

- Nramp1 (Slc11a1) and Nramp2 (Slc11a2) expressed at the plasma membrane. *Blood*, 102, 1884-92.
- FRANCHINI, M. (2006) Hereditary iron overload: update on pathophysiology, diagnosis, and treatment. *Am J Hematol*, 81, 202-9.
- FURNHAM, N., RUFFLE, S. & SOUTHAN, C. (2004) Splice variants: a homology modeling approach. *Proteins*, 54, 596-608.
- GALY, B., FERRING, D., MINANA, B., BELL, O., JANSEN, H. G., MUCKENTHALER, M., SCHUMANN, K. & HENTZE, M. W. (2005) Altered body iron distribution and microcytosis in mice deficient in iron regulatory protein 2 (IRP2). *Blood*, 106, 2580-9.
- GATTER, K. C., BROWN, G., TROWBRIDGE, I. S., WOOLSTON, R. E. & MASON, D. Y. (1983) Transferrin receptors in human tissues: their distribution and possible clinical relevance. *J Clin Pathol*, 36, 539-45.
- GEHRKE, S. G., HERRMANN, T., KULAKSIZ, H., MERLE, U., BENTS, K., KAISER, I., RIEDEL, H. D. & STREMMEL, W. (2005) Iron stores modulate hepatic hepcidin expression by an HFE-independent pathway. *Digestion*, 72, 25-32.
- GEHRKE, S. G., KULAKSIZ, H., HERRMANN, T., RIEDEL, H. D., BENTS, K., VELTKAMP, C. & STREMMEL, W. (2003) Expression of hepcidin in hereditary hemochromatosis: evidence for a regulation in response to the serum transferrin saturation and to non-transferrin-bound iron. *Blood*, 102, 371-6.
- GEORGIEVA, T., DUNKOV, B. C., HARIZANOVA, N., RALCHEV, K. & LAW, J. H. (1999) Iron availability dramatically alters the distribution of ferritin subunit messages in *Drosophila melanogaster*. *Proc Natl Acad Sci U S A*, 96, 2716-21.
- GOESSLING, L. S., DANIELS-MCQUEEN, S., BHATTACHARYYA-PAKRASI, M., LIN, J. J. & THACH, R. E. (1992) Enhanced degradation of the ferritin repressor protein during induction of ferritin messenger RNA translation. *Science*, 256, 670-3.
- GOESSLING, L. S., MASCOTTI, D. P., BHATTACHARYYA-PAKRASI, M., GANG, H. & THACH, R. E. (1994) Irreversible steps in the ferritin synthesis induction pathway. *J Biol Chem*, 269, 4343-8.
- GOESSLING, L. S., MASCOTTI, D. P. & THACH, R. E. (1998) Involvement of

- heme in the degradation of iron-regulatory protein 2. *J Biol Chem*, 273, 12555-7.
- GOSWAMI, T. & ANDREWS, N. C. (2006) Hereditary hemochromatosis protein, HFE, interaction with transferrin receptor 2 suggests a molecular mechanism for mammalian iron sensing. *J Biol Chem*.
- GOTTSCHALK, R., SEIDL, C., SCHILLING, S., BRANER, A., SEIFRIED, E., HOELZER, D. & KALTWASSER, J. P. (2000) Iron-overload and genotypic expression of HFE mutations H63D/C282Y and transferrin receptor Hin6I and BanI polymorphism in german patients with hereditary haemochromatosis. *Eur J Immunogenet*, 27, 129-34.
- GRACIA SANCHO, J. S. (2003) Expression of iron regulatory protein 1 in liver cells. B.Sc. dissertation. London Metropolitan University.
- GRIFFITHS, W. J. & COX, T. M. (2003) Co-localization of the mammalian hemochromatosis gene product (HFE) and a newly identified transferrin receptor (TfR2) in intestinal tissue and cells. *J Histochem Cytochem*, 51, 613-24.
- GRIFFITHS, W. J., SLY, W. S. & COX, T. M. (2001) Intestinal iron uptake determined by divalent metal transporter is enhanced in HFE-deficient mice with hemochromatosis. *Gastroenterology*, 120, 1420-9.
- GROFF, J. L. & GROPPER, S. A. S. (2000) *Advanced nutrition and human metabolism*, Belmont, Calif.; London, Wadsworth/Thomson Learning.
- GROSS, C. N., IRRINKI, A., FEDER, J. N. & ENNS, C. A. (1998) Co-trafficking of HFE, a nonclassical major histocompatibility complex class I protein, with the transferrin receptor implies a role in intracellular iron regulation. *J Biol Chem*, 273, 22068-74.
- GRUENHEID, S., CANONNE-HERGAUX, F., GAUTHIER, S., HACKAM, D. J., GRINSTEIN, S. & GROS, P. (1999) The iron transport protein NRAMP2 is an integral membrane glycoprotein that colocalizes with transferrin in recycling endosomes. *J Exp Med*, 189, 831-41.
- GUNSHIN, H., MACKENZIE, B., BERGER, U. V., GUNSHIN, Y., ROMERO, M. F., BORON, W. F., NUSSBERGER, S., GOLLAN, J. L. & HEDIGER, M. A. (1997) Cloning and characterization of a mammalian proton-coupled metal-ion transporter. *Nature*, 388, 482-8.
- GUO, B., PHILLIPS, J. D., YU, Y. & LEIBOLD, E. A. (1995) Iron regulates the

- intracellular degradation of iron regulatory protein 2 by the proteasome. *J Biol Chem*, 270, 21645-51.
- GUO, B., YU, Y. & LEIBOLD, E. A. (1994) Iron regulates cytoplasmic levels of a novel iron-responsive element-binding protein without aconitase activity. *J Biol Chem*, 269, 24252-60.
- HAILE, D. J., ROUAULT, T. A., HARFORD, J. B., KENNEDY, M. C., BLONDIN, G. A., BEINERT, H. & KLAUSNER, R. D. (1992) Cellular regulation of the iron-responsive element binding protein: disassembly of the cubane iron-sulfur cluster results in high-affinity RNA binding. *Proc Natl Acad Sci U S A*, 89, 11735-9.
- HALLBERG, L. (1983) Iron requirements and bioavailability of dietary iron. *Experientia Suppl*, 44, 223-44.
- HALLBERG, L. & SOLVELL, L. (1967) Absorption of hemoglobin iron in man. *Acta Med Scand*, 181, 335-54.
- HALLIWELL, B. (1987) Oxidants and human disease: some new concepts. *Faseb J*, 1, 358-64.
- HANN, H. W., STAHLHUT, M. W. & HANN, C. L. (1990) Effect of iron and desferoxamine on cell growth and in vitro ferritin synthesis in human hepatoma cell lines. *Hepatology*, 11, 566-9.
- HANSON, E. S., RAWLINS, M. L. & LEIBOLD, E. A. (2003) Oxygen and iron regulation of iron regulatory protein 2. *J Biol Chem*, 278, 40337-42.
- HARDY, L., HANSEN, J. L., KUSHNER, J. P. & KNISELY, A. S. (1990) Neonatal hemochromatosis. Genetic analysis of transferrin-receptor, H-apoferritin, and L-apoferritin loci and of the human leukocyte antigen class I region. *Am J Pathol*, 137, 149-53.
- HARFORD, J. B. (1994) Cellular iron homeostasis: a paradigm for mechanisms of posttranscriptional control of gene expression. *Prog Liver Dis*, 12, 47-62.
- HARRIS, W. R. (2002) Iron Chemistry. In: D. M. TEMPLETON, (Ed) *Molecular and cellular iron transport*, New York, N.Y., M. Dekker. pp 1-40.
- HARRIS, Z. L., TAKAHASHI, Y., MIYAJIMA, H., SERIZAWA, M., MACGILLIVRAY, R. T. & GITLIN, J. D. (1995) Aceruloplasminemia: molecular characterization of this disorder of iron metabolism. *Proc Natl Acad Sci U S A*, 92, 2539-43.
- HARRISON, P., NEILSON, J. R., MARWAH, S. S., MADDEN, L., BAREFORD,

- D. & MILLIGAN, D. W. (1996) Role of non-transferrin bound iron in iron overload and liver dysfunction in long term survivors of acute leukaemia and bone marrow transplantation. *J Clin Pathol*, 49, 853-6.
- HARRISON, P. M. & AROSIO, P. (1996) The ferritins: molecular properties, iron storage function and cellular regulation. *Biochim Biophys Acta*, 1275, 161-203.
- HARRISON, S. A. & BACON, B. R. (2003) Hereditary hemochromatosis: update for 2003. *J Hepatol*, 38 Suppl 1, S14-23.
- HEGER, P., ROSORIUS, O., HAUBER, J. & STAUBER, R. H. (1999) Titration of cellular export factors, but not heteromultimerization, is the molecular mechanism of trans-dominant HTLV-1 rex mutants. *Oncogene*, 18, 4080-90.
- HENDERSON, B. R. & KUHN, L. C. (1995) Differential modulation of the RNA-binding proteins IRP-1 and IRP-2 in response to iron. IRP-2 inactivation requires translation of another protein. *J Biol Chem*, 270, 20509-15.
- HENDERSON, B. R., SEISER, C. & KUHN, L. C. (1993) Characterization of a second RNA-binding protein in rodents with specificity for iron-responsive elements. *J Biol Chem*, 268, 27327-34.
- HENTZE, M. W. & ARGOS, P. (1991) Homology between IRE-BP, a regulatory RNA-binding protein, aconitase, and isopropylmalate isomerase. *Nucleic Acids Res*, 19, 1739-40.
- HENTZE, M. W. & KUHN, L. C. (1996) Molecular control of vertebrate iron metabolism: mRNA-based regulatory circuits operated by iron, nitric oxide, and oxidative stress. *Proc Natl Acad Sci U S A*, 93, 8175-82.
- HENTZE, M. W., MUCKENTHALER, M. U. & ANDREWS, N. C. (2004) Balancing acts: molecular control of mammalian iron metabolism. *Cell*, 117, 285-97.
- HERRMANN, T., MUCKENTHALER, M., VAN DER HOEVEN, F., BRENNAN, K., GEHRKE, S. G., HUBERT, N., SERGI, C., GRONE, H. J., KAISER, I., GOSCH, I., VOLKMANN, M., RIEDEL, H. D., HENTZE, M. W., STEWART, A. F. & STREMMLER, W. (2004) Iron overload in adult Hfe-deficient mice independent of changes in the steady-state expression of the duodenal iron transporters DMT1 and Ireg1/ferroportin. *J Mol Med*, 82, 39-48.
- HERSHKO, C., GRAHAM, G., BATES, G. W. & RACHMILEWITZ, E. A. (1978)

- Non-specific serum iron in thalassaemia: an abnormal serum iron fraction of potential toxicity. *Br J Haematol*, 40, 255-63.
- HICKMAN, P. E., HOURIGAN, L. F., POWELL, L. W., CORDINGLEY, F., DIMESKI, G., ORMISTON, B., SHAW, J., FERGUSON, W., JOHNSON, M., ASCOUGH, J., MCDONELL, K., PINK, A. & CRAWFORD, D. H. (2000) Automated measurement of unsaturated iron binding capacity is an effective screening strategy for C282Y homozygous haemochromatosis. *Gut*, 46, 405-9.
- HOLMAN, J. R. (1997) Hereditary hemochromatosis. *J Fam Pract*, 44, 304-8.
- HOLMBERG, C. G. & LAURELL, C. B. (1947) Nature of serum copper. *Scand J Clin Lab Invest*, 3, 103-7.
- HUANG, F. W., PINKUS, J. L., PINKUS, G. S., FLEMING, M. D. & ANDREWS, N. C. (2005) A mouse model of juvenile hemochromatosis. *J Clin Invest*, 115, 2187-91.
- HUBER, C. A. & WACHTERSHAUSER, G. (1998) Peptides by activation of amino acids with CO on (Ni,Fe)S surfaces: implications for the origin of life. *Science*, 281, 670-2.
- IBORRA, F. J., JACKSON, D. A. & COOK, P. R. (2001) Coupled transcription and translation within nuclei of mammalian cells. *Science*, 293, 1139-42.
- ILYIN, G., COURSELAUD, B., TROADEC, M. B., PIGEON, C., ALIZADEH, M., LEROYER, P., BRISSET, P. & LOREAL, O. (2003) Comparative analysis of mouse hepcidin 1 and 2 genes: evidence for different patterns of expression and co-inducibility during iron overload. *FEBS Lett*, 542, 22-6.
- IWAI, K., DRAKE, S. K., WEHR, N. B., WEISSMAN, A. M., LAVAUTE, T., MINATO, N., KLAUSNER, R. D., LEVINE, R. L. & ROUAULT, T. A. (1998) Iron-dependent oxidation, ubiquitination, and degradation of iron regulatory protein 2: implications for degradation of oxidized proteins. *Proc Natl Acad Sci U S A*, 95, 4924-8.
- IWAI, K., KLAUSNER, R. D. & ROUAULT, T. A. (1995) Requirements for iron-regulated degradation of the RNA binding protein, iron regulatory protein 2. *Embo J*, 14, 5350-7.
- JANOSI, A., ANDRIKOVICS, H., VAS, K., BORS, A., HUBAY, M., SAPI, Z. & TORDAI, A. (2005) Homozygosity for a novel nonsense mutation (G66X) of the HJV gene causes severe juvenile hemochromatosis with fatal

- cardiomyopathy. *Blood*, 105, 432.
- JAZWINSKA, E. C., CULLEN, L. M., BUSFIELD, F., PYPER, W. R., WEBB, S. I., POWELL, L. W., MORRIS, C. P. & WALSH, T. P. (1996) Haemochromatosis and HLA-H. *Nat Genet*, 14, 249-51.
- JOHNSON, M. B. & ENNS, C. A. (2004) Diferric transferrin regulates transferrin receptor 2 protein stability. *Blood*, 104, 4287-93.
- KAPLAN, J., JORDAN, I. & STURROCK, A. (1991) Regulation of the transferrin-independent iron transport system in cultured cells. *J Biol Chem*, 266, 2997-3004.
- KARLSSON, C. & PINES, J. (1998) Green fluorescent protein. In: J. E. Celis, (Ed). *Cell biology: a laboratory handbook*, San Diego; London, Academic Press. pp 246-252.
- KATO, J., FUJIKAWA, K., KANDA, M., FUKUDA, N., SASAKI, K., TAKAYAMA, T., KOBUNE, M., TAKADA, K., TAKIMOTO, R., HAMADA, H., IKEDA, T. & NIITSU, Y. (2001) A mutation, in the iron-responsive element of H ferritin mRNA, causing autosomal dominant iron overload. *Am J Hum Genet*, 69, 191-7.
- KAWABATA, H., FLEMING, R. E., GUI, D., MOON, S. Y., SAITO, T., O'KELLY, J., UMEHARA, Y., WANO, Y., SAID, J. W. & KOEFFLER, H. P. (2005) Expression of hepcidin is down-regulated in TfR2 mutant mice manifesting a phenotype of hereditary hemochromatosis. *Blood*, 105, 376-81.
- KAWABATA, H., GERMAIN, R. S., IKEZOE, T., TONG, X., GREEN, E. M., GOMBART, A. F. & KOEFFLER, H. P. (2001) Regulation of expression of murine transferrin receptor 2. *Blood*, 98, 1949-54.
- KAWABATA, H., GERMAIN, R. S., VUONG, P. T., NAKAMAKI, T., SAID, J. W. & KOEFFLER, H. P. (2000) Transferrin receptor 2-alpha supports cell growth both in iron-chelated cultured cells and in vivo. *J Biol Chem*, 275, 16618-25.
- KAWABATA, H., YANG, R., HIRAMA, T., VUONG, P. T., KAWANO, S., GOMBART, A. F. & KOEFFLER, H. P. (1999) Molecular cloning of transferrin receptor 2. A new member of the transferrin receptor-like family. *J Biol Chem*, 274, 20826-32.
- KELLY, A. L., LUNT, P. W., RODRIGUES, F., BERRY, P. J., FLYNN, D. M., MCKIERNAN, P. J., KELLY, D. A., MIELI-VERGANI, G. & COX, T. M.

- (2001) Classification and genetic features of neonatal haemochromatosis: a study of 27 affected pedigrees and molecular analysis of genes implicated in iron metabolism. *J Med Genet*, 38, 599-610.
- KELLY, A. L., RHODES, D. A., ROLAND, J. M., SCHOFIELD, P. & COX, T. M.
- (1998) Hereditary juvenile haemochromatosis: a genetically heterogeneous life-threatening iron-storage disease. *Qjm*, 91, 607-18.
- KELLY, J. H. & DARLINGTON, G. J. (1989) Modulation of the liver specific phenotype in the human hepatoblastoma line Hep G2. *In Vitro Cell Dev Biol*, 25, 217-22.
- KIYOKAWA, T., SEIKI, M., IWASHITA, S., IMAGAWA, K., SHIMIZU, F. & YOSHIDA, M. (1985) p27x-III and p21x-III, proteins encoded by the pX sequence of human T-cell leukemia virus type I. *Proc Natl Acad Sci U S A*, 82, 8359-63.
- KLAUSNER, R. D., ROUAULT, T. A. & HARFORD, J. B. (1993) Regulating the fate of mRNA: the control of cellular iron metabolism. *Cell*, 72, 19-28.
- KNOWLES, B. B., HOWE, C. C. & ADEN, D. P. (1980) Human hepatocellular carcinoma cell lines secrete the major plasma proteins and hepatitis B surface antigen. *Science*, 209, 497-9.
- KNUTSON, M. D., OUKKA, M., KOSS, L. M., AYDEMIR, F. & WESSLING-RESNICK, M. (2005) Iron release from macrophages after erythrophagocytosis is up-regulated by ferroportin 1 overexpression and down-regulated by hepcidin. *Proc Natl Acad Sci U S A*, 102, 1324-8.
- KOHLER, S. A., HENDERSON, B. R. & KUHN, L. C. (1995) Succinate dehydrogenase b mRNA of *Drosophila melanogaster* has a functional iron-responsive element in its 5'-untranslated region. *J Biol Chem*, 270, 30781-6.
- KRAUSE, A., NEITZ, S., MAGERT, H. J., SCHULZ, A., FORSSMANN, W. G., SCHULZ-KNAPPE, P. & ADERMANN, K. (2000) LEAP-1, a novel highly disulfide-bonded human peptide, exhibits antimicrobial activity. *FEBS Lett*, 480, 147-50.
- KRISHNAMURTHY, P., ROSS, D. D., NAKANISHI, T., BAILEY-DELL, K., ZHOU, S., MERCER, K. E., SARKADI, B., SORRENTINO, B. P. & SCHUETZ, J. D. (2004) The stem cell marker Bcrp/ABCG2 enhances hypoxic cell survival through interactions with heme. *J Biol Chem*, 279, 24218-25.

- KUDO, N., WOLFF, B., SEKIMOTO, T., SCHREINER, E. P., YONEDA, Y., YANAGIDA, M., HORINOUCHI, S. & YOSHIDA, M. (1998) Leptomycin B inhibition of signal-mediated nuclear export by direct binding to CRM1. *Exp Cell Res*, 242, 540-7.
- KUHN, L. C., MCCLELLAND, A. & RUDDLE, F. H. (1984) Gene transfer, expression, and molecular cloning of the human transferrin receptor gene. *Cell*, 37, 95-103.
- KUMAR, S., O'DOWD, C., DUNCKLEY, M. G. & LUND, T. (1994) A comparative evaluation of three transfection procedures as assessed by resistance to G418 conferred to HEPG2 cells. *Biochem Mol Biol Int*, 32, 1059-66.
- KUO, Y. M., SU, T., CHEN, H., ATTIEH, Z., SYED, B. A., MCKIE, A. T., ANDERSON, G. J., GITSCHIER, J. & VULPE, C. D. (2004) Mislocalisation of hephaestin, a multicopper ferroxidase involved in basolateral intestinal iron transport, in the sex linked anaemia mouse. *Gut*, 53, 201-6.
- LAEMMLI, U. K. (1970) Cleavage of structural proteins during the assembly of the head of bacteriophage T4. *Nature*, 227, 680-5.
- LAFTAH, A. H., RAMESH, B., SIMPSON, R. J., SOLANKY, N., BAHRAM, S., SCHUMANN, K., DEBNAM, E. S. & SRAI, S. K. (2004) Effect of hepcidin on intestinal iron absorption in mice. *Blood*, 103, 3940-4.
- LANZARA, C., ROETTO, A., DARAIO, F., RIVARD, S., FICARELLA, R., SIMARD, H., COX, T. M., CAZZOLA, M., PIPERNO, A., GIMENEZ-ROQUEPLO, A. P., GRAMMATICO, P., VOLINIA, S., GASPARINI, P. & CAMASCHELLA, C. (2004) Spectrum of hemojuvelin gene mutations in 1q-linked juvenile hemochromatosis. *Blood*, 103, 4317-21.
- LAO, B. J. & KAMEI, D. T. (2006) A compartmental model of iron regulation in the mouse. *J Theor Biol.*
- LATUNDE-DADA, G. O., SIMPSON, R. J. & MCKIE, A. T. (2006) Recent advances in mammalian haem transport. *Trends Biochem Sci*, 31, 182-8.
- LAVAUTE, T., SMITH, S., COOPERMAN, S., IWAI, K., LAND, W., MEYRON-HOLTZ, E., DRAKE, S. K., MILLER, G., ABU-ASAB, M., TSOKOS, M., SWITZER, R., 3RD, GRINBERG, A., LOVE, P., TRESSER, N. & ROUAULT, T. A. (2001) Targeted deletion of the gene encoding iron regulatory protein-2 causes misregulation of iron metabolism and

- neurodegenerative disease in mice. *Nat Genet*, 27, 209-14.
- LE, N. T. & RICHARDSON, D. R. (2003) Potent iron chelators increase the mRNA levels of the universal cyclin-dependent kinase inhibitor p21(CIP1/WAF1), but paradoxically inhibit its translation: a potential mechanism of cell cycle dysregulation. *Carcinogenesis*, 24, 1045-58.
- LEBRON, J. A., BENNETT, M. J., VAUGHN, D. E., CHIRINO, A. J., SNOW, P. M., MINTIER, G. A., FEDER, J. N. & BJORKMAN, P. J. (1998) Crystal structure of the hemochromatosis protein HFE and characterization of its interaction with transferrin receptor. *Cell*, 93, 111-23.
- LEBRON, J. A., WEST, A. P., JR. & BJORKMAN, P. J. (1999) The hemochromatosis protein HFE competes with transferrin for binding to the transferrin receptor. *J Mol Biol*, 294, 239-45.
- LEE, P. L., BEUTLER, E., RAO, S. V. & BARTON, J. C. (2004) Genetic abnormalities and juvenile hemochromatosis: mutations of the HJV gene encoding hemojuvelin. *Blood*, 103, 4669-71.
- LEE, P. L., GELBART, T., WEST, C., HALLORAN, C. & BEUTLER, E. (1998) The human Nramp2 gene: characterization of the gene structure, alternative splicing, promoter region and polymorphisms. *Blood Cells Mol Dis*, 24, 199-215.
- LEVY, J. E., JIN, O., FUJIWARA, Y., KUO, F. & ANDREWS, N. C. (1999) Transferrin receptor is necessary for development of erythrocytes and the nervous system. *Nat Genet*, 21, 396-9.
- LIEU, P. T., HEISKALA, M., PETERSON, P. A. & YANG, Y. (2001) The roles of iron in health and disease. *Mol Aspects Med*, 22, 1-87.
- LIGHT, W. R., 3RD & OLSON, J. S. (1990) Transmembrane movement of heme. *J Biol Chem*, 265, 15623-31.
- LIN, L., GOLDBERG, Y. P. & GANZ, T. (2005) Competitive regulation of hepcidin mRNA by soluble and cell-associated hemojuvelin. *Blood*, 106, 2884-9.
- LIND, M. I., EKENGREN, S., MELEFORS, O. & SODERHALL, K. (1998) Drosophila ferritin mRNA: alternative RNA splicing regulates the presence of the iron-responsive element. *FEBS Lett*, 436, 476-82.
- LOBMAYR, L., BROOKS, D. G. & WILSON, R. B. (2005) Increased IRP1 activity in Friedreich ataxia. *Gene*, 354, 157-61.
- LOMBARD, M., BOMFORD, A., HYNES, M., NAOUMOV, N. V., ROBERTS, S.,

- CROWE, J. & WILLIAMS, R. (1989) Regulation of the hepatic transferrin receptor in hereditary hemochromatosis. *Hepatology*, 9, 1-5.
- LOMBARD, M., BOMFORD, A. B., POLSON, R. J., BELLINGHAM, A. J. & WILLIAMS, R. (1990) Differential expression of transferrin receptor in duodenal mucosa in iron overload. Evidence for a site-specific defect in genetic hemochromatosis. *Gastroenterology*, 98, 976-84.
- LOMBARD, M., CHUA, E. & O'TOOLE, P. (1997) Regulation of intestinal non-haem iron absorption. *Gut*, 40, 435-9.
- LOPATA, M. A., CLEVELAND, D. W. & SOLLNER-WEBB, B. (1984) High level transient expression of a chloramphenicol acetyl transferase gene by DEAE-dextran mediated DNA transfection coupled with a dimethyl sulfoxide or glycerol shock treatment. *Nucleic Acids Res*, 12, 5707-17.
- LOU, D. Q., LESBORDES, J. C., NICOLAS, G., VIATTE, L., BENNOUN, M., VAN ROOIJEN, N., KAHN, A., RENIA, L. & VAULONT, S. (2005) Iron- and inflammation-induced hepcidin gene expression in mice is not mediated by Kupffer cells in vivo. *Hepatology*, 41, 1056-64.
- LOWRY, O. H., ROSEBROUGH, N. J., FARR, A. L. & RANDALL, R. J. (1951) Protein measurement with the Folin phenol reagent. *J Biol Chem*, 193, 265-75.
- LUDWICZEK, S., THEURL, I., BAHRAM, S., SCHUMANN, K. & WEISS, G. (2005) Regulatory networks for the control of body iron homeostasis and their dysregulation in HFE mediated hemochromatosis. *J Cell Physiol*, 204, 489-99.
- LYON, E. & FRANK, E. L. (2001) Hereditary hemochromatosis since discovery of the HFE gene. *Clin Chem*, 47, 1147-56.
- MACK, U., POWELL, L. W. & HALLIDAY, J. W. (1983) Detection and isolation of a hepatic membrane receptor for ferritin. *J Biol Chem*, 258, 4672-5.
- MARKWELL, M. A., HAAS, S. M., BIEBER, L. L. & TOLBERT, N. E. (1978) A modification of the Lowry procedure to simplify protein determination in membrane and lipoprotein samples. *Anal Biochem*, 87, 206-10.
- MARTIN, W. & RUSSELL, M. J. (2003) On the origins of cells: a hypothesis for the evolutionary transitions from abiotic geochemistry to chemoautotrophic prokaryotes, and from prokaryotes to nucleated cells. *Philos Trans R Soc Lond B Biol Sci*, 358, 59-83; discussion 83-5.

- MCCANCE, R. A. & WIDDOWSON, E. M. (1937) Absorption and excretion of iron. *The Lancet*, II, 680-684.
- MCCORD, J. M. (1998) Iron, free radicals, and oxidative injury. *Semin Hematol*, 35, 5-12.
- MCKIE, A. T. (2005) A ferrireductase fills the gap in the transferrin cycle. *Nat Genet*, 37, 1159-60.
- MCKIE, A. T., BARROW, D., LATUNDE-DADA, G. O., ROLFS, A., SAGER, G., MUDALY, E., MUDALY, M., RICHARDSON, C., BARLOW, D., BOMFORD, A., PETERS, T. J., RAJA, K. B., SHIRALI, S., HEDIGER, M. A., FARZANEH, F. & SIMPSON, R. J. (2001) An iron-regulated ferric reductase associated with the absorption of dietary iron. *Science*, 291, 1755-9.
- MCKIE, A. T., MARCIANI, P., ROLFS, A., BRENNAN, K., WEHR, K., BARROW, D., MIRET, S., BOMFORD, A., PETERS, T. J., FARZANEH, F., HEDIGER, M. A., HENTZE, M. W. & SIMPSON, R. J. (2000) A novel duodenal iron-regulated transporter, IREG1, implicated in the basolateral transfer of iron to the circulation. *Mol Cell*, 5, 299-309.
- MCLAREN, G. D., NATHANSON, M. H., JACOBS, A., TREVETT, D. & THOMSON, W. (1991) Regulation of intestinal iron absorption and mucosal iron kinetics in hereditary hemochromatosis. *J Lab Clin Med*, 117, 390-401.
- MELEFORS, O. & HENTZE, M. W. (1993) Iron regulatory factor--the conductor of cellular iron regulation. *Blood Rev*, 7, 251-8.
- MERRYWEATHER-CLARKE, A. T., CADET, E., BOMFORD, A., CAPRON, D., VIPRAKASIT, V., MILLER, A., MCHUGH, P. J., CHAPMAN, R. W., POINTON, J. J., WIMHURST, V. L., LIVESEY, K. J., TANPHAICHITR, V., ROCHELLE, J. & ROBSON, K. J. (2003) Digenic inheritance of mutations in HAMP and HFE results in different types of haemochromatosis. *Hum Mol Genet*, 12, 2241-7.
- MERRYWEATHER-CLARKE, A. T., POINTON, J. J., JOUANOLLE, A. M., ROCHELLE, J. & ROBSON, K. J. (2000) Geography of HFE C282Y and H63D mutations. *Genet Test*, 4, 183-98.
- MERRYWEATHER-CLARKE, A. T., POINTON, J. J., SHEARMAN, J. D. & ROBSON, K. J. (1997) Global prevalence of putative haemochromatosis mutations. *J Med Genet*, 34, 275-8.
- MEYRON-HOLTZ, E. G., GHOSH, M. C., IWAI, K., LAVAUTE, T.,

- BRAZZOLOTTO, X., BERGER, U. V., LAND, W., OLLIVIERE-WILSON, H., GRINBERG, A., LOVE, P. & ROUAULT, T. A. (2004a) Genetic ablations of iron regulatory proteins 1 and 2 reveal why iron regulatory protein 2 dominates iron homeostasis. *Embo J*, 23, 386-95.
- MEYRON-HOLTZ, E. G., GHOSH, M. C. & ROUAULT, T. A. (2004b) Mammalian tissue oxygen levels modulate iron-regulatory protein activities in vivo. *Science*, 306, 2087-90.
- MIMS, M. P., GUAN, Y., POSPISILOVA, D., PRIWITZEROVA, M., INDRAK, K., PONKA, P., DIVOKY, V. & PRCHAL, J. T. (2005) Identification of a human mutation of DMT1 in a patient with microcytic anemia and iron overload. *Blood*, 105, 1337-42.
- MIRET, S., MCKIE, A. T., SAIZ, M. P., BOMFORD, A. & MITJAVILA, M. T. (2003) IRP1 activity and expression are increased in the liver and the spleen of rats fed fish oil-rich diets and are related to oxidative stress. *J Nutr*, 133, 999-1003.
- MOH, M. C., LEE, L. H., YANG, X. & SHEN, S. (2003) HEPN1, a novel gene that is frequently down-regulated in hepatocellular carcinoma, suppresses cell growth and induces apoptosis in HepG2 cells. *J Hepatol*, 39, 580-6.
- MOHAMED, A. J., VARGAS, L., NORE, B. F., BACKESJO, C. M., CHRISTENSSON, B. & SMITH, C. I. (2000) Nucleocytoplasmic shuttling of Bruton's tyrosine kinase. *J Biol Chem*, 275, 40614-9.
- MOIRAND, R., ADAMS, P. C., BICHELER, V., BRISSOT, P. & DEUGNIER, Y. (1997) Clinical features of genetic hemochromatosis in women compared with men. *Ann Intern Med*, 127, 105-10.
- MONTOSI, G., CORRADINI, E., GARUTI, C., BARELLI, S., RECALCATI, S., CAIRO, G., VALLI, L., PIGNATTI, E., VECCHI, C., FERRARA, F. & PIETRANGELO, A. (2005) Kupffer cells and macrophages are not required for hepatic hepcidin activation during iron overload. *Hepatology*, 41, 545-52.
- MONTOSI, G., DONOVAN, A., TOTARO, A., GARUTI, C., PIGNATTI, E., CASSANELLI, S., TRENOR, C. C., GASPARINI, P., ANDREWS, N. C. & PIETRANGELO, A. (2001) Autosomal-dominant hemochromatosis is associated with a mutation in the ferroportin (SLC11A3) gene. *J Clin Invest*, 108, 619-23.
- MORGAN, E. H. & BAKER, E. (1986) Iron uptake and metabolism by hepatocytes.

Fed Proc, 45, 2810-6.

- MORRISON, T. B., WEIS, J. J. & WITWER, C. T. (1998) Quantification of low-copy transcripts by continuous SYBR Green I monitoring during amplification. *Biotechniques*, 24, 954-8, 960, 962.
- MUCKENTHALER, M., GRAY, N. K. & HENTZE, M. W. (1998) IRP-1 binding to ferritin mRNA prevents the recruitment of the small ribosomal subunit by the cap-binding complex eIF4F. *Mol Cell*, 2, 383-8.
- MUCKENTHALER, M., ROY, C. N., CUSTODIO, A. O., MINANA, B., DEGRAAF, J., MONTROSS, L. K., ANDREWS, N. C. & HENTZE, M. W. (2003) Regulatory defects in liver and intestine implicate abnormal hepcidin and Cybrd1 expression in mouse hemochromatosis. *Nat Genet*, 34, 102-7.
- MUCKENTHALER, M. U., RODRIGUES, P., MACEDO, M. G., MINANA, B., BRENNAN, K., CARDOSO, E. M., HENTZE, M. W. & DE SOUSA, M. (2004) Molecular analysis of iron overload in beta2-microglobulin-deficient mice. *Blood Cells Mol Dis*, 33, 125-31.
- MUIR, A. & HOPFER, U. (1985) Regional specificity of iron uptake by small intestinal brush-border membranes from normal and iron-deficient mice. *Am J Physiol*, 248, G376-9.
- MULLER-BERGHAUS, J., KNISELY, A. S., ZAUM, R., VIERZIG, A., KIRN, E., MICHALK, D. V. & ROTH, B. (1997) Neonatal haemochromatosis: report of a patient with favourable outcome. *Eur J Pediatr*, 156, 296-8.
- MULLER-EBERHARD, U., LIEM, H. H., COX, K. H. & CONWAY, T. P. (1975) Hemopexin synthesis in vitro by human fetal tissues. *Pediatr Res*, 9, 519-21.
- NEMETH, E., ROETTO, A., GAROZZO, G., GANZ, T. & CAMASCHELLA, C. (2005) Hepcidin is decreased in TFR2 hemochromatosis. *Blood*, 105, 1803-6.
- NEMETH, E., TUTTLE, M. S., POWELSON, J., VAUGHN, M. B., DONOVAN, A., WARD, D. M., GANZ, T. & KAPLAN, J. (2004) Hepcidin regulates cellular iron efflux by binding to ferroportin and inducing its internalization. *Science*, 306, 2090-3.
- NEMETH, E., VALORE, E. V., TERRITO, M., SCHILLER, G., LICHTENSTEIN, A. & GANZ, T. (2003) Hepcidin, a putative mediator of anemia of inflammation, is a type II acute-phase protein. *Blood*, 101, 2461-3.
- NEONAKI, M., GRAHAM, D. C., WHITE, K. N. & BOMFORD, A. (2002) Down-regulation of liver iron-regulatory protein 1 in haemochromatosis. *Biochem*

Soc Trans, 30, 726-8.

- NICOLAS, G., BENNOUN, M., DEVAUX, I., BEAUMONT, C., GRANDCHAMP, B., KAHN, A. & VAULONT, S. (2001) Lack of hepcidin gene expression and severe tissue iron overload in upstream stimulatory factor 2 (USF2) knockout mice. *Proc Natl Acad Sci U S A*, 98, 8780-5.
- NICOLAS, G., BENNOUN, M., PORTEU, A., MATIVET, S., BEAUMONT, C., GRANDCHAMP, B., SIRITO, M., SAWADOGO, M., KAHN, A. & VAULONT, S. (2002a) Severe iron deficiency anemia in transgenic mice expressing liver hepcidin. *Proc Natl Acad Sci U S A*, 99, 4596-601.
- NICOLAS, G., CHAUVENT, C., VIATTE, L., DANAN, J. L., BIGARD, X., DEVAUX, I., BEAUMONT, C., KAHN, A. & VAULONT, S. (2002b) The gene encoding the iron regulatory peptide hepcidin is regulated by anemia, hypoxia, and inflammation. *J Clin Invest*, 110, 1037-44.
- NICOLAS, G., VIATTE, L., LOU, D. Q., BENNOUN, M., BEAUMONT, C., KAHN, A., ANDREWS, N. C. & VAULONT, S. (2003) Constitutive hepcidin expression prevents iron overload in a mouse model of hemochromatosis. *Nat Genet*, 34, 97-101.
- NIEDERAU, C., FISCHER, R., PURSCHEL, A., STREMMLER, W., HAUSSINGER, D. & STROHMEYER, G. (1996) Long-term survival in patients with hereditary hemochromatosis. *Gastroenterology*, 110, 1107-19.
- NJAJOU, O. T., VAESSEN, N., JOOSSE, M., BERGHUIS, B., VAN DONGEN, J. W., BREUNING, M. H., SNIJDERS, P. J., RUTTEN, W. P., SANDKUIJL, L. A., OOSTRA, B. A., VAN DUIJN, C. M. & HEUTINK, P. (2001) A mutation in SLC11A3 is associated with autosomal dominant hemochromatosis. *Nat Genet*, 28, 213-4.
- NOYER, C. M., IMMENSCHUH, S., LIEM, H. H., MULLER-EBERHARD, U. & WOLKOFF, A. W. (1998) Initial heme uptake from albumin by short-term cultured rat hepatocytes is mediated by a transport mechanism differing from that of other organic anions. *Hepatology*, 28, 150-5.
- O'CONNELL, M., HALLIWELL, B., MOORHOUSE, C. P., ARUOMA, O. I., BAUM, H. & PETERS, T. J. (1986) Formation of hydroxyl radicals in the presence of ferritin and haemosiderin. Is haemosiderin formation a biological protective mechanism? *Biochem J*, 234, 727-31.
- O'DELL, B. L. & SUNDE, R. A. (1997) *Handbook of nutritionally essential mineral*

elements, New York, Dekker.

- OHGAMI, R. S., CAMPAGNA, D. R., GREER, E. L., ANTIOCHOS, B., MCDONALD, A., CHEN, J., SHARP, J. J., FUJIWARA, Y., BARKER, J. E. & FLEMING, M. D. (2005) Identification of a ferrireductase required for efficient transferrin-dependent iron uptake in erythroid cells. *Nat Genet*, 37, 1264-9.
- OLIVEIRA, L. & DRAPIER, J. C. (2000) Down-regulation of iron regulatory protein 1 gene expression by nitric oxide. *Proc Natl Acad Sci U S A*, 97, 6550-5.
- OLYNYK, J. K., CULLEN, D. J., AQUILIA, S., ROSSI, E., SUMMERSVILLE, L. & POWELL, L. W. (1999) A population-based study of the clinical expression of the hemochromatosis gene. *N Engl J Med*, 341, 718-24.
- PANTOPOULOS, K. & HENTZE, M. W. (1995) Rapid responses to oxidative stress mediated by iron regulatory protein. *Embo J*, 14, 2917-24.
- PAPANIKOLAOU, G. & PANTOPOULOS, K. (2005) Iron metabolism and toxicity. *Toxicol Appl Pharmacol*, 202, 199-211.
- PAPANIKOLAOU, G., SAMUELS, M. E., LUDWIG, E. H., MACDONALD, M. L., FRANCHINI, P. L., DUBE, M. P., ANDRES, L., MACFARLANE, J., SAKELLAROPOULOS, N., POLITOU, M., NEMETH, E., THOMPSON, J., RISLER, J. K., ZABOROWSKA, C., BABAKAIFF, R., RADOMSKI, C. C., PAPE, T. D., DAVIDAS, O., CHRISTAKIS, J., BRISSOT, P., LOCKITCH, G., GANZ, T., HAYDEN, M. R. & GOLDBERG, Y. P. (2004) Mutations in HFE2 cause iron overload in chromosome 1q-linked juvenile hemochromatosis. *Nat Genet*, 36, 77-82.
- PAPANIKOLAOU, G., TZILIANOS, M., CHRISTAKIS, J. I., BOGDANOS, D., TSIMIRIKA, K., MACFARLANE, J., GOLDBERG, Y. P., SAKELLAROPOULOS, N., GANZ, T. & NEMETH, E. (2005) Hepcidin in iron overload disorders. *Blood*, 105, 4103-5.
- PARK, C. H., VALORE, E. V., WARING, A. J. & GANZ, T. (2001) Hepcidin, a urinary antimicrobial peptide synthesized in the liver. *J Biol Chem*, 276, 7806-10.
- PARKES, J. G. & TEMPLETON, D. M. (1994) Iron transport and subcellular distribution in Hep G2 hepatocarcinoma cells. *Ann Clin Lab Sci*, 24, 509-20.
- PARKKILA, S., PARKKILA, A. K., WAHEED, A., BRITTON, R. S., ZHOU, X.

- Y., FLEMING, R. E., TOMATSU, S., BACON, B. R. & SLY, W. S. (2000) Cell surface expression of HFE protein in epithelial cells, macrophages, and monocytes. *Haematologica*, 85, 340-5.
- PARKKILA, S., WAHEED, A., BRITTON, R. S., BACON, B. R., ZHOU, X. Y., TOMATSU, S., FLEMING, R. E. & SLY, W. S. (1997) Association of the transferrin receptor in human placenta with HFE, the protein defective in hereditary hemochromatosis. *Proc Natl Acad Sci U S A*, 94, 13198-202.
- PATINO, M. M. & WALDEN, W. E. (1992) Cloning of a functional cDNA for the rabbit ferritin mRNA repressor protein. Demonstration of a tissue-specific pattern of expression. *J Biol Chem*, 267, 19011-6.
- PATTON, S. M., PINERO, D. J., SURGULADZE, N., BEARD, J. & CONNOR, J. R. (2005) Subcellular localization of iron regulatory proteins to Golgi and ER membranes. *J Cell Sci*, 118, 4365-73.
- PEDERSON, T. & AEBI, U. (2002) Actin in the nucleus: what form and what for? *J Struct Biol*, 140, 3-9.
- PIETRANGELO, A. (2004) Hereditary hemochromatosis--a new look at an old disease. *N Engl J Med*, 350, 2383-97.
- PIETRANGELO, A. (2006) Hereditary hemochromatosis. *Biochim Biophys Acta*, 1763, 700-10.
- PIETRANGELO, A., CALEFFI, A., HENRION, J., FERRARA, F., CORRADINI, E., KULAKSIZ, H., STREMMLER, W., ANDREONE, P. & GARUTI, C. (2005) Juvenile hemochromatosis associated with pathogenic mutations of adult hemochromatosis genes. *Gastroenterology*, 128, 470-9.
- PIETRANGELO, A., CASALGRANDI, G., QUAGLINO, D., GUALDI, R., CONTE, D., MILANI, S., MONTOSI, G., CESARINI, L., VENTURA, E. & CAIRO, G. (1995) Duodenal ferritin synthesis in genetic hemochromatosis. *Gastroenterology*, 108, 208-17.
- PIGEON, C., ILYIN, G., COURSELAUD, B., LEROYER, P., TURLIN, B., BRISSOT, P. & LOREAL, O. (2001) A new mouse liver-specific gene, encoding a protein homologous to human antimicrobial peptide hepcidin, is overexpressed during iron overload. *J Biol Chem*, 276, 7811-9.
- POINTON, J. J., WALLACE, D., MERRYWEATHER-CLARKE, A. T. & ROBSON, K. J. (2000) Uncommon mutations and polymorphisms in the hemochromatosis gene. *Genet Test*, 4, 151-61.

- PONKA, P. (1999) Cellular iron metabolism. *Kidney Int Suppl*, 69, S2-11.
- POPOVIC, Z. & TEMPLETON, D. M. (2005) A Northwestern blotting approach for studying iron regulatory element-binding proteins. *Mol Cell Biochem*, 268, 67-74.
- POUNTNEY, D., TRUGNAN, G., BOURGEOIS, M. & BEAUMONT, C. (1999) The identification of ferritin in the nucleus of K562 cells, and investigation of a possible role in the transcriptional regulation of adult beta-globin gene expression. *J Cell Sci*, 112 (Pt 6), 825-31.
- POWELL, L. W. (2002) Hereditary hemochromatosis and iron overload diseases. *J Gastroenterol Hepatol*, 17 Suppl, S191-5.
- POWELL, L. W., CAMPBELL, C. B. & WILSON, E. (1970) Intestinal mucosal uptake of iron and iron retention in idiopathic haemochromatosis as evidence for a mucosal abnormality. *Gut*, 11, 727-31.
- POWELL, L. W., GEORGE, D. K., MCDONNELL, S. M. & KOWDLEY, K. V. (1998) Diagnosis of hemochromatosis. *Ann Intern Med*, 129, 925-31.
- QUIGLEY, J. G., YANG, Z., WORTHINGTON, M. T., PHILLIPS, J. D., SABO, K. M., SABATH, D. E., BERG, C. L., SASSA, S., WOOD, B. L. & ABKOWITZ, J. L. (2004) Identification of a human heme exporter that is essential for erythropoiesis. *Cell*, 118, 757-66.
- RAFFIN, S. B., WOO, C. H., ROOST, K. T., PRICE, D. C. & SCHMID, R. (1974) Intestinal absorption of hemoglobin iron-heme cleavage by mucosal heme oxygenase. *J Clin Invest*, 54, 1344-52.
- RANDELL, E. W., PARKES, J. G., OLIVIERI, N. F. & TEMPLETON, D. M. (1994) Uptake of non-transferrin-bound iron by both reductive and nonreductive processes is modulated by intracellular iron. *J Biol Chem*, 269, 16046-53.
- RECALCATI, S., ALBERGHINI, A., CAMPANELLA, A., GIANELLI, U., DE CAMILLI, E., CONTE, D. & CAIRO, G. (2006) Iron regulatory proteins 1 and 2 in human monocytes, macrophages and duodenum: expression and regulation in hereditary hemochromatosis and iron deficiency. *Haematologica*, 91, 303-10.
- RHODES, D. A. & TROWSDALE, J. (1999) Alternate splice variants of the hemochromatosis gene Hfe. *Immunogenetics*, 49, 357-9.
- RIEDEL, H. D., MUCKENTHALER, M. U., GEHRKE, S. G., MOHR, I.,

- BRENNAN, K., HERRMANN, T., FITSCHER, B. A., HENTZE, M. W. & STREMMEL, W. (1999) HFE downregulates iron uptake from transferrin and induces iron-regulatory protein activity in stably transfected cells. *Blood*, 94, 3915-21.
- RIVERA, S., LIU, L., NEMETH, E., GABAYAN, V., SORENSEN, O. E. & GANZ, T. (2005) Hepcidin excess induces the sequestration of iron and exacerbates tumor-associated anemia. *Blood*, 105, 1797-802.
- ROBB, A. & WESSLING-RESNICK, M. (2004) Regulation of transferrin receptor 2 protein levels by transferrin. *Blood*, 104, 4294-9.
- ROBB, A. D., ERICSSON, M. & WESSLING-RESNICK, M. (2004) Transferrin receptor 2 mediates a biphasic pattern of transferrin uptake associated with ligand delivery to multivesicular bodies. *Am J Physiol Cell Physiol*, 287, C1769-75.
- ROETTO, A. & CAMASCHELLA, C. (2005) New insights into iron homeostasis through the study of non-HFE hereditary haemochromatosis. *Best Pract Res Clin Haematol*, 18, 235-50.
- ROETTO, A., DARAIO, F., PORPORATO, P., CARUSO, R., COX, T. M., CAZZOLA, M., GASPARINI, P., PIPERNO, A. & CAMASCHELLA, C. (2004) Screening hepcidin for mutations in juvenile hemochromatosis: identification of a new mutation (C70R). *Blood*, 103, 2407-9.
- ROETTO, A., MERRYWEATHER-CLARKE, A. T., DARAIO, F., LIVESEY, K., POINTON, J. J., BARBABETOLA, G., PIGA, A., MACKIE, P. H., ROBSON, K. J. & CAMASCHELLA, C. (2002) A valine deletion of ferroportin 1: a common mutation in hemochromatosis type 4. *Blood*, 100, 733-4.
- ROETTO, A., PAPANIKOLAOU, G., POLITOU, M., ALBERTI, F., GIRELLI, D., CHRISTAKIS, J., LOUKOPOULOS, D. & CAMASCHELLA, C. (2003) Mutant antimicrobial peptide hepcidin is associated with severe juvenile hemochromatosis. *Nat Genet*, 33, 21-2.
- ROETTO, A., TOTARO, A., CAZZOLA, M., CICILANO, M., BOSIO, S., D'ASCOLA, G., CARELLA, M., ZELANTE, L., KELLY, A. L., COX, T. M., GASPARINI, P. & CAMASCHELLA, C. (1999) Juvenile hemochromatosis locus maps to chromosome 1q. *Am J Hum Genet*, 64, 1388-93.

- ROETTO, A., TOTARO, A., PIPERNO, A., PIGA, A., LONGO, F., GAROZZO, G., CALI, A., DE GOBBI, M., GASPARINI, P. & CAMASCHELLA, C. (2001) New mutations inactivating transferrin receptor 2 in hemochromatosis type 3. *Blood*, 97, 2555-60.
- ROLFS, A., BONKOVSKY, H. L., KOHLROSER, J. G., MCNEAL, K., SHARMA, A., BERGER, U. V. & HEDIGER, M. A. (2002) Intestinal expression of genes involved in iron absorption in humans. *Am J Physiol Gastrointest Liver Physiol*, 282, G598-607.
- ROTH, J. A., HORBINSKI, C., FENG, L., DOLAN, K. G., HIGGINS, D. & GARRICK, M. D. (2000) Differential localization of divalent metal transporter 1 with and without iron response element in rat PC12 and sympathetic neuronal cells. *J Neurosci*, 20, 7595-601.
- ROUAULT, T. A. (2002) Post-transcriptional regulation of human iron metabolism by iron regulatory proteins. *Blood Cells Mol Dis*, 29, 309-14.
- ROUAULT, T. A., STOUT, C. D., KAPTAIN, S., HARFORD, J. B. & KLAUSNER, R. D. (1991) Structural relationship between an iron-regulated RNA-binding protein (IRE-BP) and aconitase: functional implications. *Cell*, 64, 881-3.
- ROUAULT, T. A., TANG, C. K., KAPTAIN, S., BURGESS, W. H., HAILE, D. J., SAMANIEGO, F., MCBRIDE, O. W., HARFORD, J. B. & KLAUSNER, R. D. (1990) Cloning of the cDNA encoding an RNA regulatory protein--the human iron-responsive element-binding protein. *Proc Natl Acad Sci U S A*, 87, 7958-62.
- ROY, C. N. & ENNS, C. A. (2000) Iron homeostasis: new tales from the crypt. *Blood*, 96, 4020-7.
- ROY, C. N., PENNY, D. M., FEDER, J. N. & ENNS, C. A. (1999) The hereditary hemochromatosis protein, HFE, specifically regulates transferrin-mediated iron uptake in HeLa cells. *J Biol Chem*, 274, 9022-8.
- SALTER-CID, L., BRUNMARK, A., LI, Y., LETURCQ, D., PETERSON, P. A., JACKSON, M. R. & YANG, Y. (1999) Transferrin receptor is negatively modulated by the hemochromatosis protein HFE: implications for cellular iron homeostasis. *Proc Natl Acad Sci U S A*, 96, 5434-9.
- SAMANIEGO, F., CHIN, J., IWAI, K., ROUAULT, T. A. & KLAUSNER, R. D. (1994) Molecular characterization of a second iron-responsive element

- binding protein, iron regulatory protein 2. Structure, function, and post-translational regulation. *J Biol Chem*, 269, 30904-10.
- SAMBROOK, J., FRITSCH, E. F. & MANIATIS, T. (1989) *Molecular cloning: a laboratory manual*, Cold Spring Harbor, N.Y., Cold Spring Harbor Laboratory.
- SASAKI, K., ZAK, O. & AISEN, P. (1993) Antisense suppression of transferrin receptor gene expression in a human hepatoma cell (HuH-7) line. *Am J Hematol*, 42, 74-80.
- SCHEUER, P. J., WILLIAMS, R. & MUIR, A. R. (1962) Hepatic pathology in relatives of patients with haemochromatosis. *J Pathol Bacteriol*, 84, 53-64.
- SCIOT, R., PATERSON, A. C., VAN DEN OORD, J. J. & DESMET, V. J. (1987) Lack of hepatic transferrin receptor expression in hemochromatosis. *Hepatology*, 7, 831-7.
- SEISER, C., POSCH, M., THOMPSON, N. & KUHN, L. C. (1995) Effect of transcription inhibitors on the iron-dependent degradation of transferrin receptor mRNA. *J Biol Chem*, 270, 29400-6.
- SELEZNEVA, A. I., CAVIGIOLIO, G., THEIL, E. C., WALDEN, W. E. & VOLZ, K. (2006) Crystallization and preliminary X-ray diffraction analysis of iron regulatory protein 1 in complex with ferritin IRE RNA. *Acta Crystallograph Sect F Struct Biol Cryst Commun*, 62, 249-52.
- SHARP, P. A., SUGDEN, B. & SAMBROOK, J. (1973) Detection of two restriction endonuclease activities in *Haemophilus parainfluenzae* using analytical agarose--ethidium bromide electrophoresis. *Biochemistry*, 12, 3055-63.
- SHAYEGHI, M., LATUNDE-DADA, G. O., OAKHILL, J. S., LAFTAH, A. H., TAKEUCHI, K., HALLIDAY, N., KHAN, Y., WARLEY, A., MCCANN, F. E., HIDDER, R. C., FRAZER, D. M., ANDERSON, G. J., VULPE, C. D., SIMPSON, R. J. & MCKIE, A. T. (2005) Identification of an intestinal heme transporter. *Cell*, 122, 789-801.
- SIMON, M., ALEXANDRE, J. L., BOUREL, M., LE MAREC, B. & SCORDIA, C. (1977) Heredity of idiopathic haemochromatosis: a study of 106 families. *Clin Genet*, 11, 327-41.
- SMITH, A. G., CARTHEW, P., FRANCIS, J. E., EDWARDS, R. E. & DINSDALE, D. (1990) Characterization and accumulation of ferritin in hepatocyte nuclei of mice with iron overload. *Hepatology*, 12, 1399-405.

- SMITH, S. R., GHOSH, M. C., OLLIVIERRE-WILSON, H., HANG TONG, W. & ROUAULT, T. A. (2006) Complete loss of iron regulatory proteins 1 and 2 prevents viability of murine zygotes beyond the blastocyst stage of embryonic development. *Blood Cells Mol Dis*, 36, 283-7.
- SOUTHERN, E. M. (1975) Detection of specific sequences among DNA fragments separated by gel electrophoresis. *J Mol Biol*, 98, 503-17.
- STARZYNSKI, R. R., GONCALVES, A. S., MUZEAU, F., TYROLCZYK, Z., SMUDA, E., DRAPIER, J. C., BEAUMONT, C. & LIPINSKI, P. (2006) STAT5 proteins are involved in down-regulation of iron regulatory protein 1 gene expression by nitric oxide. *Biochem J*.
- STARZYNSKI, R. R., LIPINSKI, P., DRAPIER, J. C., DIET, A., SMUDA, E., BARTLOMIEJCZYK, T., GRALAK, M. A. & KRUSZEWSKI, M. (2005) Down-regulation of iron regulatory protein 1 activities and expression in superoxide dismutase 1 knock-out mice is not associated with alterations in iron metabolism. *J Biol Chem*, 280, 4207-12.
- STEWART, W. B., YUILE, C. L., CLAIBORNE, H. A., SNOWMAN, R. T. & WHIPPLE, G. H. (1950) Radioiron absorption in anemic dogs; fluctuations in the mucosal block and evidence for a gradient of absorption in the gastrointestinal tract. *J Exp Med*, 92, 375-82.
- STREMMEL, W., DE GROOT, H., SIES, H. & STROHMEYER, G. (1995) [Mechanism of liver damage. Pathogenesis of primary hemochromatosis and auxiliary liver transplantation]. *Internist (Berl)*, 36, 362-6.
- STUART, K. A., ANDERSON, G. J., FRAZER, D. M., POWELL, L. W., MCCULLEN, M., FLETCHER, L. M. & CRAWFORD, D. H. (2003) Duodenal expression of iron transport molecules in untreated haemochromatosis subjects. *Gut*, 52, 953-9.
- TABUCHI, M., TANAKA, N., NISHIDA-KITAYAMA, J., OHNO, H. & KISHI, F. (2002) Alternative splicing regulates the subcellular localization of divalent metal transporter 1 isoforms. *Mol Biol Cell*, 13, 4371-87.
- TANG, C. K., CHIN, J., HARFORD, J. B., KLAUSNER, R. D. & ROUAULT, T. A. (1992) Iron regulates the activity of the iron-responsive element binding protein without changing its rate of synthesis or degradation. *J Biol Chem*, 267, 24466-70.
- TCHERNITCHKO, D., BOURGEOIS, M., MARTIN, M. E. & BEAUMONT, C.

- (2002) Expression of the two mRNA isoforms of the iron transporter Nramp2/DMT1 in mice and function of the iron responsive element. *Biochem J*, 363, 449-55.
- THE U.K. HAEMOCHROMATOSIS CONSORTIUM (1997) A simple genetic test identifies 90% of UK patients with haemochromatosis. *Gut*, 41, 841-4.
- THEIL, E. C. (2003) Ferritin: at the crossroads of iron and oxygen metabolism. *J Nutr*, 133, 1549S-53S.
- THENIE, A., ORHANT, M., GICQUEL, I., FERGELOT, P., LE GALL, J. Y., DAVID, V. & MOSSER, J. (2000) The HFE gene undergoes alternate splicing processes. *Blood Cells Mol Dis*, 26, 155-62.
- THORSTENSEN, K., TRINDER, D., ZAK, O. & AISEN, P. (1995) Uptake of iron from N-terminal half-transferrin by isolated rat hepatocytes. Evidence of transferrin-receptor-independent iron uptake. *Eur J Biochem*, 232, 129-33.
- TONG, X., KAWABATA, H. & KOEFFLER, H. P. (2002) Iron deficiency can upregulate expression of transferrin receptor at both the mRNA and protein level. *Br J Haematol*, 116, 458-64.
- TOWBIN, H., STAHELIN, T. & GORDON, J. (1979) Electrophoretic transfer of proteins from polyacrylamide gels to nitrocellulose sheets: procedure and some applications. *Proc Natl Acad Sci U S A*, 76, 4350-4.
- TOYOKUNI, S. (1996) Iron-induced carcinogenesis: the role of redox regulation. *Free Radic Biol Med*, 20, 553-66.
- TRINDER, D., ZAK, O. & AISEN, P. (1996) Transferrin receptor-independent uptake of differic transferrin by human hepatoma cells with antisense inhibition of receptor expression. *Hepatology*, 23, 1512-20.
- TRINDER, D. & MORGAN, E.H. (2002) Uptake of transferrin-bound iron by mammalian cells. In: TEMPLETON, D. M. (Ed) *Molecular and cellular iron transport*, New York, N.Y., M. Dekker. pp 427-449.
- TURNBULL, A., CLETON, F. & FINCH, C. A. (1962) Iron absorption. IV. The absorption of hemoglobin iron. *J Clin Invest*, 41, 1897-907.
- UNGER, A. & HERSHKO, C. (1974) Hepatocellular uptake of ferritin in the rat. *Br J Haematol*, 28, 169-79.
- VARGAS, J. D., HERPERS, B., MCKIE, A. T., GLEDHILL, S., MCDONNELL, J., VAN DEN HEUVEL, M., DAVIES, K. E. & PONTING, C. P. (2003) Stromal cell-derived receptor 2 and cytochrome b561 are functional ferric

- reductases. *Biochim Biophys Acta*, 1651, 116-23.
- VAULONT, S., LOU, D. Q., VIATTE, L. & KAHN, A. (2005) Of mice and men: the iron age. *J Clin Invest*, 115, 2079-82.
- VIATTE, L., LESBORDES-BRION, J. C., LOU, D. Q., BENNOUN, M., NICOLAS, G., KAHN, A., CANONNE-HERGAUX, F. & VAULONT, S. (2005) Deregulation of proteins involved in iron metabolism in hepcidin-deficient mice. *Blood*, 105, 4861-4.
- VOGEL, W., BOMFORD, A., YOUNG, S. & WILLIAMS, R. (1987) Heterogeneous distribution of transferrin receptors on parenchymal and nonparenchymal liver cells: biochemical and morphological evidence. *Blood*, 69, 264-70.
- VOGT, T. M., BLACKWELL, A. D., GIANNETTI, A. M., BJORKMAN, P. J. & ENNS, C. A. (2003) Heterotypic interactions between transferrin receptor and transferrin receptor 2. *Blood*, 101, 2008-14.
- VULPE, C. D., KUO, Y. M., MURPHY, T. L., COWLEY, L., ASKWITH, C., LIBINA, N., GITSCHEIER, J. & ANDERSON, G. J. (1999) Hephaestin, a ceruloplasmin homologue implicated in intestinal iron transport, is defective in the *sla* mouse. *Nat Genet*, 21, 195-9.
- WAHEED, A., PARKKILA, S., SAARNIO, J., FLEMING, R. E., ZHOU, X. Y., TOMATSU, S., BRITTON, R. S., BACON, B. R. & SLY, W. S. (1999) Association of HFE protein with transferrin receptor in crypt enterocytes of human duodenum. *Proc Natl Acad Sci U S A*, 96, 1579-84.
- WALLACE, D. F., PEDERSEN, P., DIXON, J. L., STEPHENSON, P., SEARLE, J. W., POWELL, L. W. & SUBRAMANIAM, V. N. (2002) Novel mutation in ferroportin1 is associated with autosomal dominant hemochromatosis. *Blood*, 100, 692-4.
- WALLACE, D. F., SUMMERSVILLE, L., LUSBY, P. E. & SUBRAMANIAM, V. N. (2005) First phenotypic description of transferrin receptor 2 knockout mouse, and the role of hepcidin. *Gut*, 54, 980-6.
- WANG, J., CHEN, G., MUCKENTHALER, M., GALY, B., HENTZE, M. W. & PANTOPOULOS, K. (2004) Iron-mediated degradation of IRP2, an unexpected pathway involving a 2-oxoglutarate-dependent oxygenase activity. *Mol Cell Biol*, 24, 954-65.
- WANG, R. H., LI, C., XU, X., ZHENG, Y., XIAO, C., ZERFAS, P.,

- COOPerman, S., ECKHAUS, M., ROUAULT, T., MISHRA, L. & DENG, C. X. (2005) A role of SMAD4 in iron metabolism through the positive regulation of hepcidin expression. *Cell Metab*, 2, 399-409.
- WEINBERG, E. D. (1996) The role of iron in cancer. *Eur J Cancer Prev*, 5, 19-36.
- WEST, A. P., JR., BENNETT, M. J., SELLERS, V. M., ANDREWS, N. C., ENNS, C. A. & BJORKMAN, P. J. (2000) Comparison of the interactions of transferrin receptor and transferrin receptor 2 with transferrin and the hereditary hemochromatosis protein HFE. *J Biol Chem*, 275, 38135-8.
- WHEBY, M. S., JONES, L. G. & CROSBY, W. H. (1964) Studies on Iron Absorption. Intestinal Regulatory Mechanisms. *J Clin Invest*, 43, 1433-42.
- WILKINS, S. J., FRAZER, D. M., MILLARD, K. N., MCLAREN, G. D. & ANDERSON, G. J. (2006) Iron metabolism in the hemoglobin-deficit mouse: correlation of diferric transferrin with hepcidin expression. *Blood*, 107, 1659-64.
- WILLIS, G., FELLOWS, I. W. & WIMPERIS, J. Z. (2000) Deaths attributed to haemochromatosis are rare in Britain. *Bmj*, 320, 1146.
- WORTHINGTON, M. T., COHN, S. M., MILLER, S. K., LUO, R. Q. & BERG, C. L. (2001) Characterization of a human plasma membrane heme transporter in intestinal and hepatocyte cell lines. *Am J Physiol Gastrointest Liver Physiol*, 280, G1172-7.
- WRIGGLESWORTH, J. M. & BAUM, H. (1980) The biochemical functions of iron. In: A. JACOBS & M. WORWOOD, (Eds) *Iron in biochemistry and medicine, II*, London, Academic Press. pp 29-86.
- YAMANAKA, K., ISHIKAWA, H., MEGUMI, Y., TOKUNAGA, F., KANIE, M., ROUAULT, T. A., MORISHIMA, I., MINATO, N., ISHIMORI, K. & IWAI, K. (2003) Identification of the ubiquitin-protein ligase that recognizes oxidized IRP2. *Nat Cell Biol*, 5, 336-40.
- YIP, R. (1998) Iron deficiency. *Bull World Health Organ*, 76 Suppl 2, 121-3.
- YOUDIM, M. B., BEN-SHACHAR, D. & RIEDERER, P. (1993) The possible role of iron in the etiopathology of Parkinson's disease. *Mov Disord*, 8, 1-12.
- YOUNG, S. P., BOMFORD, A. & WILLIAMS, R. (1984) The effect of the iron saturation of transferrin on its binding and uptake by rabbit reticulocytes. *Biochem J*, 219, 505-10.
- YU, Y., RADISKY, E. & LEIBOLD, E. A. (1992) The iron-responsive element

- binding protein. Purification, cloning, and regulation in rat liver. *J Biol Chem*, 267, 19005-10.
- ZECCA, L., YOUDIM, M. B., RIEDERER, P., CONNOR, J. R. & CRICHTON, R. R. (2004) Iron, brain ageing and neurodegenerative disorders. *Nat Rev Neurosci*, 5, 863-73.
- ZHANG, A. S., XIONG, S., TSUKAMOTO, H. & ENNS, C. A. (2004) Localization of iron metabolism-related mRNAs in rat liver indicate that HFE is expressed predominantly in hepatocytes. *Blood*, 103, 1509-14.
- ZHOU, X. Y., TOMATSU, S., FLEMING, R. E., PARKKILA, S., WAHEED, A., JIANG, J., FEI, Y., BRUNT, E. M., RUDDY, D. A., PRASS, C. E., SCHATZMAN, R. C., O'NEILL, R., BRITTON, R. S., BACON, B. R. & SLY, W. S. (1998) HFE gene knockout produces mouse model of hereditary hemochromatosis. *Proc Natl Acad Sci U S A*, 95, 2492-7.
- ZOLLER, H., KOCH, R. O., THEURL, I., OBRIST, P., PIETRANGELO, A., MONTOSI, G., HAILE, D. J., VOGEL, W. & WEISS, G. (2001) Expression of the duodenal iron transporters divalent-metal transporter 1 and ferroportin 1 in iron deficiency and iron overload. *Gastroenterology*, 120, 1412-9.
- ZOLLER, H., MCFARLANE, I., THEURL, I., STADLMANN, S., NEMETH, E., OXLEY, D., GANZ, T., HALSALL, D. J., COX, T. M. & VOGEL, W. (2005) Primary iron overload with inappropriate hepcidin expression in V162del ferroportin disease. *Hepatology*, 42, 466-72.
- ZOLLER, H., THEURL, I., KOCH, R. O., MCKIE, A. T., VOGEL, W. & WEISS, G. (2003) Duodenal cytochrome b and hephaestin expression in patients with iron deficiency and hemochromatosis. *Gastroenterology*, 125, 746-54.
- ZOLOTUKHIN, A. S., HARFORD, J. B. & FELBER, B. K. (1994) Rev of human immunodeficiency virus and Rex of the human T-cell leukemia virus type I can counteract an mRNA downregulatory element of the transferrin receptor mRNA. *Nucleic Acids Res*, 22, 4725-32.

Appendix I. Clinical characteristics and iron indices of individual samples

Table A. Iron loaded specimens

Sample ID	Sample available	Condition/ HFE mutation state	Year of Birth	Year of Biopsy	Age (at year of biopsy)	Grade of Siderosis	Hepatic Iron Concentration (µg Fe/g dry wt)	Serum Iron (µmoles·L ⁻¹)	Serum Ferritin (ng·mL ⁻¹)	Transferrin Saturation (%)	Total Iron Binding Capacity (µmoles·L ⁻¹)
KCHAB01	Explant	HH, CY	1946	1997	52	II-III	2378	26	458	45	58
KCHAB02	Explant	HH, YY	1928	2001	73	IV	9352	42	4001	100	42
KCHAB03	Explant	NH	1994	1994	neonatal	II-III	3300	-	-	-	-
KCHAB04	Percutaneous biopsy	HH, YY	1950	1998	48	III	3974	37	950	93	40
KCHAB05	Percutaneous biopsy	HH, YY	1945	1996	51	IV	11330	46.6	2104	83	56.1
KCHAB06	Percutaneous biopsy	treated HH, YY	1914	1996	82	I	388	35	30	88	40
KCHAB07	Explant	HH, YY	1945	1996	51	IV	27320	38	2954	100	38
KCHAB08	Percutaneous biopsy	PKD	1965	1996	31	IV	30000	44	3972	100	44
KCHAB09	Percutaneous biopsy	HH, YY	1961	2002	41	IV	27292	44	5165	100	44
KCHAB10	Percutaneous biopsy	HH, YY	1957	2005	48	III	1967	23	1520	56	41
KCHAB11	Percutaneous biopsy	HH, YY	1962	2005	43	III	2642	20	1311	31	65
KCHAB12	Explant	HH, YY	1946	2006	60	III-IV	2162	34	1057	69	49
KCHAB13	Percutaneous biopsy	HH, YY	1948	2005	57	IV	5398	38.5	2204	80	48
KCHAB14	Explant	treated HH, YY	1951	2004	53	0	135	38	37	84	44
KCHAB15	Explant	treated HH, YY	1936	2003	67	0	287	28	61	61	46
KCHAB16	Explant	HH, YY	1961	2002	41	III	3109	33	900	67	49

Table B. Control specimens

Sample ID	Sample available	Condition	Year of Birth	Year of Biopsy	Age (at year of biopsy)	Grade of Siderosis	Hepatic Iron Concentration ($\mu\text{g Fe/g dry wt}$)	Serum Iron ($\mu\text{moles}\cdot\text{L}^{-1}$)	Serum Ferritin ($\text{ng}\cdot\text{mL}^{-1}$)	Transferrin Saturation (%)	Total Iron Binding Capacity ($\mu\text{moles}\cdot\text{L}^{-1}$)
KCHAB17	Explant	-	1959	1999	40	0	500	18	98	37	48
KCHAB18	Explant	-	1973	2000	27	0	1114	16	112	31	52
KCHAB19	Explant	-	1962	1998	36	0	872	21	202	39	54
KCHAB20	Explant	-	1957	1999	42	0	907	18	118	35	52
KCHAB21	Percutaneous biopsy	-	1950	2002	52	0	1017	20	193	34	59
KCHAB22	Percutaneous biopsy	-	1941	2001	60	0	319	14	538	30	46
KCHAB23	Percutaneous biopsy	-	1944	2002	58	0	652	20	625	32	62
KCHAB24	Percutaneous biopsy	-	1945	2001	56	0	1260	14	78	28	50
KCHAB25	Explant	-	1962	2002	40	0	247	12	58	21	58
KCHAB26	Explant	-	1959	2002	43	0	628	18	120	36	50
KCHAB27	Explant	-	1979	2002	23	0	116	15	98	25	61
KCHAB28	Explant	-	1957	2003	46	0	89	21	178	32	66
KCHAB29	Explant	-	1961	2005	44	0	669	22	154	38	58
KCHAB30	Explant	-	1948	2001	53	0	408	14	223	22	64
KCHAB31	Explant	-	1959	2002	43	0	186	16	65	31	52
KCHAB32	Explant	-	1971	2002	31	0	220	30	92	38	61
KCHAB33	Explant	-	1968	2005	37	0	552	20	188	32	62
KCHAB34	Explant	-	-	2003	27	0	402	22	112	38	58
KCHAB35	Explant	-	-	2003	39	0	28	14	50	23	60
KCHAB36	Explant	-	-	2003	42	0	118	19	59	27	70

Appendix II

Homo sapiens mRNA for IRP1

LOCUS HSIRF 3498 bp mRNA linear PRI 09-FEB-1999
DEFINITION H.sapiens mRNA for iron regulatory factor.
ACCESSION Z11559
VERSION Z11559.1 GI:33962
KEYWORDS iron regulatory factor.
SOURCE Homo sapiens (human)
ORGANISM Homo sapiens
Eukaryota; Metazoa; Chordata; Craniata; Vertebrata;
Euteleostomi; Mammalia; Eutheria; Euarchontoglires;
Primates; Haplorrhini; Catarrhini; Hominidae; Homo.
REFERENCE 1 (bases 1 to 3498)
AUTHORS Hirling,H., Emery-Goodman,A., Thompson,N., Neupert,B.,
Seiser,C. and Kuhn,L.C.
TITLE Expression of active iron regulatory factor from a full-length human cDNA by in vitro transcription/translation
JOURNAL Nucleic Acids Res. 20 (1), 33-39 (1992)
PUBMED 1738601
REFERENCE 2 (bases 1 to 3498)
AUTHORS Hirling,H.
TITLE Direct Submission
JOURNAL Submitted (19-DEC-1991) Hirling H., Swiss Institute for Experimental Cancer Research, Chemin des Boveresses 155, Epalinges sur Lausanne, Vaud, Switzerland
FEATURES Location/Qualifiers
source 1..3498
/organism="Homo sapiens"
/mol_type="mRNA"
/db_xref="taxon:9606"
CDS 108..2777
/codon_start=1
/product="iron regulatory factor"
/protein_id="CAA77651.1"
/db_xref="GI:33963"
/db_xref="GOA:P21399"
/db_xref="UniProtKB/Swiss-Prot:P21399"
/

ORIGIN

IRPlex forward

1 gggctcgAAC gcgcAGCGA cggGAACCGG tcccgCTGCT tgggtcaggT tcGCCGGTCg
 61 cgggAGCCCC GCCGTcAGt cggAGGAACA CGTGGCCATC AGTAATCATG AGCAACCCAT
 121 tcgcACACCT TGCTGAGCCA ttggatcctg tacaaccagg aaagaaattc ttcaatttga
 181 ataaatttGGA ggattcaaga tatgggcgct taccattttc gatcagagtt cttctggaaG
 241 cagccattcg gaattgtgat gagttttgg tgaagaaaca ggatattgaa aatattctac
 301 attGGAatgt cactcAGCAC aagaACATAG aagtGCCATT taagcctgct cgtgtcatcc
 361 tgcaggactt tacGGGTGtg cccgctgtgg ttgactttgc tgcaatgcgt gatgctgtga
 421 aaaAGTTAGG aggAGATCCA gagaAAATAA accctgtctg ccctgctgat ctGtaatAG **IRP1s forward**
 481 atcattccat ccaggTTGAT ttcaacAGAA gggcAGACAG tttacAGAA aatcaAGACC
 541 tggAAATTGAA aagAAATAGA gagcGATTG aattttAAAG gtggggTTCC caggCTTTc
 601 acaACATGCG gattattccc CCTGGCTCAG gaATCATCCA CCAGGTGAAT ttGGAATATT
 661 tggcaAGAGT ggtatttGAT caggatGGAT attattACCC agacAGCCTC gtggGCACAG
 721 actcgcACAC taccatGATT gatggCTTGG gcattCTTGG ttggggTGTc ggtggTATTG
 781 aagcAGAAGC TGTcATGCTG ggtcAGCCAA tcaGtATGgt gcttcctcAG gtGATTGGCT
 841 acaggCTGAT gggGAAGCCC caccCTCTGG taACATCCAC tgACATCGT CTCACCATTa
 901 ccaAGCACCT CGGCCAGGTT gggGTAGTGG gcaAAATTGt cgAGTCTTC gggCCTGGAG
 961 tagcccAGTT gtccATTGCT gaccGAGCTA cgattGCTAA catGtGTCCA gagtacGGAG
 1021 caactGCTGC ctTTTCCCA gttGATGAAG ttagtATCAC gtacCTGGT caaACAGGTC
 1081 gtGATGAAGA aaaATTAAAG tatATTAAA AATATCTCA ggctGTagGA atGTTTcGAG
 1141 atttCAATGA ccTTTCTCAA gaccCAGACT tcACCCAGGT tGtGGAATTt gatttGAAA
 1201 cAGTAGTGCC ttGCTGTAGT ggACCCAAAA ggcCTCAGGA caaAGTTGCT gtGTCGACA
 1261 tGAAAAGGA ctTTGAGAGC tgcCTTGGAG ccaAGCAAGG ATTtAAAGGA ttccaAGTTG
 1321 ctccTGAACA tcATAATGAC cataAGACCT ttATCTATGA taACACTGAA ttCAACCCTG
 1381 ctcatGGTTc TGTGGTcATT gctGCCATT CTAGCTGCAC AAACACCAGT AATCCGTCTG
 1441 tGATGTTAGG ggcAGGATTG ttAGCAAAAGA aAGCTGTGGA tgctGGCCTG AACGTGATGc
 1501 ctTAACATCAA aactAGCCTG tCTCCTGGGA gtggcGTGGT cacCTACTAC ctacaAGAAA
 1561 gcggAGTcAT gcTTATCTG tCTCAGCTTg ggtttGAcGT ggtggcTAT ggctGcAtGA
 1621 CCTGCATTGG caACAGTGGG CCTTACCTG AACCTGTGGT agaAGCCATC ACACAGGGAG
 1681 acCTTGTAGC tGTTGGAGTA CTATCTGGAA ACAGGAATTt tGAAGGTCGA gttcacCCCA
 1741 acACCCGGGC caACTATTa GCCTCTCCCC CCTTAGTAAT AGCATATGCA attGCTGGAA
 1801 ccatcAGAAAT CGACTTTGAG AAAGAGCCAT tgggAGTAAAG tgcaaAGGGA cAGCAGGTT
 1861 ttctGAAAGA tatCTGGCCG ACTAGAGACG AGATCCAGGC AGTGGAGC GTAGTGTCA
 1921 tcccGGGGAT GTTAAGGAA GtCTATCAGA AAATAGAGAC tGtGAATGAA AGtGGAATG
 1981 ccttagcaAC cccATCAGAT aAGCTTTT tCTGGAATTc caAAATCTACG tATATCAAAT
 2041 caccACCAATTt CTtGAAAC ACTGACTTTGG ATCTTCAGCC CCCTAAATCT ATAGTGGATG
 2101 CCTATGTGCT GCTAAATTG GGAGATTcGG TAACAActGA CCACATCTCC CCAGCTGGAA
 2161 atattGCAAG AAACAGTcCT GCTGOTCGCT ACTTAACtAA CAGAGGcCTA ACTCCACGAG
 2221 aattCAACTC CTATGGCTCC CGCCGAGGTA ATGACGCCGT CATGGCACGG ggaACATTG
 2281 ccaACATTcG CTTGTTAAAC AGATTTGAT ACAAGCAGGC ACCACAGACT ATCCATCTG **IRP1s reverse**
 2341 cttctGGGA aatcTTGAT gtGTTGATG CTGCTGAGCG gtaccAGCAG gCAGGcCTTC
 2401 ccctGATCGT tCTGGCTGGC AAAGAGTACG GTGcAGGcAG CTCGGAGAC tggGAGGCTA
 2461 agggCCCTT CCTGCTGGGA ATCAAAGCCG tCCTGGCCGA gagtACGAG CGCATTcACC
 2521 gcaGTAACCT GGTGAGGATG GGTGtGATCC CACTTGAATA tCTCCCTGGT gagaATGcAG
 2581 atGCCCTGGG GCTCACAGGG CAAGAACGAT ACACtATCAT tattCCAGAA AACtCAAAC
 2641 cacaAAATGAA AGTCCAGGTC AAGCTGGATA CTGGCAAGAC CTTCCAGGCT GTCATGAGGT

2701 ttgacactga tgtggagctc acttatttcc tcaacggggg catcctcaac tacatgatcc
2761 gcaagatggc caagtaggag acgtgcactt ggtcggtgcgc ccagggagga agccgcacca
2821 ccagccagcg caggccctgg tggagaggcc tccctggctg cctctggag gggtgctgcc
2881 ttgttagatgg agcaagttag cactgagggt ctggtgccaa tcctgttaggc aaaaaaccag
2941 aagtttctac attctctatt tttgttaatc atcttcttctt tttccagaat **ttgaaagct** **IRPlex reverse**
3001 **gaatgggtggg** aatgtcagta gtgccagaaa gagagaacca agcttgtctt taaagttact
3061 gatcacagga cggtgccttt tcactgttcc ctattaatct tcagctgaac acaagcaaac
3121 cttctcagga ggtgtctcct accctcttat tgttcctctt acgctctgct caatgaaacc
3181 ttcctcttga gggtcatttt ctttctgtt ttaattatac cagttttag tgacatagat
3241 aagaactttg cacacttcaa atcagagcag tgattctctc ttctctcccc ttttcattca
3301 gagtaatca tccagactcc tcattggatag gtcgggttt aaagttttt tgattatgtt
3361 cttttgata gatccacata aaaagaaaatg tgaagttttc ttttactatac ttttcattta
3421 tcaagcagag acctttgtt ggaggcggtt tgggagaaca cattttctaat ttgaatgaaa
3481 tgaaatctat tttcagtg

Appendix III

Sequence analysis of alternatively spliced forms of IRP1

Alternatively Spliced IRP1 Transcript #01 (Δ 5-14)

Amplicon of ~550bp from nested PCR of HepG2 mRNA (oligo dT reverse transcription), 1st round PCR with IRPEx1 and IRPEx21 primers (amplifying across complete ORF) followed by 2nd round with IRP1s5 and IRP1s3 (amplifying across exons 4 - 18).

Sequence

>6001.MN.h1RP1.F sequence exported from 6001.MN.h1RP1.F.Seq
TCTCCATCCAGTTGATTCAACACGAAGGAGTAATGCAAAGGGACAGCAGGTATT
TCTGAAAAGATATCTGGCCGACTAGAGACGAGATCCAGGCAGTGGAGCGTCAGTATGTCAT
CCCCGGGATGTTAACCGAAGTCTATCAGAAAATAGAGACTGTGAATGAAAGCTGGAATGC
CTTAGCAACCCCCATCAGATAAGCTGTTCTGAAATTCCAATCTACGTATATCAAATC
ACCACCAATTCTTGAAACACTGACTTGGATCTCAGCCCCCTAAATCTATAGTGGATGC
CTATGTGCTGCTAAATTGGGAGATTGGTAACAACGACCATCTCCCCAGCTGGAAA
TATTGCAAGAACAGTCCTGCTCGCTACTTAACAAACAGAGGCCTAACTCCACGAGA
ATTCAACTCCTATGGCTCCCGCCGAGGTAATGACGCCGTATGGCN

The sequence at the 5' from the automatic readout has been modified by careful inspection of the chromatogram.

Alignment with IRP1 cDNA

6001.MN.h1RP1	1	TCTCCATCC--AGT-----TG--ATT-----T
18		..
IRP1	1751	tat tagcctccccccttagtaatagcatatgcaatttgtggaaaccat
1800		
6001.MN.h1RP1	19	C--AA-C-AC-----GAA-----GGAGTAAATGCAAAGGGACAGC
49		
IRP1	1801	cagaatcgactttgagaaagagccattggagtaatgcaaaggacagc
1850		
6001.MN.h1RP1	50	AGGTATTCTGAAAGATATCTGGCCGACTAGAGACGAGATCCAGGCAGTG
99		
IRP1	1851	aggtattctgaaagatatctggccgactagagacgagatccaggcagt
1900		
6001.MN.h1RP1	100	GAGCGTCAGTATGTCATCCGGGATGTTAAGGAAGTCTATCAGAAAAT
149		
IRP1	1901	gagcgtcagtatgtcatccgggatgttaaggaagtctatcagaaaat
1950		
6001.MN.h1RP1	150	AGAGACTGTGAATGAAAGCTGGAATGCCTAGCAACCCATCAGATAAGC
199		
IRP1	1951	agagactgtgaatgaaagctggaatgccttagcaacccatcagataagc
2000		

Alignment run with EBI's EMBOSS-Align with open gap penalty 1.0, gap penalty extension 0.5, Blosum 62 matrix; parameters intended to penalise gaps as little as possible.

Most of the sequence is aligned, but little correspondance at 5' end, with alignment mostly starting at exon 15 (in blue).

Run Align again with first 20 or bases:

6001.MN.h1RP1	1	TC -- TCCATCCA-GTTGATT
17		
IRP1	451	ccctgtctgccctgctgatctttaatagatcattccatccagggttggatt
500		
6001.MN.h1RP1	18	TCAACA-----C-GA-AG
28		
IRP1	501	tcaacagaggggcagacagttagacaagaatcaagacacctggaaattgaaa
550		

Reasonable match to an upstream region identified as exon 4 (in red).

Alignments indicate exons 5 to 14 (inclusive) are absent in the transcript, with a predicted amplicon size of 576.

Translation Product

Analysis of exon ends indicates that the Δ5-14 splice form would not have the IRP1 reading frame maintained. Does the splice product encode a meaningful protein?

Sequence from initiation ATG onwards run in EMBOSS-Transeq:

EMBOSS_001_1

```
MSNPFAHLAEPPLDPVQPGKKFFNLNKLEDSRYGRLPFSIRVLLEAAIRNCDEFLVKKQDI  
ENILHWNVTQHKNIEVPFKPARVILQDFTGVPAVVDFAAMRDAVKKLGGDPEKINPVCAPA  
DLVIDHSIQVDFNRRE*MQRDSRYF*KISGRLETRSRSRQWSVSMSSRGCLRKSIRK*RL*M  
KAGMP*QPHQISCFSGIPNLRISNHHSLKT*LWIFSPLNL*WMPMCC*IWEIR*QLTTS  
PQLEILQETVLLLAT*LTEA*LHENSTPMAPAEVMTPSWHGEHLPTFAC*TDF*TSRHHR  
LSICLLGKSLMCLMLSGTSRQAFP*SFWLAKSTVQAAPETGQLRALSCWESKPSWPRAT  
SAFTAVTWLGWV*SHLNISLVRMQMPWGSQGKNDTLSLFQKTSNHK*KSRSSWILARPSR  
LS*GLTLMWSSLISSTGASSTT*SARWPSRRRALGAAPREEAAPASAGPGGEASLAASG  
RGAAL*MEQVSTEGLVPIL*AQNQKFLHSLFLLIIIFSFSRIWKLEWWECQ*CQKERTKLV  
FKVTDHRTLLFHCFLLIFS*TQANLLRRCLLPSYCSSYALLNETFLLRVIFLSVLIIPVL  
SDIDKNFAHKSEQ*FSLLSPFPSE*IIQTPHG*VGC*SCFDYVPFDRST*KEM*SFLLL  
SFHLSSRDLCWEAVWENTFLI*MK*NLFSVKTC*L*VLLCLWLEFWDI*YRVNLTPYHWE  
A*ITFIFSHFYNSIRTVRV*RKCLGTIMLALPCIGADKKEE*PGGSGNDIST*GKADKLO  
DTKNQLSAHFYPCSHFWACLSLLGLL*CNAIDWLKEQKCIFSQLWRLEF*DQS*SHFIFW  
*GHSSWFTDGHLLACSHMAFLWYVPGGGER
```

Using the original initiation ATG a peptide of 135 + 1 aa would be translated. The 135 aa are IRP1 sequence encoded in exons 1-4. The last aa (in red) new sequence. The predicted protein size is 15.5kDa.

Using the next ATG (exon2/3 junction) only small peptides are predicted.

Conclusion

The Δ5-14 alternatively spliced transcript is unlikely to have any biological function.

Alternatively Spliced IRP1 Transcript #02 ($\Delta?$)

Amplicon of ~500bp amplified using template from HepG2 cells, 1st round PCR with IRPex1 and IRPex21 primers (amplifying across complete ORF) followed by 2nd round with IRP1s5 and IRP1s3 (amplifying across exons 4 - 18).

>9698.MN.h1RP1.500.s3R sequence exported from 9699.MN.h1RP1.700.s5F
TCCTCGTGGTGCCTGTTCAAAATCTGTTAACAGCGAATGTTCGGCCAATGTTCCCC
GTGCCATGAANGNGNGCTTACCTTNGCGGNTGCCATANNANTGAATTGNACCGACAN
TTAGGTTTNTATGTAGCTAAGTAGACNNAGCTNNCTAGNTNCNGTCTNAGNAAGNCA
TAGCNCNNGCAGNANCNTAGCCNNCTATTNTCNNAGNAATNTCCCATGCACTNGNNG
NGGGGNTGATNTNCTCGNGCNAAGNCAANACTNNNCNTCCATGAACNCCNAAATACCN
TGGNGNACCTNNAACTNTNGAAACGATNNTGNACNTNCNTNGNNCCNNAACAACGNGTNC
TNNTNATNNTCTNANNNTANACGGTTNNACNNCATCTAAACAATTGTCACCGNNGA
GTCGTNNTCNACAAGAAGNANACCNGNCNTNNTTANAATTCTCCATNTNNNNCNNATG
ANACCGTTNCAGACANCGGGTNCACCGCGANANNANCACGCTTCTGNCNACTGCNNGCA
CCANGCGTCACGACNCTACGNNNTNTNNNNANNANATCACACTTATANTNNG

Inverted:

<IRP1 alt splice transcript #02 inverted
CNNANTATAAGTGTGATNTNNNNNNNNNNNNNNCGTAGNGTGTGACGCNTGGTGCNNNGCA
GTNGNCAGAACCGCGCAGTNTNTCGCGGTGNACCGCGTCTNGNAACGGTNTCATNNNN
NNANATGGAGAATTNTAAANNANGNCNGGTNTNCTCTTGNGANNACGACTCNCGGTG
ACAAATTGTTAGATGNNGGTNNAACCGTNTANNNNTNAGANANNATNANNAGNACNCGT
TGTNNNGNNCNANGNANGTNCANNATCGTTCNANAGTTNNAGGTNCNCANGTATT
NGGNGTTCATGGAGNGNNNAGTNTGNCTTNGCGNCAGNANATCANCCCNCNNCNATG
CATGGGANATTNCTNNGANAAATAGNNGCTANTAGNTNCNGNGCTATGNCTTNC
TNAGGAACNGNANCTAGNNAGCTNGTCTACTTAGCTACATANAAAACCTAANTGTCGGT
NCAATTCAANTNNTATGGCANCCGNNAAGGTAAGCNCNCNTTATGGCACGGGGAAACA
TTTGGCGAACATTCGCTTGTAAACAGATTGAAACAAGCAGGACCACGAGGA

Sequence too poor to interpret.

Second sequence reaction

10048.MN.hIRP	1	TGAGNNNGCCCTTCC--CNGTTGNTT
25	
IRP1	451	ccctgtctgcccgtctgatctttaatagatcattccatccagggttgatt
500		
10048.MN.hIRP	26	CC--CAGAAGGGCAGACAGTTACAGAAGAATCAAGACCTGGAATTGAA
73		. .
IRP1	501	tcaacagaaggcagacagtttacagaagaatcaagacctggaatttgaa
549		
10048.MN.hIRP	74	AGAAATAGAGAGCGATTGAAATTAAAGTGGGTTCCCAGGCTTTCA
123		.
IRP1	550	agaaatagagagcgatttgaattttaaagtgggttcccaggctttca
599		

Exon 5 is in blue and exon 6 in green. Sequence after exon 6 is not clear, but may not be exon 7.

>10169.MN.hIRP1.500R.seq; complement, reversed
CCNNNNNTANNNNNTNCATNNNNNTGATTNNNNNNNAATNGNANANAGNTTCCNGNAGNTT
CCAGANNTNGCATTNNNTAGAAATTGANAGCGATTGAATTTTAAAGAGGGTTNCAGG
NNNTTCAANACNTTGGNTTNTCCCCCTGNNTAGGAATCATCCANCATGTGAATTGG
NATNTTGGCAAGANNTGTATTCATCAGGATNGNTATTNTTATACNAGACNAGCCNTG
TGGGNAANNANCACTCGGNACGATTATNTNNTGANTANATGNGTCTTNTGGNNNTCCCT
TGC GTGAAAGTAGTTGCGTAGGTAAATCANTANCTAGAAGCTNGNCTATGTTANGTCACA
GNNNCCTANNTGGTGCNCANTNGAANTATTNATGGCTANNCGNATGAGGGTAAGNNCN
NCCNNATGGCACGGGAACATGTTGCCAACATTGGCTTAAACGAGATTTTGAAACA
AGCAGGGACCACCTAGGCTTNC

No improvement - need to re-sequence.

Second Round of Sequencing

PCR fragment subcloned into pTBlue and sequenced from vector with T7 and 3' primer in *lacZ* sequence.

10637.MN.hIRP1500.T7 reverse complement aligned with human IRP1 cDNA:

IRP1 501 tcaacagaaggcagacagttacagaagaatcaagacctgaaatttggaa
550

10637.MN.hIRP 1
2

IRP1 551 gaaatagagagcgattgaattttaaagtgggtccaggctttcac
600

10637.MN.hIRP 3 GAAATAGAGAGCGA-TTGAATCTTAAAGTGGGTTCCAGGCTTCAC
51

IRP1 601 aacatgcggattattccccctggctcaggaatcatccaccaggtaatt
650

10637.MN.hIRP 52 TACATGCAGATTATTCCCCCTGGCTCAGGAATCATCCACCAGGTGAATT
101

IRP1 651 ggaatatttgcaagagtggtatttgcatttcaggatggatatttacccag
700

10637.MN.hIRP 102 GGAATATTGGCAAGAGTGGTATTGATCAGGATGGATTATTACCCAG
151

IRP1 701 acagcctcggtggcacagactgcacactaccatgattgatggcttggc
750

10637.MN.hIRP 152 ACAGCCTCGTGGGCACAGACTCGCACACTACCATGATTGATGGCTTGGC
201

IRP1 751 attcttggttgggtgtcggttgttgcattgcaggactgtcatgttgg
800

10637.MN.hIRP 202 ATTCTTGTTGGGTGTCGGTGGTATTGAAGCAGAACGCTGTCATGCTGG
251

IRP1 801 tcagccaatcagtatggtgcttcctcaggtgattggctacaggctatgg
850

10637.MN.hIRP 252 TCAGCCAATCAGTATGGTGCCTCAGGTGATTGGCTACAGGCTGATGG
301

IRP1 851 ggaagccccaccctctggtaacatccactgacatcggtcaccattacc
900

10637.MN.hIRP 302 GGAAGCCCCACCCTCTGG-----CACGGGAAACAT-----TTGCC
336

IRP1 901 aagcacctccgccaggttgggttagtggcaaatgtcgagttttcgg
950

10637.MN.hIRP 337 A---ACATT CGC---TTG-----TTAACACAGATTTTGA
364

IRP1 951 gcctggagtagcc-cagt-tgtccattgtcaccgagctacgattgctaa
998

10637.MN.hIRP 365 ACAAGCAGGCACCACAGACTATCCAT--CTGCC-----
395

IRP1 1048	999	catgtgtccagagtacggagcaactgctgcctttcccagttatgaag
10637.MN.hIRP 427	396	-----TTCTGGGAAAT-CATCCATATGA CTAGTAGAT -----
IRP1 1095	1049	ttagtatcacgt---acctggtgcaaacaggctgtatgaagaaaaatta
10637.MN.hIRP 454	428 ---- CCTCTAGANCACCNG ----- CAGG-CGTGAAG
IRP1 1145	1096	aagtatattaaaaaatatcttcaggctgttaggaatttcgagattcaa
10637.MN.hIRP 454	455	

Sequence in blue is exon 7.

Expected vector sequence from T7 primer to amplicon subcloned into EcoRV:

gggaaagcttgcattgcctgcaggcgactctagaggatctactgtcatatggat

Reverse complement:

atccatatgactagtagatcctctagactcgacctgcaggcatgcaagcttccc

Alignment of vector sequence and T7 sequence:

10637.MN.hIRP 41	1 CTT-CACGCCTGCNGGTCGN-TCTAGAGGATCTACTAGTCATA
pTBlue 50	1 . . . 1 gggaaagctgcatgcctgcaggtcgactctagaggatctactagtata
10637.MN.hIRP 91	42 TGGATGATTCCCCAGAAGGCAGATGGATAGTCTGTGGTGCCTGCTTGT
pTBlue 55	51 tggat

Perfect alignment up to EcoRV site. First 36 bases of sequence are vector.

Sequence in red identified as vector.

Expected vector sequence from EcoRV site to 3' primer:

atcgatccccgggtaccgagctcgaattcactggccgtcgtttacaa

Analysis of the sequence:

>10637.MN.hIRP1500.T7 reverse complement
AAGAAATAGAGAGCGATTGAATCTTAAAGTGGGTTCCCAAGGCTTCACTACATGCGG
ATTATTCCCCCTGGCTCAGGAATCATCCACCAAGGTGAATTGGAATATTGGCAAGAGTG
GTATTTGATCAGGATGGATATTATTACCCAGACAGCCTCGTGGCACAGACTCGCACACT
ACCATGATTGATGGCTTGGGCATTCTGGTGGGTGTCGGTGGTATTGAAGCAGAACGCT
GTCATGCTGGGTCAAGCAATCAGTATGGTGCCTCCTCAGGTGATTGGCTACAGGCTGATG
GGGAAGCCCCACCCTCTGGCACGGGAACATTGCCAACATTGCTTGTAAACAGATTT
TTGAACAAGCAGGCAACCACAGACTATCCATCTGCCTCTGGGAAATCATCCATATGACT
AGTAGATCCTCTAGANCGACCGNGCAGGCGTGAAG

Sequence in blue is exon 7, up to perfect alignment (see above); sequence in red is vector; sequence in purple is unaligned.

Purple sequence re-aligned against IRP1 cDNA:

Unknown	1	
0		
IRP1	2201	gcctaactccacgagaattcaactcctatggctccgcccaggtaatgac
2250		
Unknown	1	CACGGGAAACATTGCCAACATTCGCTTAAACAGATT
40		
IRP1	2251	gccgtcatggcacgggaacattgccaacattcgctttaaacagatt
2300		
Unknown	41	TTTGAACAAGCAGGCACCACAGACTATCCATCTGCCTCTGGGAAATCA
90		
IRP1	2301	tttgaacaaggcaggcaccacagactatccat <u>ctgcctctgggaaatcc</u>
2350		
Unknown	91	TCCATATGA
99		
IRP1	2351	ttgatgtgtttagtgctgctgagcggtaccagcaggcaggcctccctg
2400		

The sequence shown in green above maps to exon 18, but a cryptic splice site has been used. The primer sequence used for the PCR is double underlined. Does the sequence encode a viable protein?

The splicing, although not conventional maintains the reading frame.

>EMBOSS_001_1
MSNPFAHLAEPLDPVQPGKKFFNLNKLEDSRYGRLPFSIRVLLEAAIRNCDEFLVKKQDI
ENILHWNVTQHKNIEVPFKPARVILQDFTGVPAVVDFAAAMDRAVKKLGGDPEKINPVCPA
DLVIDHSIQVDFNRRADSLQKNQDLEFERNRERFEFLWKGSQAFHNMRIIPPGSGIIHQV
NLEYLARVVFQDGYYYPSLGVGTDSHTMIDGLGILGWGVGGIEAEAVMLGQPISMVLP
QVIGYRLMGKPHPLARGTFANIRLLNRFLNKQAPQTIHLPSGEILDVFDAEERYQQAGLP
LIVLAGKEYGAGSSRDWAAKGPFLLGIAKVALAESYERIHRNSNLVGMGVIPLEYLPGENAD
ALGLTGQERYTIIIPENLKPKQMVKVQVKLDTGKTFQAVMRFDTDVELTYFLNGGILNYMIR
KMAK

SWISS-PROT ANNOTATION:

ID EMBOSST 001 STANDARD; PRT; 424 AA.

number of residues: 424; molecular weight: 47.6 kdal

1 MSNPFAHLAE PLDPVQPGKK FFNLNKLEDS RYGRLPFSIR VLLEAAIRNC DEFLVKKQDI
61 ENILHWNVTQ HKNIEVPFKP ARVILQDFTG VPAVVdfaAM RDAVKKLGGD PEKINPVCPA
121 DLVIDHSIQV DFNRRADSLQ KNQDLEFERN RERFEFLKGW SQAFHNMRRII PPGSGIIHQV
181 NLEYLARVVF DQDGYYYPDS LVGTDSDHTTM IDGLGILGWG VGGIEAEAVM LGQPISMVL
241 QVIGYRLMGK PHPLARGTFA NIRLLNRFLN KQAPQTIHLP SGEILDVFDA AERYQQAGLP
301 LIVLAGKEYG AGSSRDWAAK GPFLLGKAV LAESYERIHR SNLVGMGVIP LEYLPGENAD
361 ALGLTGQERY TIIIPENLKP QMKVQVKLDT GKTFQAVMRF DTDVELTYFL NGGILNYMIR
421 KMak

Sequence from 3' primer aligned against sequence of the aberrant splice product:

IRP1	251	gaattgtatgatgttttgtgaagaaaacaggatattgaaaatattctac
300		
10638.MN.hIRP	1	AACCCGGC-
8		. .
IRP1	301	attgaaatgtcactcagcacaagaacatagaagtgcatttaagcctgt
350		
10638.MN.hIRP	9	CGTG--ATTC-----GACT---CG---GTACCC-----
28		. .
IRP1	351	cgtgtcatcctgcaggacttacgggtgtgcccgtgtggttgactttgc
400		
10638.MN.hIRP	29	-----GGGGATCC---GA-----
38		.
IRP1	401	tgcaatgcgtatgtgtaaaaagtttaggaggagatccagagaaaataa
450		
10638.MN.hIRP	39	---TGTCTGCCCTGCTGATCTTGTAAATAGATCATCCATCCAGGTTGAT
84		
IRP1	451	accctgtctgcctgctgtatcttgcataagatcattccatccagggttat
500		
10638.MN.hIRP	85	TTCAACAGAAGGGCAGACAGTTACAGAAGAATCAAGACCTGGAATTGAA
134		
IRP1	501	ttcaacagaagggcagacagttaacagaagaatcaagacctggaatttga
550		
10638.MN.hIRP	135	AAGAAAATAGAGAGCGATTGAAATCTTAAAGTGGGTTCCCAGGCTTTCA
184		.
IRP1	551	aagaaaatagagagcgatttgcattttaaagtgggttcaggctttc
600		
10638.MN.hIRP	185	ACTACATGCGGATTATTCCCCCTGGCTCAGGAATCATCCACCAGGTGAAT
234		.
IRP1	601	acaacatgcggattattccccctggctcaggaatcatccaccaggtaat
650		
10638.MN.hIRP	235	TTGGAATATTGGCAAGAGTGGTATTGATCAGGATGGATATTATTACCC
284		
IRP1	651	ttggaatattggcaagagtggatttgcattcaggatggatatttaccc
700		
10638.MN.hIRP	285	AGACAGCCTCGTGGGCACAGACTCGCACACTACCATGATTGATGGCTTGG
334		
IRP1	701	agacagcctcggtggcacagactcgcacactaccatgattgatggcttgg
750		
10638.MN.hIRP	335	GCATTCTGGTTGGGTGTCGGTGGTATTGAAGCAGAAGCTGTCATGCTG
384		
IRP1	751	gcattcttgggtgggtgtcggtggattgaagcagaagctgtcatgctg
800		

10638.MN.hIRP	385	GGTCAGCCAATCAGTATGGTGCTTCCTCAGGTGATTGGCTACAGGCTGAT
	434	
IRP1	801	ggtcagccaatcagtatggtgcttcctcaggtgattggctacaggctgat
	850	
10638.MN.hIRP	435	GGGGAAGCCCCACCCTCTGGCACGGGAACATTGCCAACATTCGCTTGT
	484	
IRP1	851	ggggaagccccaccctctggcacgggaacattgccaacattcgcttgt
	900	
10638.MN.hIRP	485	TAA
	487	
IRP1	901	taaacagat ttt gaacaaggcaggcaccacagactatcc <u>atctgccttct</u>
	950	
10638.MN.hIRP	488	
	487	
IRP1	951	<u>qqqgaaatc</u> cttgatgtgttgatgctgctgagcggtaccaggcagg
	1000	
10638.MN.hIRP	488	
	487	
IRP1	1001	ccttcccctgatcg ttctggctgg caaagagtacggcaggcagctccc
	1050	

Exon 7, up to splice site, in blue; exon 18 from splice site in green; PCR primer IRP1s3 is double underlined. Confirms sequence splice site perfectly. Bases 871-2265 excised.

Alternatively Spliced IRP1 Transcript #03 (Δ 5-13?)

Amplicon of ~710bp amplified using template from HepG2 cells, 1st round PCR with IRPEx1 and IRPEx21 primers (amplifying across complete ORF) followed by 2nd round with IRP1s5 and IRP1s3 (amplifying across exons 4 - 18).

0047.MN.hIRP1.700F.Seq LENGTH: 461 Fri, Jun 04, 2004 6:24 PM
CHECK: 9130 ..

1	ATNCCATCCT	CCGGTTGGAG	TCTTCTGGAA	ACAGGAATT	TGAAGGTCGA
51	GTTCCCCCAA	CACCCGGGCC	AACTATTTAG	CCTCTCCCCC	CTTAGTAATA
101	GCATATGCAA	TTGCTGGAAC	CATCAGAAC	GACTTTGAGA	AAGAGCCATT
151	GGGAGTAAAT	GCAAAGGGAC	AGCAGGTATT	TCTGAAAGAT	ATCTGGCCGA
201	CTAGAGACGA	GATCCAGGCA	GTGGAGCGTC	AGTATGTCAT	CCCAGGGATG
251	TTTAAGGAAG	TCTATCAGAA	AATAGAGACT	GTGAATGAAA	GCTGGAATGC
301	CTTAGCAACC	CCATCAGATA	AGCTGTTTT	CTGGAATTCC	AAATCTACGT
351	ATATCAAATC	ACCACCATTC	TTTGAAACC	TGACTTTGGA	TCTTCAGCCC
401	CCTAAATCTA	TAGTGGATGC	CTATGTGCTG	CTAAATTG	GAGATTCGGT
451	AAACACTGACC	C			

EMBOSS-Align Results

EMBOSS_001	1	ATNCCAT-----CCT---CCGGTTGGAGT-CT-T
24		
IRP1	1651	tgtggtagaaagccatcacacagggagacctttagctgttgaggactat
1700		
EMBOSS_001	25	CTGGAAACAGGAATTGAGGTGAGTTC-CCCCAACACCCGGGCCAAC
73		
IRP1	1701	ctggaaaacaggaatttgaaggtcgagttcccccaacaccgggccaac
1750		
EMBOSS_001	74	TATTTAGCCTCTCCCCCTTAGTAATAGCATATGCAATTGCTGGAACCAT
123		
IRP1	1751	tat tagcctctcccccttagtaatagcatatgcaattgctgaaaccat
1800		
EMBOSS_001	124	CAGAATCGACTTTGAGAAAGAGCCATTGGGAGTAAATGCAAAGGGACAGC
173		
IRP1	1801	cagaatcgactttgagaaagagccattggagtaaatgcaaaggacagc
1850		
EMBOSS_001	174	AGGTATTTCTGAAAGATATCTGGCCGACTAGAGACGAGATCCAGGCAGTG
223		
IRP1	1851	aggtat ttctgaaagat atctggccgactagagacgagatccaggcagtg
1900		
EMBOSS_001	224	GAGCGTCAGTATGTCATCCCGGGATGTTAAGGAAGTCTATCAGAAAAT
273		
IRP1	1901	gagcgtcagtgatgtcatcccgggatgttaaggaagtctatcagaaaat
1950		

EMBOSS_001	274	AGAGACTGTGAATGAAAGCTGGAATGCCTTAGCAACCCCATCAGATAAGC
323		
IRP1	1951	agagactgtgaatgaaagctggaatgccttagcaaccccatcagataagc
2000		
EMBOSS_001	324	TGTTTTCTGGAATTCCAATCTACGTATATCAAATCACCACCATTCTT
373		
IRP1	2001	tgttttctggaattccaaatctacgtatatcaaattcaccaccattctt
2050		
EMBOSS_001	374	GAAAACCTGACTTTGGATCTTCAGCCCCCTAAATCTATAGTGGATGCCTA
423		
IRP1	2051	gaaaacctgactttggatcttcagccccctaaatctatagtgatgccta
2100		
EMBOSS_001	424	TGTGCTGCTAAATTGGGAGATTGGTAAC- ACTGACCC
461		.
IRP1	2101	tgtgctgctaaattgggag- ttggtaacaactgaccacatctccccag
2149		.

Amplicon maps from exon 14 (in red) to exon 17 (which ends at 2201 on IRP1 sequence)

If the transcript is Δ5-13, expected size for IRP1s5 and IRP1s3 primers is 732bp.

Extra sequence cannot be read from 5' end from Chromas file. Need to sequence 5' end carefully. 5' primer ends 36bp from end of exon 4; first 50 bases of sequence reaction are poor quality.

```
>10168.MN.h1RP1.700RI; reverse seq (inverse, complement); 15th June
2004
AAAGATATCTGGCCGACTAGAGACGAGATCCAGGCAAGTGGAGCGTCAGTATGTCATCCC
GGGGATGTTAACGGAAAGTCTATCAGAAAATAGAGACTGTGAATGAAAGCTGGAATGCCTT
AGCAACCCCATCAGATAAGCTGNTTTCTGGAATTCCAATCTACGTATATCAAATCACC
ACCATTCTTGAAAACCTGACTTTGGATCTTCAGCCCCCTAAATCTATAGTGGATGCCTA
TGTGCTGCTAAATTGGGAGATTGGTAACAACGTGACCACATCTCCCCAGCTGAAATAT
TGCAAGAAACAGTCCTGCTCGCTACTTAACAAAGAGGCCCTAATCCACGAGAATT
CAACTCCTATGGCTCCCGCCGAGGTAATGACGCCGTATGGCACGGGAACATTGCCAA
CATTCGCTTGTAAACAGATTAAACAAGCANGCACCACA
```

10168.MN.h1RP	1	AAAGATATCTGGCCGACTAGAGACGAGATCCAGGCAAGT
39		
IRP1	1851	aggatattctgaaagatatctggccactagagacgagatccaggc-agt
1899		
10168.MN.h1RP	40	GGAGCGTCAGTATGTCATCCGGGGATGTTAACGGAAAGTCTATCAGAAAA
89		
IRP1	1900	ggagcgtcagtatgtcatccggggatgttaaggaaagtctatcagaaaa
1949		

10168.MN.h1RP 139	90 TAGAGACTGTGAATGAAAGCTGGAATGCCTAGCAACCCATCAGATAAG
IRP1 1999	1950 tagagactgtgaatgaaagctggaatgccttagcaacccatcagataag
10168.MN.h1RP 189	140 CTGNTTTCTGGAATTCCAATCTACGTATATCAAATCACCACCATTCTT
IRP1 2049	2000 ctgttttctggaattccaaatctacgtatatcaaattaccaccattctt
10168.MN.h1RP 239	190 TGAAAACCTGACTTGGATCTTCAGCCCCCTAAATCTATAGTGGATGCCT
IRP1 2099	2050 tgaaaacctgactttggatcttcagccccctaaatctatagtggatgcct
10168.MN.h1RP 289	240 ATGTGCTGCTAAATTGGGAGATTGGTAACAACTGACCACATCTCCCCA
IRP1 2148	2100 atgtgctgctaaattggag- <i>ttcggt</i> aacaactgaccacatctcccc
10168.MN.h1RP 339	290 GCTGGAAATATTGCAAGAACAGTCCTGCTCGCTACTTAACAAACAG
IRP1 2198	2149 <i>gctggaaatattgcaagaaacagtcctgctgctacttaactaacag</i>
10168.MN.h1RP 389	340 AGGCCTAACTCCACGAGAACATTCAACTCCTATGGCTCCGCCGAGGTAATG
IRP1 2248	2199 <i>aggctaactccacgagaattcaactcctatggctccgcaggtaatg</i>
10168.MN.h1RP 439	390 ACGCCGTCATGGCACGGGAACATTGCCAACATTGCTTGTAAACAGA
IRP1 2298	2249 <i>acgcgtcatggcacgggaacattgccaacattcgcttgttaaacaga</i>
10168.MN.h1RP 461	440 TTTT-AACAAGCANGCACCACA
IRP1 2348	2299 <i>ttttgaacaagcaggcaccacagactatccATCTGCCTCTGGGAAAT</i>

Sequence reaction starts 8 bases from end of primer (in CAPS); confirms presence of exon 18 (**in red**) in the amplicon. No new info about 5' end.

Translation Product

Analysis of exon ends indicates that the Δ5-13 splice form would not have the IRP1 reading frame maintained. Does the splice product encode a meaningful protein?

Sequence from initiation ATG onwards run in EMBOSS-Transeq:

```
>EMBOSS_001_1
MSNPFAHLAEPLDPVQPGKKFFNLNKLEDSRYGRLPFSIRVLLEAAIRNCDEFLVKKQDI
ENILHWNVTQHKNIEVPFKPARVILQDFGTGVPAVVDFAACMRDAVKLGGDPEKINPVCPA
DLVIDHSIQVDFNRRETL*LLEYYLET GILKVEFTPTPGPTI*PLPP***HMQLLEPSSES
TLRKSHWE*MQRDSRYF*KISGRLETRSRQWSVSMSSRGCLRKSIRK*RL*MKAGMP*QP
HQISCFSGIPNLRISNHHSLKT*LWIFSPNLN*WMPMCC*IWEIR*QLTTSPQLEILQE
TVLLLAT*LTEA*LHENSTPMAPAEVMTPSWHGEHLPFAC*TDF*TSRHRLSICLLGK
SLMCLMLLSGTSRQAFP*SFWLAKSTVQAAPETGQLRALSCWESKPSWPRATSFTAFTAVTW
LGWV*SHLNISLVRMQMPWGSQGKNDTLSLFQKTSNHK*KSRSWILARPSRLS*GLTLM
WSSLISSTGASSTT*SARWPSRRRALGAAPREEAPPASAGPGGEASLAASGRGAAL*ME
QVSTEGLVPIL*AQNQKFLHSLFLIIIFSFSRRIWKLEWWECQ*CQKERTKLVFKVTDHRT
LLFHCFLLIFs*TQANLLRRCLLPSYCSSYALLNETFLLRVIFLSVLIIPVLSIDKNFA
HFKSEQ*FSLLSPFPSE*IQTPHG*VGC*SCFDYVPFDRST*KEM*SFLLSFHLSSRD
LCWEAWENTFLI*MK*NLF SVKTC*L*VLLCLWLEFDI*YRVNLTPYHWEA*ITFIFS
HFYNSIRTDRV*RKCLGTIMLALPCLGADKKEE*PGGSGNDIST*GKADKLQDTKNQLSA
HFYPCSHFWACLSLLGLL*CNAIDWLKEQKCIFS SQLWRLEF*DQS*SHFIFW*GHSSWFT
DGHLLACSHMAFLWYVPGGGER
```

Using the original initiation ATG a peptide of 135 + 3 aa would be translated, corresponding to a protein of 15.7kDa.

Conclusions

Sequence at 5' end needs to be confirmed, either by repeating the forward sequencing reaction or by subcloning the fragment and sequencing from a plasmid.

The data indicate that exons 5 to 13 are skipped, but sequence at the 5' end of exon 14 is poor - there may be a cryptic splice site at the beginning of exon 14 (needs to be checked) - and there is no sequence data upstream of exon 14 (expect 36 bases from primer to end of exon 4).

The transcript is unlikely to have significant biological function.